

Static Analysis of Laminated Composite Structures by Finite Element and Semi-Analytical Methods

Thesis submitted by

ARNAB CHOUDHURY

**Doctor of Philosophy
(Engineering)**

**DEPARTMENT OF MECHANICAL ENGINEERING
FACULTY COUNCIL OF ENGINEERING & TECHNOLOGY
JADAVPUR UNIVERSITY
KOLKATA, INDIA
2022**

1. Title of the Thesis:

Static Analysis of Laminated Composite Structures by Finite Element and Semi-Analytical Methods

2. Name, Designation and Institution of the Supervisors:

Prof. (Dr.) Samar Chandra Mondal

Professor
Dept. of Mechanical Engineering
Jadavpur University
Kolkata, India

Prof. (Dr.) Susenjit Sarkar

Professor
Dept. of Mechanical Engineering
Jadavpur University
Kolkata, India

3. List of Publications (Referred Journals):

- i. Arnab Choudhury, Samar Chandra Mondal, Susenjit Sarkar: "Effect of Lamination angle and thickness on analysis of composite plate under thermo mechanical loading", Journal of Mechanical Engineering-Strojnícky časopis (ISSN 0039-2472), 67(1), pp. 5- 22, 2017. SCOPUS Indexed Journal.

- ii. Arnab Choudhury, Samar Chandra Mondal, Susenjit Sarkar, Mintu Karmakar "Analysis of Simply Supported Laminated Composite Plate for Different Orientation Angles", Journal of Mechanical Engineering-Strojnícky časopis (ISSN 0039-2472), 73(2), 2023. SCOPUS Indexed Journal (Accepted for publication)

4. List of Patents

Nil

5. List of Presentations in National/International/Conferences/Workshops:

- i. Arnab Choudhury, Samar Chandra Mondal, Susenjit Sarkar: “Effect of Fiber Orientation Angle on Deflection of Simply Supported Composite Beam”, 1st International Conference on Emerging Trends in Engineering and Science (ETES 2018) organized by Asansol Engineering College, March 23-24, 2018.

- ii. Arnab Choudhury, Samar Chandra Mondal, Susenjit Sarkar: “Finite Element Analysis of Buckling of Simply Supported Composite Plate for Different Orientation Angles”, National Conference on Trends & Advances in Mechanical Engineering (TAME 2019) jointly organized by The Association of Engineers, India & Kalyani Govt. Engineering College, Feb 15-16, 2019.

“Statement of Originality”

I **Shri Arnab Choudhury** registered on **16.02.2015** do hereby declare that this thesis entitled **“Static Analysis of Laminated Composite Structures by Finite Element and Semi-Analytical Methods”** contains literature survey and original research work done by the undersigned candidate as part of Doctoral studies.

Although information in this thesis have been obtained and presented in accordance with existing academic rules and ethical conduct. I declare that, as required by these rules and conduct, I have fully cited and referred all materials and results that are not original to this work.

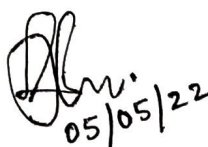
I also declare that I have checked this thesis as per the “Policy on Anti Plagiarism, Jadavpur University, 2019”, and the level of similarity as checked by iThenticate software is 8%.

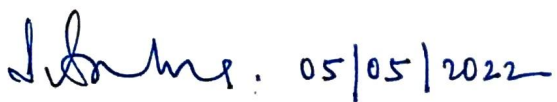
Arnab Choudhury
Signature of Candidate

Date: 05-05-22

Certified by Supervisor (s):

(Signature with date, seal)


1.  05/05/22
Professor
Dept. of Mechanical Engineering
Jadavpur University, Kolkata-32

2.  05/05/2022
Professor
Dept. of Mechanical Engineering
Jadavpur University, Kolkata-32

**DEPARTMENT OF MECHANICAL ENGINEERING
FACULTY COUNCIL OF ENGINEERING & TECHNOLOGY
JADAVPUR UNIVERSITY
KOLKATA, INDIA**


CERTIFICATE FROM THE SUPERVISOR/S

This is to certify that the thesis entitled “Static Analysis of Laminated Composite Structures by Finite Element and Semi-Analytical Methods” submitted by Shri Arnab Choudhury, who got his name registered on 16.02.2015 for the award of Ph.D. (Engineering) degree of Jadavpur University is absolutely based upon his own work under the supervision of Prof. (Dr.) Samar Chandra Mondal and Prof. (Dr.) Susenjit Sarkar and that neither his thesis nor any part of the thesis has been submitted for any degree/diploma or any other academic award anywhere before.

1.  05/05/22

Prof. (Dr.) Samar Chandra Mondal
Professor
Dept. of Mechanical Engineering
Jadavpur University
Kolkata
India
Supervisor

Professor
Dept. of Mechanical Engineering
Jadavpur University, Kolkata-32

2.  .05/05/2022

Prof. (Dr.) Susenjit Sarkar
Professor
Dept. of Mechanical Engineering
Jadavpur University
Kolkata
India
Supervisor

Professor
Dept. of Mechanical Engineering
Jadavpur University, Kolkata-32

ABOUT THE AUTHOR

Name: ARNAB CHOUDHURY

Address:

C/12, Sector-1, Bidhanpark
P.O- Fuljhore, Durgapur, District- Paschim Burdwan
PIN-731206, West Bengal, India

Email: arnabmech001@gmail.com

Education:

B.E (Mechanical Engineering), 2007
Pt. RavishankarShukla University, Raipur (C.G)
College: Bhilai Institute of Technology, Bhilai (C.G)

M.Tech (Automobile Engineering), 2009
Mumbai University, Maharastra
College: VeermataJijabai Technological Institute, Mumbai

GATE 2009 Qualified, AIR- 1221

Experience:

Mr. Arnab Choudhury is presently working as Junior Engineer (Mechanical) in Public Health Engineering Directorate, Government of West Bengal from 01/10/2018 to till date. Earlier, Sri Choudhury had worked in the capacity of Assistant Professor of Mechanical Engineering Department at Dr.B.C.Roy Engineering College, Durgapur from 17/2/2014 to 29/9/2018, at Birbhum Institute of Engineering & Technology, Suri, Birbhum from 2/4/2013 to 15/02/2014 and at Bhilai Institute of Technology, Bhilai house, Chhattisgarh from 03/08/2009 to 30/03/2013.

ACKNOWLEDGEMENT

I wish to express my profound regards to my supervisor, Prof. (Dr.) Samar Chandra Mondal, Professor, Department of Mechanical Engineering, Jadavpur University, Kolkata, for his unconditional support, guidance and advice towards me during preparation of this dissertation. No word would be sufficient to express my gratitude towards him.

I would like to express my sincere thanks to my another supervisor, Prof. (Dr.) Susenjit Sarkar, Professor, Department of Mechanical Engineering, Jadavpur University, Kolkata, for his important suggestions, encouragement, and constant motivation in completing this research work. Without him, this research work would never have been completed.

I would like to express my most sincere thanks to Mintu Karmakar, Space Instrumentation Engineer in Mechanical Engineering, CESSI, IISER Kolkata, Mohanpur, W.B for his support and help to my work.

It has been a distinct privilege for me to work with Prof. Samar Chandra Mondal and Prof. Susenjit Sarkar.

Words are inadequate to express deep sense of gratitude to the members of the doctoral committee, Mechanical Engineering Dept., Jadavpur University, Kolkata.

I am also thankful to Dr. Subhas Ch. Moi, Assistant Professor, Dr. B.C Roy Engineering College, Durgapur and Amalendu Biswas, Assistant Professor, Heritage Institute of Technology for their kind cooperation.

Lastly, I would like to thank my Grandfather and Grandmother, Late Debnarayan Chaudhury and Late Annapurna Chaudhury for their blessings. I would also like to thank my Parents, Mr. Nirmalendu Chaudhury and Mrs. Tapati Chaudhury, my wife Lipi and my sister Anushree for their saintly patience and constant inspiration. I want to give special thanks to Mr. Swapan Kumar Roy (Uncle) for his heartening support.

Arnab Choudhury
ARNAB CHOUDHURY 5/5/22

DEDICATED TO

My

Grandfather & Grandmother

Late Debnarayan Chaudhury & Late Annapurna Chaudhury

&

My Parents

Mr. Nirmalendu Chaudhury and Mrs. Tapati Chaudhury

&

My Wife

Mrs. Lipi Choudhury

&

My Daughter

Alivia Choudhury

TABLE OF CONTENTS

Title of Thesis		ii
Statement of Originality		iv
Certificate of Supervisors		v
About the Author		vi
Acknowledgement		vii
Dedication		viii
Table of Contents		ix
Brief Nomenclatures		xvi
List of Figures		xviii
List of Tables		xxii
Chapter 1	Introduction	1
	1.1 Background	1
	1.2 Objectives of the present research work	3
	1.3 Plan of the present research work	4
	1.4 Outline of the thesis	6
Chapter 2	Theory and Literature Review	8
	2.1 Composite material basics	8
	2.1.1 Applications	8
	2.1.2 Advantages and limitations	9
	2.1.3 Classification of Composite material	10
	2.1.4 Fibers and Matrix	10
	2.1.5 Lamina and Laminates	11
	2.1.6 Coordinate System	12
	2.1.7 Laminate Lay up	12
	2.1.7.1 Symmetric laminate	14
	2.1.7.2 Anti symmetric Laminate	14
	2.1.7.3 Balanced Laminate	14
	2.1.7.4 Angle ply laminate	14

	2.1.7.5	Cross ply laminate	14
	2.1.7.6	Hybrid laminate	15
	2.1.7.7	Sandwich laminate	15
	2.1.8	Manufacturing of Fiber-Reinforced Composite Materials	15
	2.2	Literature Review	16
	2.3	Closure	24
Chapter 3		Macro mechanical analysis of Laminate	26
	3.1	Constitutive equations of Lamina	26
	3.1.1	Hook's Law in 3D	26
	3.1.2	Hook's Law in 2 D	27
	3.2	Constitutive equations of Laminate	29
	3.2.1	Calculation of ABD matrix (laminate stiffness)	30
	3.3	Closure	32
Chapter 4		Finite element analysis: Introduction	33
	4.1	Introduction	33
	4.2	Basic Finite Element method (FEM) steps	33
	4.3	Basic steps of FEA package (ANSYS)	34
	4.4	Basic steps of analysis of Laminated composite structure	34
	4.4.1	Properties of the laminate	35
	4.4.2	Element Type	35
	4.4.3	Algorithm of FEM	36
	4.5	Closure	38
Chapter 5		Analysis of Laminated Composite Plate	39
	5.1	Stress analysis of single lamina under in plane load	39
	5.1.1	Semi-analytical method & FEM	40
	5.1.2	Validation of semi-analytical and FEM	40
	5.1.3	Numerical problem	42
	5.1.3.1	Result and discussion	43
	5.1.3.2	Effect of orientation angle on displacement	44
	5.1.3.3	Effect of length to thickness ratio	44

5.2	Stress analysis of laminate under in plane load	45
5.2.1	Determination of stress of laminate	45
5.2.2	Semi-analytical method & FEM	47
5.2.3	Validation of Semi-analytical Method and FEA model	47
5.2.4	Numerical problem	48
5.2.4.1	Result and discussion	49
5.2.4.2	Effect of orientation angle	52
5.2.4.3	Effect of length to thickness ratio	54
5.2.4.4	Effect of no. of lamina	54
5.2.4.5	Symmetric cross ply laminate	56
5.2.5	Closure	57
Chapter 6	Bending & Buckling of Laminated composite plate	58
A	Bending of Laminated composite plate under uniform transverse loading	58
6.1	Classical Lamination Theory (CLT)	58
6.1.1	Governing equation of laminated plate using CLT	59
6.1.2	Equation of motion	59
6.2	Bending of Specially orthotropic simply supported plate	61
6.2.1	The Navier Method	62
6.3	Bending of Symmetric angle ply simply supported plate	63
6.4	Semi-Analytical Method	64
6.5	Finite element method	64
6.6	Validation of the semi-analytical method & FEM	64
6.7	Numerical Problem	65
6.7.1	Convergence analysis	66
6.7.2	Results and Discussion	67
6.7.2.1	Effect of stacking sequence	70
6.7.2.2	Effect of no. of plies	71
6.7.2.3	Effect of length to thickness ratio	72
6.8	Analysis of Percentage error of laminated composite Plate	72

6.8.1	Thickness of lamina (or Ply)	73
6.8.2	Number of Lamina (or Ply)	73
6.8.3	Orientation angle (Stacking sequence)	74
6.8.4	Statistical Analysis of Percentage Error in deflection	75
6.8.5	(a) Regression equation	76
	(b) Validation of model	76
	(c) Effect of Process Parameters	79
6.8.6	Discussion	82
B	Buckling of laminated Composite plate	82
6.9	Semi-analytical Method	83
6.10	Finite element method	84
6.10.1	Convergence analysis	85
6.11	Validation of semi-analytical method & FEM	85
6.12	Numerical Problem	86
6.12.1	Results & Discussion	86
6.12.2	Effect of fiber orientation angle and number of lamina	88
6.13	Closure	90
Chapter 7	Bending of Laminated Composite Beam	91
7.1	Introduction	91
7.1.1	Assumptions.	92
7.2	Theoretical formulation	92
7.2.1	Analysis of laminated beam using CLT	93
7.2.1.1	General solution of Bending Equation	94
7.2.1.2	Calculation of stresses	95
7.2.2	Analysis of laminated beam using FSDT	95
7.2.2.1	General solution of bending equation	96
7.2.2.2	Non dimensional quantity	97
7.3	Semi-analytical method	98
7.3.1	Validation of Semi-analytical method	98
7.4	Finite element Method (FEM)	99

7.4.1	Convergence analysis	99
7.4.2	Validation of the FEM	100
7.4.3	Numerical problem	101
7.4.3.1	Analysis of the results	101
7.4.3.2	Effect of Orientation angle	104
7.4.3.3	Effect of boundary conditions	105
7.4.3.4	Effect of length to thickness ratio	105
7.4.3.5	Effect of no. of lamina	106
7.5	Analysis of Percentage error of laminated composite beam	108
7.5.1	Length to width ratio (L/W)	108
7.5.2	Mesh size unit	109
7.5.3	Thickness of laminate	109
7.5.4	Orientation angle	111
7.5.5	Statistical Analysis of Percentage Error in deflection	113
	(a) ANOVA	113
	(b) Regression equation	115
	(c) Validation of model	116
	(d) Effect of Process Parameters	117
7.6	Closure	125
	Failure analysis of laminate composite	126
8.1	Introduction	126
8.2	Methodology to find Strength ratio & First ply failure load	127
8.2.1	Thermo mechanical stress	128
8.2.2	Hygro thermal stress	129
8.3	Failure Theories	129
8.3.1	Maximum stress criteria	130
8.3.2	Maximum strain criteria	130
8.3.3	Tsai–Wu Failure Theory	130
8.3.4	Tsai–Hill failure theory	130

Chapter 8

8.3.5	Strength ratio	131
8.4	Failure of laminated composite plate under in-plane tensile load	131
8.4.1	Numerical Problem	131
8.4.1.1	Validation of semi-analytical & FEM model	132
8.4.1.2	Comparison of semi-analytical method and FEM	133
8.4.2	Effect of fiber orientation angle on failure analysis	134
8.4.2.1	Symmetric Angle ply composite subjected to different mechanical loading condition	134
8.4.3	Comparative study of different failure criteria based on first ply failure load	136
8.4.4	Last ply failure analysis of laminate under tensile loading	139
8.4.5	Mode of failure	140
8.4.6	Effect of hygro-thermo mechanical loading on strength ratio	141
8.5	Failure analysis of Laminated Composite Beam	144
8.5.1	Numerical Problem	144
8.5.2	Results and discussion	145
8.5.2.1	Comparative study of different failure theories for beam fixed at both ends under UDL	145
8.5.2.2	Effect of fiber orientation angle on strength ratio for different boundary conditions of composite beam subjected to mechanical load (Uniformly distributed load)	147
8.5.2.3	Effect of thermal load on strength ratio of composite beam	148
8.5.2.4	Effect of length to thickness ratio (a/h) on strength ratio based on FPF load	150
8.5.2.5	Mode of failure	151
8.6	Comparison of FEM results with Semi-analytical method (FSDT)	153
8.7	Closure	154
Chapter 9	Analysis of hybrid laminated composite	155
9.1	Introduction	155
9.2	Analysis of Hybrid composite Laminate	156

9.2.1	Numerical Problem	157
9.2.2	Semi-analytical method	157
9.2.3	Finite element Method	157
9.3	Results and Discussion	159
9.3.1	Stress and displacement	159
9.3.2	Failure analysis	162
9.4	Analysis of hybrid composite beam and plate	164
9.5	Closure	166
Chapter 10	Conclusion	167
Chapter 11	Future scope	169
References		171
Appendix		177

BRIEF NOMENCLATURE

Symbols	Details
E	Young's modulus
E_1	longitudinal Young's modulus (in direction 1)
E_2	transverse Young's modulus (in direction 2)
ν_{12}	Major Poisson's ratio
ν_{21}	Minor Poisson's ratio
G_{12}	in-plane shear modulus (in plane 1–2)
G	Shear modulus
τ	Shear stress at plane (MPa)
ν	Poisson's ratio
$\sigma_x, \sigma_y, \tau_{xy}$	Stress in global coordinate system
$\sigma_1, \sigma_2, \tau_{12}$	Stress in local coordinate system
$\varepsilon_x, \varepsilon_y, \gamma_{xy}$	Strain in global coordinate system
$\varepsilon_1, \varepsilon_2, \gamma_{12}$	Strain in local coordinate system
ε	Strain tensor
θ	Orientation angle (degree)
γ	Shear strain at plane (MPa)
ϕ_x	Rotations of the transverse normal about the x axis
ϕ_y	Rotations of the transverse normal about the y axis
x, y, z	Global coordinate system
$1, 2, 3$	Local coordinate system
w_{bar}	Non dimensional deflection
w_0	Displacements along the coordinate line of a material point on the x - y plane
w_{max}	Maximum deflection
M_{max}	Maximum bending moment
σ	Stress tensor (MPa)
M	Bending moment
T	Transformation matrix
K	Shear correction coefficient
h	Total thickness of laminate
z	Distance from neutral axis
$E_{xx}^b I_{yy}$	Bending stiffness
Q_{ij}	Reduced stiffness coefficient
S_{ij}	Compliance matrix
$[R]$	Reuter matrix
$N_x, N_y,$	Normal force per unit length
N_{xy}	Shear force per unit length
$M_x, M_y,$	Bending moment per unit length

M_{xy}	Twisting moments per unit length
ε^0	Mid-plane strain of laminate in x-y coordinate
k	Laminate curvature
A_{ij}	Extensional stiffness matrix
B_{ij}	Extension – bending coupling matrix
D_{ij}	Bending stiffness matrix
u, v, w	Displacement in x, y, z directions
$I_0, I_1 \& I_2$	Rotary inertia terms
SR	Strength ratio
q	Applied Distributed Force
FEM	Finite element model
CLT	Classical Lamination theory
FSDT	First Order shear deformation theory
FEA	Finite element analysis
V	Total Potential energy
I_F	Failure index
T	Thermal effect

LIST OF FIGURES

Figure No.	Description	Page No.
2.1(a)	Formation of a composite material using fibers and resin for continuous fiber composite	11
2.1(b)	Structure of continuous fiber and short fiber composites	11
2.2	Laminate made up of lamina at different orientations	11
2.3	Lamina (1, 2) and Laminate (x, y) coordinate system	12
2.4	Composite manufacturing technologies (a) Hand Layup (b) Filament winding	16
3.1	3 D Stress Tensor in Cartesian rectangular coordinate	27
3.2	2 D Stress Tensor in Cartesian rectangular coordinate	28
3.3	Coordinate of plies within laminate	30
5.1	Local or lamina reference axis (1-2) and global or laminate reference axis (x, y)	39
5.2	Geometry of a Lamina	43
5.3	Influence of orientation angle on displacement vector sum (USUM)	44
5.4(a)	Stacking sequence of lamina within laminate	49
5.4(b)	Geometry of laminate under loading in x direction	49
5.5	Effect of orientation angle on local and global stress for different orientation angle $[+\theta/-\theta]_s$ for loading in x direction	53
5.6	Effect of orientation angle on deflection- x for different orientation angle $[+\theta/-\theta]_s$ for loading in x direction.	54
5.7	Effect of orientation angle on deflection- x for different orientation angle $[0/90/+\theta/-\theta]_s$ for loading in x direction.	54
5.8	Effect of Length to thickness ratio (a/h) on deflection in x direction and Global Stress in x direction.	55
5.9 (a)	Effect of no. of lamina on deflection in x direction and Global Stress in x direction	55
5.9 (b)	Effect of no. of lamina on Global Stress in x direction	56
5.10	Deflection of symmetric angle ply laminate using ANSYS 15.0	57
6.1	Boundary conditions of simply supported rectangular plate on all sides	61
6.2	Convergence analysis for different mesh size	66
6.3(a)	Boundary conditions of plate simply supported on all the sides	69
6.3(b)	Uniform pressure loading of plate simply supported on all the sides	69
6.3(c)	Deflection of $[+30/-30]_s$ composite plate	69

6.4	Variation of deflection with orientation angle for different methods	70
6.5 (a)	Variation of deflection with no. of plies for sym. Angle ply composite.	71
6.5 (b)	Variation of deflection with no. of plies for sym. cross ply composite.	71
6.6	Variation of deflection with length to thickness ratio using two ways: Keeping thickness constant, length varies (left) and length constant, thickness varies (right).	72
6.7	Variation of thickness per lamina with % error for 4 ply, 45 deg angle square plate subjected to transverse load of 1 N/m	74
6.8	Variation of No. of lamina with % error for 45 deg angle square plate subjected to transverse load of 1 N/m	74
6.9	Variation of Orientation angle with % error for square plate subjected to transverse load of 1 N/m of thickness per lamina of 5mm.	75
6.10	Residual plot of % error	77
6.11(a,b)	Surface plot of factors with response (% Error)	80
6.11(c)	Surface plot of factors with response (% Error)	81
6.12	2 D plot of factors with response (% Error)	82
6.13	Meshed Geometry of simply supported composite plate with constraint and loading	84
6.14	Convergence analysis	85
6.15	Effect of orientation angle on critical buckling load (left) and % age error (right)	87
6.16(a)	Critical buckling load for different orientation angle for simply supported graphite/ epoxy composite plate under compressive load $N_y \neq 0, N_x = N_{xy} = 0$	88
6.16(b)	Critical buckling load for different orientation angle for simply supported graphite/ epoxy composite plate under compressive load $N_y \neq 0, N_x \neq 0, N_{xy} = 0$	89
6.17	Critical buckling load for number of lamina for simply supported graphite/ epoxy composite plate under compressive load ($N_x \neq 0, N_y = N_{xy} = 0$).	89
6.18	Buckling mode of simply supported composite plate for 45° fiber orientation angle.	90
7.1	Geometry of laminated composite beam	93
7.2	Laminated composite beam subjected to UDL for different boundary conditions.	98

7.3	Convergence analysis in ANSYS for Clamped-Clamped beam of stacking seq. $[\pm 30^\circ]_s$.	100
7.4	Geometry of hinged-hinged laminated composite beam under UDL	100
7.5(a)	Comparison of the semi-analytical method (CLT & FSDT) with FEM	103
7.5(b)	Deflection of H-H beam for $[0/-0]_s$	104
7.6	Effect of fiber orientation angle on non dimensional deflection for (a) different methods (b) boundary conditions.	105
7.7	Effect of length to thickness ratio on non dimensional deflection for different methods.	106
7.8	Effect of no. of lamina on non dimensional deflection solved by FSDT	106
7.9	Distribution of maximum normal stress along the thickness of the beam for fiber orientation angle $\pm 0^\circ$ to $\pm 90^\circ$ for boundary conditions: (a) both end hinged (b) both end clamped (c) one end clamped and other end free. (d) Comparison of the variation of maximum normal stress along the beam thickness for different boundary conditions for $\pm 45^\circ$ fiber orientation angle.	107
7.10	Variation of percentage error with (a) L/W ratio from 1 and above, (b)L/W ratio from 10 and above for orientation angle of $[45/-45]_s$, mesh unit size of 0.25, thickness 0.5mm.	108
7.11(a)	Variation of percentage error with mesh size (size of element) for L/W ratio of 20	109
7.11 (b)	Variation of percentage error with mesh size (size of element) for L/W ratio of 10	110
7.12	Percent error for different L/W and thickness of angle $[45/-45]_s$	111
7.13	Effect of Orientation angle on % error	112
7.14	Residual plot of % error	116
7.15(a,b)	Surface plot of factors with response (% Error)	118
7.15(c,d)	Surface plot of factors with response (% Error)	119
7.16(a,b)	2 D plot of factors with response (% Error)	120
8.1	Strength ratio calculated using Maximum stress criteria base on FPF for angle ply laminate for a range of fiber orientation angle subjected to (a) in plane normal and shear loading (only $N_x = 1$, $N_y = 1$, $N_{xy} = 1$, $N_x = N_y = N_{xy} = 1$) (b) bending and twisting moment (only $M_x = 1$, $M_y = 1$, $M_{xy} = 1$, $M_x = M_y = M_{xy} = 1$) and (c) combination of all loading ($N_x = M_x = 1$, $N_y = M_y = 1$, $N_{xy} = M_{xy} = 1$)	135
8.2	Strength ratio calculated using interactive and non interactive	138

	failure criteria for angle ply laminate subjected to (a) in plane normal tensile loading ($N_x \neq 0$) (b) twisting moment $M_{xy} \neq 0$ and (c) in plane loading ($N_y \neq 0$) for range of fiber orientation angle.	
8.3	Comparison of Strength ratio calculated using Max. Stress, Tsai –Wu and modified failure criteria for angle ply laminate subjected to inplane normal tensile loading ($N_x \neq 0$) for range of fiber orientation angle	138
8.4	Strength ratio calculated using interative and non interactive failure criteria for cross ply laminate subjected to in plane normal tensile loading ($N_x \neq 0, N_y \neq 0$)	139
8.5	Comparison of the Strength ratio calculated using Tsai-Wu criteria based on FPF for angle ply laminate for a range of fiber orientation angle subjected to (a) Hygro thermo mechanical loading (b) Combined Hygro thermo mechanical loading for positive temperature difference	142
8.6	Comparison of the Strength ratio calculated using Tsai-Wu criteria subjected to Hygro thermo mechanical loading for negative temperature difference.	143
8.7	Comparison of the Strength ratio calculated using Tsai-Wu criteria subjected to thermo mechanical loading for a range of temperature difference.	143
8.8	Comparison of the Strength ratio calculated using Tsai-Wu criteria subjected to Hygro thermo mechanical loading for cross ply composite.	144
8.9	Comparative study of different failure criteria for fixed – fixed symmetric angle ply composite beam.	146
8.10	Comparative study of different failure criteria for fixed – fixed symmetric Cross ply composite beam.	147
8.11	Effect of fiber orientation angle on strength ratio for different boundary conditions	148
8.12	Comparison of strength ratio obtained for mechanical and thermo mechanical load for different fiber orientation angle for composite fixed beam	150
8.13	Effect of aspect ratio on strength ratio for fixed composite beam for Mechanical and thermo mechanical load	151
9.1	(a) Stacking sequence of laminate	159
	(b) Quad. Mapped meshing of laminate	159
9.2	USUM of G-C-C-G	162
9.3	Deflection of G-C-C-G hybrid composite beam	166

LIST OF TABLES

Table No.	Description	Page No.
2.1	Layup code for different composite laminate	13
5.1	Properties of composite material	41
5.2	Validation with published literature	41
5.3	Comparison of the local stress in Pa determined by Semi-analytical method and FEM	43
5.4	Semi-analytical model verification with published literature for [0/30/-45] Graphite/Epoxy Laminate subjected to $N_x = N_y = 1000 N/m$ for 5 mm lamina thickness.	48
5.5	FEM model verification with published literature for [0/90/45/-45] _s AS4D/9310 Laminate subjected to $N_x = 100 N/mm$ for 10 mm laminate thickness.	48
5.6	Comparison of the Local stress from Semi-analytical method with FEM for different stacking sequence of symmetric angle ply laminate.	50
5.7	Comparison of the Local stress from Semi-analytical method with FEM for different stacking sequence of symmetric cross ply laminate.	51
5.8	Comparison of the Global stress from Semi-analytical method with FEM for different stacking sequence of symmetric angle ply laminate.	51
5.9	Comparison of the Global stress from Semi-analytical method with FEM for different stacking sequence of symmetric cross ply laminate.	52
5.10	Comparison of the Global stress from Semi-analytical model with FEM for symmetric cross ply laminate.	56
6.1	Validation of model with published literature Manahan (2011)	65
6.2	Validation of model with published literature of Kenneth Carroll (2013)	65
6.3	Convergence analysis for different mesh size	66
6.4	Rayleigh- Ritz method coefficients	67
6.5	Comparison of Semi-analytical method and FEM for Symmetric angle plies composite plate simply supported on all the sides under transverse uniform pressure.	70
6.6	Effect of thickness per lamina for 4 ply square plate (L/W=1), angle= [45/-45] _s	73
6.7	Effect of No. of lamina for square plate (L/W=1), angle= [45/-	74

	45]s, thickness/lamina is 5mm	
6.8	ANOVA table	77
6.9	Variables for statistical analysis with levels.	78
6.10	Results for one way ANOVA	78
6.11	Results for two way ANOVA	79
6.12	Validation of results with existing literature	85
6.13	Comparison of Critical buckling load (N/mm) found by Finite element Method and semi-analytical method (CLT)	87
7.1	Maximum Transverse deflections of laminated composite beam for different boundary conditions and subjected to point load and uniformly distributed load according to CLT and FSDT	97
7.2	Validation of Semi-analytical Model for Hinged-Hinged (H-H) beam	98
7.3	Comparison of the semi-analytical model with FEM model for H-H beam, length=0.1m, width= 5mm, UDL= 200 N/m, thickness of each ply= 0.125mm	103
7.4	Percent error for different L/W and thickness of angle [45/-45]s	110
7.5	Variation of % error with orientation angle	112
7.6	Percentage error in deflection (E) of MATLAB result with FEA (ANSYS) for simply supported beam under UDL of 200 N/m	121
7.7	Variables for statistical analysis with levels.	121
7.8	Arrangement of data for ANOVA of simply supported beam	121
7.9	Results for one way ANOVA	123
7.10	Results for two way ANOVA	123
7.11	Arrangement of data for ANOVA eliminating the insignificant term	124
7.12	Results of ANOVA eliminating the insignificant term	124
8.1	Comparison of FEM results with published literature	132
8.2	Comparison of CLT with published literature	133
8.3	Comparison of CLT with ANSYS	133
8.4	Comparison of CLT with FEM for 4 layer laminated composite plate under in plane load (Nx) of 1 N/m, a/h= 10.	134
8.5	First ply failure load (FPF) and last ply failure load (LPF) for different laminate under tensile load (1MN), thickness/ply: 5 mm, Graphite epoxy composite laminate.	139
8.6	Mode of failure of symmetric angle ply composite laminate under in plane tensile load	140
8.7	Mode of failure of symmetric cross ply composite laminate under in plane tensile load	141

8.8	Comparison of strength ratio from different failure criteria for different fiber orientation angle	146
8.9	Strength ratio and transverse deflection of composite beam for different boundary conditions under UDL. (Graphite/Epoxy composite material)	148
8.10	Comparison of strength ratio of composite beam subjected to mechanical (UDL=1000 N/m) and thermo mechanical load ($\Delta T = -75^{\circ}\text{C}$, $UDL = 1000 \text{ N/m}$)	149
8.11	Mode of failure of composite beam for different boundary conditions subjected to mechanical and thermo mechanical load	152
8.12	Percentage error of FEA results with FSDT results for Tsai-Wu Criteria	154
9.1	Validation of FEM model with existing literature	158
9.2	Validation of Semi-analytical model with existing literature	158
9.3(a)	Comparison of the Local stress of G-C-C-G hybrid composite of FEM with Semi-analytical method	160
9.3(b)	Comparison of the Global stress of G-C-C-G hybrid composite of FEM with Semi-analytical method	160
9.4	Comparison of different hybrid composite laminate	161
9.5	Comparison of four layers Cross ply [0/90/90/0] Glass/Epoxy and Graphite/ Epoxy composite with Hybrid composite, thickness/layer: 5 mm, length: 1m and width: 0.2 m under in plane tensile load (1N) based on Tsai-Wu Criteria.	163
9.6	Strength ratio of G-C-C-G sym. Angle ply hybrid composite [45/-45] _s	163
9.7	Comparison of four layers Angle ply [45/-45/-45/45] Glass/Epoxy and Graphite/ Epoxy composite with Hybrid composite, thickness/layer: 5 mm, length: 1m and width: 0.2 m under in plane tensile load (1N) based on Tsai-Wu Criteria and Max. Stress Criteria.	164
9.8	Comparison of four layers Angle ply [60/-60] _s Glass/Epoxy and Graphite/ Epoxy composite with Hybrid composite beam, thickness/layer: 0.125 mm, length: 0.1m and width: 5mm under UDL (200N/m) based on Tsai-Wu Criteria.	165
9.9	Comparison of the semi-analytical results (FSDT) with FEM results for four layers Angle ply [60/-60] _s Glass/Epoxy and Graphite/ Epoxy composite with Hybrid composite beam, thickness/layer: 0.125 mm, length: 0.1m and width: 5mm under UDL (200N/m) based on Tsai-Wu Criteria.	165
9.10	Comparison of the semi-analytical results (Navier Method) with	166

FEM results for simply supported laminated composite plate for G-C-C-G combination under uniform transverse load (100 N/m) of thickness per lamina of 5mm

CHAPTER 1

INTRODUCTION

Outline of the Chapter: 1.1 Background, 1.2 Objective of the present research work, 1.3 Plan of the present research work, 1.4 Outline of the thesis

1.1 Background

The concept of combining two or more materials to produce a new, stronger and lighter material whose properties are superior to those of its constituent materials was developed by human beings thousands of years ago. Around 1500 B.C., Egyptians and Mesopotamians created the first composite by combining mud and straw to build their houses. In 1200 A.D., the Mongols invented the composite bow by combining wood, bow, and animal glue. Although many types of composites have been developed throughout the history of mankind, the first artificial fiber reinforced plastic composite was developed in 1935 by Simison and Arthur D. Little of the Owens Corning Company. Later, many developments occurred in the field of composite manufacturing. Composites have grown in popularity in the aerospace, marine, sports, and automotive industries due to their appealing properties of high strength to weight ratio [1].

While designing a structure made of laminated composite material, there are many aspects to investigate because the behaviour of composite material under loading depends upon many factors. The properties of fiber and matrix, orientation of fiber in the matrix, stacking sequence of lamina or ply within the laminate, and different combinations of composite materials are some of the important factors which affect the response of the composite laminate under loads. The flexibility in producing different composite materials mainly depends upon the combination of these factors in an optimum way. Different theories are available in the literature to study the behaviour of composite structures under load. The most commonly used theories are classical lamination theory, first order shear deformation theory, and higher order shear deformation theory. All these theories require a complicated computer programme in MATLAB, C++, and FORTRAN to determine the deflection and three-dimensional stress and

strain of a composite structure. Solving the complicated equations of composite materials using the above theories requires high programming skills and strong mathematical foundations. Finite element analysis (FEA) software such as ANSYS, ABAQUS, etc., is the most efficient and robust tool for advanced modeling and analysis. This software package can solve a variety of problems, from linear static analysis to nonlinear dynamic analysis, easily. These software packages provide a variety of analysis modules along with geometric modeling and visualization of results in color code. As a result, this software may be useful in a larger platform for composite laminate design and manufacturing [2].

The Finite element analysis (FEA) software is divided into four phases: pre-processor, processor, solution, and post-processor. In the preprocessing phase, an FEA model is built up by defining the geometry, material properties, and element type. The model is then divided into a number of sub domains called elements. Load and boundary conditions may also be applied at this stage. In the processor phase, the stiffness matrices and force vectors are computed based on the information provided in the preprocessor phase. In the solution phase, load and boundary conditions are applied if they are not applied in the preprocessor phase, and matrices are solved using the loads and boundary conditions. In the post-processing phase, results are viewed in terms of displacement, stress, and strain in different color codes. Since FEA software uses numerical methods to solve the equations, the results that are obtained are an approximate solution to the problem. The failure of a composite structure is a complicated phenomenon since the whole laminate does not fail at the same time. Failure takes place in a progressive way. It happens that, due to an increase in load, the first ply fails but the other plies in the laminate continue to take the load. Due to a further increase in load, the next ply fails, and it continues till all the plies fail. To accurately predict these complex failure mechanisms of composite laminate, reliable analysis tools are required that can integrate failure theories and damage propagation methodologies.

Here in this thesis, static analysis of different types of composite structures under different loadings and boundary conditions is carried out by semi-analytical methods and finite element methods (2 dimensional finite element model) using available commercial software (ANSYS 15.0).

1.2 Objective of the present research work

A comparative study of different semi analytical methods (Classical Lamination Theory & First order shear deformation theory) and finite element method (using Finite element software, ANSYS 15.0) is conducted for different laminated composite structures (Plate and beam) from simpler to complex problems under different loadings and boundary conditions. The objective of the study is to find out the variation of percentage error which is the difference of the results obtained from the above two methods with respect to the semi analytical method, from simple problems to the complex problems and to find out the reasons behind the percentage error. The percentage errors are also determined for composite structure problems by changing the different design variables of composite material such as orientation angle, thickness of laminate, number of lamina, length to thickness ratio, length to width ratio and size of mesh. Mesh size can be neglected by convergence analysis. The objective is to find out the dependencies of these design variables on percentage error by statistical methods and how to reduce the percentage errors by changing these variables. Due to assumptions in solving the equations, both semi-analytical and FEA software give approximate solutions to the problems. As the complexity of the problem increases, the higher order terms also increase. Therefore, to solve the equations, certain assumptions are made, which introduces the error. The relationship of percentage error with design variables is found out by regression analysis, to establish the dependency by mathematical form.

To conclude the objective of the thesis is to study the different semi analytical methods for solving different problems of laminated composite structures and analysis of 2 D finite element model of those problems. To study the percentage errors obtained by comparing the results from different semi analytical methods with finite element methods by varying different design variables evaluate the dependencies of the percentage error and proposed way to reduce them. Finally this study may be helpful in having an idea of the solution of laminated composite problem by using finite element software easily by following few steps rather than writing complex programme in mathematical tools for solving problem by semi analytical methods.

1.3 Plan of the present research work

A comparative study of semi analytical method and finite element method is conducted for different laminated composite structure from simpler to complex problems. Finite element analysis is done using a two dimensional finite element model. Percentage error is the percentage difference of the results obtained from the two methods i.e. Percentage error is the difference of the results obtained from semi analytical method and finite element method with respect to semi analytical method. The angle between the lamina coordinate system (1-axis) and laminate coordinate system (x-axis) is called orientation angle " θ " (fig 2.3). Percentage error between the results from semi analytical and finite element model is determined for different problems of laminated composite structure under different boundary conditions and loadings. Two types of laminated composite structure are studied: Laminated composite Plate and beam. Two types of stacking sequence of laminate are studied: symmetric angle ply and symmetric cross ply. Problems discussed in this thesis as:

1. Laminated composite plate under in-plane loads (simplest problem)
2. Simply supported laminated composite plate under transverse uniform pressure.
3. Buckling of simply supported laminated composite plate under compressive load.
4. Laminated composite beam under different boundary conditions (Hinged-hinged, Clamped-clamped, fixed-fixed) subjected to uniformly distributed loads.
5. Hybrid composite laminated structure under different loads and boundary conditions.

The problems of Laminated composite plate under in-plane load is solved by laminate equations whereas for simply supported plate under transverse loading is solved by classical lamination theory and the equations obtained from this theory is solved by Navier method and Rayleigh Ritz method. The problems of laminated composite beam under different boundary condition subjected to different loading conditions are solved by Classical lamination theory (CLT) and first order shear deformation theory (FSDT). The objectives of this thesis are as:

1. Deflection, stress and strength ratio based on first ply failure load for the above problems are found out by semi analytical methods and finite element method using FEA software ANSYS 15.0.
2. The percentage error of deflection and failure load are found out by comparing the results obtained each by classical lamination theory and first order shear deformation theory with

the results obtained by analyzing 2 dimensional laminated composite static structure by using FEA package ANSYS 15 for different types of loads (i.e. point load, uniformly distributed load etc.) and boundary conditions (simply supported, cantilever, fixed etc.)

3. Orientation angle is the angle between Lamina coordinate system and Laminate coordinate system. Fibers are aligned along the lamina coordinate system. Whereas for laminate, a number of lamina are stacked or arranged (symmetrically, anti symmetrically, cross ply etc. arrangement) one upon the other in a sequence called **laminate stacking sequence**. In case of laminate keeping the laminate stacking sequence constant (for eg. for symmetric arrangement $[+\theta/-\theta]_s$), orientation angle ' θ ' can be changed which is done in the thesis. The effect of orientation angle, thickness of laminate, number of lamina, length to thickness ratio and length to width ratio on percentage error are studied. The significance of these factors on percentage error is studied by statistical method: ANOVA and relationship between them is established by regression analysis.
4. The analysis is further extended to study the effect of these factors on deflection and strength ratio based on first ply failure load.
5. A comparative study of different failure criteria is conducted based on first ply failure load. Mode of failure is determined by maximum stress or maximum strain theory.
6. The effect of hygro thermal load on strength ratio for composite laminate and beam is studied.
7. This study is further extended for analysis of hybrid composite laminate, which is a combination of lamina of different material arranged in a particular order. In this thesis, two composite materials are considered, graphite/epoxy (G) and glass/epoxy (C) composite. The problem of hybrid composite structure (Plate and beam) under different loads (plane tensile load and simply supported) is solved by classical lamination theory and finite element method using ANSYS. The reason behind the difference in the results of semi analytical method and finite element method is discussed and the probable way to reduce them is also discussed.
8. In this thesis two dimensional finite element model of laminated composite structure is used to solve the problem.

1.4 Outline of the thesis

Chapter 1 gives a brief description of the history and evolution of composite materials. It gives a brief description of FEA software and its modules. This chapter also provides a brief description of the objective of the thesis.

Chapter 2 provides a brief description of the basics, properties, classification, advantages, disadvantages, and applications of composite materials. It gives a brief description of the manufacturing of composite materials. It provides a brief literature review of research work on analysis of laminated composite plate and beam by different semi analytical and finite element methods for different loads and boundary.

Chapter 3 presents the constitutive equation of lamina, Hook's Law in 3D and 2D form. The equations of each lamina are combined to give the constitutive equations of the laminate. It shows the calculation of the ABD matrix (laminate stiffness).

Chapter 4 gives a brief description of the finite element method and its steps. It explains the basic steps of the analysis of a laminated composite structure in the FEA software ANSYS using two dimensional finite element model.

Chapter 5 discusses the stress analysis of lamina and laminate under in-plane load by classical lamination theory (CLT). The CLT model is compared with a 2 Dimensional FEM model built using FEA packages ANSYS 15.0. The results obtained from both methods are compared and discussed.

Chapter 6 discusses the bending of simply supported laminated plates under uniform transverse load. The deflection equation is solved by the Navier method and the Rayleigh-Ritz method. The FEM model of the plate is compared with the Navier and Rayleigh-Ritz models and percentage errors are calculated. The effect of stacking sequence, number of plies, and length to thickness ratio on deflection is studied. This chapter discusses the effect of orientation angle, thickness, length to width ratio, and mesh size on the percentage error for laminated composite plates under uniform transverse load. It also discusses the significance of these factors on percentage error by statistical method and establishes the relationship between them by regression analysis. This chapter also presents the buckling analysis of laminated composite plates, and a comparison of the results of FEM and semi-analytical methods is made. This

chapter also discusses the effect of fiber orientation angle and the number of the lamina on buckling load.

Chapter 7 discusses the bending of laminated composite beams using CLT and FSDT. This chapter also discusses the FEM model of the beam and compares the FEA software results with those of the CLT and FSDT, and percentage errors are noted. This chapter discusses the effect of orientation angle, boundary condition, length to thickness ratio, and the number of the lamina on the deflection of a beam. This chapter discusses the effect of orientation angle, thickness, length to width ratio, and mesh size on the percentage error for laminated composite beams under uniform transverse load. It also discusses the significance of these factors on percentage error by statistical method and establishes the relationship between them by regression analysis.

Chapter 8 describes the methodology to determine the strength ratio and first ply failure load of laminated composite plates and beams by both semi-analytical methods (CLT) and FEM using FEA software ANSYS under different boundary conditions and loadings. The results from both methods are compared and the percentage errors between the two methods are calculated. Different failure criteria are studied and compared. The mode of failure is studied. This chapter also investigates the effect of orientation angle, the number of lamina, and length to thickness ratio on the strength ratio. It also studied the strength ratio for different boundary conditions and loadings. This chapter also describes the effect of thermal and hygro-thermo-mechanical loads on the strength ratio and first ply failure load for different orientation angles and thicknesses.

Chapter 9 discusses hybrid composite laminates under in-plane tensile load by classical lamination theory (CLT). The semi-analytical method's results are compared to those obtained using finite element software. In this chapter, strength ratios are calculated for different combinations of hybrid composites by Tsai-Wu and maximum stress criteria. A comparative study of the deflection, strength ratio, cost, and mass of graphite epoxy and glass epoxy composite beams for different boundary conditions is discussed in this chapter.

Chapter 10 gives the conclusion of the present work and a detailed discussion of the outcome of the present research. Chapter 11 discusses the future scope of the present research.

CHAPTER 2

THEORY AND LITERATURE REVIEW

Outline of Chapter: 2.1 Composite material basics, 2.1.1 Applications, 2.1.2 Advantages and limitations, 2.1.3 Classification of Composite material, 2.1.4 Fibers and Matrix, 2.1.5 Lamina and Laminates, 2.1.6 Coordinate System, 2.1.7 Laminate Lay up, 2.1.7.1 Symmetric laminate, 2.1.7.2 Anti symmetric Laminate, 2.1.7.3 Balanced Laminate, 2.1.7.4 Angle ply laminate, 2.1.7.5 Cross ply laminate, 2.1.7.6 Hybrid laminate, 2.1.7.7 Sandwich laminate, 2.1.8 Manufacturing of Fiber-Reinforced Composite Materials, 2.2 Literature Review, 2.3 Closure

2.1 Composite Material basics

A composite material is defined as a new material that is composed of two or more existing materials combined at the macroscopic level and is not soluble in each other. The property of the newly formed material is superior to its constituents and, in some cases, possesses a property that neither of its constituents possesses. One of the constituents is called the reinforcing phase (fibers, particles, or flakes) and the other in which it is embedded is called the matrix phase, which is generally continuous. Fibers usually have high strength as compared to the matrix. The matrix holds the fibers in place and at proper orientations. The behaviour of the composite material depends upon the orientation of fibers in the matrix. The advantages of composite materials are high strength, stiffness, corrosion resistance, strength-to-weight ratio, stiffness-to-weight ratio, low specific gravities, fatigue damage tolerance, noncorrosive behavior, chemical resistance, temperature-dependent behavior, and impact resistance. Examples of composite materials are glass-epoxy, where glass fibers are reinforced in an epoxy matrix, graphite-epoxy, boron epoxy, etc.

2.1.1 Applications

Composite materials find wide application in many industries, such as the aerospace industry, marine, sports applications, and the automotive industry. The composite material is highly suitable for military and civil aircraft such as Boeing 777 and Airbus A380 due to its high stiffness and strength and low weight properties. They also find wide use in making automobile parts like leaf springs and propeller shafts. Sandwich structures and composites such as carbon

and glass fiber composites are widely used in the construction of ship structures. Graphite composites are used to make light-weight, extremely stiff aerospace structures and optical instruments. Carbon composite finds application in power generation in manufacturing the blades of wind turbine generators. Composite materials are also widely used in offshore oil drilling installations such as drilling risers and biomedical fields such as prosthetic devices and artificial limbs. They are also used in making entertainment products such as bicycles, tennis/badminton rackets, golf balls, finishing poles, skis, etc. Recently, the development of composite materials can be found in the field of infrastructure application also. They are used to produce structural members for buildings and bridges. An example of such a long cable-stayed composite foot bridge, 114m long, is found in Aberfeldy, Scotland [1]. Glass/polyester composites are used to make deck structure rails and A-frame towers. They are also used to make pipelines for the transport of oil and water.

2.1.2 Advantages and limitations

Composite materials have high strength-to-weight ratios (specific strength ratios) and stiffness-to-weight ratios (specific weight ratios), and they offer excellent resistance to corrosion, chemical attack, and outdoor weathering. Though the cost of raw materials such as fibers, resins, etc. and manufacturing processes of composite materials is high, they help to reduce the cost of acquisition and life cycle cost of products through savings in weight, lower maintenance, tooling costs, and the number of assembly operations and parts. Composites have a long fatigue life and can be easily maintained and repaired.

The design and manufacturing of composite materials is a challenging task, and the behaviour of composite materials is less predictable. Monitoring the structural health of composite materials is much more difficult than metals. Also, testing of compositing materials through non-destructive tests is also difficult as compared to metal. Composite materials absorb moisture, which affects their properties and dimensional stability. Another disadvantage of composite materials is de lamination, which is the de bonding of one layer from another.

2.1.3 Classification of Composite material

Most manmade composite materials are generally made from two materials. One material is called the reinforcing phase, i.e., fibers, and another material is called the base material, i.e., matrix. Composite materials are generally divided into three categories:

1. Fibrous composite: It consists of fibers of one material embedded in matrix of another material. Fibrous composite is of two types:
 - (a) Discontinuous or short fiber composite which contains short fibers, Nano tubes, or whiskers as the reinforcing phase. Examples of such a composite are Nano composite reinforced with carbon Nano tubes.
 - (b) Continuous –fiber composite which contains long continuous fibers as the reinforcing phase. Continuous fibers can be arranged all parallel (unidirectional) or at right angle to each other (cross ply) or it can be oriented at different direction (multi direction) in the matrix.
2. Particulate composites: It consists of particles of different sizes embedded in the matrix. An example of such a composite is concrete reinforced with mica flakes.
3. Laminated composite: It consist of layers of different or same material including composite of first two types bonded together.

2.1.4 Fibers and Matrix

Fibers are stiffer and stronger than the matrix. There may be short fibers or long continuous fibers. The strength of a fibrous composite mainly depends on the strength of the fibers. Short fibers have better strength than long fibers. The fibers carry between 70 and 90 percent of the load. Fibers provide stiffness, strength, and thermal stability to the composites. The matrix material helps to keep the fibers together and transfers the load to the fibers. It also provides rigidity and shape to the structure and protects the fibers from chemical attack and damage. The mode of failure is affected by the type of matrix material and its compatibility with the fiber. Fig. 2.1 (a) shows the formation of a composite material using fibers and resin for continuous fiber composites, and Fig. 2.1 (b) shows the structure of continuous and short-fiber composites.

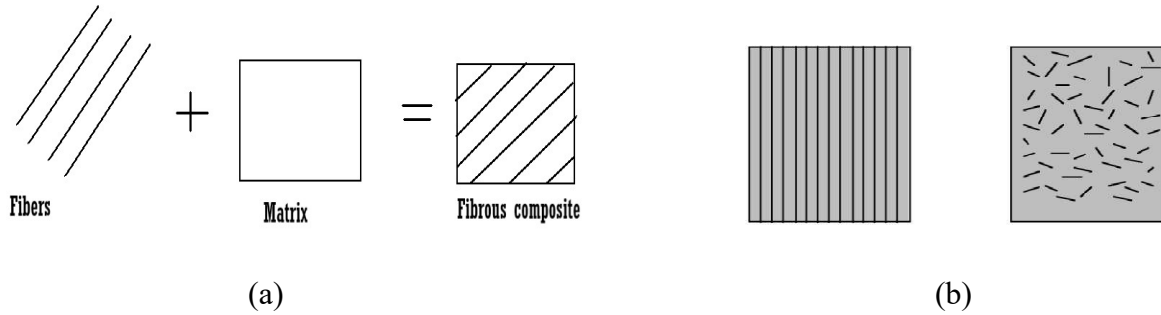


Figure 2.1 (a) Formation of a composite material using fibers and resin for Continuous fiber composite (b) structure of continuous and short fiber composites [1]

2.1.5 Lamina and Laminates

The basic building block of a laminated composite structure is a thin layer of very small thickness. A laminate is a collection of a number of such laminae, stacked in the direction of the lamina thickness in such a way that it can achieve the desired strength and stiffness. A lamination scheme, or stacking sequence, is the sequence of the orientation of fiber-reinforced composite lamina within the laminate. Fig 2.2 shows the stacking of lamina of different fiber orientation on above the other to form laminate. Here 0° , 90° shows the fiber orientation of each lamina with respect to laminate coordinate system (x axis), whereas lamina coordinate system (1-axis) is oriented along the fiber. The behaviour of a composite structure under loads such as deflection, failure load, and stress and strain depends upon the stacking sequence of the lamina within the laminate and the properties of the material of the lamina. But due to the mismatch between the properties of the material and the orientation of each lamina, shear stress developed between the lamina, which caused the layer to delaminate.

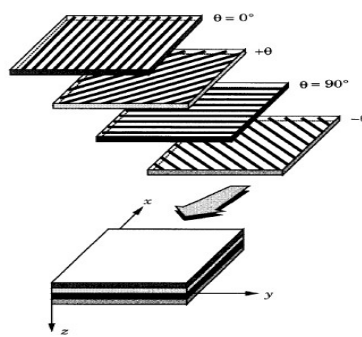


Figure 2.2 Laminate made up of lamina at different orientations [3]

2.1.6 Coordinate System

There are two coordinate systems used in composite material design. One is the lamina coordinate system, and another is the laminate coordinate system. In two dimensions, lamina coordinate system (or material coordinate system) is represented by 1, 2. Axis 1 is oriented along the fiber whereas axis 2 is on the surface of the composite and perpendicular to axis-1. Each lamina has its own lamina coordinate system aligned along the orientation of fiber in that lamina.

The laminate coordinate system (or global coordinate system) is represented by x, y which is common to all the laminas within the laminate. The angle between the lamina coordinate system (1-axis) and laminate coordinate system (x-axis) is called orientation angle " θ " (fig 2.3).

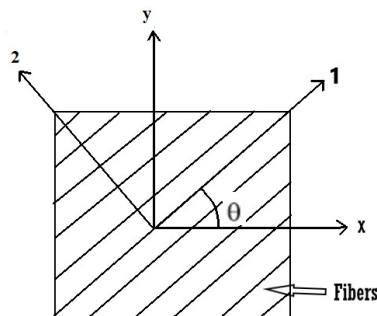


Figure 2.3 Lamina (1, 2) and Laminate (x, y) coordinate system [2]

2.1.7 Laminate Lay up

Based on the design criteria of composite structure, a laminate may have a specific layup or arrangement of ply within the laminate. Laminate layup means the orientation of fibers in the matrix of successive lamina within the laminate with respect to a coordinate system.

Each layer within the laminate can be defined by its location, material system, and orientation with respect to the reference coordinate system (x-y axis). Each lamina is represented by a number that defines the orientation of fibers in degree with respect to reference coordinate system separated by a slash or space, and the whole code of the laminate is within a bracket. Different arrangements of lamina are used for symmetric, anti-symmetric, cross ply and hybrid laminates. For symmetric arrangement suffix "s" and for anti-symmetric arrangement suffix "as" is used outside the bracket. Suffix "T" is used for total laminate. '+' and '-' are used for direction of fiber orientation angle. Laminate Layup code must specify the

orientation and direction of fibers in each ply relative to reference axis (x-y axis), number of ply, arrangement of ply (symmetric or anti symmetric) with respect to mid layer and type of material (in case of hybrid and sandwich laminate).

Table 2.1 Layup code for different composite laminate

Code	Description	Laminate lay up
[30/45/60 ₂ /0/90] _T	Total laminate	30
		45
		60
		60
		0
		90
[±30/+45/-45/60] _T	Total laminate	30
		-30
		45
		-45
		60
[90/45/0] _s	Symmetric layup	90
		45
		0
		0
		45
		90
[0/45/90] _s	Symmetric layup	0
		45
		90
		45
		0
[0 _{GR} /45 _{GL} /90 _{GR}] _s	Hybrid Laminate	0 _{GR}
		45 _{GL}
		90 _{GR}
		90 _{GR}
		45 _{GL}
		0 _{GR}
[±45] _s	Sym Angle ply laminate	45
		-45
		-45
		45

Code	Description	Laminate lay up
[0/90] _s	Sym Cross ply laminate	0
		90
		90
		0
[±45] _s	Anti symmetric laminate	45
		-45
		45
		-45
	Sandwich Laminate	Carbon/epoxy
		foam
		Carbon epoxy

2.1.7.1 Symmetric laminate

In symmetric laminate, the laminae of the same thickness, material, and orientations are arranged symmetrically with respect to the middle layer. For symmetric laminate bending-extension coupling $B_{ij} = 0$ [4]. For symmetric notation, subscript “s” is used outside the bracket and only half of the stacking sequence is given. For example, refer to table 1.

2.1.7.2 Anti symmetric Laminate

In anti symmetric laminate, pairs of laminae of the same material, thickness but with opposite orientation are arranged with respect to the middle layer. For anti symmetric laminate, $A_{16} = A_{26} = D_{16} = D_{26} = 0$. For example, [45/-45/45/-45] and [0/90/0/90] are anti symmetric angle ply and cross ply laminates respectively [4].

2.1.7.3 Balanced Laminate

In case of balanced laminate, the laminae are arranged in such a way that for every $+\theta$ lamina, there is another $-\theta$ lamina of the same thickness and material. For balanced laminate A_{16} and A_{26} is always equal to zero.

2.1.7.4 Angle ply laminate

Angle ply laminate has laminae oriented at $\pm\theta$ of same material and thickness. For symmetric angle ply laminate, $A_{16} = A_{26} = 0$, $B_{ij} = 0$ and for anti symmetric laminate, $A_{16} = A_{26} =$

$D_{16} = D_{26} = 0$. For example $[45/-45/-45/45]$ and $[0/90/90/0]$ are symmetric angle ply and cross ply laminate respectively.

2.1.7.5 Cross ply laminate

Cross ply laminate has laminas oriented at 0 degree and 90 degree. For cross ply laminate $A_{16} = A_{26} = D_{16} = D_{26} = \overline{Q}_{16} = \overline{Q}_{26} = H_{45} = 0$. Cross ply laminate may be symmetric or anti symmetric.

2.1.7.6 Hybrid laminate

Hybrid laminate composed of laminas of different materials oriented with respect to middle layer. Example of hybrid laminate is shown in table 1.

2.1.7.7 Sandwich laminate

It is a special type of composite that is made of two thin face sheets and a lightweight, thicker, and low-stiffness core. Face sheets may be made from composites and metals, whereas the core is made of metallic or non-metallic honeycomb, cellular foams, wood, etc. They are suitable for lightweight structures with high in-plane and flexural stiffness [1].

2.1.8 Manufacturing of Fiber-Reinforced Composite Materials

The manufacturing process is the most important step in the design and application of composite materials. A variety of fabrication processes for composite materials are available, which depend on the type of matrix and fibers, their curing temperature, and cost-effectiveness. Some of the manufacturing processes are autoclave molding, filament winding, pultrusion, and resin transfer molding. The first manufacturing technique is hand lay-up (fig 2.4 a), which is a simple and widely used technique. In this method, dry fibers in the form of woven, knitted, stitched, or bond fabrics are first manually placed in the mould, and then a brush is used to apply the resin matrix on the reinforcing material.

The general fabrication process follows the following operations [4]:

1. Placing the fibers in predetermined orientations
2. Impregnation of fibers in the matrix (resins).
3. Consolidation of the impregnated fibers to remove excess resin, air, etc.
4. Cure and extraction of the mold.
5. Finishing operations

Another method of composite manufacturing is the open mold process with spray-up of chopped fibers, which is used for prototype fabrication. A great development in the composite fabrication field occurred with the development of "prepreg" tape. It is a tape composed of fibers pre-impregnated in resin. Autoclave molding is a process of composite manufacturing for fabrication with prepreg tape. This process is widely used for high-quality, complex parts. Filament winding technology (fig 2.4b) is widely used to produce composite structures that have a body of revolution, such as pipes, pressure vessels, shafts, etc. This technique involves the winding of resin-coated fibers onto a rotating mandrel. Other manufacturing techniques include bag molding, compression molding, and resin transfer molding. As compared to conventional material fabrication, composite manufacturing involves, to some extent, highly skilled hand labor with limited automation and standardization. This makes composite manufacturing costly with complex quality control procedures.

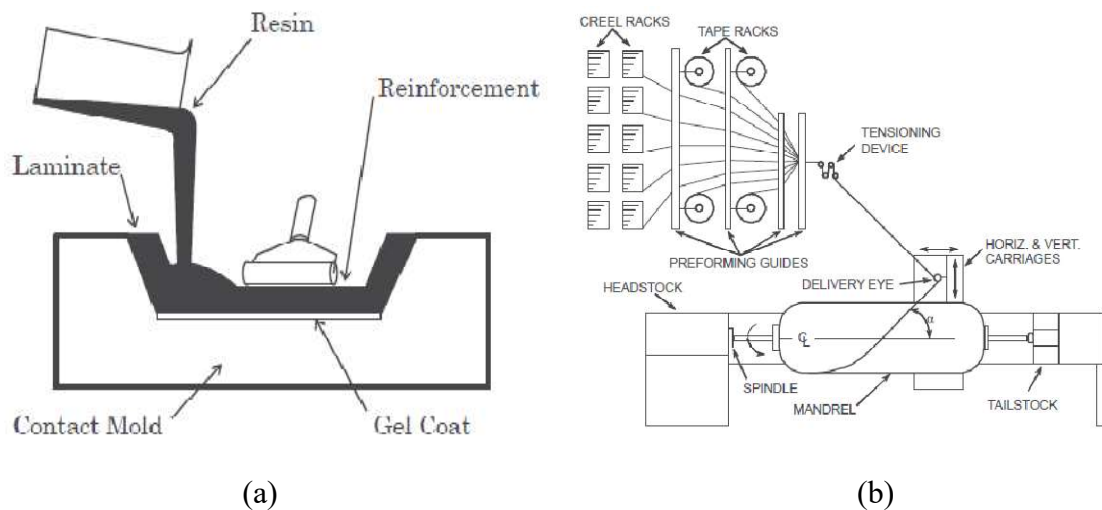


Figure 2.4 Composite manufacturing technologies (a) Hand layup (b) Filament winding [4]

2.2 Literature Review

Unlike conventional materials, the behaviour of composite materials is complex because they are composed of many layers of different or same thickness, materials and orientation stacked together. The behaviour of composite materials depends upon the thickness, orientation of fibers, stacking sequence, and materials of each ply.

Therefore, many types of composite laminate can be obtained by possible combinations of different plies or laminas in the laminate. All the plies are glued together. The study of their

behaviour is complicated because delamination of the ply can occur under high heat and load. Due to the increase in thermal and or mechanical load, failure of the weakest ply can occur, which substantially reduces the strength of the laminate. So it is very essential to study the deflection and stress-strain relationship of composite laminates under load.

Composite structure problems subjected to different loadings and boundary conditions can be solved by classical lamination theory, first-order shear deformation theory, etc. But these methods are not sufficient to provide the exact solution when complex geometries, arbitrary boundary conditions, or nonlinearities are introduced. So, for solving complex problems, approximate results are considered. The finite element method is one such technique that provides an approximate solution to a complex or simple problem by using a numerical method. As a result, the finite element method can be formulated using either computer programming in MATLAB, C++, Fortran, and so on, or by using pre programmed commercial FEA packages such as ANSYS, ABAQUS, and so on.

There are several theories available for analyzing transverse deflection, stress, and strain of composite plates and beams: classical lamination theory, first-order shear deformation theory, higher-order shear deformation theory, Zig-zag theory, and layer-wise lamination theory. B.N. Pandya et al. [5] presented a C^0 continuous displacement finite element model of a higher-order theory to determine the flexure of thick laminated composite plates subjected to transverse loads. The element used for finite element formulation is a nine-noded quadrilateral with nine degrees of freedom per node, and this method eliminates the use of shear correction coefficients. Kam T.Y et al. [6] used a total Lagrangian finite element formulation which is based on the assumptions of Von Karman and first order shear deformation theory to perform the reliability analysis of laminated composite plate structures subjected to large deflections. Han Wanmin et al. [7] used the hierarchical finite element method to study the geometrically nonlinear analysis of laminated composite rectangular plates.

C. Sridhar and K.P Rao [8] introduce a 48 d.o.f., four-node quadrilateral shell finite element for solving large deformation problems of circular composite laminated plates, and the Newton-Raphson method is used to solve this non-linear problem. This method can handle both symmetric and unsymmetrical lay-up schemes. They can also be used to estimate the failure rate of composite plates caused by low-velocity impacts. M. Ganapathi et al. [9] used a new

eight-node C^0 membrane plate quadrilateral finite element which is based on the Reissner–Mindlin plate theory for the analysis of large deflections for static and dynamic problems of thick composite laminates, including buckling problems and the effect of coupling of membrane plate. G.Bao et al. [10] present an analytical solution for the buckling and bending of rectangular thin plates for different boundary conditions under in-plane compression and out-of-plane pressure loads, respectively, and the solutions are compared with finite element solutions. They used an orthotropic rescaling technique to simplify the solution. K.Y. Sze et al. [11] introduce predictor-corrector methods for the analysis of laminated composite plates using Mindlin finite element models without using shear correction factors. The new procedure was tested by using first, second, and third-order Mindlin nine-node plate elements. For the linear analysis of thin and thick laminates, Y.X. Zhang et al. [12] proposed a 4 node 20 DOF, RDKQ-L24 displacement-based quadrilateral element, and a 24 node 24 DOF, RDKQ-L24 displacement-based quadrilateral element based on first order shear deformation theory (FSDT). For analysis of geometrically non-linear problems, they [13] proposed the displacement-based 3-node, 18-degree-of-freedom flat triangular shell element LDT18, which is based on FSDT. A geometrically nonlinear approach is used to formulate the element for geometrically nonlinear analysis. The deflection and rotation functions are determined based on Timoshenko’s beam theory. Y.X. Zhang and C.H. Yang [14] present a review paper on recent developments from 1990 to future in finite element analysis of free vibration and dynamics, buckling and post-buckling, geometric nonlinearity and large deformation, and failure and damage analysis problems of composite laminated plates based on the various laminated plate theories. Mauricio F. Caliri Jr. et al. [15] reviewed over 100 papers on plate and shell theories of laminated structure and explained the coupling between plate and shell theory. They also help to set a new platform for new theories and solution methods for laminated and sandwich structures. They also explained how the finite element method can simplify the complex analysis. Chalida Anakpotchanakul and Pongtorn Prombut [16] studied the influence of the aspect ratio on vibration and bending analysis of T300/934 composite laminates with a symmetric stacking sequence of $[0/90/0/90/0]$ s. Classical Laminated Plate Theory (CLPT) is used to model the bending and vibration behaviour of composite laminates, and the results are verified with a finite element model. They also studied the composite cantilever beam with different stacking sequences.

In the early 18th century, Euler and Bernoulli formulated the classical beam theory to describe the nature of the deflection of a laminated beam. This theory was modified later by Timoshenko by considering transverse shear deflection in the bending equation. Reddy proposed a third-order theory [3] that takes quadratic variation in shear strain into account. Third order theory provides an increase in accuracy in solution relative to FSDT since it eliminates the shear correction factor of FSDT. K.H. Lo et al. [17] proposed a higher order theory for the deformation of plates. Deepak Ku. Maity et al. [18] presented a higher-order shear deformation and a first-order theory to perform a finite element analysis of the bending and free vibration of laminated composite beams using nine-noded isoperimetric elements. They also studied the effects of fiber orientation angle, stacking sequence, length-to-thickness ratio, and boundary condition on the non-dimensional deflections, stresses, and fundamental frequencies of a laminated composite beam. Hemendra Arya et al. [19] present a zigzag model for a symmetric laminated beam. Sine and cosine term was used to represent the non-linear displacement and transverse shear stress and strain across the thickness of the beam. The results obtained from the model were very accurate for displacement and stresses of symmetric cross-ply laminated beams, even for small length to thickness ratios. Many papers are available on the analysis of laminated composite beams for different boundary conditions, materials, sections, and fiber orientations. Masoud Tahani [20] adapted two theories to analyse laminated beams. One is the layer wise laminated plate theory, and the other theories are simpler theories such as CLT, FSDT, and HSDT. Equations of motion are obtained by using Hamilton's principle. Borkar et al. [21] performed bending analysis of a simply supported composite beam by using refined beam theories that account for the parabolic variation of shear strain through the depth of the beam, thus eliminating the use of a shear correction factor. Mohammed Fahmy Aly et al. [22] studied the effects of fiber orientation and laminate sequences on the torsional natural frequencies of laminated composite beams of doubly symmetrical cross sections by classical lamination theory, which takes into accounts the coupling of flexural and torsional modes. Also, they studied the torsional vibrations of the laminated beams by the shear deformation theory, considering the shear deformation effects. The results obtained by FEM package ANSYS 10, classical lamination theory, and shear deformation theory are used to predict the effects of fiber orientation and layer stacking sequence on the torsional frequencies of the beams. Trung-Kien Nguyen et al. [23] present a new analytical solution based on a

higher-order beam theory for the static, buckling, and vibration of laminated composite beams for different boundary conditions. Lagrange's equations are used to derive the governing equations of motion. The equations are solved by trigonometric series, which satisfies various boundary conditions. Atteshamuddin S. Sayyad et al. [24] present a review article on the bending, buckling, and free vibration of laminated composite and sandwich beams. Atilla and Emrah et al. [25] present a static analysis of a laminated composite beam based on higher order shear deformation theory. They used a mixed finite element method, obtained by using the Gâteaux differential, to solve the problem. Krishna Chaitanya et al. [26] developed an analytical method for the analysis of inter-laminar stress of laminated composite I-beams. A finite element model is created using ANSYS 15 to compare the results obtained analytically. Nivedan Pandey et al. [27] studied the static behavior of a laminated composite beam subjected to transverse loading using the finite element method which is established by using higher order shear deformation theory (HSDT). The results are compared with available literature and finite element software, ABAQUS.

Buckling is the loss of stability of a structure due to geometric effects, leading to failure if the resulting deformations are not restrained. The minimum load at which the equilibrium condition of the plate is disturbed is called the critical buckling load. Studies on buckling analysis of hybrid and sandwich composite plates under compressive load are few. Joshi & Biggers [28] studied the effects of transverse shear stiffness on the optimum design of composite laminated plates and also determined the optimum buckling load for different width/thickness ratios. They show the improvement in buckling load by optimizing the thickness. A semi-analytical method based on the principle of virtual work and the Kantorovich method is used by Shufrin et al. [29] for the analysis of pre-buckling and buckling behaviour of laminated rectangular plates with a variety of boundary conditions and various combinations of the in-plane shear, compressive, and tensile loads. The results are compared with published literature and finite element analysis. In their paper, Lakshmi Narayana et al. [30] studied the effect of square and rectangular cut outs on the buckling load of a 16-ply laminated composite plate subjected to a linearly varying in-plane compressive load. They also find out the effect of plate aspect ratio, length to thickness ratio, and boundary conditions on the laminated composite plate under the above-stated load. Volkan Kahya [31] studied buckling behaviour of laminated composite beam using finite element method for different boundary condition and

stacking sequence and the results are compared with published literature. Many researchers work on the buckling, pre buckling and post buckling analysis of laminated composite structure using a variety of methods like digital image correlation technique, Koiter's approach, NURBS iso geometric finite element method, shear deformable finite element model [32,33]. The first ply analysis of laminated composite structure with variety of boundary conditions and load, draw much attention in the recent years. Turvey, G.J [34-37] in their papers uses analytical method based on classical lamination theory for the analysis of first ply failure load of angle ply and cross ply symmetric or anti symmetric laminated composite plate. Reddy et al. [38, 39] introduces finite element method based on first order shear deformation theory to study the linear and non linear first ply failure load of laminated composite plate subjected to transverse load. S. Tolson and N. Zabaras [40] developed seven degree of freedom finite element model to determine the stresses in laminated composite plate subjected to complex loading. Using the stresses and based on failure theories, they determined first ply failure (FPF) and last ply failure (LPF) by a progressive stiffness reduction technique and found that the results show good agreement with experimental results. T. Y. Kam & T. B. Jan [41] developed a finite element model based on layer-wise linear displacement theory to study the first ply failure of a thick laminate composite plate. They compared the stress and displacement with experimental results and published literature. They also investigate the capability of the failure theories to predict the first ply failure load by comparing them with the experimental results. Flexural analysis of symmetric laminated composite beams was investigated by P. Subramanian [42] using a two-noded C^1 finite element of 8 d.o.f. per node, based on a higher-order shear deformation theory. Numerical results for simply supported, symmetric laminated composite beams, loaded equally at the top and bottom surfaces of the beams, were compared with available literature by Pagano. A.K. Onkar et al. [43] predict the statistics of first-ply failure of laminated composite plates with random material properties under random loading using a stochastic finite element method solved by layer wise plate theory. The analytical solution was obtained by using Kirchhoff–Love plate theory, and the first-ply failure load was computed by using Tsai-Wu and Hoffman criteria, as well as a first-order perturbation technique was used to find the mean and variance of failure statistics. The solutions from the finite element method are compared with those obtained from the analytical method. Y.X. Zhang and H.S. Zhang [44] developed a multiscale nonlinear finite element modelling

technique using a 4-node, 24-DOF shear-locking free rectangular plate element. They proposed a micromechanical elastic–plastic bridging constitutive model to study the behaviour of composite laminates. M. Meng et al. [45] formulate a 3D finite element model to study the effect of fiber layup on the initiation of failure of laminated composites in bending. They used the Tsai-Wu failure theory to determine the mode of failure of a laminated composite for different stacking sequences. The 3D FEA showed that the transverse normal and in-plane shear stress are significant in the angle ply and cross ply laminates, respectively. The analytical results are compared with the FEA. Ever J. Barbero and Mehdi Shahbazi [46] studied a method to determine the material parameters used by the progressive damage analysis material model (PDA) in ANSYS. Their method is based on fitting the results obtained from PDA experimental data by using Design of Experiments and Direct Optimization. They also studied mesh sensitivity by using p- and h-mesh refinement. The proposed PDA method may be used to study the damage response of their lamination process. A detailed review in the field of applications of the finite element method in the failure analysis of laminated glasses was done by Meenu Teotia and R.K. Soni [47]. They also review different modelling approaches like equivalent single layer theories, layerwise theories, zig-zag models, and finite element techniques such as erosion, cohesive zone, etc. to understand the fundamental concept of FEA in failure analysis. Dhiraj Biswas and Chaitali Ray [48] studied the first ply failure analysis of hybrid laminated plate panels subjected to transverse static load. They fabricated hybrid laminates in the laboratory by combining carbon and glass fiber with epoxy resin and tested the hybrid laminates (CFRP and GFRP) with all edges fixed and subjected to transverse static load. They developed a higher-order zigzag theory to analyse the inter laminar stresses of laminated composites using an improved eight-noded quadratic iso parametric element. The finite element model is compared with published literature and experimental results. M. Patni et al. [49] investigated 3D stress fields, based on the Unified Formulation, that account for geometric nonlinearity in laminated composites for predicting the failure load. The modelling approach uses the hierarchical Serendipity Lagrange finite elements, which include high-order shear deformation and local cross-sectional warping. The failure mode determined by this method matches well with experimental values. Ravi Joshi et al. [50] studied the ply-by-ply failure load of anti-symmetric and symmetric angle-ply and cross-ply laminated plates with simply supported and clamped edges. Different stress-based failure theories were used on composite

plates subjected to uniformly distribute transverse load. The failure load is determined by writing a computer programme in FORTRAN based on the finite element method using an eight-noded element having seven degrees of freedom at each node. The results are validated with published literature. They also studied the effect of the stacking sequence on the failure load. Many researchers investigate the failure behaviour of composite structures under a hygro-thermal environment. They studied the effects of temperature and moisture on the failure analysis of composite structures. Through a hygro-thermal model, Jianyu Zhang et al. [51] studied the failure of composite structures in hygro-thermal environments. This model uses a constitution equation using hygro-thermal strain. They solved the progressive failure model by formulating a subroutine incorporating the hygro-thermal effect in the FEA package ABAQUS and the results were compared with experimental values.

Manahan [55] presents the deflection of simply supported, symmetrically laminated composite plates subjected to a uniformly distributed load by using classical lamination theory and the finite element method. The FEA software ANSYS was used to model and perform analysis on the plate of a 4-ply composite plate by the finite element method. The equations developed by using classical lamination theory were solved by the Navier method in the MATLAB platform. Both methods were compared, and the percentage error was found. Errors were minimized by changing the orientation and increasing the number of plies. Kenneth Carroll [56] discussed the deflection of a simply supported plate under uniform pressure applied to the surface for both symmetric angle ply and cross-ply laminated plates. Two methods were used to solve the equations developed using classical lamination theory. He used the Navier method for cross-ply laminates and the Rayleigh-Ritz method for angle-ply laminates. The results were compared with the deflection results of an aluminum plate. Results were compared with the finite element modeling programme ANSYS, and a percentage error was noted, but he did not discuss the analysis of the error percentage. He analyzed different symmetric ply arrangements, ranging from four plies to sixteen plies. A failure analysis was also conducted. Qiao Jie Yang [57] studied the buckling of both simply supported and clamped edges plated subjected to uni axial compression load by CLT and FSDT and the results are compared with ANSYS and percentage error was noted.

There are numerous research works in the field of analysis of hybrid composite structures. Jin Zhang et al. [58] find the effect of stacking sequence on the strength of hybrid composites which are composed of materials of different strengths and stiffness. The author investigates the strength of hybrid composites, which are manufactured by using varying ratios of glass woven fabric and carbon woven fabric in an epoxy matrix by static tests like tension, compression, and three point bending. The results of the paper present that hybrid composite laminates having reinforcement of 50% carbon fiber give the best flexural properties where the carbon layers are arranged at the outside of laminate, and when the carbon and glass lay-up are arranged in the alternating fashion, it shows the highest compressive strength. M.M.W. Irina et al. [59] investigated the mechanical properties of three different arrangements of glass fiber hybrid composites (plain-woven and stitched bi-axial 45) and plain-woven carbon fiber. The hybrid composite panels were manufactured by Vacuum assisted resin transfer molding method. Experimental results show that mechanical properties such as tensile strength, flexural strength, and volume fraction of the $[CWW]_6$ arrangement, where C and W are weaved carbon fiber and glass fiber respectively, were superior. M. Akbulut et al. [61] minimize the thickness of laminated composite plate subjected to both in plane and out of plane loading by using a new variant of the simulated annealing algorithm. To investigate the influence of transverse shear deformation on the deflection and stresses of laminated composite plates subjected to uniformly distributed load, Krishna Chaitanya et al. [62] developed an analytical method for inter-laminar stress analysis of laminated composite I-beams by extending the applicability of lamination theory usually used at the laminate level to the composite structure level and the results are compared with FEA software ANSYS 15.

2.3 Closure

Most of the research is concentrated on the analysis of laminated composite plates and beams subjected to different loadings under different boundary conditions by different semi-analytical and finite element methods. Researchers compared the results obtained from both the methods and an error was found. But the study of the dependency of the error on different variables like orientation angle, mesh size, length to width ratio (aspect ratio) and thickness of the laminate is rare. Analysis of the error is very essential to determine the exactness of the results obtained from the semi-analytical methods. A study of the significance of the factors affecting the percentage error has not been done. In the present thesis, the deflection and stress of a

laminated composite structure subjected to various loadings and boundary conditions are determined by both semi-analytical methods and FEM, and then both the results are compared to find out the percentage error. The dependencies of the abovementioned variables on percentage error are studied. The statistical method is used to investigate the significance of these factors as well as the relationship between these factors and percentage error. The effects of orientation angle, the thickness of the laminate, and the number of ply on deflection, stress, buckling load, strength ratio, and first ply failure load is also studied in this thesis. The semi-analytical model is also used to study the deflection of hybrid composite structures and the effect of hygro-thermal load on the first ply failure load of hybrid composite structures.

CHAPTER 3

MACRO MECHANICAL ANALYSIS OF LAMINATE

Outline of Chapter: 3.1 Constitutive equation of lamina, 3.1.1 Hook's Law in 3D, 3.1.2 Hook's Law in 2 D, 3.2 Constitutive equations of Laminate, 3.2.1 Calculation of ABD matrix (laminate stiffness), 3.3 Closure.

1.1 Constitutive equations of Lamina

A lamina is a thin layer of composite material whose thickness is of the order of 0.125 mm. A laminate is built by stacking the lamina in a specific order. Design and failure analysis of laminated structures demand knowledge of stress and strain. Since laminate is constructed by stacking the lamina in the direction of the laminate thickness, knowledge of stress and strain on lamina is essential to studying the mechanics of laminate.

Lamina is made of isotropic homogenous fibers embedded in an isotropic homogenous matrix. Therefore, the modeling of lamina becomes complicated since the stiffness varies from point to point, which depends upon whether the point lies on the fiber, the matrix, or the interface of fiber and matrix. So the properties of lamina also vary from point to point, which makes the mathematical formulation difficult. For ease of analysis, lamina is considered homogenous and is analyzed based on the average properties of fiber and matrix. Though lamina is considered homogenous, its behaviour is different from that of isotropic homogenous material.

3.1.1 Hook's Law in 3D

Composite material is elastic in nature but is not isotropic. So it follows the Hook's law but the constant relating the stress and strain is many in number. 3D stress tensor in Cartesian coordinate is shown in fig 3.1. The stress and strain relation for general 3 Dimensional bodies in 1-2-3 Cartesian coordinate system is as follows:

$$\begin{bmatrix} \sigma_1 \\ \sigma_2 \\ \sigma_3 \\ \tau_{23} \\ \tau_{31} \\ \tau_{12} \end{bmatrix} = \begin{bmatrix} C_{11} & \cdots & C_{16} \\ \vdots & \ddots & \vdots \\ C_{61} & \cdots & C_{66} \end{bmatrix}_{6 \times 6} \begin{bmatrix} \varepsilon_1 \\ \varepsilon_2 \\ \varepsilon_3 \\ \gamma_{23} \\ \gamma_{31} \\ \gamma_{12} \end{bmatrix} \quad (3.1)$$

Where $[C]_{6 \times 6}$ is stiffness matrix which consists of 36 constants.

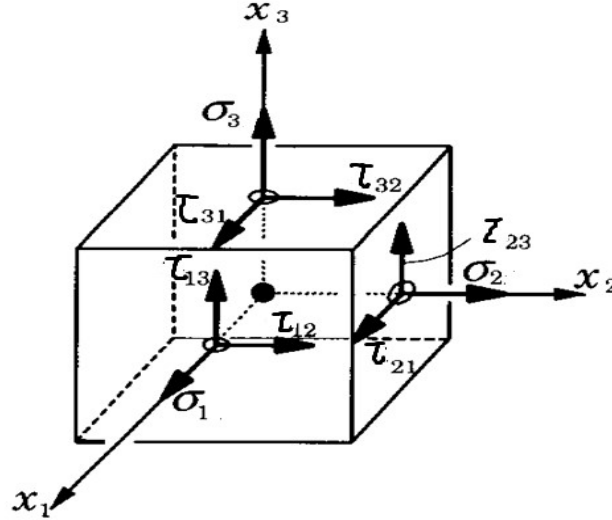


Figure 3.1 3 D Stress Tensor in Cartesian rectangular coordinate

3.1.2 Hook's Law in 2 D

Lamina is a thin member, so out of plane load is zero. Therefore it can be considered under plane stress problem. The upper and lower surfaces of the plate are free from external load, therefore $\sigma_3 = \tau_{31} = \tau_{23} = 0$ and $\varepsilon_3 = \gamma_{23} = \gamma_{31} = 0$. This assumption reduces the three-dimensional stress-strain equations into two-dimensional equations. A fig 3.2 shows 2 D stress tensor in Cartesian rectangular coordinate, where stress (in 1 and 2 direction) and shear stress is applied.

The stress- strains relations in 1-2 axes in 2 D form from Hook's law using the plane stress assumptions for unidirectional lamina [52]:

$$\begin{bmatrix} \sigma_1 \\ \sigma_2 \\ \tau_{12} \end{bmatrix} = \begin{bmatrix} Q_{11} & Q_{12} & Q_{11} \\ Q_{12} & Q_{22} & 0 \\ 0 & 0 & Q_{66} \end{bmatrix} \begin{bmatrix} \varepsilon_1 \\ \varepsilon_2 \\ \gamma_{12} \end{bmatrix} \quad (3.2)$$

Where $Q_{11} = \frac{E_1}{1-\nu_{12}\nu_{21}}$, $Q_{22} = \frac{E_2}{1-\nu_{12}\nu_{21}}$, $Q_{12} = \frac{\nu_{12}E_2}{1-\nu_{12}\nu_{21}}$, $Q_{66} = G_{12}$, $\frac{\nu_{12}}{E_1} = \frac{\nu_{21}}{E_2}$

Q_{ij} is called reduced stiffness coefficient.

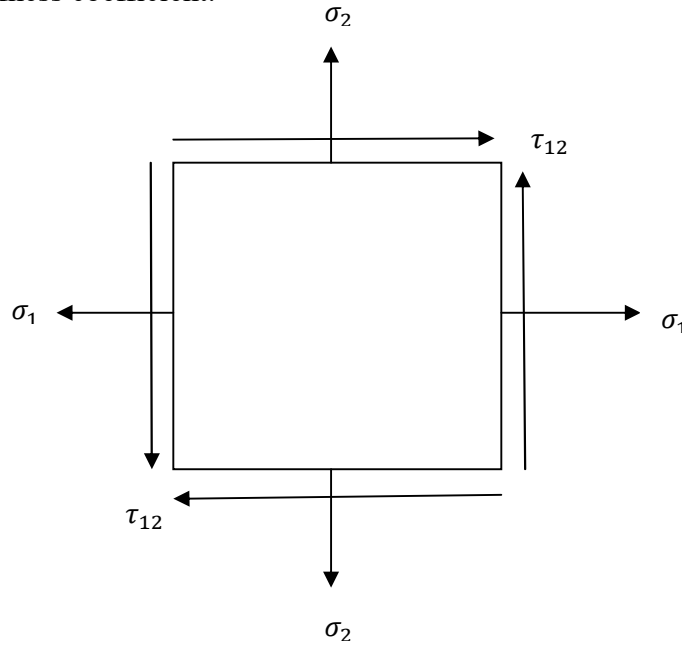


Figure 3.2 2 D Stress Tensor in Cartesian rectangular coordinate

Inverting the equation 3.2

$$\begin{bmatrix} \varepsilon_1 \\ \varepsilon_2 \\ \gamma_{12} \end{bmatrix} = \begin{bmatrix} S_{11} & S_{12} & S_{11} \\ S_{12} & S_{22} & 0 \\ 0 & 0 & S_{66} \end{bmatrix} \begin{bmatrix} \sigma_1 \\ \sigma_2 \\ \tau_{12} \end{bmatrix} \quad (3.3)$$

S_{ij} is the elements of compliance matrix.

Unidirectional lamina is weak in transverse direction. So laminae are placed at angle within the laminate. The coordinate system used for angle lamina: the axis in the 1–2 coordinate system is called the local axis or the material axes. The direction 1 is parallel to the fibers and the direction 2 is perpendicular to the fibers. The axis in the x – y coordinate system is called the global axis. The angle between the two axis is denoted by an angle θ (Fig 2.3). θ is called the orientation angle.

The relationship between stresses in x – y and 1-2 coordinate systems for angle lamina is given as [52]:

$$\begin{bmatrix} \sigma_x \\ \sigma_y \\ \tau_{xy} \end{bmatrix} = [T]^{-1} \begin{bmatrix} \sigma_1 \\ \sigma_2 \\ \tau_{12} \end{bmatrix} \quad (3.4)$$

Where $[T]$ is called the transformation matrix.

$$[T] = \begin{bmatrix} \cos^2\theta & \sin^2\theta & 2\cos\theta\sin\theta \\ \sin^2\theta & \cos^2\theta & -2\cos\theta\sin\theta \\ -2\cos\theta\sin\theta & \cos\theta\sin\theta & \cos^2\theta - \sin^2\theta \end{bmatrix} \quad (3.5)$$

The global stress can be calculated as:

$$\begin{bmatrix} \sigma_x \\ \sigma_y \\ \tau_{xy} \end{bmatrix} = [T]^{-1}[Q] \begin{bmatrix} \varepsilon_1 \\ \varepsilon_2 \\ \gamma_{12} \end{bmatrix} \quad (3.6)$$

The local strain can be calculated as:

$$\begin{bmatrix} \varepsilon_1 \\ \varepsilon_2 \\ \gamma_{12} \end{bmatrix} = [R][T][R]^{-1} \begin{bmatrix} \varepsilon_x \\ \varepsilon_y \\ \gamma_{xy} \end{bmatrix} \quad \text{And } [R] = \begin{bmatrix} 1 & 0 & 0 \\ 0 & 1 & 0 \\ 0 & 0 & 2 \end{bmatrix} \text{ where } [R] \text{ is called Reuter matrix} \quad (3.7)$$

The stress- strain relationship in $x - y$ global coordinate system:

$$\begin{bmatrix} \sigma_x \\ \sigma_y \\ \tau_{xy} \end{bmatrix} = [T]^{-1}[Q] [R][T][R]^{-1} \begin{bmatrix} \varepsilon_x \\ \varepsilon_y \\ \gamma_{xy} \end{bmatrix} \quad (3.8)$$

$$\begin{bmatrix} \sigma_x \\ \sigma_y \\ \tau_{xy} \end{bmatrix} = \begin{bmatrix} \bar{Q}_{11} & \bar{Q}_{12} & \bar{Q}_{16} \\ \bar{Q}_{12} & \bar{Q}_{22} & \bar{Q}_{26} \\ \bar{Q}_{16} & \bar{Q}_{26} & \bar{Q}_{66} \end{bmatrix} \begin{bmatrix} \varepsilon_x \\ \varepsilon_y \\ \gamma_{xy} \end{bmatrix} \quad (3.9)$$

Where \bar{Q}_{ij} are called the elements of the transformed reduced stiffness matrix.

$$\begin{bmatrix} \varepsilon_x \\ \varepsilon_y \\ \gamma_{xy} \end{bmatrix} = \begin{bmatrix} \bar{S}_{11} & \bar{S}_{12} & \bar{S}_{16} \\ \bar{S}_{12} & \bar{S}_{22} & \bar{S}_{26} \\ \bar{S}_{16} & \bar{S}_{26} & \bar{S}_{66} \end{bmatrix} \begin{bmatrix} \sigma_x \\ \sigma_y \\ \tau_{xy} \end{bmatrix} \quad (3.10)$$

Where \bar{S}_{ij} are called the elements of the transformed reduced Compliance matrix.

3.2 Constitutive equations of Laminate

The laminate strain can be written as [52]:

$$\begin{Bmatrix} \varepsilon_x \\ \varepsilon_y \\ \gamma_{xy} \end{Bmatrix} = \begin{Bmatrix} \varepsilon_x^0 \\ \varepsilon_y^0 \\ \gamma_{xy}^0 \end{Bmatrix} + z \begin{Bmatrix} K_x \\ K_y \\ K_{xy} \end{Bmatrix} \quad (3.11)$$

Where $\begin{Bmatrix} K_x \\ K_y \\ K_{xy} \end{Bmatrix}$ is mid plane curvature and $\begin{Bmatrix} \varepsilon_x^0 \\ \varepsilon_y^0 \\ \gamma_{xy}^0 \end{Bmatrix}$ is the mid plane strain and z is the location of

lamina from mid plane. Global Stress and strain relation in terms of mid plane strain and curvature from eq. 3.9 and eq. 3.11 [52]

$$\begin{bmatrix} \sigma_x \\ \sigma_y \\ \tau_{xy} \end{bmatrix} = \begin{bmatrix} \bar{Q}_{11} & \bar{Q}_{12} & \bar{Q}_{16} \\ \bar{Q}_{12} & \bar{Q}_{22} & \bar{Q}_{26} \\ \bar{Q}_{16} & \bar{Q}_{26} & \bar{Q}_{66} \end{bmatrix} \begin{bmatrix} \varepsilon_x^0 \\ \varepsilon_y^0 \\ \gamma_{xy}^0 \end{bmatrix} + z \begin{bmatrix} \bar{Q}_{11} & \bar{Q}_{12} & \bar{Q}_{16} \\ \bar{Q}_{12} & \bar{Q}_{22} & \bar{Q}_{26} \\ \bar{Q}_{16} & \bar{Q}_{26} & \bar{Q}_{66} \end{bmatrix} \begin{bmatrix} K_x \\ K_y \\ K_{xy} \end{bmatrix} \quad (3.12)$$

Global stress can be converted to local stress using equation 3.4 and global strain can be converted to local strain using eq. 3.7. From eq. 3.12, it is obtained that the stress varies linearly throughout the thickness of the lamina and also the stress jump from ply to ply depending upon the orientation and transformed reduced-stiffness matrix. Mid plane strain and curvature are the unknown parameters which can be found out from the $[A \ B \ D]$ matrix. Global stress and strain in each ply can be found from the Mid plane strain and curvature forces using eq. 3.12.

3.2.1 Calculation of ABD matrix (laminate stiffness)

Consider a laminate made of n plies shown in Fig 3.3. Each ply has a thickness of t_k . Then the thickness of the laminate h is $h = \sum_{k=1}^n t_k$ (3.13)

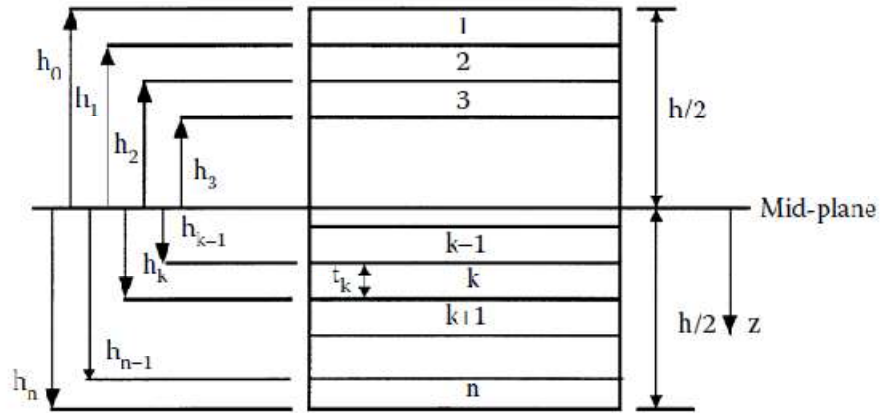


Figure 3.3 Coordinate of plies within laminate [52]

Then, the location of the mid plane is $h/2$ from the top or the bottom surface of the laminate.

The z -coordinate of each ply k surface (top and bottom) is given by:

Ply 1: $h_0 = -\frac{h}{2}$ (*top surface*)

$$h_1 = -\frac{h}{2} + t_1 \text{ (top surface)}$$

Ply k : ($k = 2, 3, \dots, n-2, n-1$):

$$h_{k-1} = -\frac{h}{2} + \sum_1^{k-1} t \text{ (top surface)}$$

$$h_{k-1} = -\frac{h}{2} + \sum_1^k t \text{ (bottom surface)}$$

Ply n : $h_{n-1} = \frac{h}{2} - t_n$ (*top surface*)

$$h_n = \frac{h}{2} \text{ (bottom surface)} \quad (3.14)$$

Force per unit length (N) and the bending moment per unit length (M) of a laminate are given as:

$$\begin{bmatrix} N_x \\ N_y \\ N_{xy} \end{bmatrix} = \begin{bmatrix} A_{11} & A_{12} & A_{16} \\ A_{12} & A_{22} & A_{26} \\ A_{16} & A_{26} & A_{66} \end{bmatrix} \begin{bmatrix} \varepsilon_x^0 \\ \varepsilon_y^0 \\ \gamma_{xy}^0 \end{bmatrix} + \begin{bmatrix} B_{11} & B_{12} & B_{16} \\ B_{12} & B_{22} & B_{26} \\ B_{16} & B_{26} & B_{66} \end{bmatrix} \begin{bmatrix} k_x \\ k_y \\ k_{xy} \end{bmatrix} \quad (3.15)$$

$$\begin{bmatrix} M_x \\ M_y \\ M_{xy} \end{bmatrix} = \begin{bmatrix} B_{11} & B_{12} & B_{16} \\ B_{12} & B_{22} & B_{26} \\ B_{16} & B_{26} & B_{66} \end{bmatrix} \begin{bmatrix} \varepsilon_x^0 \\ \varepsilon_y^0 \\ \gamma_{xy}^0 \end{bmatrix} + \begin{bmatrix} D_{11} & D_{12} & D_{16} \\ D_{12} & D_{22} & D_{26} \\ D_{16} & D_{26} & D_{66} \end{bmatrix} \begin{bmatrix} k_x \\ k_y \\ k_{xy} \end{bmatrix} \quad (3.16)$$

N_x, N_y , = normal force per unit length, N_{xy} = shear force per unit length.

M_x, M_y , = Bending moment per unit length, M_{xy} = Twisting moments per unit length

ε^0 = Mid-plane strain of laminate in x-y coordinates and k =laminate curvature.

Combining the eq. 3.15 and 3.16:

$$\begin{Bmatrix} N \\ M \end{Bmatrix} = \begin{bmatrix} A_{ij} & B_{ij} \\ B_{ij} & D_{ij} \end{bmatrix} \begin{bmatrix} \varepsilon^0 \\ k \end{bmatrix} \quad (3.17)$$

$$A_{ij}(\text{extensional stiffness matrix}) = \sum_{k=1}^n [\overline{Q}_{ij}]_k (h_k - h_{k-1}), \quad i = 1, 2, 6, \quad j = 1, 2, 6$$

$$B_{ij}(\text{extension - bending coupling matrix}) = \frac{1}{2} \sum_{k=1}^n [\overline{Q}_{ij}]_k (h_k^2 - h_{k-1}^2), \quad i = 1, 2, 6 \quad j = 1, 2, 6$$

$$D_{ij}(\text{bending stiffness matrix}) = \frac{1}{3} \sum_{k=1}^n [\overline{Q}_{ij}]_k (h_k^3 - h_{k-1}^3), \quad i = 1, 2, 6, \quad j = 1, 2, 6 \quad (3.18)$$

Therefore mid plane strain and curvature can be determined from the eq. 3.17 after applying force and moments. Then substituting the mid plane strain and curvature in eq. 3.11 and 3.12,

global stress and strain (along x - y axis) can be calculated. Local stress and strain (along 1 - 2 axis) can be calculated from the eq. 3.4 and eq. 3.7 respectively.

In this thesis, for symmetric angle ply laminated structures (plate or beam), the stacking sequence $[\theta/-\theta]_s$ is represented by the orientation angle “ θ ” in the y axis. For example, a stacking sequence of $[45/-45]_s$ is represented by 45° (orientation angle). A stacking sequence is the arrangement of lamina within the laminate.

3.3 Closure

- A composite structure or laminate consists of more than one lamina bonded together through their thickness. Stress–strain equations were developed for a single lamina in both local and global coordinate systems.
- Equations for the macro mechanical analysis of laminates are developed by combining the equations of lamina.
- Global Stress and strain of laminate is developed based on mid plane strain and curvature.
- Mid plane strain and curvature can be calculated by using $[A \ B \ D]$ matrix and applied force and moments.
- $A \ B \ D$ matrix is developed for laminates using the sequence of steps as:
 - I. Reduced stiffness matrix $[Q]$ is calculated for each ply from the eq. 3.2 using elastic moduli, E_1 , E_2 , ν_{12} and G_{12} from the properties of composite material.
 - II. The transformed reduced stiffness matrix $[\bar{Q}]$ is calculated from eq. 3.8 for each ply using reduced stiffness matrix $[Q]$, Reuter matrix $[R]$ and the transformation matrix $[T]$.
 - III. Using the thickness t_k , of each ply the coordinate of location of ply (top and bottom surface), h_i ($i = 1 \dots n$) with respect to mid plane is determined from the eq. 3.14.
 - IV. $[A]$, $[B]$ and $[D]$ matrix are calculated from the eq. 3.18 using $[\bar{Q}]$ from step II and location of each ply from step III.
- Local stress and strain can be calculated by using the transformation matrix, Reuter matrix and global stress and strain.

CHAPTER 4

FINITE ELEMENT ANALYSIS: INTRODUCTION

Outline of the chapter: 4.1 Introduction, 4.2 Basic Finite element method(FEM) steps, 4.3 Basic steps of FEA package (ANSYS), 4.4 Basic steps of analysis of laminated composite structure, 4.4.1 Properties of the laminate, 4.4.2 Element Type, 4.4.3 Algorithm of FEM, 4.5 Closure

4.1 Introduction

The finite element method is used as a tool in this thesis to compare the results obtained from the semi analytical method. Different FEA commercial packages are available in the market. ANSYS is used in this thesis to compare the results. A basic understanding of the finite element method is necessary to use the FEA package effectively and efficiently. Also, it is necessary to study the different elements of FEA packages to effectively model a problem.

4.2 Basic Finite Element method (FEM) steps

The FEA method, first introduced by Turner et al. (1956) is a powerful computational technique for approximate solutions to a variety of complex problems subjected to boundary conditions and loads. The steps followed in the finite element method are as:

- [1] Discretization of the problem domain into a finite number of sub domains called elements.
- [2] Select an interpolation function. The unknown field variable is expressed in terms of interpolation function within each element at specific points known as nodes. Nodes are located at the element boundaries and they connect adjacent elements.
- [3] An element matrix is developed for each element.
- [4] The element matrix obtained from each element is assembled to obtain a global matrix for the entire domain.
- [5] Apply boundary conditions and loads.
- [6] Then a solution of the equation is obtained.
- [7] Derive the results.

4.3 Basic steps of FEA package (ANSYS)

The finite element package consists of mainly three blocks:

- [1] **Pre processor:** Model is built defining the geometry, material properties and element type. Load and boundary condition may also be applied at this stage.
- [2] **Processor:** It computes the stiffness matrix and force vector based on the information provided in pre-processor.
- [3] **Solution:** This phase solves the equation and solution is obtained in terms of displacement.
- [4] **Post processor:** In this phase results are derived i.e. Stress, strain and failure component. Results may be visualized in graphical form also.

4.4 Basic steps of analysis of laminated composite structure

Finite element analysis of laminated structure can be done at different levels which depend upon the level of post processing needed.

1. **Level 1:** Only displacements, buckling loads and modes, or vibration frequencies and their modes are required.
2. **Level 2:** Both displacement and stress, strain need to be calculated at lamina level.

Based on the level of post processing, the analysis of laminated composite structure can be categorized under three approaches:

I. Macroscopic approach:

- The whole laminate is approximated as a homogeneous equivalent shell and analysis is done using the orthotropic properties.
- Stress distribution in the laminate cannot be obtained.
- Only displacements, buckling loads and modes, or vibration frequencies and modes can be calculated.
- Only laminate stiffness is required for the analysis.

II. Mesoscale approach:

This method is also called laminate stacking sequence approach.

- This method compute the stress and strain of each lamina
- It computes the displacements, buckling loads and modes, or vibration frequencies and modes can be calculated.
- The elastic properties of each lamina must be given

- The thickness and fiber orientation of every lamina must be given.

III. **Micromechanical approach:**

- This method computes the stress and strain of fiber and matrix.
- The micro structural properties such as the fiber shape and geometrical distribution, and the material properties of the constituents must be given.
- Microstructure modeling is used to generate the properties of composite material for different combination of fiber and matrix using the properties of fibers and matrix.
- This approach is difficult to adopt, so most of the laminate is analyzed using the plates and shell simplifications.

4.4.1 Properties of the laminate

Properties of the laminate can be inserted in the FEA software in three ways:

1. By using the matrices A, B, D and H:

It can compute only displacements, buckling loads and their modes, or vibration frequencies and their modes. It can also calculate strain along the thickness of the laminate. But it is not able to compute stress since it does not have information about laminate stacking sequence, so it cannot distinguish between laminas. [H] matrix is called the transverse shear stiffness matrix which relates transverse shear force to transverse shear strain. In case of CLT, this matrix is not used because both transverse shear strain is zero.

2. By using the laminate stacking sequence (LSS) and properties for each lamina:

This method can compute both displacement and stress and strain at the lamina level. With the help of LSS, software calculates the A, B, D and H matrix internally.

3. Using Element Orthotropic properties for laminate:

This approach is used when FEA software does not accept the [A B D H] matrix as input. This method is applicable to balanced symmetric laminates. The FEA software uses orthotropic elements and equivalent properties of the laminate should be calculated and introduced into the FEA software.

4.4.2 Element Type

The shell elements used by the commercial FEA packages for the analysis of composite materials are SHELL 181 /SHELL 281(ANSYS). Shell elements are used to model thin to moderately thick shells, down to a side-to-thickness ratio of 10. SHELL 181 has 4 nodes while

SHELL 281 has 8 nodes. So they used an interpolation function to a higher degree. While some of them have 3 or 4 nodes, others have 8 nodes, thus using interpolation functions of higher degree. Shell elements are specified in 3D space and have 5 or 6 degrees of freedom (DOF) at each node (translations in the nodal x, y, and z directions and rotations about the nodal x, y, and z axis). Elements SHELL181 and SHELL281 are used for the transverse shear deflection using an energy equivalence method, which is recommended for sandwich shells.

4.4.3 Algorithm of FEM

Basic steps in the analysis of laminated composite structure using FEA software (ANSYS):

➤ **Model Generation**

- Define the element type using the menu path:

Main Menu > Preprocessor > Element Type > Add/Edit/Delete > SHELL 281 > OK > close.

- Specify the material properties using the menu path:

Main Menu > Preprocessor > Material properties > Material models > structural > linear > elastic > orthotropic > Ex, Ey etc.

- Specify section using the menu path:

Main Menu > Preprocessor > Section > Shell > Layup > Add/delete > define the layer, thickness and material.

➤ **Geometry and mesh**

In this section geometry of the structure is created. Then the geometry is divided into elements connected by nodes (meshing).

- Create key points using the menu path

Main Menu > Preprocessor > Modeling > Create > Key points > In Active

- Create area using the menu path

Main Menu > Preprocessor > Modeling > Create > Areas > Arbitrary > Through Kps.

➤ **Meshing**

Meshing means dividing the geometry in elements and nodes.

- Create Meshing using the menu path:

Main Menu > Preprocessor > Meshing > Size Cntrl > ManualSize > Lines > All Lines

Main Menu > Preprocessor > Meshing > Mesh > Areas > Mapped > 3 or 4 sided

➤ **Solution**

- Apply degree of freedom (DOF) constraint on the model using the following menu path:

Main Menu > Solution > Define Loads > Apply > Structural > Displacement > On Nodes

- Apply load on the model using the following menu path:

Main Menu > Solution > Define Loads > Apply > Structural > Pressure > On nodes

- Solve the model using the following menu path

Main Menu > Solution > Solve > Current

➤ **Post processing**

Review the deformed shape using the following menu path:

Main Menu > General Post Processing > Plot Results > Deformed Shape

Obtain the contour plot of the displacement using the following menu path

Main Menu > General Postprocessor > Plot Results > Contour Plot > Nodal Solution

Obtain the contour plot of the stress using the following menu path

Main Menu > General Postprocessor > Plot Results > Contour Plot > Nodal Solution

4.5 Closure

1. FEA is a powerful numerical technique to determine an approximate solution to the problem.
2. FEA packages have three basic phases: Pre processor, Solution and Post processor.
3. There are three approaches to analyzing laminated composite structures: microscopic, mesoscale, and macroscopic approach.
4. The properties of the laminate can be inserted in FEA packages by using three methods: A B D H matrix, Laminate stacking sequence (LSS) and element orthotropic properties.
5. The shell elements used by the commercial FEA packages for the analysis of composite materials are 4 noded SHELL 181 /SHELL 281(ANSYS).
6. A mesoscale approach is used in this thesis, because stress is required at lamina level along with deflection and properties of laminate is inserted in FEA software by using a laminate stacking sequence (LSS) i.e. properties and orientation of each lamina is specified.
7. SHELL element is used to build a two dimensional finite element model of a laminated composite structure.

CHAPTER 5

ANALYSIS OF LAMINATED COMPOSITE PLATE

Outline of chapter: 5.1 Stress analysis of single lamina under in plane load, 5.1.1 Semi analytical method & FEM 5.1.2 Validation of semi analytical and FEA model 5.1.3 Numerical problem on lamina, 5.1.3.1 Result and discussion 5.1.3.2 effect of orientation angle on displacement, 5.1.3.3 effect of length to thickness ratio, 5.2. Stress analysis of laminate under in plane load, 5.2.1 Determination of stress of laminate, 5.2.2 Semi analytical method & FEM 5.2.3 Validation of semi analytical and FEM 5.2.4 Numerical problem on laminate, 5.2.4.1 Result and discussion 5.2.4.2 effect of orientation angle, 5.2.4.3 effect of length to thickness ratio, 5.2.4.4 effect of no. of lamina, 5.2.4.5 Symmetric cross ply laminate, 5.2.5 Closure

5.1 Stress analysis of single lamina under in-plane load

The lamina is considered a thin plate of small thickness. The lamina is considered under plane stress because the lamina is thin and there are no out-of-plane loads. Fig. 5.1 shows the geometry of single lamina. The 1-2 axis is the local axis, and x-y is the global axis. Axis 1 is aligned along the fiber direction and axis 2 is perpendicular to axis 1. The angle between the axis 1 and the axis x is called the orientation angle, θ .

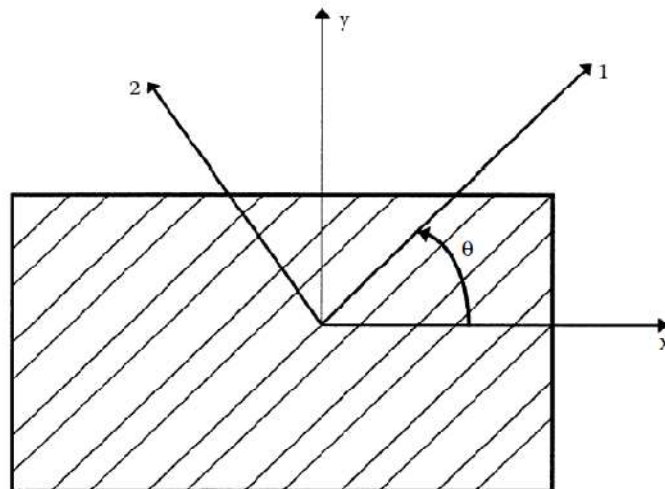


Figure 5.1 Local axis (1-2) and global axis (x-y) of Lamina [52]

The constitutive equations of stress and strain tensor for a lamina, discussed in the chapter 3 are given by the expression:

$$\begin{bmatrix} \sigma_1 \\ \sigma_2 \\ \tau_{12} \end{bmatrix} = \begin{bmatrix} Q_{11} & Q_{12} & Q_{11} \\ Q_{12} & Q_{22} & 0 \\ 0 & 0 & Q_{66} \end{bmatrix} \begin{bmatrix} \varepsilon_1 \\ \varepsilon_2 \\ \gamma_{12} \end{bmatrix} \quad (5.1a)$$

where $Q_{11} = \frac{E_1}{1-\nu_{12}\nu_{21}}$, $Q_{22} = \frac{E_2}{1-\nu_{12}\nu_{21}}$, $Q_{12} = \frac{\nu_{12}E_2}{1-\nu_{12}\nu_{21}}$, $Q_{66} = G_{12}$, $\frac{\nu_{12}}{E_1} = \frac{\nu_{21}}{E_2}$

Where Q_{ij} is called reduced stiffness coefficient.

Inverting the eq. 5.1(a)

$$\begin{bmatrix} \varepsilon_1 \\ \varepsilon_2 \\ \gamma_{12} \end{bmatrix} = \begin{bmatrix} S_{11} & S_{12} & S_{11} \\ S_{12} & S_{22} & 0 \\ 0 & 0 & S_{66} \end{bmatrix} \begin{bmatrix} \sigma_1 \\ \sigma_2 \\ \tau_{12} \end{bmatrix} \quad (5.1 b)$$

Where S_{ij} are the elements of compliance matrix.

5.1.1 Semi-analytical method and Finite element method (FEM)

A semi analytical model of single lamina using the equations 5.1(a) and 5.1(b) is built up in mathematical tool MATLAB and stress in the local coordinate is found out by applying load in either the x or y direction. An FEA model of single lamina is built up using quadrilateral 4 nodes 182 elements. Material properties are specified in an input field in lamina coordinate system (1-2 planes) i.e. in the fiber direction. The global Cartesian coordinates and the fiber directions are at an angle of θ . For this purpose a local coordinate system is created and aligned with the fiber orientation. The geometry is meshed by quadrilateral mapped meshing of suitable mesh size. The results depend on the mesh size. As mesh size increases, the results change. After a certain mesh size, the same results are repeated. The mesh size after which the same results were obtained is selected to make the results mesh independent (convergence analysis). In the solution phase, pressure is applied on the top and bottom sides of the lamina or on left and right sides of the lamina. In the post processor phase, stresses are viewed.

5.1.2 Validation of Semi-Analytical and FEM model

The code built in the MATLAB tool for semi-analytical methods is validated with a problem given in KAW [52] and the FEA (Finite element analysis) code built by following the procedure discussed in section 5.1.1 in ANSYS software is validated with the problem of Guven et. al. [53]. The problem chosen for checking from the published literature is given in

the table 5.2, where σ_1 , σ_2 and τ_{12} are calculated and checked. It ascertains that the semi analytical code and FEA code are correct and may be extended for different problems for solution.

Table 5.1 Material properties of composite material [52]

Property	Symbol	Unit	Graphite/Epoxy	Glass/Epoxy
Longitudinal elastic modulus	E_1	GPa	181	38.6
Transverse elastic modulus	E_2	GPa	10.3	8.27
Major Poisson's ratio	ν_{12}		0.28	0.26
Shear modulus	G_{12}	GPa	7.17	4.14
Ultimate longitudinal tensile strength	$(\sigma_1^T)_{ult}$	MPa	1500	1062
Ultimate longitudinal compressive strength	$(\sigma_1^c)_{ult}$	MPa	1500	610
Ultimate transverse tensile strength	$(\sigma_2^T)_{ult}$	MPa	40	31
Ultimate transverse compressive strength	$(\sigma_2^c)_{ult}$	MPa	246	118
Ultimate in-plane shear strength	$(\tau_{12})_{ult}$	MPa	68	72

Table 5.2 Validation with published literature

Model	Condition	Ref.	Present			Literature		
			σ_1	σ_2	τ_{12}	σ_1	σ_2	τ_{12}
FEM	Uniform axial tension on top & bottom = 20 Ksi, fiber orientation = 45 deg.	Güven et. al. (2006) [53]	10e3 Ksi	10e3 Ksi	10e3 Ksi	10e3 Ksi	10e3 Ksi	10e3 Ksi

Model	Condition	Ref.	Present			Literature		
			σ_1	σ_2	τ_{12}	σ_1	σ_2	τ_{12}
Semi-Analytical method	$\sigma_x = 2$ MPa, $\sigma_y = -3$ MPa, $\tau_{xy} = 4$ MPa, Orientation angle = 60 deg, Graphite/ epoxy material	KAW (2006) [52]	0.17 e7 Pa	-0.271 e7 Pa	-0.416 e7 Pa	0.1714 e7 Pa	-0.271 e7 Pa	-0.416 e7 Pa

5.1.3 Numerical Problem

A fiber reinforced composite square plate of 200 x 200 mm² of single lamina subjected to uniform tensile in plane load on the top and bottom surface (y direction) of 1Pa are considered for the study. The fibers are oriented at different angles ranging from 0° to 90°. The material used is graphite- epoxy composite material (table 5.1). Stresses are determined by semi analytical and finite element methods and results from both the methods are compared.

Stresses are determined by using the semi analytical method as discussed in chapter 3 (eq. 5.1a and 5.1b). The equations are solved in MATLAB platform for different orientation angles ranging from 0° to 90°. The semi analytical results are compared with FEM by using finite element software (ANSYS 15.0). The steps followed to model the problem in FEA software is discussed in section 5.1.1. Fig 5.2 shows the geometry and loading of the lamina. The stress in the y direction is applied to the lamina. The meshed geometry of the lamina is shown in fig 5.2. Quadrilateral mapped meshing is used.

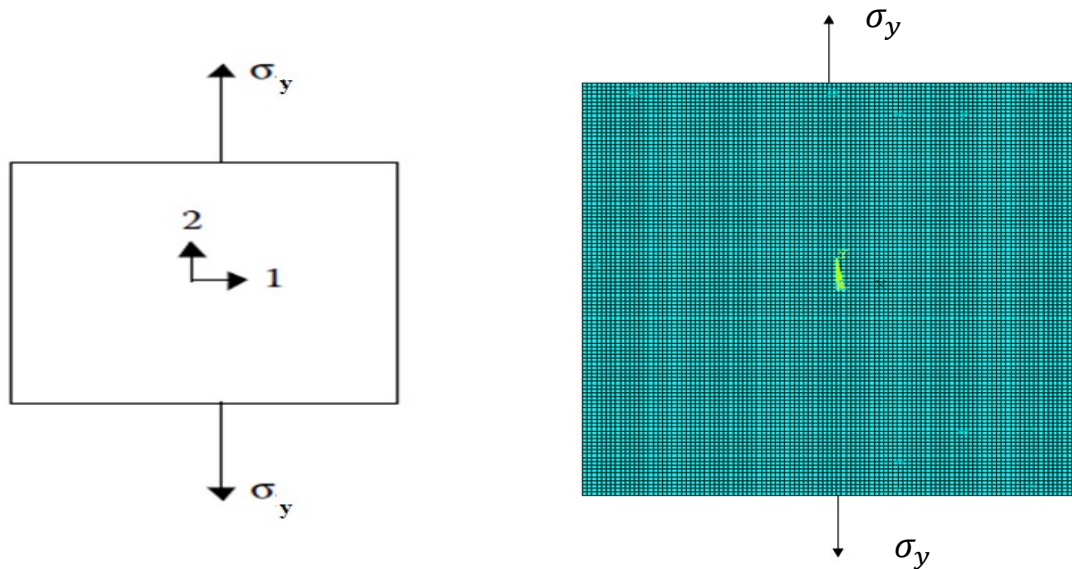


Figure 5.2 Geometry of a Lamina

5.1.3.1 Results and Discussion

Results (local stress) obtained from the semi analytical methods are compared with FEM (FEA software) in Table 5.3. It is found that both the results show good agreement with each other with zero error. This is due to the reasons that the equations used in the semi analytical method to determine stress are free from higher order terms and the equations are formulated in terms of the matrix, which is solved by simple matrix operations. Therefore, the results of the semi analytical method are same as the FEM results. This can be proved for other loading conditions, i.e. $\sigma_x \neq 0, \sigma_y = \tau_{xy} = 0$ or $\tau_{xy} \neq 0, \sigma_x = \sigma_y = 0$ or $\sigma_x \neq \sigma_y \neq 0, \tau_{xy} = 0$ etc. by applying the above model.

Table 5.3 Comparison of the local stress in Pa determined by Semi analytical method and FEM

Orientation angle	Semi analytical method			FEM			%age error
	σ_1	σ_2	τ_{12}	σ_1	σ_2	τ_{12}	
Unit	Pa	Pa	Pa	Pa	Pa	Pa	
0°	0	1	0	0	1	0	0
15°	0.067	0.933	0.25	0.067	0.933	0.25	0
30°	0.25	0.75	0.433	0.25	0.75	0.433	0
45°	0.5	0.5	0.5	0.5	0.5	0.5	0

Orientation angle	Semi analytical method			FEM			%age error
	σ_1	σ_2	τ_{12}	σ_1	σ_2	τ_{12}	
60°	0.75	0.25	0.433	0.75	0.25	0.433	0
75°	0.933	0.067	0.25	0.933	0.067	0.25	0
90°	1	0	0	1	0	0	0

5.1.3.2 Effect of orientation angle on displacement

The FEM model is used to determine the displacement for the above numerical problem for different orientation angles to study the effect of orientation angle on displacement. The displacement decreases as the orientation angles vary from 0° to 90° having maximum and minimum displacement at 0° and 90° respectively (fig 5.3). Fig 5.3 shows the graph between displacement vector sum and orientation angle. Displacement vector sum means the sum of displacements in x , y and z direction.

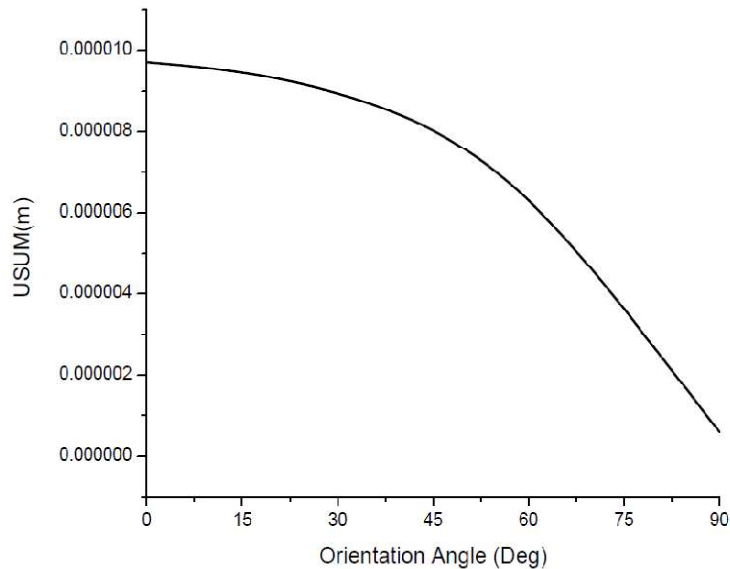


Figure 5.3 Influence of orientation angle on displacement vector sum (USUM)

5.1.3.3 Effect of length to thickness ratio

The displacement and stress has no effect on length to thickness ratio since lamina is thin.

5.2 Stress analysis of laminate under in-plane load

It is not possible to construct a structure made of a single lamina because the thickness of the lamina is very small (in the order of 0.125 mm). Therefore, many laminas are stacked one above the other to form a laminated structure that is able to take a realistic load [64]. So a laminated structure is a collection of lamina arranged in a specified manner within the laminate (Laminate Stacking Sequence, LSS). The properties of a lamina are limited to a particular direction, so if a number of unidirectional laminas are stacked together, they can be able to take a unidirectional load. For complex loads, therefore laminas are stacked together in different orientation within the lamina. Therefore, the properties of the laminae depend upon the optimum combination of:

1. Stacking sequence of laminas within laminate
2. Thickness of laminate
3. Modulus of elasticity
4. Orientation angle
5. Coefficient of thermal and moisture expansion

In chapter 3, macro mechanical analysis of laminate is developed. Stresses in local and global coordinate system can be found out for each ply within the laminate under in plane loads. Stiffness of whole laminate i.e.[A B D] matrix is calculated in chapter 3.

5.2.1 Determination of stress of laminate

The strain displacement equation can be written as [52]

$$\begin{Bmatrix} \varepsilon_x \\ \varepsilon_y \\ \gamma_{xy} \end{Bmatrix} = \begin{Bmatrix} \frac{\partial u_0}{\partial x} \\ \frac{\partial v_0}{\partial y} \\ \left(\frac{\partial u_0}{\partial y} + \frac{\partial v_0}{\partial x} \right) \end{Bmatrix} + z \begin{Bmatrix} -\frac{\partial^2 w_0}{\partial x^2} \\ -\frac{\partial^2 w_0}{\partial y^2} \\ -2\frac{\partial^2 w_0}{\partial x \partial y} \end{Bmatrix} \quad (5.2)$$

Therefore laminate strain can be written as

$$\begin{Bmatrix} \varepsilon_x \\ \varepsilon_y \\ \gamma_{xy} \end{Bmatrix} = \begin{Bmatrix} \varepsilon_x^0 \\ \varepsilon_y^0 \\ \gamma_{xy}^0 \end{Bmatrix} + z \begin{Bmatrix} K_x \\ K_x \\ K_{xy} \end{Bmatrix} \quad (5.3)$$

Where $\begin{Bmatrix} K_x \\ K_x \\ K_{xy} \end{Bmatrix}$ is mid plane curvature and $\begin{Bmatrix} \varepsilon_x^0 \\ \varepsilon_y^0 \\ \gamma_{xy}^0 \end{Bmatrix}$ is the mid plane strain. Global Stress and strain relation in terms of mid plane strain and curvature [52]

$$\begin{bmatrix} \sigma_x \\ \sigma_y \\ \tau_{xy} \end{bmatrix} = \begin{bmatrix} \bar{Q}_{11} & \bar{Q}_{12} & \bar{Q}_{16} \\ \bar{Q}_{12} & \bar{Q}_{22} & \bar{Q}_{26} \\ \bar{Q}_{16} & \bar{Q}_{26} & \bar{Q}_{66} \end{bmatrix} \begin{bmatrix} \varepsilon_x \\ \varepsilon_y \\ \gamma_{xy} \end{bmatrix} \quad (5.4)$$

Using eq. 5.3 in eq. 5.4

$$\begin{bmatrix} \sigma_x \\ \sigma_y \\ \tau_{xy} \end{bmatrix} = \begin{bmatrix} \bar{Q}_{11} & \bar{Q}_{12} & \bar{Q}_{16} \\ \bar{Q}_{12} & \bar{Q}_{22} & \bar{Q}_{26} \\ \bar{Q}_{16} & \bar{Q}_{26} & \bar{Q}_{66} \end{bmatrix} \begin{bmatrix} \varepsilon_x^0 \\ \varepsilon_y^0 \\ \gamma_{xy}^0 \end{bmatrix} + z \begin{bmatrix} \bar{Q}_{11} & \bar{Q}_{12} & \bar{Q}_{16} \\ \bar{Q}_{12} & \bar{Q}_{22} & \bar{Q}_{26} \\ \bar{Q}_{16} & \bar{Q}_{26} & \bar{Q}_{66} \end{bmatrix} \begin{bmatrix} K_x \\ K_x \\ K_{xy} \end{bmatrix} \quad (5.5)$$

The mid plane strain and curvature are unknown to determine the stress and strain. The mid plane strain and curvature can be determined from ABD matrix (eq. 3.18) from the equation

$$\begin{bmatrix} \varepsilon_x^0 \\ \varepsilon_y^0 \\ \gamma_{xy}^0 \\ K_x \\ K_x \\ K_{xy} \end{bmatrix} = \begin{bmatrix} A_{11} & A_{12} & A_{16} & B_{11} & B_{12} & B_{16} \\ A_{12} & A_{22} & A_{26} & B_{12} & B_{22} & B_{26} \\ A_{16} & A_{26} & A_{66} & B_{16} & B_{26} & B_{66} \\ B_{11} & B_{12} & B_{16} & D_{11} & D_{12} & D_{16} \\ B_{12} & B_{22} & B_{26} & D_{12} & D_{22} & D_{26} \\ B_{16} & B_{26} & B_{66} & D_{16} & D_{26} & D_{66} \end{bmatrix}^{-1} \begin{bmatrix} N_x \\ N_y \\ N_{xy} \\ M_x \\ M_y \\ M_{xy} \end{bmatrix} \quad (5.6)$$

Where N and M are external in-plane loads and moments applied to the laminate.

Local Stresses of laminate in the k^{th} lamina can be calculated by

$$[\sigma]_{1,2}^k = [T][\bar{Q}]_k \{[\varepsilon^0] + h [k]\} \quad (5.7)$$

Global Strain of laminate in the k^{th} lamina as:

$$[\varepsilon]_{x,y}^k = [\varepsilon_0] + h[k] \quad (5.8)$$

h is the thickness of laminate.

Local Strain of laminate in the k^{th} lamina can be calculated from eq. 3.7.

$$\begin{bmatrix} \varepsilon_1 \\ \varepsilon_2 \\ \gamma_{12} \end{bmatrix} = [R][T][R]^{-1} \begin{bmatrix} \varepsilon_x \\ \varepsilon_y \\ \gamma_{xy} \end{bmatrix} \text{ and } [R] = \begin{bmatrix} 1 & 0 & 0 \\ 0 & 1 & 0 \\ 0 & 0 & 2 \end{bmatrix} \text{ where } [R] \text{ is called Reuter matrix} \quad (5.9)$$

5.2.2 Semi-analytical Method and FEM

A semi analytical model of a laminated plate consisting of many lamina stacked one upon the other in the specific stacking sequence is built up using the laminate equations as discussed in section 5.2.2 in mathematical tool MATLAB, and stress in local and global coordinates is found out by applying load in the x and y directions. A FEA model of laminate is built up using Shell 281 elements. Material properties, orientation, and thickness are specified in an input field in the lamina coordinate system ($1-2$ plane), i.e. in the fiber direction for each lamina. The geometry is meshed by the quadrilateral mapped meshing of a suitable mesh size. The results depend on the mesh size. As mesh size increases, the results change. After a certain mesh size, the same results are repeated. The mesh size, after which the same results are obtained is selected to make the results mesh independent (convergence analysis). In the solution phase, load is applied on the top and bottom sides or on the left and right sides or a combination of both. In the post processor phase, stress and strain are viewed in both coordinate systems.

5.2.3 Validation of Semi-Analytical and FEM

The code built in the MATLAB tool for semi-analytical method (Classical lamination theory) is checked and validated with a problem given in KAW [52] and the FEA code built by following the procedure discussed in section 5.2.3 in ANSYS software is validated with the work of Barberio et. al. [2]. The problem chosen for checking from the published literature for the semi analytical model is given in table 5.4 where σ_x , σ_y and τ_{xy} are calculated and verified. Similarly, local stress can also be verified. A problem is taken from Barberio [2] and FEM model is verified in table 5.5. It ascertains that the semi analytical code and FEM code are correct and may be extended to solve different problems. Table 5.4 and 5.5 show stresses in the global coordinate system (x, y, z) for the top and bottom surfaces of each lamina within the laminate. In table 5.5, stress is shown for lamina above the mid plane; due to the symmetric arrangement stress of lamina below the mid plane is same and therefore not shown in table 5.5.

Table 5.4 Semi analytical model verification with published literature [52] for [0/30/-45] Graphite/Epoxy Laminate subjected to $N_x = N_y = 1000 \text{ N/m}$ for 5 mm lamina thickness.

Global stress (Pa)								
Lamina No.	Position	σ_x		σ_y		τ_{xy}		%age error
		Present	Ref.(2006)	Present	Ref.(2006)	Present	Ref.(2006)	
1. (0°)	Top	33510	33510	61880	61880	-27500	-27500	0
	Bottom	55770	55770	45310	45310	-12800	-12800	0
2. (30°)	Top	69300	69300	73910	73910	33810	33810	0
	Bottom	143400	143400	81020	81020	84260	84260	0
3. (-45°)	Top	123500	123500	156300	156300	-38880	-38880	0
	Bottom	-25470	-25470	-18400	-18400	40910	40910	0

Table 5.5 FEM model verification with published literature [2] for [0/90/45/-45]_s AS4D/9310 Laminate subjected to $N_x = 100 \text{ N/mm}$ for 10 mm laminate thickness.

Global stress (MPa)									Displacement in X direction (UX) in mm		% error
Lamina No.	Position	σ_x		σ_y		τ_{xy}		% ge error	Present	Ref. (2014)	
		Present	Ref. (2014)	Present	Ref. (2014)	Present	Ref. (2014)				
1. (0°)	Top	26.391	26.391	-0.0136	-0.0136	0	0	0	0.197	0.197	0
	Bottom	26.391	26.391	-0.0136	-0.0136	0	0	0			
2. (90°)	Top	1.385	1.385	-7.7621	-7.7621	0	0	0			
	Bottom	1.385	1.385	-7.7621	-7.7621	0	0	0			
3. (45°)	Top	6.112	6.112	3.887	3.887	4.314	4.314	0			
	Bottom	6.112	6.112	3.887	3.887	0	0	0			
4. (-45°)	Top	6.112	6.112	3.887	3.887	-4.314	-4.314	0			
	Bottom	6.112	6.112	3.887	3.887	0	0	0			

5.2.4 Numerical Problem

A fiber reinforced laminated composite square plate of $200 \times 200 \text{ mm}^2$, subjected to uniform tensile in plane load on top and bottom surface (y direction) or on the side surface (x direction) or a combination of both of 100 N/mm are considered. The laminae are stacked together symmetrically about the mid plane and the fibers are oriented at different angles ranging from 0° to 90° in each lamina. The thickness of each lamina is 1.5 mm . The material used is graphite- epoxy composite material (table 5.1). Stresses on local (1-2) and global (x-y) coordinates are determined using semi analytical and FEM and compared. The effects of the number of lamina, length to thickness ratio, and orientation angle are studied.

Stresses are determined by using the semi analytical method as discussed in section 5.2.2. The equations are solved in MATLAB platform for different orientation angles ranging from 0° to 90° . For symmetric angle ply laminate stacking sequence of $[\theta/-\theta]_s$ is represented by orientation angle “ θ ” in the y -axis. For example stacking sequence of $[45/-45]_s$ is represented by 45° (orientation angle). The semi analytical results are compared with FEM by using finite element software (ANSYS 15.0). The steps followed to model the problem in FEA software are discussed in section 5.2.3. Fig 5.4 shows the geometry and stacking of the lamina within the laminate. Fig 5.4 (a) shows stacking sequence of each lamina within the laminate along with fiber orientation of each lamina on one side of middle axis because it is symmetric about the middle axis. 0, 90, 45, -45 are the fiber orientation angle of each lamina and 1 shows the material code of each lamina, 1,2,3,4 shows the stacking sequence of lamina from outer to middle axis. Fig 5.4 (b) shows the meshing of laminate by ANSYS. Quadrilateral mapped meshing is shown.

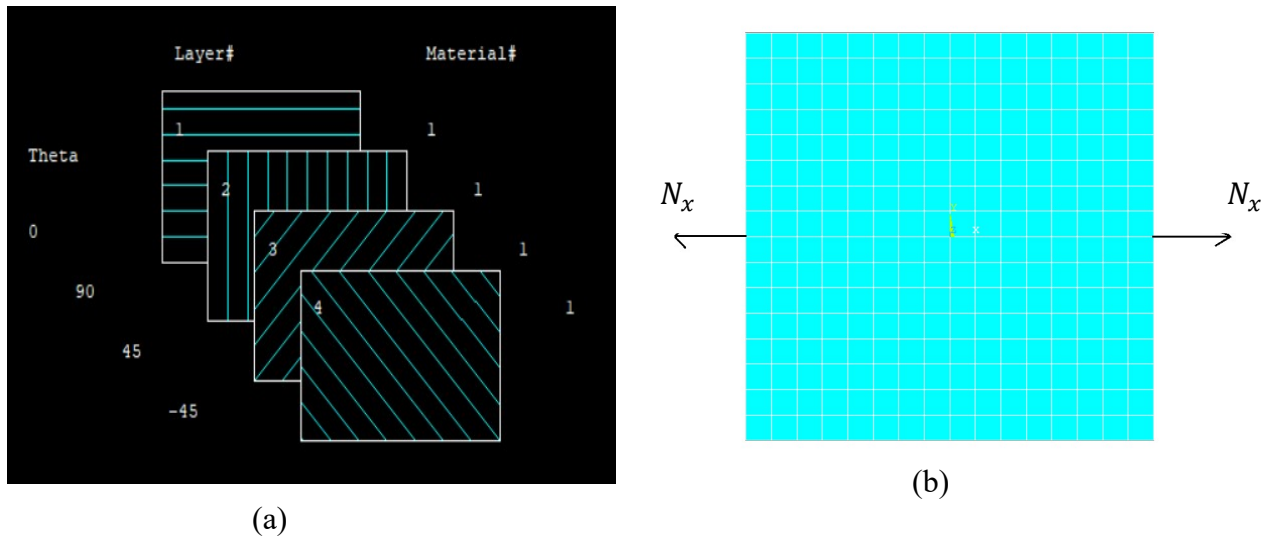


Figure 5.4 (a) Stacking sequence of lamina within laminate (b) Geometry of laminate under loading in x direction

5.2.4.1 Results and Discussion

Results obtained from the semi analytical method are compared with FEM (FEA software) in Table 5.6 - 5.9. It is found that both the results show good agreement with each other with zero error. This is due to the fact that the equations used in the semi analytical method to determine stress are free from higher order terms and the equations are formulated in terms of a matrix which is solved by simple matrix operations. Therefore, the results of the semi analytical

method are the same as the FEM results. In table 5.6, local stresses are determined by both the methods for the symmetric angle ply laminate of stacking sequence $[\theta/-\theta]_s$ subjected to in plane load in x direction (100 N/mm) as shown in fig 5.4. Stress (σ_1 and σ_2) in the top and bottom surfaces of each lamina is the same. Stress τ_{12} for the top and bottom surfaces of each lamina is the same but opposite in signs except 0° and 90° whose stress is 0 in both the top and bottom of each lamina. Table 5.7 shows the local stress determined by both the methods for the symmetric cross ply laminate of the stacking sequence $[0/90/\theta/-\theta]_s$ subjected to in plane load in the x direction. Stress at both the top and bottom of each lamina is the same. Stresses above the mid plane are shown; due to symmetry stress below the mid plane is same as top and therefore not shown in the table. The top of the table shows the orientation of each lamina in the laminate $[0/90/\theta/-\theta]_s$ and the extreme left side of the table shows the value of θ . The value of θ is changed from 0° to 90° and the local stress on the top and bottom surfaces of the lamina is determined. Similarly, global stresses are determined in tables 5.8 and 5.9 for symmetric angle ply laminates ($[\theta/-\theta]_s$) and cross ply laminates ($[0/90/\theta/-\theta]_s$) respectively.

Table 5.6 Comparison of the Local stress from Semi analytical method with FEM for different stacking sequence of symmetric angle ply laminate.

Stacking sequence (Orientation angle)	σ_1 (MPa)		σ_2 (MPa)		τ_{12} (MPa)		%age error
	FEM	Semi-Analytical	FEM	Semi-Analytical	FEM	Semi-Analytical	
	Top (T) /Bottom (B)	T/B	T/B	T/B	T/B	T/B	
$[0/-0]_s$	16.67	16.67	0	0	0	0	0
$[15/-15]_s$	17.471	17.471	-0.804	-0.804	± 0.839	± 0.839	0
$[30/-30]_s$	18.438	18.438	-1.771	-1.771	± 3.789	± 3.789	0
$[45/-45]_s$	15.552	15.552	1.115	1.115	± 8.33	± 8.33	0
$[60/-60]_s$	8.256	8.256	8.41	8.41	± 9.578	± 9.578	0
$[75/-75]_s$	2.107	2.107	14.56	14.56	± 5.883	± 5.883	0
$[90/-90]_s$	0	0	16.67	16.67	0	0	0

N.B: T- top of lamina, B- bottom of lamina, + for top and - for bottom.

Table 5.7 Comparison of the Local stress from Semi analytical method with FEM for different stacking sequence of symmetric cross ply laminate.

Stacking sequence [0/90/θ/-θ] _s	Local Stress (MPa)								% error
	σ ₁ (Top/Bottom) 0°		σ ₁ (Top/Bottom) 90°		σ ₁ (Top/Bottom) θ°		σ ₁ (Top/Bottom) - θ°		
	FEM	Semi-Analytical	FEM	Semi-Analytical	FEM	Semi-Analytical	FEM	Semi-Analytical	
0	10.91	10.91	-0.42	-0.42	10.91	10.91	10.91	10.91	0
30	15.47	15.47	-4.34	-4.34	10.51	10.51	10.51	10.51	0
45	21.64	21.64	-6.09	-6.09	7.78	7.78	7.78	7.78	0
60	26.59	26.59	-4.16	-4.16	3.52	3.52	3.52	3.52	0
90	28.50	28.50	-0.14	-0.14	-0.14	-0.14	-0.14	-0.14	0
Stacking sequence [0/90/θ/-θ] _s	σ ₂ (Top/Bottom) 0°		σ ₂ (Top/Bottom) 90°		σ ₂ (Top/Bottom) θ°		σ ₂ (Top/Bottom) - θ°		% error
	FEM	Semi-Analytical	FEM	Semi-Analytical	FEM	Semi-Analytical	FEM	Semi-Analytical	
	0	0.14	0.14	0.61	0.61	0.14	0.14	0.14	
30	-0.01	-0.01	0.81	0.81	0.19	0.19	0.19	0.19	0
45	-0.02	-0.02	1.13	1.13	0.56	0.56	0.56	0.56	0
60	0.16	0.16	1.44	1.44	1.12	1.12	1.12	1.12	0
90	0.42	0.42	1.61	1.61	1.61	1.61	1.61	1.61	0
Stacking sequence [0/90/θ/-θ] _s	τ ₁₂ (Top/Bottom) 0°		τ ₁₂ (Top/Bottom) 90°		τ ₁₂ (Top/Bottom) θ°		τ ₁₂ (Top/Bottom) - θ°		% error
	FEM	Semi-Analytical	FEM	Semi-Analytical	FEM	Semi-Analytical	FEM	Semi-Analytical	
	0	0.00	0.00	0.00	0.00	0.00	0.00	0.00	
30	0.00	0.00	0.00	0.00	-0.69	-0.69	0.69	0.69	0
45	0.00	0.00	0.00	0.00	-1.11	-1.11	1.11	1.11	0
60	0.00	0.00	0.00	0.00	-1.07	-1.07	1.07	1.07	0
90	0.00	0.00	0.00	0.00	0.00	0.00	0.00	0.00	0

Table 5.8. Comparison of the Global stress from Semi analytical method with FEM for different stacking sequence of symmetric angle ply laminate.

Stacking sequence	σ _x (MPa)		σ _y (MPa)		σ _{xy} (MPa)		%age error
	FEM	Semi-Analytical	FEM	Semi-Analytical	FEM	Semi-Analytical	
	Top/Bottom	T/B	T/B	T/B	T/B	T/B	
[0/-0] _s	16.67	16.67	0	0	0	0	0
[15/-15] _s	16.67	16.67	0	0	±3.841	±3.841	0
[30/-30] _s	16.67	16.67	0	0	±6.856	±6.856	0
[45/-45] _s	16.67	16.67	0	0	±7.218	±7.218	0
[60/-60] _s	16.67	16.67	0	0	±4.722	±4.722	0
[75/-75] _s	16.67	16.67	0	0	±1.982	±1.982	0
[90/-90] _s	16.67	16.67	0	0	0	0	0

N.B: T- top of lamina, B- bottom of lamina, + for top and - for bottom.

Table 5.9 Comparison of the Global stress from Semi analytical method with FEM for different stacking sequence of symmetric cross ply laminate.

Stacking sequence [0/90/θ/- θ] _s	Global stress (MPa)								
	σ _x (Top/Bottom) 0°		σ _x (Top/Bottom) 90°		σ _x (Top/Bottom) θ°		σ _x (Top/Bottom) -θ°		% error
	FEM	Semi-Analytical	FEM	Semi-Analytical	FEM	Semi-Analytical	FEM	Semi-Analytical	
0	10.91	10.91	0.61	0.61	10.91	10.91	10.91	10.91	0
30	15.47	15.47	0.81	0.81	8.53	8.53	8.53	8.53	0
45	21.64	21.64	1.13	1.13	5.28	5.28	5.28	5.28	0
60	26.59	26.59	1.44	1.44	2.65	2.65	2.65	2.65	0
90	28.50	28.50	1.61	1.61	1.61	1.61	1.61	1.61	0
Stacking sequence [0/90/θ/- θ] _s	σ _y (Top/Bottom) 0°		σ _y (Top/Bottom) 90°		σ _y (Top/Bottom) θ°		σ _y (Top/Bottom) -θ°		% error
	FEM	Semi-Analytical	FEM	Semi-Analytical	FEM	Semi-Analytical	FEM	Semi-Analytical	
	0°	0.14	0.14	-0.42	-0.42	0.14	0.14	0.14	0.14
30°	-0.01	-0.01	-4.34	-4.34	2.18	2.18	2.18	2.18	0
45°	-0.02	-0.02	-6.09	-6.09	3.06	3.06	3.06	3.06	0
60°	0.16	0.16	-4.16	-4.16	2.00	2.00	2.00	2.00	0
90°	0.42	0.42	-0.14	-0.14	-0.14	-0.14	-0.14	-0.14	0
Stacking sequence [0/90/θ/- θ] _s	τ _{xy} (Top/Bottom) 0°		τ _{xy} (Top/Bottom) 90°		τ _{xy} (Top/Bottom) θ°		τ _{xy} (Top/Bottom)- θ°		% error
	FEM	Semi-Analytical	FEM	Semi-Analytical	FEM	Semi-Analytical	FEM	Semi-Analytical	
	0	0.00	0.00	0.00	0.00	0.00	0.00	0.00	0.00
30	0.00	0.00	0.00	0.00	4.13	4.13	-4.13	-4.13	0
45	0.00	0.00	0.00	0.00	3.61	3.61	-3.61	-3.61	0
60	0.00	0.00	0.00	0.00	1.57	1.57	-1.57	-1.57	0
90	0.00	0.00	0.00	0.00	0.00	0.00	0.00	0.00	0

5.2.4.2 Effect of orientation angle

The models as described above are further extended to study the effect of orientation angle on stress and deflection. Tables 5.6 and 5.8 show the effects of orientation angle on local and global stress, respectively, for symmetric angle ply laminates under in plane load in the x direction. Tables 5.7 and 5.9 show the effects of orientation angle on local and global stress respectively, for symmetric cross ply laminates under in plane load in x direction. Figure 5.5 shows that local stress decreases from 0° to 90° with a minimum and maximum deflection at 90° and 0° respectively, for stress in the ‘1’ direction in local coordinate systems, and the opposite case takes place for stress in the ‘2’ direction. Whereas the global stresses in the x

direction remain constant from 0° to 90° and in the y direction is zero for all orientation angles because the load is applied in the x direction only. A FEM model is used to find the deflection in the x direction for different orientation angles. Figures 5.6 and 5.7 show that the deflection increases as the orientation angle increases from 0° to 90° with a minimum and maximum deflection of 0° and 90° respectively. Fig 5.10 shows the deflection in the x direction for a symmetric angle ply laminate $[30/-30]_s$ in FEM (ANSYS) for loading in the x direction. The colour code represent the deflection at various section of laminate. From the discussion 5.2.4.2 and figures 5.5, it may be conclude that local stress decreases from 0 to 90 degree with a minimum and maximum deflection at 90 and 0 degree respectively, for stress in the ‘1’ direction in local coordinate systems, and maximum stress is obtained at 30 degree angle and the opposite case happened for stress in direction “2” with minimum stress obtained at 30 degree. The opposite case will happen, if the problem of composite laminate under in plane tensile load in y direction is studied. Therefore, it may be concluding that the optimum orientation angle is 30 degree, because at this angle stress is maximum or minimum. Whereas for deflection in x direction or in y direction depending on applied load, (fig 5.6 & fig 5.7) the deflection rises sharply after 30 degree angle starting from minimum at 0 degree and maximum at 90 degree. Therefore the optimum angle is 30 degree because after that angle stress rises sharply. The model may be extended further for other loading conditions i.e. $N_y \neq 0, N_x = N_{xy} = 0$ or $N_{xy} \neq 0, N_x = N_y = 0$ or $N_x \neq N_y \neq 0, N_{xy} = 0$.

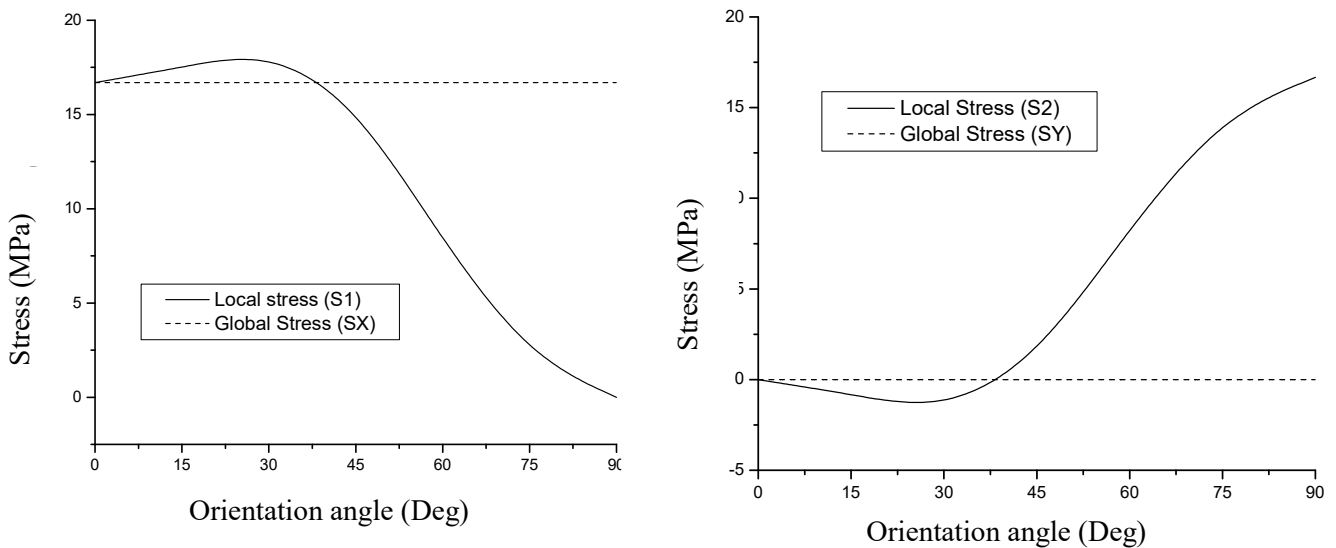


Figure 5.5 Effect of orientation angle on local and global stress for different orientation angle $[+\theta/-\theta]_s$ for loading in x direction

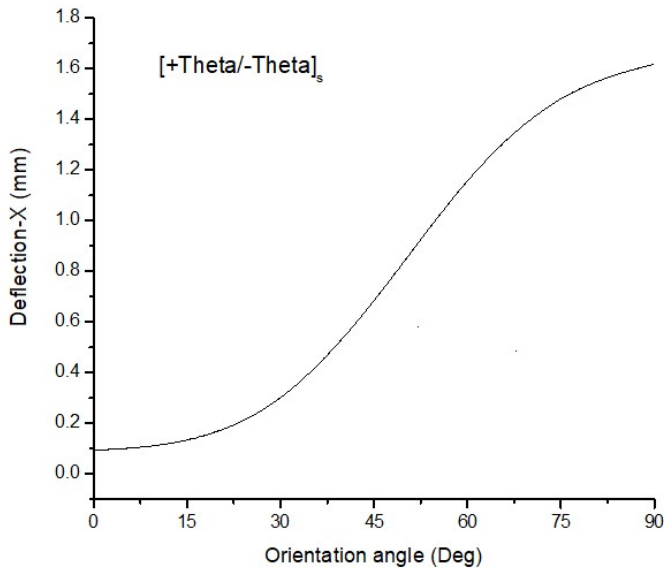


Figure 5.6 Effect of orientation angle on deflection-x (Deflection in x direction) for different orientation angle. $[+\theta/-\theta]_s$ for loading in x direction.

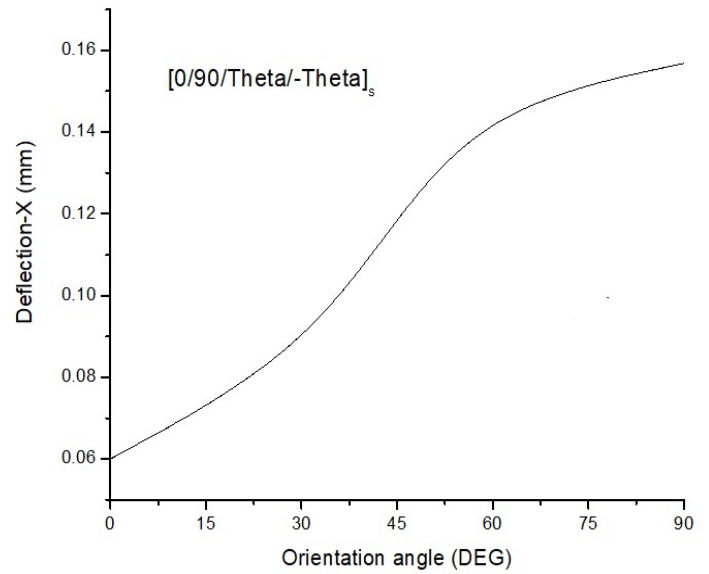


Figure 5.7 Effect of orientation angle on deflection-x for different orientation angle. $[0/90/+\theta/-\theta]_s$ for loading in x direction

5.2.4.3 Effect of length to thickness ratio (a/h)

Both deflection and stress increase (fig 5.8) with the increase in length to thickness ratio (a/h). As the a/h ratio increases, the thickness of the laminate decreases, and therefore stress and deflection increase.

5.2.4.4 Effect of No. of Lamina

From figs 5.9a and 5.9b, it is seen that stress and deflection decrease with the increase in the number of lamina within the laminate. Because with the increase in the number of the lamina, the thickness of laminate increases, so deflection and stress decrease.

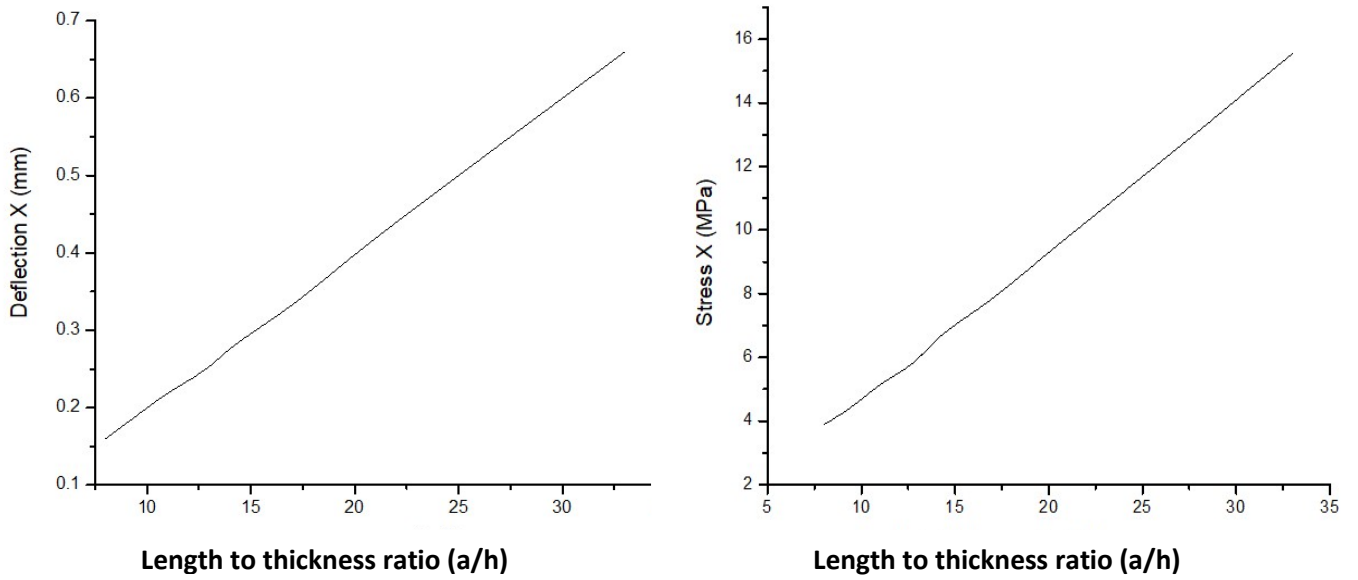


Figure 5.8 Effect of Length to thickness ratio (a/h) on deflection in x direction (Deflection x) and Global Stress in x direction (Stress x)

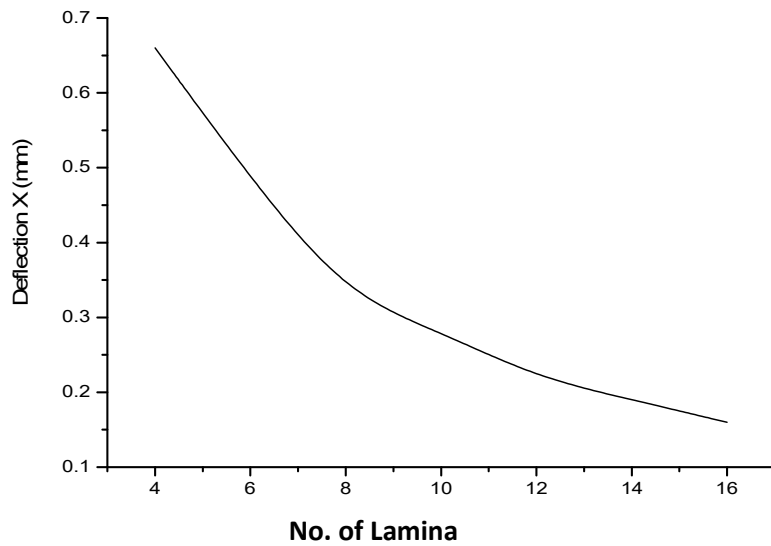


Figure 5.9(a) Effect of no. of lamina on (Deflection x) deflection in x direction and Global Stress in x direction

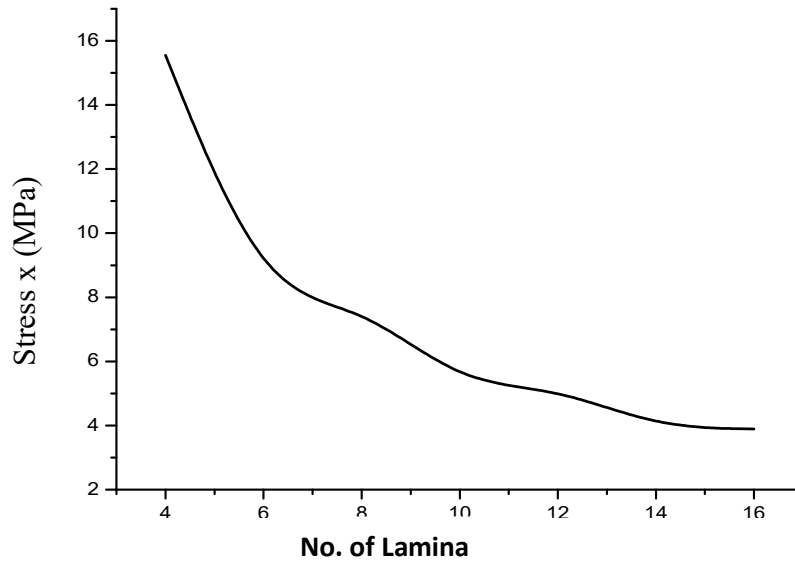


Figure 5.9 (b) Effect of no. of lamina on Global Stress in x direction (Stress x)

5.2.4.5 Symmetric Cross ply Laminate

The stress on the local and global coordinate systems is shown in table 5.10 for four layers symmetric cross ply laminate $[0/90/90/0]$ under loading in the x direction ($N_x = 100$ N/mm) using FEA software (FEM) and a semi analytical model. Stresses in two laminae 0° and 90° in the laminate $[0/90/90/0]$ above the mid plane are shown in table 5.10. Due to symmetry, the stresses in the other two lamina below the mid plane are the same, and therefore not shown in table 5.10. The displacement in the x direction obtained by both the methods is 0.174 mm. The percentage error of the two methods is zero. This concludes that both the methods yield the same result because the equations of laminate analysis are free from higher order terms and the solution of the equations involves simple matrix operations.

Table 5.10 Comparison of the Global stress from Semi analytical model with FEM for symmetric cross ply laminate.

Stacking sequence [0/90/90/0]	σ_1 (MPa)		σ_2 (MPa)		τ_{12} (MPa)		%age error
	FEM	Semi-Analytical	FEM	Semi-Analytical	FEM	Semi-Analytical	
	T/B	T/B	T/B	T/B	T/B	T/B	
0	31.55	31.55	0.45	0.45	0	0	0
90	-0.45	-0.45	1.78	1.78	0	0	0

	σ_x (MPa)		σ_y (MPa)		τ_{xy} (MPa)		
0	31.55	31.55	0.45	0.45	0	0	0
90	1.78	1.78	-0.45	-0.45	0	0	0

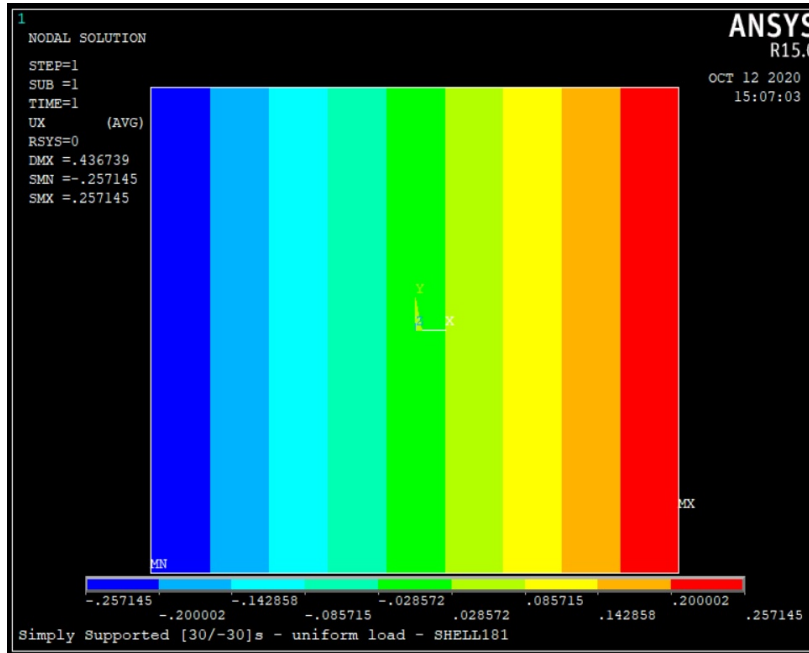


Figure 5.10 Deflection of symmetric angle ply laminate using ANSYS 15.0

5.2.5 Closure

A semi analytical model of single lamina and laminate under in-plane load is developed by laminate equations and solved by using the MATLAB tool. A FEM model of a single lamina and laminate under in-plane load is built and solved by FEA software ANSYS. Both the models are compared and good agreement is found because the equations of the lamina and laminate is free from higher order terms and can be easily solved without making many assumptions. Numerical problems on lamina and laminate are taken to compare the two methods and to study the effects of various parameters like orientation angle, length to thickness ratio, and the number of the lamina on stress and deflection. In the next chapter, a complex problem of laminated structure is discussed whose equations contain higher order terms.

CHAPTER 6

BENDING & BUCKLING OF LAMINATED COMPOSITE PLATE

A Bending of Laminated Composite plate under uniform transverse loading, 6.1. Classical Lamination Theory (CLT), 6.1.1. Governing equation of laminated plate using CLT, 6.1.2 Equation of motion, 6.2 Bending of Specially orthotropic simply supported plate, 6.2.1 The Navier Method, 6.3 Bending of Symmetric angle ply simply supported plate, 6.4 Semi-Analytical Model, 6.5 Finite Element Method, 6.6 Validation of the model, 6.7 Numerical Problem, 6.7.1 Convergence analysis, 6.7.2 Results and Discussion, 6.7.2.1 Effect of stacking sequence, 6.7.2.2 Effect of no. of plies, 6.7.2.3 Effect of length to thickness ratio, 6.8 Analysis of Percentage error of laminated composite Plate, 6.8.1 Thickness of lamina (or Ply), 6.8.2 Number of lamina (or ply) 6.8.3 Orientation angle (Stacking sequence), 6.8.4 Statistical Analysis of Percentage Error in deflection, 6.8.5 (a) Regression equation, 6.8.5 (b) Validation of model, 6.8.5 (c) Effect of Process Parameters, 6.8.6 Discussion, B Buckling of laminated Composite plate, 6.9 Semi-analytical Method, 6.10 Finite element method, 6.10.1 Convergence analysis, 6.11 Validation of models, 6.12 Numerical Problem, 6.12.1 Results & Discussion, 6.12.2 Effect of fiber orientation angle and number of lamina, 6.13 Closure

A Bending of Laminated Composite plate under uniform transverse loading

Deflection of laminated composite plate under transverse load can be found out by the semi analytical method and the result is compared with Finite element method using FEA software. Classical lamination theory is used to find the deflection by the semi analytical method. The semi analytical method is solved in MATLAB and the results are compared with FEA software.

6.1. Classical Lamination Theory (CLT)

Classical lamination theory, an extension of classical plate theory to composite laminate is based upon Kirchhoff's Hypothesis which states that, the transverse displacement does not depend upon transverse or thickness coordinate and transverse normal and shear strains are zero i.e. $\varepsilon_{zz} = \varepsilon_{xz} = \varepsilon_{yz} = 0$. (6.1)

Assumption of Classical lamination theory (CLT):

The assumptions of classical lamination theory are stated as [52]:

1. Each layer of the laminate is quasi-homogeneous and orthotropic.
2. The laminate is thin compared to the lateral dimensions and is loaded in its plane.

3. State of stress is plane stress.
4. All displacements are small compared to the laminate thickness.
5. Displacements are continuous throughout the laminate.
6. Straight lines normal to the middle surface remain straight and normal to that surface after deformation.
7. Transverse normal strain ϵ_z is negligible compared to the in-plane strains ϵ_x and ϵ_y .
8. Strain-displacement and stress-strain relations are linear.

6.1.1 Governing equation of laminated plate using CLT

Deflection of laminated composite plate under transverse load can be found out by the semi analytical method and the result is compared with Finite element method using FEA software. Classical lamination theory is used to find the deflection by the semi analytical method. The semi analytical method is solved in MATLAB and the results are compared with FEA software.

$$u(x, y, z, t) = u_0(x, y, t) - z \frac{\partial w_0}{\partial x}$$

$$v(x, y, z, t) = v_0(x, y, t) - z \frac{\partial w_0}{\partial y}$$

$$w(x, y, z, t) = w_0(x, y, t) \quad (6.2)$$

u^0, v^0 and w^0 are the displacements along the coordinate line in a material point in x - y plane and $\frac{\partial w_0}{\partial x}, \frac{\partial w_0}{\partial y}$ are the rotations about x and y axis respectively. If the mid-point displacement can be found, then the displacement at any point in the plate can be determined by the eq. 6.2.

6.1.2 Equation of motion

The three general equations which govern the response of laminated plates are as [55]:

$$\frac{\partial N_{xx}}{\partial x} + \frac{\partial N_{xy}}{\partial y} = I_0 \frac{\partial^2 u_0}{\partial t^2} - I_1 \frac{\partial^2}{\partial t^2} \left(\frac{\partial w_0}{\partial x} \right) \quad (6.3)$$

$$\frac{\partial N_{xy}}{\partial x} + \frac{\partial N_{yy}}{\partial y} = I_0 \frac{\partial^2 v_0}{\partial t^2} - I_1 \frac{\partial^2}{\partial t^2} \left(\frac{\partial w_0}{\partial y} \right) \quad (6.4)$$

$$\frac{\partial^2 M_{xx}}{\partial x^2} + 2 \frac{\partial^2 M_{xy}}{\partial y \partial x} + \frac{\partial^2 M_{yy}}{\partial y^2} + N(w_0) + q = I_0 \frac{\partial^2 w_0}{\partial t^2} - I_2 \frac{\partial^2}{\partial t^2} \left(\frac{\partial^2 w_0}{\partial x^2} + \frac{\partial^2 w_0}{\partial y^2} \right) + I_1 \frac{\partial^2}{\partial t^2} \left(\frac{\partial u_0}{\partial x} + \frac{\partial v_0}{\partial y} \right) \quad (6.5)$$

The terms I_0, I_1 & I_2 are the rotary inertia terms which are neglected for static equilibrium of the plate. The eq. of motion can be expressed in terms of displacement by substituting the force and moment resultant from the eq. 6.6 in Eq. 6.3 to 6.5 takes the form for homogenous laminate (eq.6.7-6.9).

$$\begin{bmatrix} \frac{\partial u_0}{\partial x} \\ \frac{\partial v_0}{\partial y} \\ \frac{\partial u_0}{\partial y} + \frac{\partial v_0}{\partial x} \\ -\frac{\partial^2 w_0}{\partial x^2} \\ -\frac{\partial^2 w_0}{\partial y^2} \\ -2\frac{\partial^2 w_0}{\partial x \partial y} \end{bmatrix} = \begin{bmatrix} A_{11} & A_{12} & A_{16} & B_{11} & B_{12} & B_{16} \\ A_{12} & A_{22} & A_{26} & B_{12} & B_{22} & B_{26} \\ A_{16} & A_{26} & A_{66} & B_{16} & B_{26} & B_{66} \\ B_{11} & B_{12} & B_{16} & D_{11} & D_{12} & D_{16} \\ B_{12} & B_{22} & B_{26} & D_{12} & D_{22} & D_{26} \\ B_{16} & B_{26} & B_{66} & D_{16} & D_{26} & D_{66} \end{bmatrix}^{-1} \begin{bmatrix} N_x \\ N_y \\ N_{xy} \\ M_x \\ M_y \\ M_{xy} \end{bmatrix} \quad (6.6)$$

$$\begin{aligned} & A_{11} \left(\frac{\partial^2 u_0}{\partial x^2} + \frac{\partial w_0}{\partial x} \frac{\partial^2 w_0}{\partial x^2} \right) + A_{12} \left(\frac{\partial^2 v_0}{\partial x \partial y} + \frac{\partial w_0}{\partial y} \frac{\partial^2 w_0}{\partial x \partial y} \right) + A_{16} \left(\frac{\partial^2 u_0}{\partial x \partial y} + \frac{\partial v_0}{\partial x^2} + \frac{\partial^2 w_0}{\partial x^2} \frac{\partial w_0}{\partial y} + \frac{\partial w_0}{\partial x} \frac{\partial^2 w_0}{\partial x \partial y} \right) - \\ & B_{11} \frac{\partial^3 w_0}{\partial x^3} - B_{12} \frac{\partial^3 w_0}{\partial x \partial y^2} - 2B_{16} \frac{\partial^3 w_0}{\partial x^2 \partial y} + A_{16} \left(\frac{\partial^2 u_0}{\partial x \partial y} + \frac{\partial w_0}{\partial x} \frac{\partial^2 w_0}{\partial x \partial y} \right) + \\ & A_{26} \left(\frac{\partial^2 v_0}{\partial y^2} + \frac{\partial w_0}{\partial y} \frac{\partial^2 w_0}{\partial y^2} \right) + A_{16} \left(\frac{\partial^2 u_0}{\partial x^2} + \frac{\partial w_0}{\partial x} \frac{\partial^2 w_0}{\partial x \partial y} \right) - B_{16} \frac{\partial^3 w_0}{\partial x^2 \partial y} - B_{26} \frac{\partial^3 w_0}{\partial y^3} - 2B_{66} \frac{\partial^3 w_0}{\partial x \partial y^2} - \\ & \left(\frac{\partial N_{xx}^T}{\partial x} + \frac{\partial N_{xy}^T}{\partial y} \right) = I_0 \frac{\partial^2 u_0}{\partial t^2} - I_1 \frac{\partial^3 w_0}{\partial x \partial t^2} \end{aligned} \quad (6.7)$$

$$\begin{aligned} & A_{16} \left(\frac{\partial^2 u_0}{\partial x^2} + \frac{\partial w_0}{\partial x} \frac{\partial^2 w_0}{\partial x^2} \right) + A_{26} \left(\frac{\partial^2 v_0}{\partial x \partial y} + \frac{\partial w_0}{\partial y} \frac{\partial^2 w_0}{\partial x \partial y} \right) + A_{66} \left(\frac{\partial^2 u_0}{\partial x \partial y} + \frac{\partial^2 v_0}{\partial x^2} + \frac{\partial^2 w_0}{\partial x^2} \frac{\partial w_0}{\partial y} + \frac{\partial w_0}{\partial x} \frac{\partial^2 w_0}{\partial x \partial y} \right) - \\ & B_{16} \frac{\partial^3 w_0}{\partial x^3} - B_{26} \frac{\partial^3 w_0}{\partial y^2 \partial x} - 2B_{66} \frac{\partial^3 w_0}{\partial x^2 \partial y} + A_{12} \left(\frac{\partial^2 u_0}{\partial x \partial y} + \frac{\partial w_0}{\partial x} \frac{\partial^2 w_0}{\partial x \partial y} \right) + A_{22} \left(\frac{\partial^2 v_0}{\partial y^2} + \frac{\partial w_0}{\partial y} \frac{\partial^2 w_0}{\partial y^2} \right) + \\ & A_{26} \left(\frac{\partial^2 u_0}{\partial y^2} + \frac{\partial^2 v_0}{\partial x \partial y} + \frac{\partial^2 w_0}{\partial x \partial y} \frac{\partial w_0}{\partial y} + \frac{\partial w_0}{\partial x} \frac{\partial^2 w_0}{\partial y^2} \right) - B_{12} \frac{\partial^3 w_0}{\partial x^2 \partial y} - B_{22} \frac{\partial^3 w_0}{\partial y^3} - 2B_{26} \frac{\partial^3 w_0}{\partial y^2 \partial x} - \left(\frac{\partial N_{xy}^T}{\partial x} + \right. \\ & \left. \frac{\partial N_{yy}^T}{\partial y} \right) = I_0 \frac{\partial^2 v_0}{\partial t^2} - I_1 \frac{\partial^3 w_0}{\partial y \partial t^2} \end{aligned} \quad (6.8)$$

$$\begin{aligned} & B_{11} \left(\frac{\partial^3 u_0}{\partial x^3} + \frac{\partial^2 w_0}{\partial x^2} \frac{\partial^2 w_0}{\partial x^2} + \frac{\partial w_0}{\partial x} \frac{\partial^3 w_0}{\partial x^3} \right) + B_{12} \left(\frac{\partial^3 v_0}{\partial x^2 \partial y} + \frac{\partial^2 w_0}{\partial x \partial y} \frac{\partial^2 w_0}{\partial x \partial y} + \frac{\partial w_0}{\partial y} \frac{\partial^3 w_0}{\partial x^2 \partial y} \right) + B_{16} \left(\frac{\partial^3 u_0}{\partial x^2 \partial y} + \right. \\ & \left. \frac{\partial^3 v_0}{\partial x^3} + \frac{\partial w_0}{\partial y} \frac{\partial^3 w_0}{\partial x^3} + 2\frac{\partial^2 w_0}{\partial x^2} \frac{\partial^2 w_0}{\partial x \partial y} + \frac{\partial w_0}{\partial x} \frac{\partial^3 w_0}{\partial x^2 \partial y} \right) - D_{11} \frac{\partial^4 w_0}{\partial x^4} - D_{12} \frac{\partial^4 w_0}{\partial x^2 \partial y^2} - 2D_{16} \frac{\partial^4 w_0}{\partial x^3 \partial y} + \\ & 2B_{16} \left(\frac{\partial^3 u_0}{\partial x^2 \partial y} + \frac{\partial^2 w_0}{\partial x^2} \frac{\partial^2 w_0}{\partial x \partial y} + \frac{\partial w_0}{\partial y} \frac{\partial^3 w_0}{\partial x^2 \partial y} \right) + 2B_{26} \left(\frac{\partial^3 v_0}{\partial y^2 \partial x} + \frac{\partial^2 w_0}{\partial y^2} \frac{\partial^2 w_0}{\partial x \partial y} + \frac{\partial w_0}{\partial y} \frac{\partial^3 w_0}{\partial y^2 \partial x} \right) + \\ & 2B_{66} \left(\frac{\partial^3 u_0}{\partial y^2 \partial x} + \frac{\partial^3 v_0}{\partial x^2 \partial y} + \frac{\partial w_0}{\partial y} \frac{\partial^3 w_0}{\partial x^2 \partial y} + \frac{\partial^2 w_0}{\partial x \partial y} \frac{\partial^2 w_0}{\partial x \partial y} + \frac{\partial^2 w_0}{\partial x^2} \frac{\partial^2 w_0}{\partial y^2} + \frac{\partial w_0}{\partial x} \frac{\partial^3 w_0}{\partial y^2 \partial x} \right) - 2D_{16} \frac{\partial^4 w_0}{\partial x^3 \partial y} - \\ & 2D_{26} \frac{\partial^4 w_0}{\partial y^3 \partial x} + 4D_{66} \frac{\partial^4 w_0}{\partial x^2 \partial y^2} + B_{12} \left(\frac{\partial^3 u_0}{\partial y^2 \partial x} + \frac{\partial^2 w_0}{\partial x \partial y} \frac{\partial^2 w_0}{\partial x \partial y} + \frac{\partial w_0}{\partial x} \frac{\partial^3 w_0}{\partial y^2 \partial x} \right) + B_{22} \left(\frac{\partial^3 u_0}{\partial y^3} + \frac{\partial^2 w_0}{\partial y^2} \frac{\partial^2 w_0}{\partial y^2} + \right. \end{aligned}$$

$$\begin{aligned}
& \frac{\partial w_0}{\partial y} \frac{\partial^3 w_0}{\partial y^3} + B_{26} \left(\frac{\partial^3 u_0}{\partial y^3} + \frac{\partial^3 v_0}{\partial y^2 \partial x} + \frac{\partial w_0}{\partial y} \frac{\partial^3 w_0}{\partial y^2 \partial x} + 2 \frac{\partial^2 w_0}{\partial y^2} \frac{\partial^2 w_0}{\partial x \partial y} + \frac{\partial w_0}{\partial x} \frac{\partial^3 w_0}{\partial y^3} \right) - D_{22} \frac{\partial^4 w_0}{\partial y^4} - \\
& D_{12} \frac{\partial^4 w_0}{\partial x^2 \partial y^2} - 2D_{26} \frac{\partial^4 w_0}{\partial y^3 \partial x} - \left(\frac{\partial^2 M_{xx}^T}{\partial x^2} + 2 \frac{\partial^2 M_{xy}^T}{\partial y \partial x} + \frac{\partial^2 M_{yy}^T}{\partial y^2} \right) + N(w_0) + q = I_0 \frac{\partial^2 w_0}{\partial t^2} - \\
& I_2 \frac{\partial^2}{\partial t^2} \left(\frac{\partial^2 w_0}{\partial x^2} + \frac{\partial^2 w_0}{\partial y^2} \right) + I_1 \frac{\partial^2}{\partial t^2} \left(\frac{\partial u_0}{\partial x} + \frac{\partial v_0}{\partial y} \right)
\end{aligned} \tag{6.9}$$

These are the general non linear equations which govern the response of laminated plate. The equations can be simplified depending on boundary conditions, lamination scheme, type of laminate etc.

6.2 Bending of Specially orthotropic simply supported plate

For static bending of specially orthotropic plates, coupling terms of the bending stiffness matrix (bending twisting coefficient and bending stretching coupling coefficient), D_{16} and D_{26} are taken zero. Also [B] matrix is zero for symmetric plate. The non linear terms are neglected to reduce the complexity. In the absence of thermal effects, in-plane forces, and moments, eq. 6.9 reduce to:

$$D_{11} \frac{\partial^4 w_0}{\partial x^4} + 2(D_{12} + 2D_{66}) \frac{\partial^4 w_0}{\partial x^2 \partial y^2} + D_{22} \frac{\partial^4 w_0}{\partial y^4} = q \tag{6.10}$$

In this paper, simply supported boundary conditions on all the four edges of the rectangular plate are considered for study. The boundary conditions are as:

$$\begin{aligned}
w_0(x, 0) = 0, w_0(x, b) = 0, w_0(0, y) = 0, w_0(a, y) = 0 \\
M_{xx}(0, y) = 0, M_{xx}(a, y) = 0, M_{yy}(x, 0) = 0, M_{yy}(x, b) = 0
\end{aligned} \tag{6.11}$$

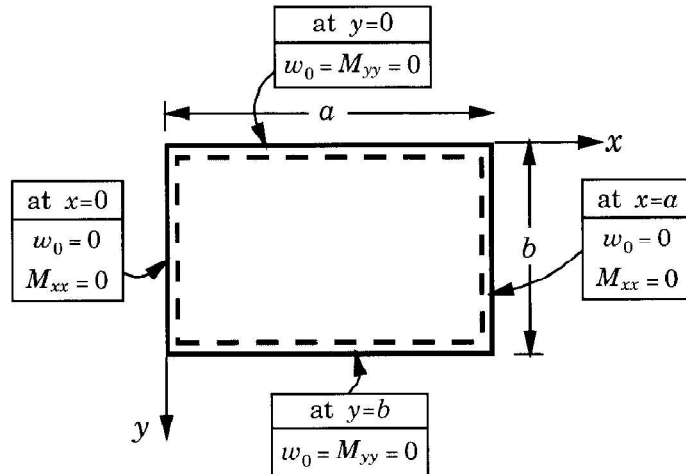


Figure 6.1 Boundary conditions of simply supported rectangular plate on all sides [3]

The equation 6.10 can be solved by Navier method, the Levy method with state space approach and Rayleigh-Ritz method. Navier solution is used for plate when all the edges are simply supported, whereas Levy method is used when two opposite edges are simply supported and the remaining edges have any possible combination of boundary conditions. The Rayleigh-Ritz method can be used to find out the approximate solution for more general boundary conditions. Fig 6.1 shows the dimension of plate and boundary condition of simply supported rectangular plate on all sides. i.e displacement and moment are constrained on all the sides.

6.2.1 The Navier Method

The Navier method uses double trigonometric series (Fourier) to solve the equations and the choice of trigonometric function depends on the boundary condition of the problem. The displacement and load are expanded as [55]:

$$w_0(x, y) = \sum_{n=1}^{\infty} \sum_{m=1}^{\infty} W_{mn} \sin \alpha x \sin \beta y \quad (6.12a)$$

$$q(x, y) = \sum_{n=1}^{\infty} \sum_{m=1}^{\infty} Q_{mn} \sin \alpha x \sin \beta y \quad (6.12b)$$

Where

$$Q_{mn} = \frac{4}{ab} \int_0^b \int_0^a q(x, y) \sin \alpha x \sin \beta y \, dx dy \quad (6.13)$$

$\alpha = \frac{m\pi}{a}$, $\beta = \frac{n\pi}{b}$ and W_{mn} are the coefficients to be determined such that governing equation 6.9 are satisfied. a and b are the dimension of plate (fig 6.1).

Substituting the expansions 6.8-6.10 in the governing equation 6.6 gives

$$\sum_{n=1}^{\infty} \sum_{m=1}^{\infty} \{-W_{mn} [D_{11}\alpha^4 + 2(D_{12} + 2D_{66})\alpha^2\beta^2 + D_{22}\beta^4] + Q_{mn}\} \sin \alpha x \sin \beta y = 0 \quad (6.14)$$

The solution of the equation becomes

$$w_0(x, y) = \sum_{n=1}^{\infty} \sum_{m=1}^{\infty} \frac{Q_{mn}}{d_{mn}} \sin \alpha x \sin \beta y \quad (6.15)$$

Where $d_{mn} = \frac{\pi^4}{b^4} [D_{11}m^4s^4 + 2(D_{12} + 2D_{66})(mns)^2 + D_{22}(ns)^4]$ and s denotes the aspect ratio $= \frac{a}{b}$. For any loading condition, load can be expressed as

$$q(x, y) = \sum_{n=1}^{\infty} \sum_{m=1}^{\infty} Q_{mn} \sin \alpha x \sin \beta y \quad (6.16)$$

Q_{mn} is the loading coefficient which depends upon the load. For uniformly distributed load $Q_{mn} = \frac{16q_0}{\pi^2 mn}$ for $m, n, \text{ odd}$, $q(x, y) = q_0$, a constant.

Substituting the value of Q_{mn} and d_{mn} in eq. 6.15, the deflection becomes

$$w(x, y) = \sum_{m=1}^{\infty} \sum_{n=1}^{\infty} \frac{16q_0 \sin \frac{m\pi x}{a} \sin \frac{n\pi y}{b}}{\pi^6 mn [D_{11} \left(\frac{m}{a}\right)^4 + 2(D_{12} + 2D_{66}) \left(\frac{m}{a}\right)^2 \left(\frac{n}{b}\right)^2 + D_{22} \left(\frac{n}{b}\right)^4]} \quad \text{where } m, n = 1, 3, 5, \dots \quad (6.17)$$

After simplification

$$w = \frac{a^4 Q_{mn}}{\pi^4 [D_{11} m^4 + 2(D_{12} + 2D_{66})(mns)^2 + D_{22}(ns)^4]} \quad (6.18)$$

Where $s = \frac{a}{b}$, plate aspect ratio.

6.3 Bending of Symmetric angle ply simply supported plate

For static bending of Symmetric angle ply plates, bending twisting coefficient and bending stretching coupling coefficient are not zero. Also [B] matrix is zero for symmetric plate. The non linear terms are neglected to reduce the complexity. In the absence of thermal effects, in-plane forces, and moments, eq. 6.9 reduce to:

$$D_{11} \frac{\partial^4 w_0}{\partial x^4} + 2(D_{12} + 2D_{66}) \frac{\partial^4 w_0}{\partial x^2 \partial y^2} + D_{22} \frac{\partial^4 w_0}{\partial y^4} + 4D_{16} \frac{\partial^4 w_0}{\partial x^3 \partial y} + 4D_{26} \frac{\partial^4 w_0}{\partial y^3 \partial x} = q \quad (6.19)$$

This eq. cannot be solved by Navier solution because separations of variables are not possible and the Fourier expansion does not satisfy the eq. 6.19. The alternative method to solve the problem is the Rayleigh-Ritz Method which is based on the principal of total potential energy.

The total potential energy of the laminated plate is given by [56]

$$V = \iint (D_{11} \frac{\partial^4 w^0}{\partial x^4} + 2D_{12} \frac{\partial^4 w^0}{\partial x^2 \partial y^2} + D_{22} \frac{\partial^4 w^0}{\partial y^4} + 4D_{66} \left(\frac{\partial^2 w^0}{\partial x \partial y} \right)^2 + 4D_{16} \frac{\partial^4 w^0}{\partial x^3 \partial y} + 4D_{26} \frac{\partial^4 w^0}{\partial y^3 \partial x} - 2pw) dx dy \quad (6.20)$$

Deflection of the laminated plate by the Rayleigh-Ritz Method is given by [56]

$$w = \sum_{n=1}^{\infty} \sum_{m=1}^{\infty} C_{ij} \sin \frac{m\pi x}{a} \sin \frac{n\pi y}{b} \quad (6.21)$$

Where C_{ij} are the coefficients to be determined. Integrating the eq. 6.20 yield an equation which contain $m \cdot n$ unknown coefficient. Total potential energy principle is used to solve the

eq. which yields $m \times n$ equations with a single unknown in each eq. After solving all the equations using any computing software, deflection is find out.

6.4 Semi-Analytical Method

A semi-analytical method of laminated composite plate simply supported on all the sides subjected to UDL transverse load is built up in mathematical tool, MATLAB and MAPPLE using the equations of 6.18 for the specially orthotropic plate and 6.21 for symmetric angle ply plate. First five material properties are entered for each layer because of plane stress assumptions for simplification of calculation. Compliance matrix S_{ij} is calculated for each layer. Then Stiffness matrix $[\overline{Q}_{ij}]$ is calculated for each layer by transforming and inverting a compliance matrix. Then program code calculates the distance h from the mid-plane. Then, using h and $[\overline{Q}_{ij}]$, bending stiffness matrix $[D]$ is calculated by the eq. 3.18. Then the deflection function of Navier and Rayleigh-Ritz method is calculated from the eq.6.18 and 6.21 using $[D]$ matrix respectively.

6.5 Finite Element Method

A finite element model of laminated composite plate simply supported on all the sides subjected to UDL transverse load is built up in FEA software, ANSYS. Due to symmetry, a quarter of the plate is modeled using SHELL 281 element. The model is meshed with quadrilateral mapped meshing. Simply supported boundary condition is applied on two adjacent sides of quarter of plate and symmetric condition is applied on the other two adjacent sides. Uniform pressure load is applied on the top sides of the plate and the model is solved in solution phase. Transverse deflection is noted in post processor phase for different stacking sequence. Convergence analysis is performed to determine the solution which is mesh independent. Fig 6.3a and 6.3b show the boundary conditions, quadrilateral mapped meshing and uniform pressure loading of the simply supported plate in ANSYS. Fig 6.3c shows the variation of deflection of $[30/-30]$ s simply supported plate under uniform pressure loading for quarter of geometry of plate.

6.6 Validation of the models

The model built up by semi-analytical method using Navier method solved by MATLAB tool is validated with the published literature of M.A Manahan [55] and the model built up by Finite

element method of laminated composite plate under transverse load as discussed above is validated with Manahan [55] in table 6.1. The semi-analytical models prepared by Rayleigh-Ritz method using MAPLE tool is validated with the published literature of Kenneth Carroll [56] in table 6.2.

Table 6.1 Validation of model with published literature Manahan (2011) [55]

Stacking sequence	Mesh size	FEM deflection (m)		Navier Method deflection (m)		% error of FEM & Navier Method		Bending coefficient (N-m)	
		Manahan	Present	Manahan	Present	Manahan	Present	D ₁₆	D ₂₆
[0 90] _s (specially symmetric Orthotropic)	20 mm x 20 mm	0.0681	0.0682	0.0680	0.0680	0.1468	0.232	0.00	0.00
[60 90] _s (Sym Angle ply)		0.1165	0.1170	0.0436	0.0436	62.5751	62.73	193.8	565.8

Table 6.2 Validation of model with published literature of Kenneth Carroll (2013) [56]

Stacking sequence	Rayleigh-Ritz Method deflection (in)	
	Caroll	Present
[0 90 0 90] _s (specially symmetric Orthotropic)	0.7146	0.7146
[+/- 45 0 +/- 45] _s (Sym Angle ply)	0.1304	0.1304

6.7 Numerical Problem

A fiber reinforced laminated composite square plate of length to width ratio of unity, simply supported on all the sides is considered. The plate is, subjected to a pressure of 1 N/m² on the top surface. The laminae are stacked together symmetrically about the mid plane and the fibers are oriented at different orientation angle. Two type of stacking sequence is considered: symmetric cross ply and angle ply arrangement. The thickness of each lamina is 5mm. The material used is graphite- epoxy composite material (table 5.1). Deflection is found out by semi analytical method and FEM and both the methods are compared. Effect of number of lamina, length to thickness ratio and orientation angle are studied.

The model of semi analytical method and FEM as discussed above is used to solve the numerical problem for four ply simply supported symmetric angle ply laminated composite plate under uniform pressure on top surface for orientation angles ranging from 0° to 90° . For symmetric angle ply laminated plate stacking sequence of $[\theta/-\theta]_s$ is represented by orientation angle “ θ ” in the y -axis. For example stacking sequence of $[45/-45]_s$ is represented by 45° (orientation angle). Deflection is found out by using Navier and Rayleigh-Ritz method and compared with the results from FEM by using FEA software ANSYS. Percentage error is noted for each orientation angle. Also bending coefficient is determined for different orientation angle.

6.7.1 Convergence analysis

A convergence analysis is conducted in FEA software to finalize the size of the mesh. Convergence analysis is done by running the FEA code for different mesh size until a size of mesh is obtained at which same result is repeated. In this thesis, model is first validated with published literature for 20×20 mesh size which is mentioned in the literature. Now a convergence analysis is performed with ANSYS, to find out the exact mesh size at which result is repeated. From table 6.3 and fig 6.2, it is seen that after 40×40 mesh size same result is repeated. Therefore, at 40×40 mesh size, a converged result is obtained.

Table 6.3 Convergence analysis for different mesh size

Mesh size	FEM deflection (m)
10 x10	0.01983
20 x 20	0.02005
30 x 30	0.02013
40 x 40	0.02018
50 x 50	0.02018

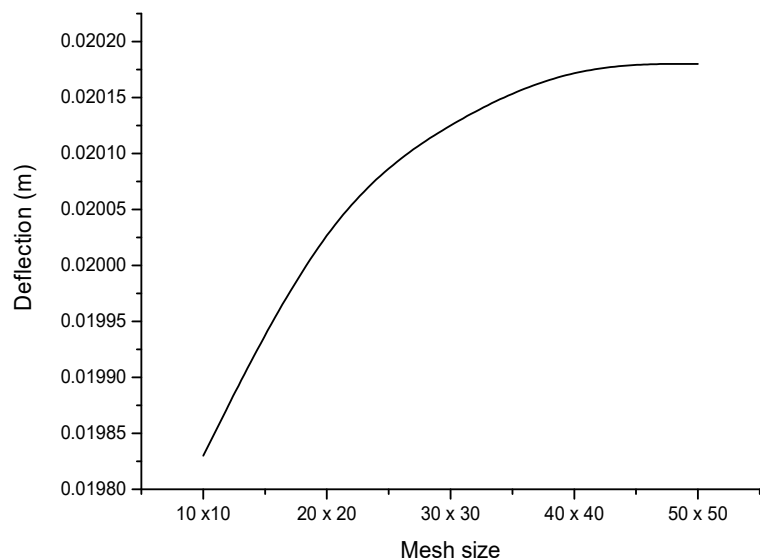


Figure 6.2 Convergence analyses for different mesh size

Rayleigh- Ritz method solves $m * n$ equations with $m * n$ unknown coefficients using matrix elimination method. Therefore the solution of the Rayleigh-Ritz method depends on the number of equations chosen for the solution. So to make the solution independent of the numbers of equations, convergence analysis are performed shown in table 6.4. So it is found out from the table that after the number of equations 49, same results are obtained, which states that the number of equations at which results converge is 49 ($m = n = 7$).

Table 6.4 Rayleigh- Ritz method coefficients

m, n	No. of equations.	Results (m)
2	4	0.0526
3	9	0.0549
4	16	0.0560
7	49	0.0570
8	64	0.0570

6.7.2 Results and Discussion

Deflection of simply supported composite plate determined using Navier Method and Rayleigh-Ritz method is compared with FEA software results for symmetric angle ply composite (table 6.5). It is found from the table 6.5 that the percentage error of Navier and Rayleigh method with FEA results is within acceptable limit for 0° and 90° but it exceeds the limit for other angles. The percentage error first increases from 0° to 45° , maximum at 45° and then decreases up to 90° . Maximum error occurs at 45° and minimum at 0° and 90° . This is due to the reason that coefficients D_{16} and D_{26} are zero for 0° and 90° . Also the coefficient varies in the same way as that of percentage error, i.e. as the error increases coefficient increases and decreases as they decrease which inferred that percentage error depends on the value of coefficient. Also the percentage error of Rayleigh- Ritz method is less as compared to Navier method for all the angles except 0° and 90° . This is because 0° and 90° are considered under specially orthotropic composite (cross ply composite). Therefore one of the ways to reduce the error may be by reducing the value of D_{16} and D_{26} coefficients. Navier method takes D_{16} and D_{26} coefficients as zero to solve the equations whereas Rayleigh-Ritz method considers the coefficient as non zero. That is why the percentage error of Navier method is greater than Rayleigh-Ritz method for all angles of angle ply composite except 0° and 90° whose D_{16} and

D_{26} are zeros. Manahan in his paper discussed how to reduce the error by reducing the coefficients by changing the stacking sequence and number of ply but he did not discuss in detail the dependability of error percentage on different factors i.e. laminate thickness, orientation angle, number of ply and mesh size. Whereas Carroll in his paper finds out the percentage error, but the dependability of percentage error on different factors were absent. For cross ply laminate bending coefficients are zero, therefore eq. 6.10 can be used to determine the deflection which is solved by Navier method because eq. 6.10 is taken by assuming the bending coefficient zero. From table 6.5, it is found that the percentage error of Navier method with FEA is zero for cross ply laminate and angle ply laminate of 0° and 90° , which shows that eq. 6.10 is effective to solve cross ply laminate and 0° and 90° angle ply laminate because they come under specially orthotropic laminate (Bending coefficient is zero). But in eq. 6.19 which is formed by considering bending coefficient, is used to solve cross ply laminate, it is found that the percentage error is 2.9 % which is below 5 %, therefore acceptable. But eq. 6.10 is more effective in solving cross ply laminate. For angle ply laminate, opposite thing happened because, bending coefficient are not zero. But using eq. 6.19 for angle ply, percentage error is reduced but not acceptable because error is greater than 5%. This may be due to the reason that, eq. 6.19 solved by Rayleigh-Ritz method gives approximate solution because, its solution depends on number of equations and it solved equations by matrix elimination method. Therefore semi analytical method formed by classical lamination theory (CLT) solved by Navier method and Rayleigh-Ritz method gives an approximate solution to problems of laminated composite plate under uniform pressure because the equations for different stacking arrangement (angle ply, cross ply laminate etc.) is derived from general plate equations by assuming some assumptions which is based upon different factors like stacking arrangement, symmetric or non symmetric conditions etc. The equations are solved by different methods like Navier method, Rayleigh-Ritz method etc. which gives an approximate solution because they solve the equations by Fourier expansion, matrix elimination etc. Also they neglect the higher order terms for simplification. So, all these assumptions make the solution approximate and dependent on different factors which are taken for solution. To study the deviation of analytical results from the actual, they are compared with FEM, and percentage error is found out. Therefore from the above discussion it may be conferred that the percentage error also depends on the above factors. The study of percentage error is discussed in next section.

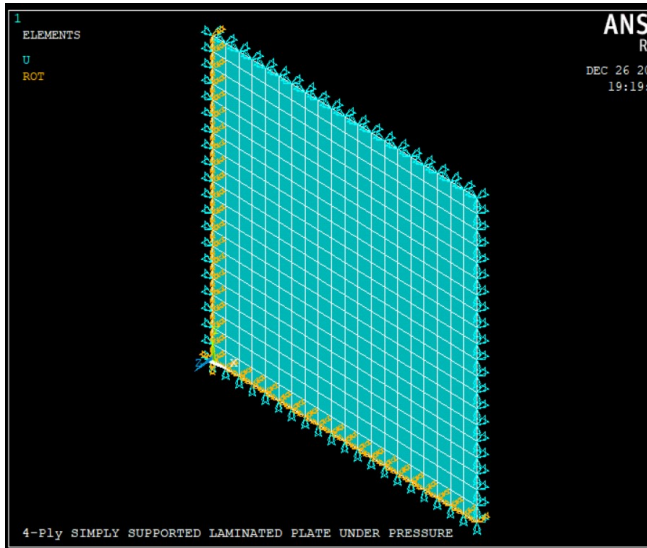


Figure 6.3(a) Boundary conditions of the quarter of plate simply supported on all the sides

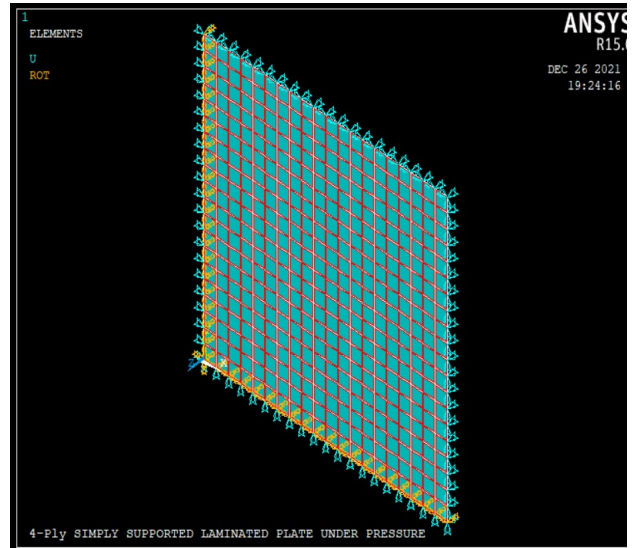


Figure 6.3(b) Uniform pressure loading of the quarter of plate simply supported on all the sides

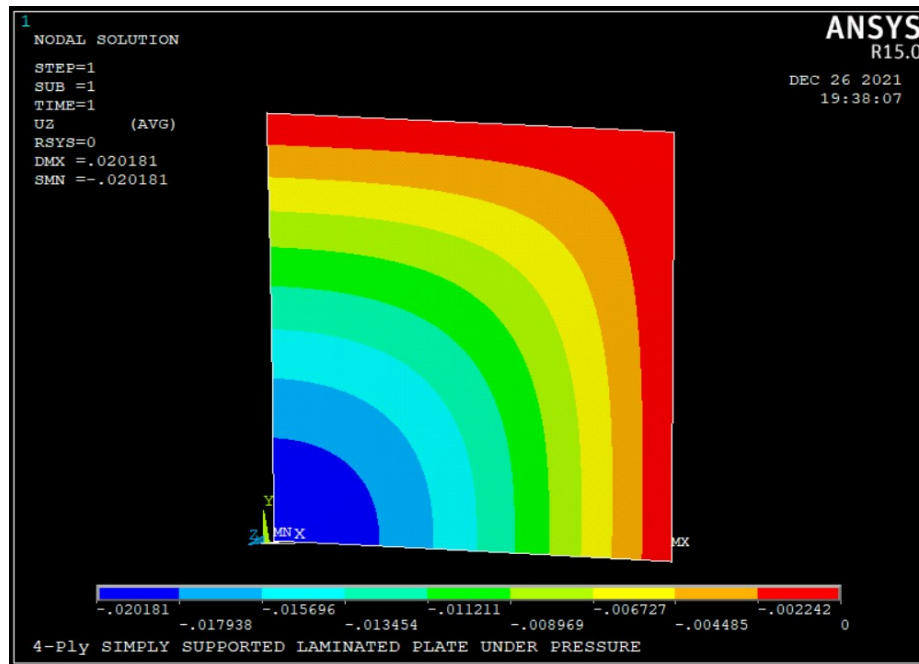


Figure 6.3(c) Deflection of $[+30/-30]_s$ of the quarter of composite plate

Table 6.5 Comparison of Semi analytical method and FEM for Symmetric angle plies composite plate simply supported on all the sides under transverse uniform pressure.

Angle Orientation [+ θ /- θ] _s	Semi-Analytical Method		Deflection (m) (FEM)	Bending Coefficient		Percentage Error	
	Deflection (m) (Navier Method)	Deflection (m) (Rayleigh- Ritz Method)		D16 (N- m)	D26 (N- m)	Navier method with FEM	Rayleigh- Ritz method with FEM
0	0.0166	0.0177	0.0166	0	0	0.00	6.33
15	0.0143	0.0160	0.0211	1.93e4	2.18e3	32.13	24.20
30	0.0112	0.0131	0.0202	2.71e4	1.00e4	44.50	35.28
45	0.0101	0.0119	0.0188	2.14e4	2.14e4	46.39	37.10
60	0.0112	0.0131	0.0202	1.00e4	2.71e4	44.42	35.19
75	0.0143	0.0160	0.0211	2.18e3	1.93e4	32.09	24.11
90	0.0166	0.0177	0.0166	0	0	0.29	6.02
Symmetric Crossply							
[90/0] _s	0.0171	0.0176	0.0171	0	0	0	2.9

6.7.2.1 Effect of stacking sequence (Orientation angle)

The model is now extended to study the effect of orientation angle on the deflection of simply supported composite plates for symmetric angle ply plates of stacking sequence (orientation angle) of [+ θ /- θ]_s (fig 6.4) in table 6.5. Maximum deflection takes place at of [+0/-0]_s and [+90/-90]_s orientation angle. Minimum deflection occurs at a 45° angle ([+45/-45]_s). The deflection decreases as the orientation angle increases and becomes minimum at 45° angle, then increases and becomes maximum at 90°angle (fig 6.4). For representation [+ θ /- θ]_s, is represented by θ in the y axis of fig 6.4.

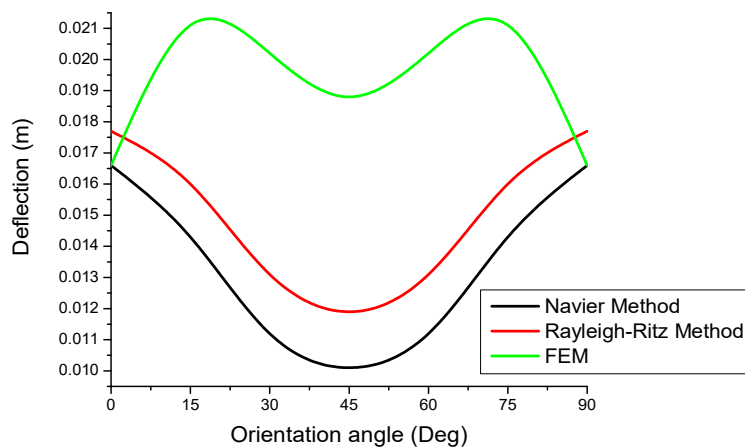


Figure 6.4 Variation of deflection with orientation angle for different methods

6.7.2.2 Effect of no. of ply (Lamina)

The model is further extended to study the effect of a number of plies or lamina on the deflection of simply supported plate. From the fig 6.5 (a) and fig 6.5 (b) it is seen that deflection decreases as the number of plies increases for both symmetric angle ply and cross ply composite. For cross ply composite it is seen from the fig 6.5 (b) that the results of the three method are almost same, due to the reason as discussed above. The bending coefficients D_{16} and D_{26} are zeros.

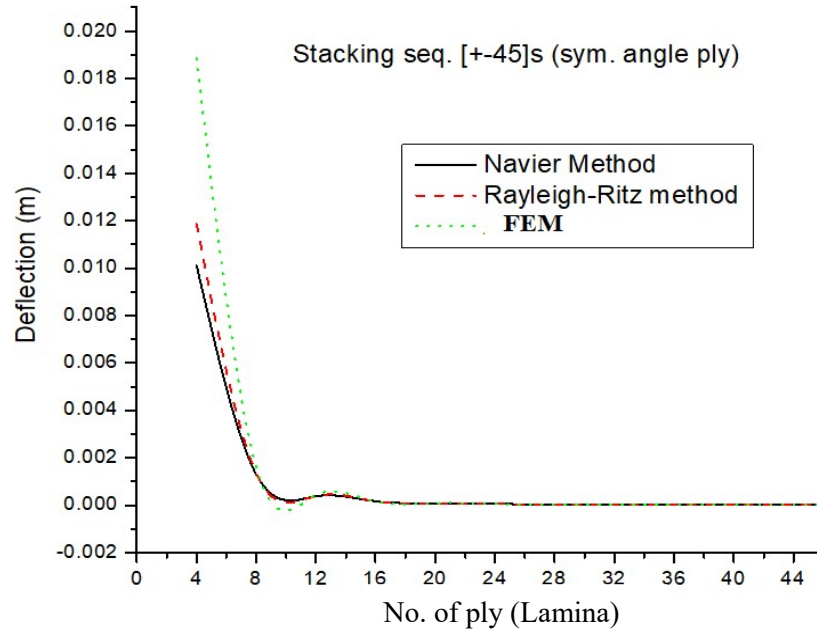


Figure 6.5 (a) variation of deflection with no. of plies for sym. Angle ply composite.

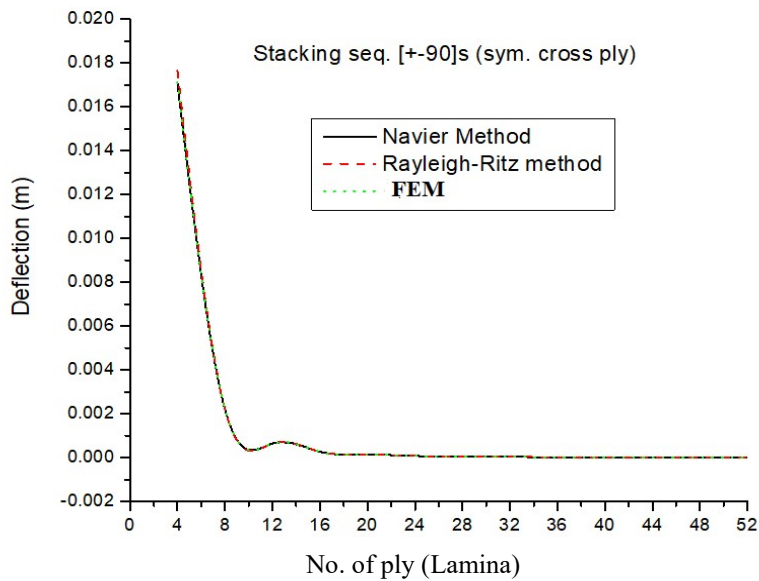


Figure 6.5 (b) variation of deflection with no. of plies for sym. cross ply composite.

6.7.2.3 Effect of length to thickness ratio

Fig 6.6 shows that as the length to thickness ratio increases, deflection of the plate increases. Length to thickness ratio increases can be varied in two ways: keeping the thickness constant and vary the length or vice versa. When thickness is kept constant and length is increased, ratio increases at the same time deflection also increases. On the other hand, when the length is kept constant and thickness decreases, ratio increases and deflection increases. It shows that deflection increases with the increase in length of the plate and decrease in thickness of the plate.

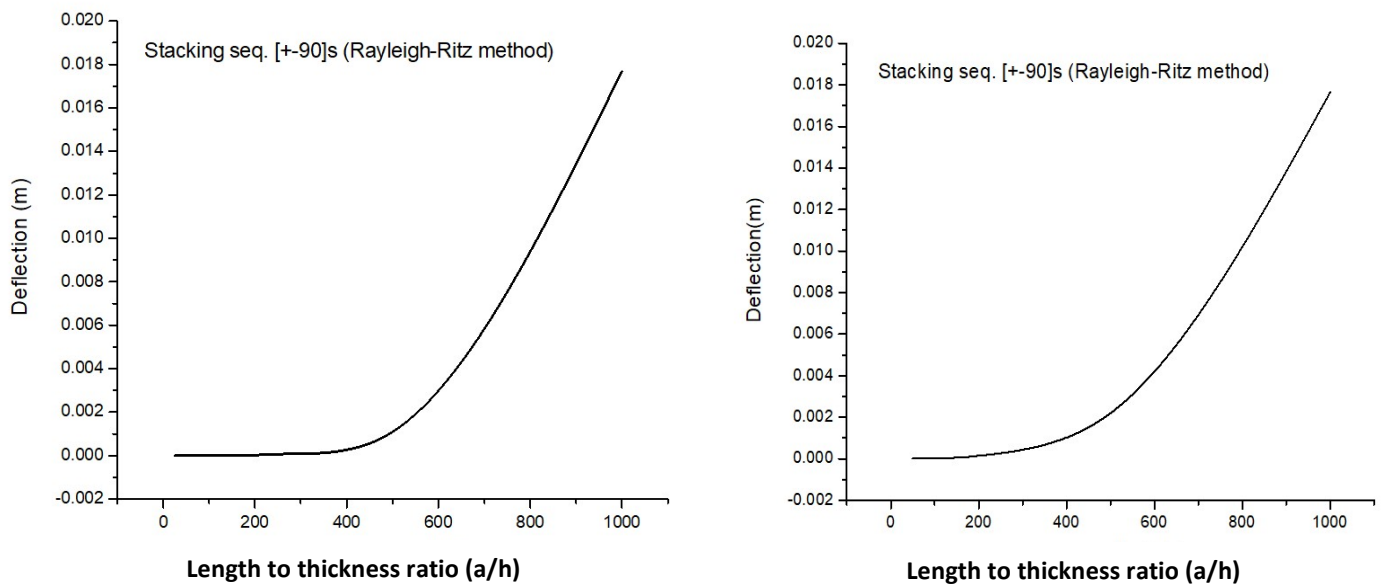


Figure 6.6 Variation of deflection with length to thickness ratio using two ways: Keeping thickness constant, length varies (left) and length constant, thickness varies (right).

6.8 Analysis of Percentage error of laminated composite Plate

As discussed above, the results from FEM are compared with semi-analytical method (Navier Method) solved in MATLAB platform for different orientation angles (or stacking sequence), thickness of the lamina, no. of ply or lamina for simply supported laminated symmetric angle ply composite plate under the uniform distributed load. As discussed above stacking sequence of symmetric angle ply laminate of $[\theta/-\theta]_s$ is represented by “ θ ” (orientation angle) in this thesis. Percentage error is the difference in the results of FEM (FEA software) with semi-analytical method with respect to semi-analytical results. In the above discussion, it is seen that

deflection depends on the number of lamina or ply, thickness of the lamina and orientation angle. The variable Length to width ratio is not considered because square laminated plate ($L/W=1$) is taken for analysis and mesh size is eliminated in the present analysis by convergence. The effect of these variables on %age error is discussed in this section to determine the significance of the variables in reducing the percentage error.

6.8.1 Thickness of lamina (or Ply)

The variation of percentage error in thickness per lamina is investigated keeping the other factors constant i.e. orientation angle and number of lamina. From the table 6.6 and fig 6.7, it is seen that the effect of thickness per lamina is very less significant on %age error because the variation of the graph is almost constant. The significance of thickness per lamina is studied for different orientation angle and number of lamina by ANOVA and its relation with %age error is established by regression analysis in the next section for detailed investigation.

6.8.2 Number of Lamina (or Ply)

Another important variable is the number of lamina (or ply). The significance of this variable is studied keeping the other variable viz. Orientation angle and thickness per ply constant. From the fig 6.8 and table 6.7 it is seen that no. of lamina has a significant effect on %age error. As the no. of lamina increases %age error decreases. It shows a sharp decrease from 4 to 8 and after 8, the variation in curve is less. Since the thickness per lamina is constant, the increase in the number of lamina increases the laminate thickness. Therefore, in other words, it may be say that as the laminate thickness increases, % error decreases which are already seen in the case of beam in the previous section.

Table 6.6 Effect of thickness per lamina for 4 ply square plate ($L/W=1$), angle= $[45/-45]$ s

Sl. No.	Thickness of Lamina (m)	% Error
1	0.00125	41.59
2	0.0025	41.61
3	0.00375	42.02
4	0.005	41.58
5	0.00625	43.53
6	0.0075	41.53
7	0.00875	40.95
8	0.01	38.46

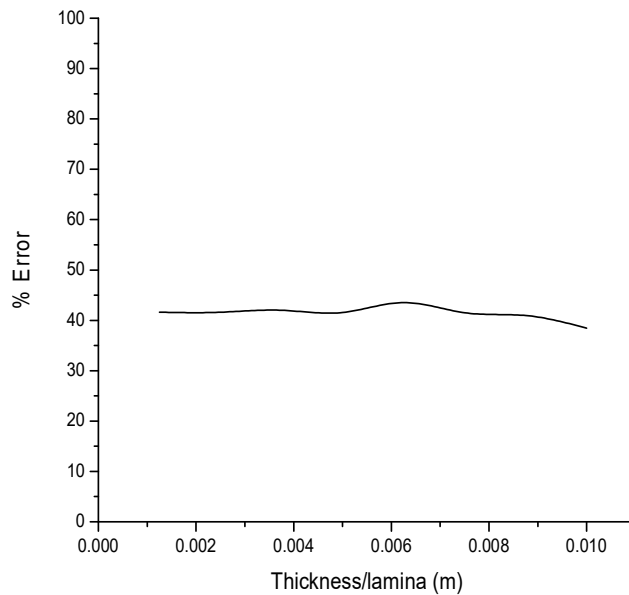


Figure 6.7 Variation of thickness per lamina with % error for 4 ply, 45 deg angle square plate subjected to transverse load of 1 N/m

Table 6.7 Effect of No. of lamina for square plate (L/W=1), angle= [45/-45]s, thickness/lamina is 5mm

Sl. No.	Thickness per Lamina (m)	% Error
1	0.00125	41.59
2	0.0025	41.61
3	0.00375	42.02
4	0.005	41.58
5	0.00625	43.53
6	0.0075	41.53
7	0.00875	40.95
8	0.01	38.46

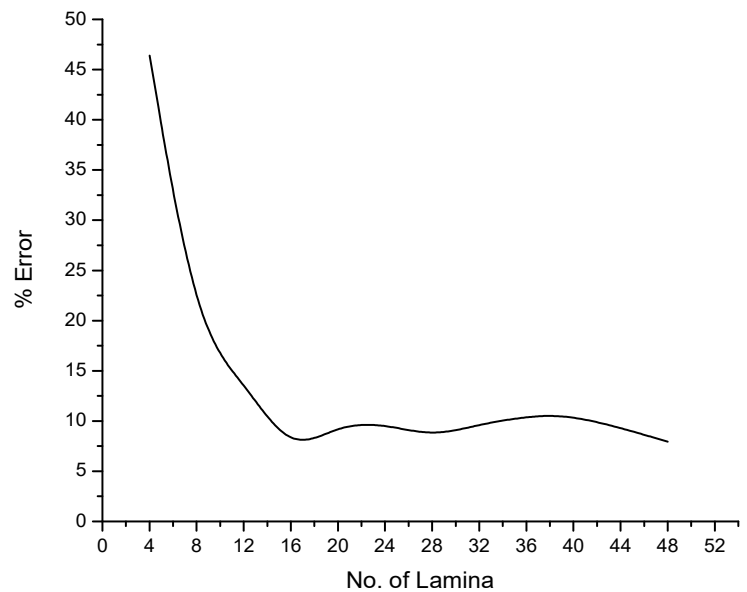


Figure 6.8 Variation of No. of lamina with % error for 45 deg angle square plate subjected to transverse load of 1 N/m

6.8.3 Orientation angle (Stacking sequence)

Another important variable is orientation angle. In this section symmetric arrangement of angle ply laminated composite plate is taken. As seen in the chapter 6, the percentage error varies as the orientation angle changes from 0 deg to 90 deg. From the graph fig 6.9 it is seen that for angle 0 deg and 90 deg, the %age error is zero because the bending stiffness D16 and D26 is

zero as discussed above in details. Also it is found that the curve first increases as the angle increases up to 45 deg and then decreases to zero at 90 deg. Therefore 45 deg angle poses the highest %age error. So while selecting the levels for ANOVA statistical analysis, angle 0 deg and 90 deg are excluded because %age error is negligible.

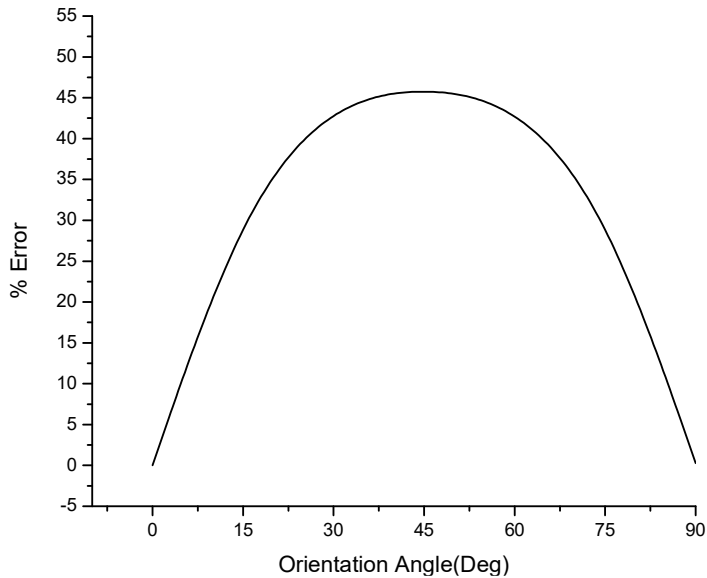


Figure 6.9 Variation of Orientation angle with %age error for square plate subjected to transverse load of 1 N/m of thickness per lamina of 5mm.

6.8.4 Statistical Analysis of Percentage Error in deflection

To understand the effect of these variables, No. of Lamina (A), thickness per lamina (B) and orientation angle (C) on percentage error (E), data from the table 6.8 are analyzed using analysis of variance (ANOVA) statistical tool. Three levels of these variables are chosen for creating an ANOVA table (table 6.9). In this analysis, No. of Lamina (A), thickness per lamina (B) and orientation angle (C) is independent variables whereas percentage error (E) is dependent variable or response factor. The significance level was based on the P-value, i.e. Significant if $P < 0.05$ and insignificant for $P > 0.05$ (5% significance level or 95% confidence level). MATLAB tool is used to solve the ANOVA table.

Both one way and two ways ANOVA test is conducted on response variable: percentage error and the output are presented in table 6.10 and 6.11 respectively. In both the tables it is found that the variable thickness per lamina is insignificant with probability greater than 5%. The

variable number of the lamina and orientation angle is significant with probability of zero. From one way ANOVA table, it may be predicted that the significance of factor A is more than B because the probability value of A is less than B, though the probability of both are less than 0.05.

The interaction between No. of lamina (A) and orientation angle (C) i.e. AC is significant with a probability value zero since A and C is significant. The interaction of thickness per lamina (B) with A and C (AB & BC) is not significant with probability value 0.3875 and 0.4663 respectively. The interaction between thickness per lamina (B) and orientation angle (C) i.e. BC is much higher than AB, which shows that the significance of the number of lamina (A) on response is more than orientation angle (C).

6.8.5 (a) Regression equation

In this thesis Design Expert 13.0 software has been applied to the data to obtain the mathematical equations for % error. In the present study responses, % age errors (E) are functionally of No. of Lamina (A), thickness per lamina (B) and orientation angle (C). The regression equations developed by RSM, used for predicting responses of % error (E) in terms of these variables are given as:

$$E = 10.99 - 9.27125 * A + 0.52375 * B + 2.9275 * C + 1.595 * A*B - 4.1675 * A*C + 0.1625 * B*C + 10.6925 * A^2 + 4.3425 * B^2 - 9.27 * C^2 \quad (6.22)$$

The equation in terms of coded factors can be used to make predictions about the response for given levels of each factor. By default, the high levels of the factors are coded as +1 and the low levels are coded as -1. The coded equation is useful for identifying the relative impact of the factors by comparing the factor coefficients.

6.8.5 (b) Validation of model

The adequacy of the developed model for % error has been tested using the statistical analysis of variance (ANOVA) technique, which shows that the regression is significant with linear and quadratic terms for % error at 95% confidence level as its p-value is less than 0.05. Adequate precision measures the signal to noise ratio. A ratio greater than 4 is desirable. This model shows a ratio of 8.09 which indicates an adequate signal. Therefore, this model can be used to navigate the design space. The validation of the developed model has also been checked by the

normal probability plot of the residuals for % error as shown in Fig. 6.10 and it is seen that the residuals fall on the straight line, which means the errors are distributed normally and the mathematical relationship is correctly developed.

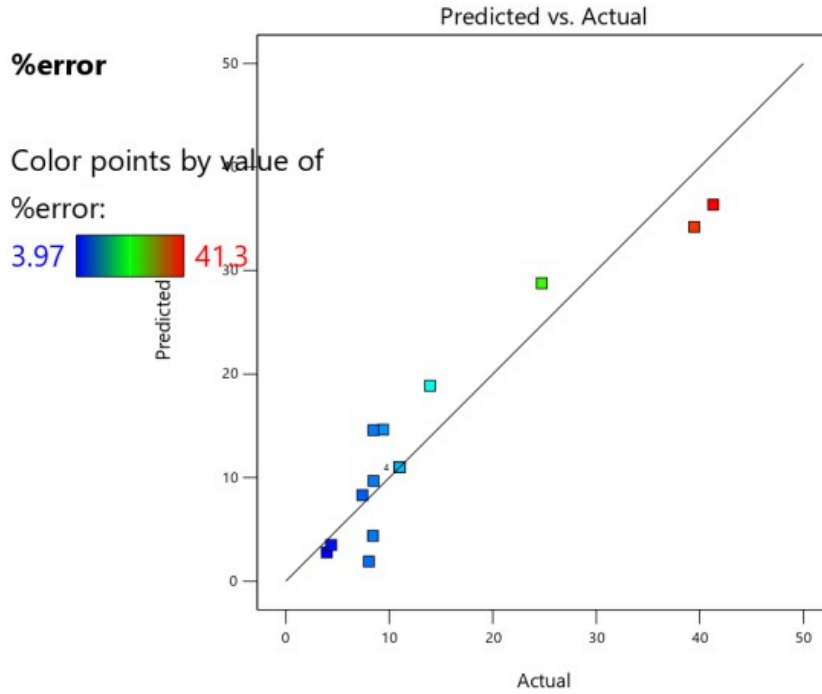


Figure 6.10: Residual plot of % age error

Table 6.8 ANOVA table

SL NO.	A	B	C	M	A	% error
1	4	0.005	10	0.0155	0.0168	8.39
2	4	0.005	40	0.0102	0.0144	41.30
3	4	0.005	70	0.0131	0.0164	25.23
4	4	0.0075	10	0.0046	0.0050	8.46
5	4	0.0075	40	0.003	0.0043	42.77
6	4	0.0075	70	0.0039	0.0049	24.74
7	4	0.01	10	0.0019	0.0021	10.84
8	4	0.01	40	0.0013	0.0018	39.46
9	4	0.01	70	0.0016	0.002	25.00
10	12	0.005	10	5.73E-04	5.96E-04	3.97
11	12	0.005	40	3.77E-04	4.13E-04	9.53
12	12	0.005	70	4.86E-04	5.22E-04	7.41
13	12	0.0075	10	1.70E-04	1.77E-04	4.21
14	12	0.0075	40	1.12E-04	1.24E-04	10.99
15	12	0.0075	70	1.57E-04	1.55E-04	1.08

SL NO.	A	B	C	M	A	% error
16	12	0.01	10	7.17E-05	7.48E-05	4.39
17	12	0.01	40	4.71E-05	5.28E-05	12.03
18	12	0.01	70	6.07E-05	6.59E-05	8.48
19	20	0.005	10	1.24E-04	1.29E-04	4.18
20	20	0.005	40	8.14E-05	8.91E-05	9.40
21	20	0.005	70	1.05E-04	1.12E-04	6.70
22	20	0.0075	10	3.67E-05	3.36E-05	8.42
23	20	0.0075	40	0.00002	2.69E-05	11.47
24	20	0.0075	70	3.11E-05	3.36E-05	8.03
25	20	0.01	10	1.55E-05	1.62E-05	4.66
26	20	0.01	40	1.02E-05	1.16E-05	13.94
27	20	0.01	70	1.31E-05	1.43E-05	8.99

Table 6.9 Variables for statistical analysis with levels.

Variables	Unit	Notation	Level		
			1	2	3
No. of lamina	unit less	A	4	12	20
Thickness/ply	m	B	0.005	0.0075	0.01
Angle	deg	C	10	40	70

Table 6.10 Results for one way ANOVA

Source	Sum of Square	Degree of freedom	Mean Square	F	Probability (P)	Remarks
No. of Lamina (A)	1842.0985	2	921.0492	25.4411	3.19e-06 < 0.05	significant
Thickness per Lamina (B)	7.8137	2	3.9068	0.1079	0.898 > 0.05	In significant
Angle (C)	993.6062	2	496.8031	13.7226	1.77e-4 < 0.05	significant
Error	724.0627	20	36.2031			
Total	3567.5812	26				

Table 6.11 Results for two way ANOVA

Source	Sum of Square	Degree of freedom	Mean Square	F-value	P-value	Remark
A	1842.0985	2	921.0492	253.1965	0 < 0.05	Significant
B	7.8137	2	3.9068	1.07399	0.386 > 0.05	In Significant
C	993.6062	2	496.8031	136.5712	0 < 0.05	Significant
A*B	17.2164	4	4.3041	1.1832	0.3875 > 0.05	In Significant
A*C	663.3711	4	165.8427	45.5902	0 < 0.05	Significant
B*C	14.3736	4	3.5934	0.9878	0.466 > 0.05	In Significant
Error	29.1014	8	3.6376			
Total	3567.5812	26				

6.8.5 (c) Effect of Process Parameters

Fig 6.11 and 6.12 show the variation of factors with the response in surface plot and 2D plot respectively. From the plot 6.12:B it is seen that the variation of %error with thickness per the lamina is almost constant, because the graph is almost horizontal which shows that the thickness per lamina is insignificant. Also the 2D plot of the no. of lamina (fig 6.12 A) and orientation angle (fig 6.12 B) with %age error shows the same nature of graph as discussed in section 6.8.2 and 6.8.3. In the graph 6.12, the black line is the mean of upper limit and lower limit blue line. The 3 D surface plot (fig 6.11) shows the combined effect of the parameters on the % error. From the fig 6.11(a) and 6.11(c), it shows that the effect of thickness per lamina on % error is not significant because the curve is smoothly decreasing in fig.6.11(a) and increasing to a peak value and then decreasing in fig 6.11(c) as discussed above for no. of lamina and orientation angle. But for fig 6.11(b) the curve is bending which shows the combined effect both significant variable numbers of lamina and orientation angle. Fig. 6.12 is the 2 dimensional representation of the variation of parameters with the % age error of fig 6.11.

Factor Coding: Actual

3D Surface

%error (unitless)

Design Points:

● Above Surface

○ Below Surface

3.97  41.3

X1 = A

X2 = B

Actual Factor

C = 40

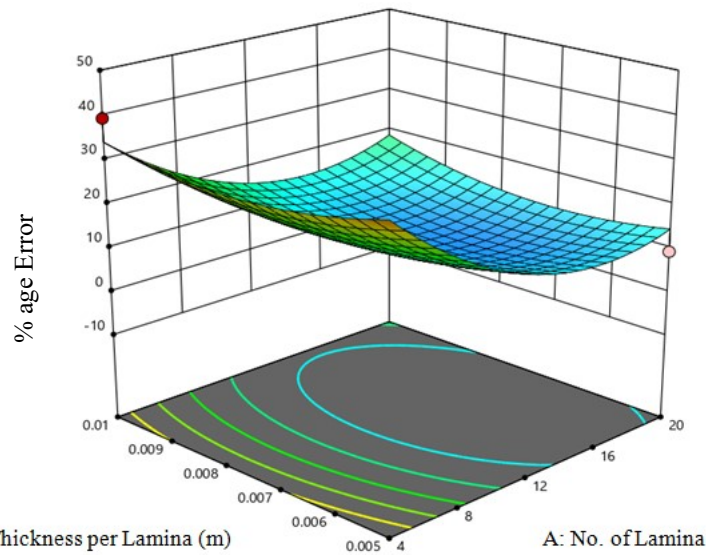


Figure 6.11(a) Surface plot of factors with response (% age Error)

Factor Coding: Actual

3D Surface

%error (unitless)

Design Points:

● Above Surface

○ Below Surface

3.97  41.3

X1 = A

X2 = C

Actual Factor

B = 0.0075

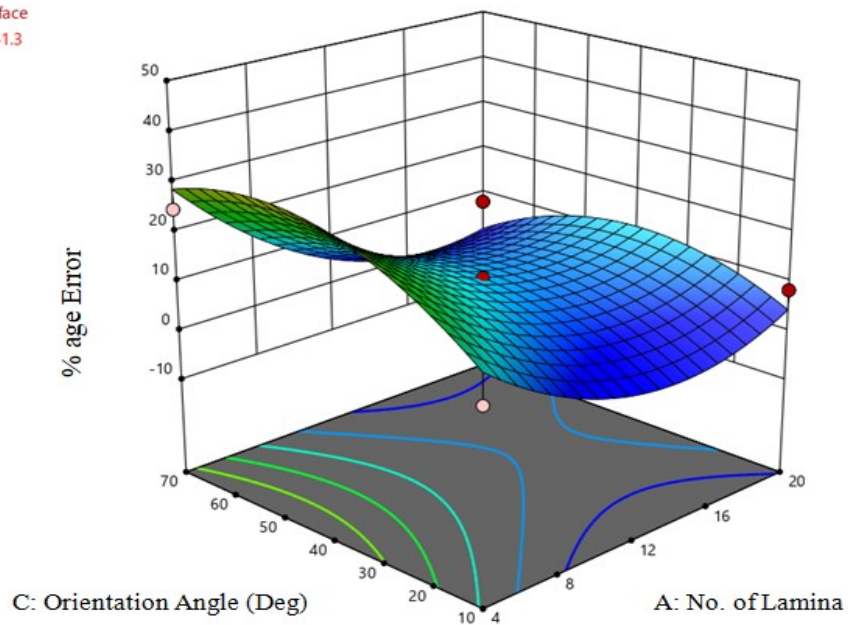


Figure 6.11(b) Surface plot of factors with response (% Error)

Factor Coding: Actual

3D Surface

%error (unitless)

Design Points:

● Above Surface

○ Below Surface

3.97  41.3

X1 = B

X2 = C

Actual Factor

A = 12

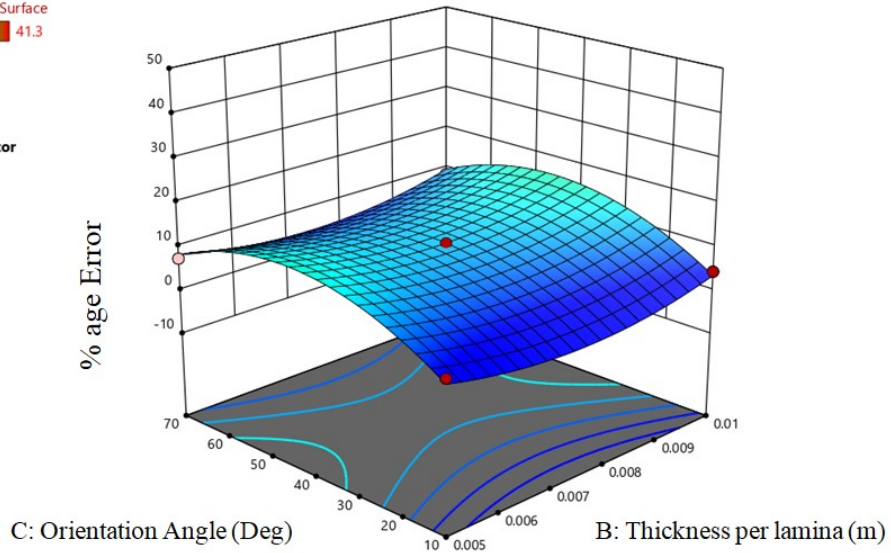
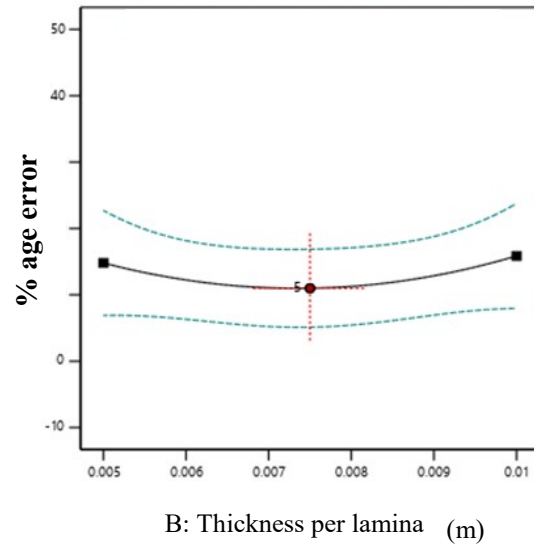
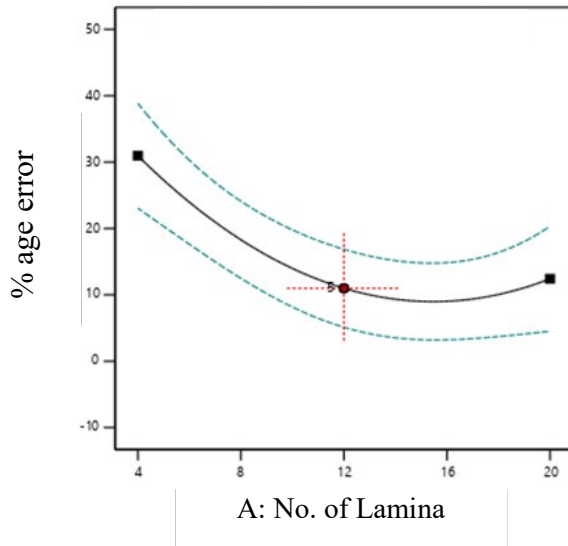


Figure 6.11(c) Surface plot of factors with response (% Error)



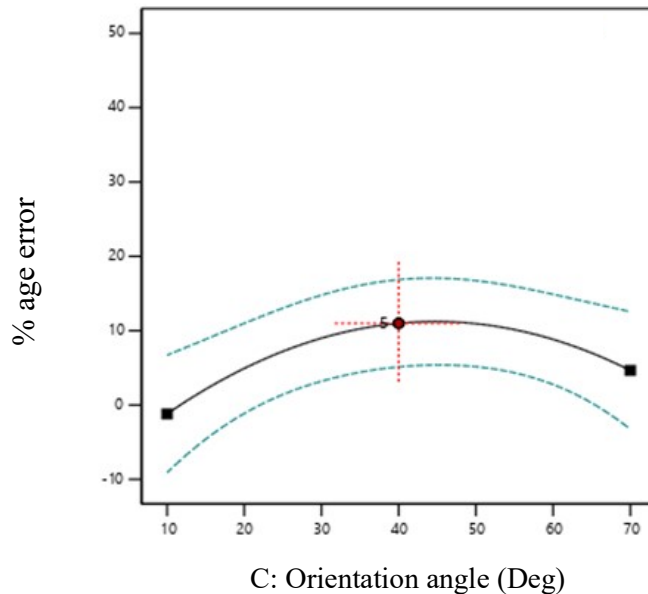


Figure 6.12 2 D plot of factors with response (% age Error)

6.8.6 Discussion

It may be concluded that the percentage error for laminated composite plate under transverse load depends on the number of lamina and orientation angle (or stacking sequence). If the thickness of each lamina is kept constant, then increase in the number of lamina means increase in total thickness of the laminate. So, number of lamina can be predicted as laminate thickness. Therefore, in other way it can be said that, % error of the plate depends on laminate thickness and orientation angle. Mesh size is an insignificant variable because mesh size can be converged by convergence analysis. Statistical analysis is conducted to reduce the number of variables by testing their significance at 5% significance level. Therefore the percentage error may be reduced by proper optimization of these variables.

B. Buckling of laminated Composite plate

The model as discussed above is further extended for buckling analysis of simply supported laminated composite plate under axial compressive load for different orientation angle. A finite element model of buckling is built up using ANSYS software and the results from the ANSYS software is compared with existing literature and a semi-analytical model built up using

classical lamination theory (CLT) solved by MATLAB software. The equations of buckling formulated by CLT are solved by Navier method and calculation is done on MATLAB platform.

6.9 Semi-analytical Method

Buckling is the loss of stability of the structure due to geometric effects leading to the failure if the resulting deformations are not restrained. During buckling, if permanent deformation takes place in composite structure, then matrix cracking occurs. Consider a simply supported column of area A , length L , and moment of inertia I . If the column geometry, loading, and material have no imperfections, the axial deformation is [2]

$$u = \frac{PL}{EA} \quad (6.23)$$

With no lateral deformation $w = 0$. The deformation of the structure (u, v, w) before buckling occurs is called the primary path. The slightest imperfection will make the column buckle when

$$P_{cr} = \frac{\pi^2 EI}{L^2} \quad (6.24)$$

The simply supported structure experiences no deformations in the shape of the buckling mode before buckling actually happens since it behaves like a perfect structure with perfectly aligned loading. For these types of structures, buckling occurs at the bifurcation point which is the intersection of primary path with secondary path ie. Post buckling. The bifurcation loads, one for every possible mode of buckling, can be obtained by FEM software easily. This type of analysis is called eigen value buckling analysis because the critical loads are the eigen values λ_i of the discretized system of equations [2]

$$([K] - \lambda[K_s])\{v\} = 0 \quad (6.25)$$

Whereas $[K]$ and $[K_s]$ are the stiffness and stress stiffness matrix, respectively, and v is the column of eigenvectors (buckling modes).

The equilibrium of the plate remains stable under in plane compressive force, until a certain load called buckling load is reached. The buckling load depends upon geometry, material properties and buckling mode shape. The governing equation for buckling deflection is derived by CLT method. The critical buckling load (N_0) is determined by solving the buckling equation using Navier method. [3]

$$N_0(m, n) = \frac{\pi^2 D_{22}}{b^2} \left[m^2 \frac{D_{11}}{D_{22}} \left(\frac{b}{a} \right)^2 + 2 \frac{(D_{12} + 2D_{66})}{D_{22}} + \frac{1}{m^2} \left(\frac{a}{b} \right)^2 \right] \quad (6.26)$$

The smallest value of N_0 occurs at $n = 1$ for any value of m . a, b are plate dimensions. D_{ij} is bending stiffness matrix. The critical buckling load is determined by finding the minimum value of N_0 . The mathematical model is solved in MATLAB platform and the MATLAB code is verified with the existing literature.

6.10 Finite element method

A finite element model of laminated composite plate composed of four layers of composite plate simply supported at both the end is built up using 8 node shell 281 elements by using finite element software ANSYS. In the pre-processor phase material properties are inserted in the orthotropic tab. The meshing is done using quadrilateral mapped element (fig 6.13). In the solution phase simply supported boundary conditions and loadings is applied to the model and the solution is done keeping pre stress effect on. In the next step Eigen value buckling analysis is selected from solution tab and a number of modes to be extracted is inserted in the analysis option. Then the problem is again solved and Eigen values are noted in the post processor phase. The minimum Eigen value multiplied by the length is the critical buckling load. The programme code for buckling analysis is written in the command prompt of ANSYS following the programming language and run several times for different fiber orientation angle and number of plies. A code is written using ANSYS programming language and the same is verified with existing literature.

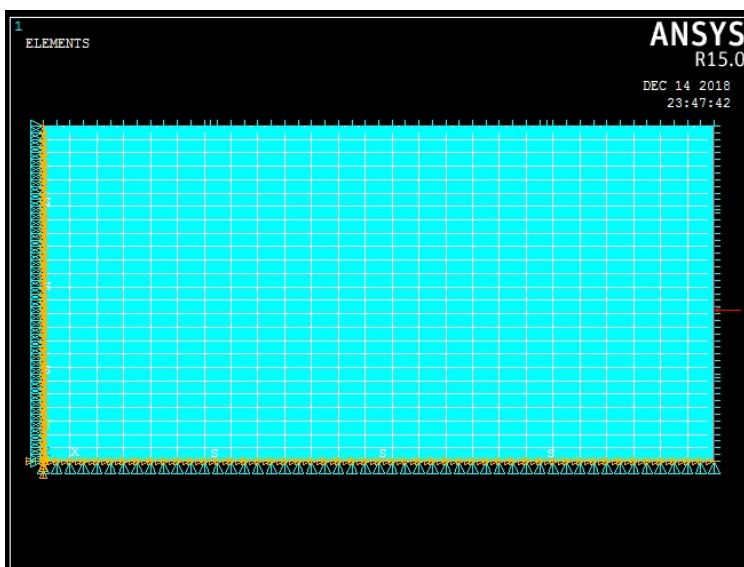


Figure 6.13 Meshed Geometry of simply supported composite plate with constraint and loading

6.10.1 Convergence analysis

A convergence analysis is conducted to finalize the size of the mesh. Convergence analysis is done by running the ANSYS code and critical buckling load is determined for different mesh size until a size of mesh is obtained at which same result is repeated. In this problem (fig 6.14) 12 x12 mesh size is finalized since same result is obtained at 12 x 12, 25 x 25 and so on mesh size.

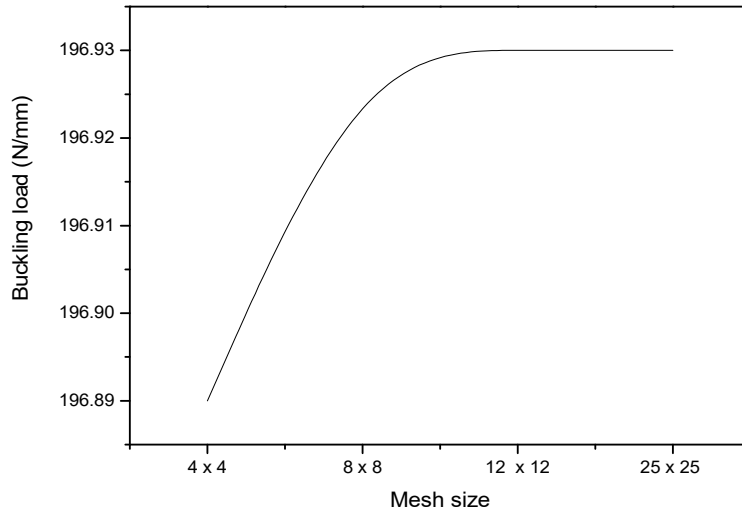


Figure 6.14 Convergence analysis

6.11 Validation of models

The result obtained from the finite element software ANSYS is validated with Barberio [2] and semi-analytical model result is validated with published results by Qiao Jie Yang [57] and it is found out that the results are very close which shows that both the models are correct to solve the defined problem (table 6.12).

Table 6.12 Validation of results with existing literature

500 x 500 plate with orientation [0/45/90/-45] _s	Validation of mathematical model using CLT	
Plate thickness	Buckling Load	
	Qiao Jie Yang [57]	Present result
8 mm	179.4 N/mm	179.1 N/mm
16 mm	1484.2 N/mm	1484 N/mm
1000 x 500 plate with orientation [(0/90) ₃] _s , AS4/9310	Validation of FEA model using LLS (laminated stacking sequence and lamina properties)	
Plate thickness	Buckling load	
	Barberio [7]	Present result
10.2 mm	209.42 N/mm	209.4N/mm

6.12 Numerical Problem

Consider a simply supported laminated composite plate made up of number of lamina bonded together perfectly and reinforced by fibers in a definite orientation and which is symmetric to its mid plane. The plate is subjected to axial compressive load. The Composite materials chosen for analysis is graphite/epoxy composite. The laminated composite plate is composed of four plies or lamina of composite material arranged symmetrically within the laminate in stacking sequence of angle ply ($[\theta/-\theta]_s$). The fiber orientation varies from 0° to 90° . Critical buckling load is determined for each orientation angle by semi analytical and finite element method and compared.

The model of semi analytical method and FEM as discussed above is used to solve the numerical problem for four ply simply supported symmetric angle ply laminated composite plate under axial compressive load for orientation angle ranging from 0° to 90° . Critical buckling load is found out by using Navier method and compared with the results from FEM by using FEA software ANSYS. Percentage error is noted for each orientation angle.

6.12.1 Results & Discussion

Now the validated models as discussed above are extended for analysis of the present problem. The result obtained from the finite element software ANSYS is compared with the semi analytical model for the problem defined in this thesis for buckling and the percentage errors are noted. The errors are within the acceptable limit for 0° and 90° fiber orientation angle but it show a significant error for the other angles shown in table 6.13. The difference in the results is probably due to some reasons. The First, reason as discussed above, the governing equation of buckling is derived by taking into consideration of some assumptions. Also, it neglects bending coefficient D_{16} and D_{26} , which is zero for cross ply (0° & 90°) but it is non zero for angle ply. Therefore, it shows negligible error for 0° & 90° stacking sequence, but the error becomes significant for other angles where D_{16} and D_{26} are not zero. The buckling equation is solved by Navier method, which finds an approximate solution to the problem because it considers Fourier expansion. Secondly, the finite element model of composite plate is built up by approximating all the laminas as the single entity. Each lamina is not modeled separately to reduce the time for simulation, but it introduces an error in the results. The ANSYS will simulate the problem by taking the average of the properties of each lamina which depends on

the degree of orientation of each lamina. That is why the error is more significant for all the orientations except 0° and 90°. The reasons for this type of error may be found out if the results are compared with experimental results. Navier method simplifies the equations by taking some assumptions as discussed above including D_{16} and D_{26} as zero. This may be proved for 0° and 90° angles, where percentage error is negligible due to the absence of bending coefficients. Present problem is solved by CLT, which neglects the higher order terms, but FEM uses higher order theories to solve the problem.

The percentage error may be reduced, if the general governing equation used to solve the problem is built up without neglecting the bending coefficients. Second, if the problem is solved by higher order theories. FEM results may be improved further by improving the model by modeling each lamina separately and joined them using a function.

Table 6.13 Comparison of Critical buckling load (N/mm) found by Finite element Method and semi analytical method (CLT)

Fiber angles	Critical buckling load (N/mm)		Percentage error
	Semi analytical method (CLT)	Finite element Method	
[0/0] _s	199.50	196.93	1.30
[30/-30] _s	549.08	305.23	79.80
[45/-45] _s	632.17	432.80	46.00
[60/-60] _s	515.99	333.04	55.00
[90/90] _s	199.55	205.92	3.00

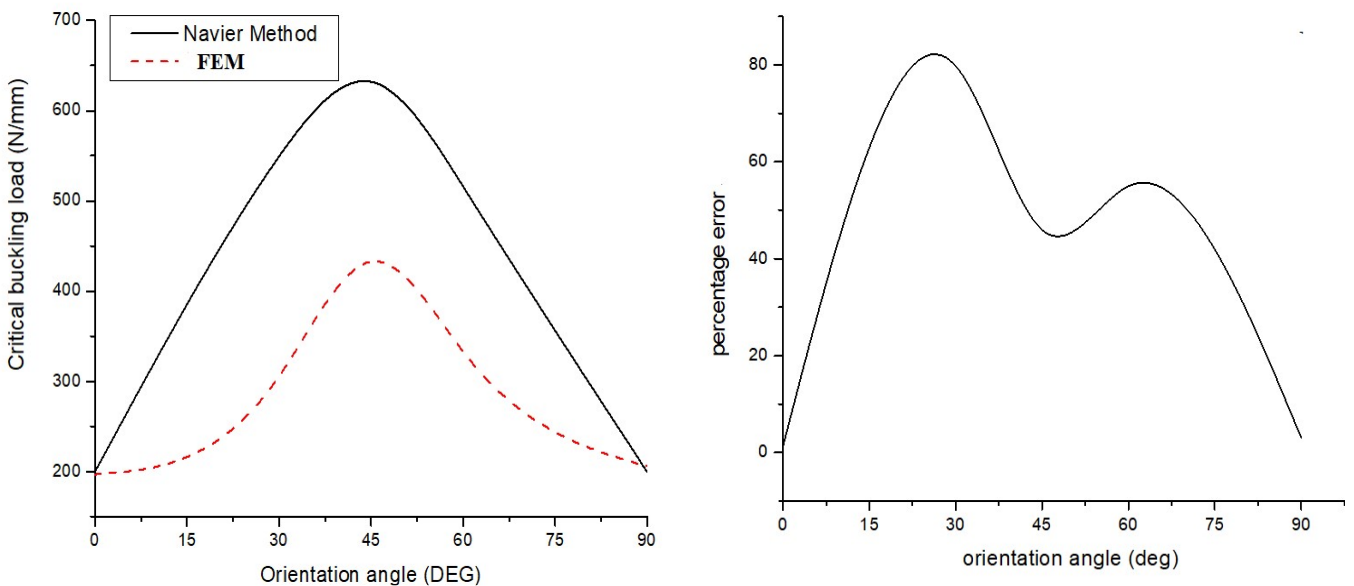


Figure 6.15 Effect of orientation angle on critical buckling load (left) and % age error (right)

6.12.2 Effect of fiber orientation angle and number of lamina

Critical buckling load is determined by using finite element method for simply supported composite plate subjected to axial compressive load ($N_x = 1N/mm$) for different fiber orientation angle. It is found that critical buckling load is maximum at 45° fiber orientation angle (fig 6.15). Therefore optimum stacking sequence of the lamina at which the load bearing capacity of composite structure is maximum is $[45/-45]_s$ for loading $N_x = 1N/mm$. The analysis is also extended for different loading conditions i.e. $N_y \neq 0, N_x = N_{xy} = 0$ and $N_y \neq 0, N_x \neq 0, N_{xy} = 0$ shown in fig 6.16(a) and fig 6.16(b) respectively. It is found that the critical buckling load increases as the fiber orientation angle increases and become maximum at 90° orientation angle. Fig 6.17 shows that the critical buckling load increases as the number of ply increases which concludes that load carrying capacity of composite structure under buckling can be increased by increasing the number of ply but it increases the mass as well as the cost. Fig 6.18 shows the shape of buckling modes of simply supported composite plate for 45° fiber orientation angle.

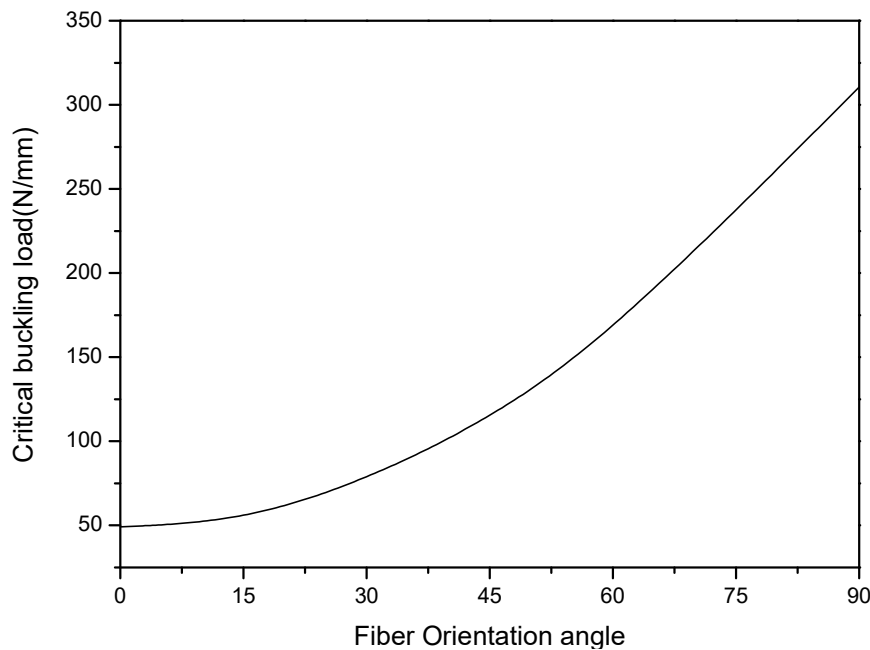


Figure 6.16 (a) Critical buckling load for different orientation angle for simply supported graphite/ epoxy composite plate under compressive load $N_y \neq 0, N_x = N_{xy} = 0$

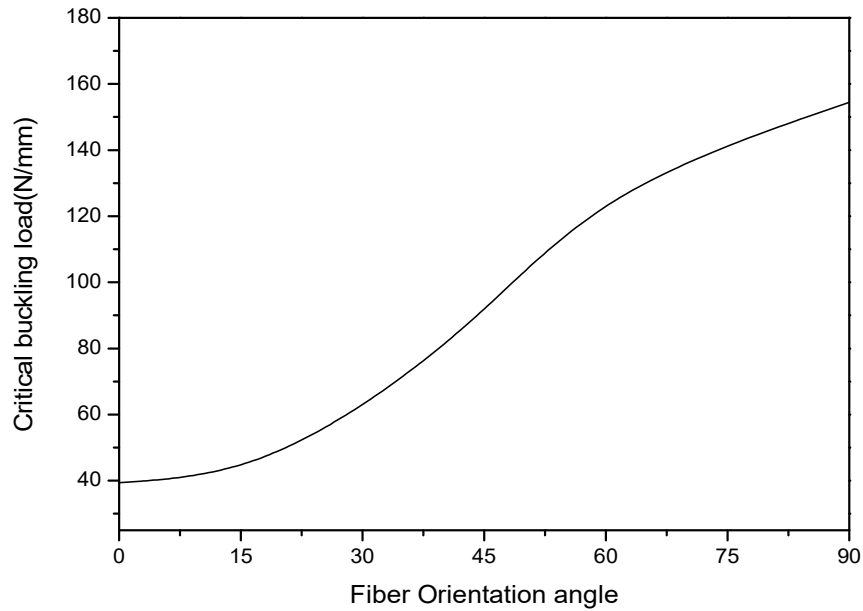


Figure 6.16 (b) Critical buckling load for different orientation angles for simply supported graphite/ epoxy composite plate under compressive load $N_y \neq 0, N_x \neq 0, N_{xy} = 0$

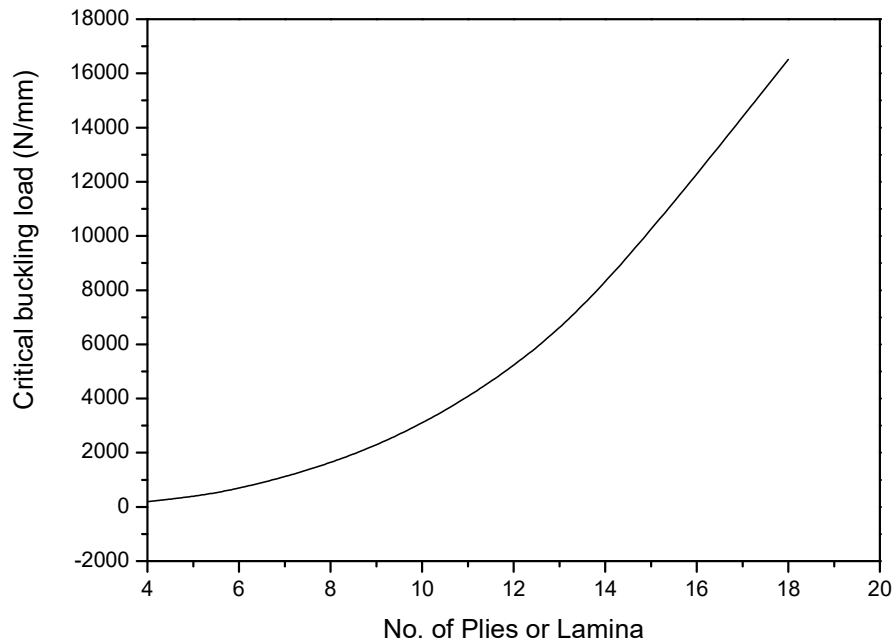


Figure 6.17 Critical buckling loads for number of lamina for simply supported graphite/ epoxy composite plate under compressive load ($N_x \neq 0, N_y = N_{xy} = 0$) .

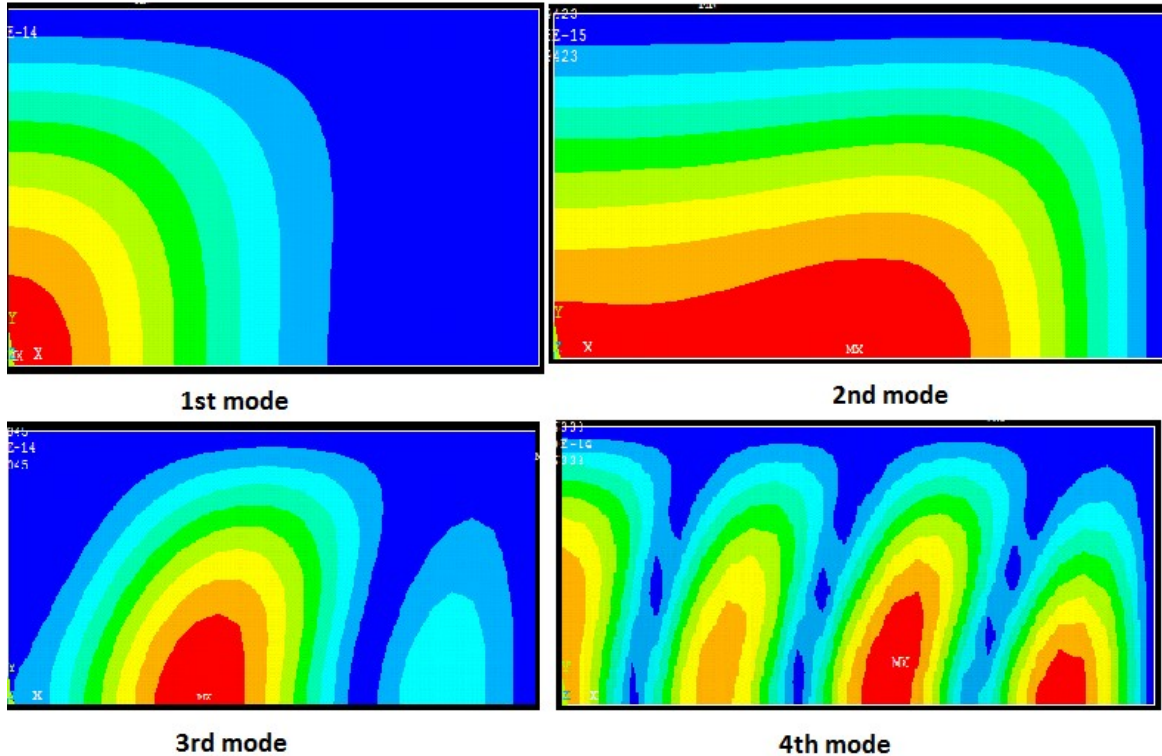


Figure 6.18: Buckling mode of simply supported composite plate for 45° fiber orientation angle.

6.13 Closure

It may be concluded from the discussion of this chapter, Navier method is more efficient to solve cross ply composite problem, whereas Rayleigh-Ritz method is used to solve angle ply composite problem. Percentage error for laminated composite plate under transverse load depends on laminate thickness and orientation angle. Therefore, the percentage error for a laminated composite plate can be reduced by the optimum combination of laminate thickness and orientation angle. The same conclusion can be obtained from the buckling analysis of simply supported plate for symmetric angle ply and cross ply composite. The percentage error with FEA software may be reduced, if the general governing equation is used to solve the problem without neglecting the bending coefficients. Second, if the problem is solved by higher order theories. ANSYS results may be improved by improving the model by modeling each lamina separately and joined them using a function. The analysis of percentage error for buckling of simply supported plate under compressive load is same as that of simply supported plate under transverse load, because the plate equations are solved in the same way as discussed above.

CHAPTER 7

BENDING OF LAMINATED COMPOSITE BEAM

7.1 Introduction, 7.1.1 Assumptions. 7.2. Theoretical formulation, 7.2.1 Analysis of laminated beam using CLT, 7.2.1.1 General solution of Bending Equation, 7.2.1.2 Calculation of stresses 7.2.2. Analysis of laminated beam using FSDT, 7.2.2.1 General solution of bending equation, 7.2.2.2 Non dimensional quantity, 7.3 Semi-Analytical method, 7.3.1 Validation of Semi analytical model, 7.4 Finite Element Method (FEM), 7.4.1 Convergence analysis, 7.4.2 Validation of the FEM model, 7.4.3 Numerical problem, 7.4.3.1 Analysis of the results, 7.4.3.2 Effect of Orientation angle, 7.4.3.3 Effect of boundary conditions, 7.4.3.4 Effect of length to thickness ratio, 7.4.3.5 Effect of no. of lamina, 7.5 Analysis of Percentage error of laminated composite beam, 7.5.1 Length to width ratio (L/W), 7.5.2 Mesh size unit, 7.5.3 Thickness of laminate, 7.5.4 Orientation angle, 7.5.5 Statistical Analysis of Percentage Error in deflection 7.5.5 (a) ANOVA, 7.5.5 (b) Regression equation, 7.5.5 (C) Validation of model, 7.5.5 (d) Effect of Process Parameters, 7.6 Closure

7.1 Introduction

Laminated beam is considered a one dimensional problem of laminated plate where displacements are function of one coordinate. When the width of a laminated plate (length along y axis) is very small compared to the length along x axis and the lamination scheme and loading is such that displacement are function of x only, the laminate is treated as a beam[52]. So plate theory can be used to model beam. Beam problem is considered as plane stress problem. Classical laminated theory (CLT) is based on Euler- Bernoulli's beam theory which disregards the effect of transverse shear deformation and transverse shear strain. Whereas first order shear deformation theory (FSDT) is based on Timoshenko's beam theory which considers the linear variation of shear deformation in thickness direction of beams together with rotary inertia [52]. The transverse shear strain is constant through the thickness and the transverse shear stress is constant layer wise. Therefore shear correction factor is introduced for appropriate representation of strain energy of deformation which depends on material and geometric properties of beam as well as loading and boundary conditions [3]. This factor can be eliminated by using higher order theory which satisfies shear stress free boundary condition. Transverse deflection of the FSDT consists of two parts, one due to pure bending and the other

due to transverse shear. When transverse shear deflection goes to zero, Timoshenko beam theory solution reduces to classical beam theory. The in plane stresses are the same for both the theories.

There are two types of solutions: Exact (analytical) solution and Numerical solution. Exact (analytical) solution is one which satisfies the equations and boundary conditions in every domain, whereas a numerical solution satisfies in an approximate sense. Since the beam equations are simplified form of plate equations in one dimension and considering assumptions, exact solutions of beam equations are possible. In this chapter, the beam problem is also solved by a numerical method using FEA software, and the results from both the methods are compared.

7.1.1 Assumptions

In order to obtain the exact solution of the beam equations by analytical method, certain assumptions are taken:

1. Beam problem is considered as 1 D problem of plate.
2. When the width (b) of a laminated plate (length along y axis) is assumed very small compared to the length along x axis such that displacement are function of x only. Therefore deflection (w_0), displacement (u_0, v_0) and load (q) are function of x only.
3. In this thesis, symmetrical problem is solved i.e the equations for bending deflection are coupled from stretching displacement. $[B_{ij}] = 0$ for symmetric problem.
4. In plane forces and in plane displacement are assumed zero.
5. M_{yy} and $M_{xy} = 0$ are assumed everywhere in the beam problem.
6. Beam problem is considered as plane stress problem.
7. Large beam is assumed whose aspect ratio is large.

7.2. Theoretical formulation

A laminated composite beam of rectangular section ($b \times h$) and length a as shown in figure are considered for study. The beam is composed of four angle ply laminate of composite material of different fiber orientations with respect to x axis.

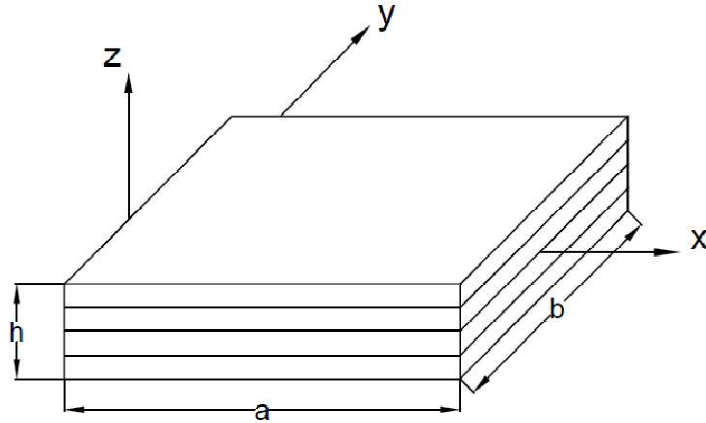


Figure 7.1 Geometry of laminated composite beam

7.2.1 Analysis of laminated beam using CLT

Classical laminated theory (CLT) holds the assumptions of Kirchhoff hypothesis. The assumptions states that the transverse displacement is independent of the transverse coordinate and the transverse normal strain ϵ_{zz} is zero. Also it assumes that the transverse shear strain is zero. The displacement (u, v, w) can be written as

$$\begin{aligned}
 u(x, y, z, t) &= u_0(x, y, t) - z \frac{\partial w_0}{\partial x}, \\
 v(x, y, z, t) &= v_0(x, y, t) - z \frac{\partial w_0}{\partial y}, \\
 w(x, y, z, t) &= w_0(x, y, t)
 \end{aligned}
 \tag{7.1}$$

Where (u_0, v_0, w_0) are the displacements along the coordinate line of a material point on x-y plane. If the inplane forces and displacement are zero, then the problem is reduced to one dimensional problem. For computing the deflection and stresses in laminated beam, it is assumed that

$$M_{yy} = M_{xy} = 0 \quad \text{every where in the beam.} \tag{7.2}$$

The constitutive equations for symmetric laminates in the absence of in-plane forces and considering symmetric conditions ie. $[B_{ij}] = 0$ given by

$$\begin{Bmatrix} M_{xx} \\ M_{yy} \\ M_{xy} \end{Bmatrix} = - \begin{bmatrix} D_{11} & D_{12} & D_{16} \\ D_{12} & D_{22} & D_{26} \\ D_{16} & D_{26} & D_{66} \end{bmatrix} \begin{Bmatrix} \frac{\partial^2 w_0}{\partial x^2} \\ \frac{\partial^2 w_0}{\partial y^2} \\ 2 \frac{\partial^2 w_0}{\partial x \partial y} \end{Bmatrix} \quad (7.3)$$

It is assumed that the laminated beam under consideration is long enough (length to width ratio is large) such that the effects of the Poisson ratio and shear coupling on the deflection can be neglected (i.e. $D_{16}^* = D_{26}^* = 0$). Then the transverse deflection can be taken only as the function of x coordinate.

$$\frac{\partial^2 w_0}{\partial x^2} = -D_{11}^* M_{xx}, \frac{\partial^2 w_0}{\partial y^2} = -D_{22}^* M_{xx}, 2 \frac{\partial^2 w_0}{\partial x \partial y} = -D_{16}^* M_{xx} \quad \text{and}$$

$$w_0 = w_0(x) \quad (7.4)$$

$$\text{Then it can be written as: } \frac{\partial^2 w_0}{\partial x^2} = -D_{11}^* M_{xx} \quad (7.5)$$

In order to cast the equation 7.5 in familiar form following quantities are introduced:

$$M = bM_{xx}, Q = bQ_x, E_{xx}^b = \frac{12}{h^3 D_{11}^*} = \frac{b}{I_{yy} D_{11}^*}, I_{yy} = \frac{bh^3}{12} \quad (7.6)$$

From eq. 7.5

$$\frac{\partial^2 w_0}{\partial x^2} = -\frac{M}{E_{xx}^b I_{yy}}, M(x) = -E_{xx}^b I_{yy} \frac{\partial^2 w_0}{\partial x^2} \quad (7.7a)$$

$$\text{Shear force and bending moments are related by: } Q_x = \frac{\partial M_{xx}}{\partial x}, \text{ or } Q = \frac{\partial M}{\partial x} \quad (7.7b)$$

Where b is the width and h is the total thickness of the laminate.

7.2.1.1 General solution of Bending Equation

Considering static bending and in the absence of axial forces, equation (7.7a, b) take the form

$$\frac{\partial^2 w_0}{\partial x^2} = -\frac{M}{E_{xx}^b I_{yy}} \quad (7.8a)$$

$$E_{xx}^b I_{yy} \frac{\partial^4 w_0}{\partial x^4} = \hat{q} \quad (7.8b)$$

Where $\hat{q} = bq$. Eq. 7.8a is used to express bending moment M in terms of applied load whereas eq. 7.8b is applicable for indeterminate beams. The general solution of eq. 7.8a can be obtained by integration as:

$$E_{xx}^b I_{yy} w_0(x) = - \int_0^x \left[\int_0^\eta M(\xi) d\xi \right] d\eta + b_1 x + b_2 \quad (7.9a)$$

The general solution of eq. 7.8b is as

$$E_{xx}^b I_{yy} w_0(x) = \int_0^x \left\{ \int_0^\xi \left[\int_0^\eta \left(\int_0^\zeta \hat{q}(\mu) d\mu \right) d\zeta \right] d\eta \right\} d\xi + c_1 \frac{x^3}{6} + c_2 \frac{x^2}{2} + c_3 x + c_4 \quad (7.9b)$$

The constant of integration can be determined from the boundary conditions of the problem.

Boundary conditions for different type of supports are as [52]:

$$\text{Free:} \quad Q = \frac{dM}{dx} = 0, M = 0$$

$$\text{Hinged:} \quad w_0 = 0, M = 0$$

$$\text{Clamped:} \quad w_0 = 0, \frac{\partial w_0}{\partial x} = 0 \quad (7.10)$$

7.2.1.2 Calculation of stresses

The in-plane stresses in the k^{th} layer can be determined as:

$$\begin{Bmatrix} \sigma_{xx} \\ \sigma_{yy} \\ \sigma_{xy} \end{Bmatrix}^{(k)} = z \begin{bmatrix} \bar{Q}_{11} & \bar{Q}_{12} & \bar{Q}_{16} \\ \bar{Q}_{12} & \bar{Q}_{22} & \bar{Q}_{26} \\ \bar{Q}_{16} & \bar{Q}_{26} & \bar{Q}_{66} \end{bmatrix}^{(k)} \begin{Bmatrix} \frac{\partial^2 w_0}{\partial x^2} \\ \frac{\partial^2 w_0}{\partial y^2} \\ 2 \frac{\partial^2 w_0}{\partial x \partial y} \end{Bmatrix} \quad (7.11)$$

7.2.2. Analysis of laminated beam using FSDT

The bending of symmetrically laminated beam using the first order shear deformation theory is considered for study. The displacement field of the first order theory is:

$$u(x, y, z, t) = u_0(x, y, t) - z\phi_x(x, y, t),$$

$$v(x, y, z, t) = v_0(x, y, t) - z\phi_y(x, y, t),$$

$$w(x, y, z, t) = w_0(x, y, t) \quad (7.12)$$

where ϕ_x, ϕ_y are the rotations of the transverse normal about the y and x axis respectively.

In the absence of in-plane forces, the laminate constitutive equations for symmetric laminates are as:

$$\begin{Bmatrix} M_{xx} \\ M_{yy} \\ M_{xy} \end{Bmatrix} = \begin{bmatrix} D_{11} & D_{12} & D_{16} \\ D_{12} & D_{22} & D_{26} \\ D_{16} & D_{26} & D_{66} \end{bmatrix} \begin{Bmatrix} \frac{\partial \phi_x}{\partial x} \\ \frac{\partial \phi_y}{\partial y} \\ \frac{\partial \phi_x}{\partial y} + \frac{\partial \phi_y}{\partial x} \end{Bmatrix} \quad (7.13a)$$

$$\begin{Bmatrix} Q_y \\ Q_x \end{Bmatrix} = K \begin{bmatrix} A_{44} & A_{45} \\ A_{45} & A_{55} \end{bmatrix} \begin{Bmatrix} \frac{\partial w_0}{\partial y} + \phi_y \\ \frac{\partial w_0}{\partial x} + \phi_x \end{Bmatrix} \quad (7.13b)$$

K is the shear correction coefficient. For computing the deflection and stresses in laminated beam, it is assumed that

$$M_{yy} = M_{xy} = Q_y = \phi_y = 0 \quad (7.14a)$$

$$\text{And } w_0 \text{ and } \phi_x \text{ is function of only } x \text{ coordinate. } w_0 = w_0(x), \phi_x = \phi_x(x) \quad (7.14b)$$

From eq.7.12, the displacement field takes the form:

$$u(x, z) = z\phi_x(x), w(x, z) = w_0(x) \quad (7.15a)$$

Strain- displacement relation:

$$\varepsilon_{xx} = z \frac{\partial \phi_x}{\partial x}, 2\varepsilon_{xz} = \frac{\partial w_0}{\partial x} + \phi_x \quad (7.15b)$$

Taking inverse of eq. (7.13 a,b)

$$\frac{\partial \phi_x}{\partial x} = D_{11}^* M_{xx}, \frac{\partial w_0}{\partial x} + \phi_x = \frac{A_{55}^*}{K} Q_x \quad (7.16)$$

$$\text{or } E_{xx}^b I_{yy} \frac{\partial \phi_x}{\partial x} = M(x), M(x) = bM_{xx}, E_{xx}^b = \frac{12}{D_{11}^* h^3} \quad (7.17a)$$

$$KG_{xz}^b bh \left(\frac{\partial w_0}{\partial x} + \phi_x \right) = Q(x), Q(x) = bQ_x, G_{xz}^b = \frac{1}{A_{55}^* h} \quad (7.17b)$$

7.2.2.1 General solution of bending equation

Considering static bending and in the absence of axial forces, bending eq. reduce to

$$KG_{xz}^b bh \left(\frac{d^2 w_0}{dx^2} + \frac{d\phi_x}{dx} \right) + \hat{q} = 0 \quad (7.18a)$$

$$E_{xx}^b I_{yy} \frac{d^2 \phi_x}{dx^2} - KG_{xz}^b bh \left(\frac{\partial w_0}{\partial x} + \phi_x \right) = 0 \quad (7.18b)$$

Integrating the eq. (7.18a) with respect to x substituting the result in eq. (7.18b) and simplifying and integrating, we get

$$w_0(x) = -\frac{1}{E_{xx}^b I_{yy}} \left[-\int_0^x \int_0^\xi \int_0^\eta \int_0^\mu \hat{q}(\zeta) d\zeta d\mu d\eta d\xi + c_1 \frac{x^3}{6} + c_2 \frac{x^2}{2} + c_3 x + c_4 \right] + \frac{1}{KG_{xz}^b bh} \left[-\int_0^x \int_0^\xi \hat{q}(\zeta) d\zeta d\xi + c_1 x \right] \quad (7.19a)$$

$$w_0(x) = w_0^b(x) + w_0^s(x) \quad (7.19b)$$

Where, the constant of integration can be determined from the boundary condition of the beam. The transverse deflection, $w_0(x)$ consist of two parts: one is due to pure bending, $w_0^b(x)$ as that of CLT and the other is due to transverse shear, $w_0^s(x)$. when the deflection due to transverse shear becomes zero then FSDT approaches CLT. The in-plane stresses are same for both the theories.

Table 7.1 Maximum Transverse deflections of laminated composite beam for different boundary conditions and subjected to point load and uniformly distributed load according to CLT and FSDT [53].

Boundary conditions	Loading	Maximum Bending Moment (M_{max})	Maximum transverse deflections (w_{max})		
			CLT	FSDT	Location (x)
Hinged-hinged	Uniformly distributed load ($q_0 b$)	$-\frac{1}{8} b_4$ at $x = \frac{a}{2}$	$\frac{5}{384} b_2$	$\frac{5}{384} b_2 + \frac{1}{8} s_2$	$\frac{a}{2}$
Clamped-Clamped	Uniformly distributed load ($q_0 b$)	$\frac{1}{12} b_4$ at $x = 0$	$\frac{1}{384} b_2$	$\frac{1}{384} b_2 + \frac{1}{8} s_2$	$\frac{a}{2}$
Clamped-Free	Uniformly distributed load ($q_0 b$)	$\frac{1}{2} b_4$ at $x = 0$	$\frac{1}{8} b_2$	$\frac{1}{8} b_2 + \frac{1}{2} s_2$	a

The constants in the expressions are defined as

$$b_1 = \frac{F_0 b a^3}{E_{xx}^b I_{yy}}, \quad b_2 = \frac{q_0 b a^4}{E_{xx}^b I_{yy}}, \quad b_3 = -F_0 b a, \quad b_4 = -q_0 b a^2, \quad s_1 = \frac{F_0 b a}{KG_{xz}^b bh}, \quad s_2 = \frac{q_0 b a^2}{G_{xz}^b bh}$$

7.2.2.2 Non dimensional quantity

Non dimensional transverse deflection, $\hat{w} = w_{max} (E_2 h^3 / q_0 a^4) * 10^2$

Non dimensional normal stress, $\hat{\sigma} = \sigma_{max} \left(\frac{1}{R} * q_0 \right)$ where $R = \frac{a^2}{h^2}$ & $F_0 = q_0 a$ (7.20)

7.3 Semi-Analytical method

A semi analytical model of a laminated composite beam of rectangular section ($b \times h$) and length a , composed of four symmetric angle ply laminates of graphite epoxy composite material of different fiber orientations with respect to the x axis is built up by using semi analytical methods: CLT and FSDT as discussed, which is solved by using the MATLAB tool. Three boundary conditions are investigated: Hinged-Hinged (H-H), Clamped-Clamped (C-C) and Clamped-Free (C-F) under uniformly distributed load ($q_0 b$) (Fig 7.2). The steps required to develop an algorithm in MATLAB are as:

- I. Enter the basic lamina properties ($E_1, E_2, G_{12}, \vartheta_{12}$)
- II. Compute the ply stiffness $[Q]_{12}$ referred to their principle material axis.
- III. Enter the orientation θ_k , number of layers n , through the thickness coordinate z .
- IV. Find out the transformed layer stiffness $[\bar{Q}]_{xy}^k$ referred to the laminate coordinate system (x, y).
- V. Calculate the laminate stiffness matrix $[A], [B], [D]$ and their compliance matrix.
- VI. Then bending equation is derived and their solutions are obtained by direct integration.
- VII. Using the boundary conditions, the constants of integration are determined and the non dimensional normal stress and transverse deflection is calculated using $[D]$ matrix.

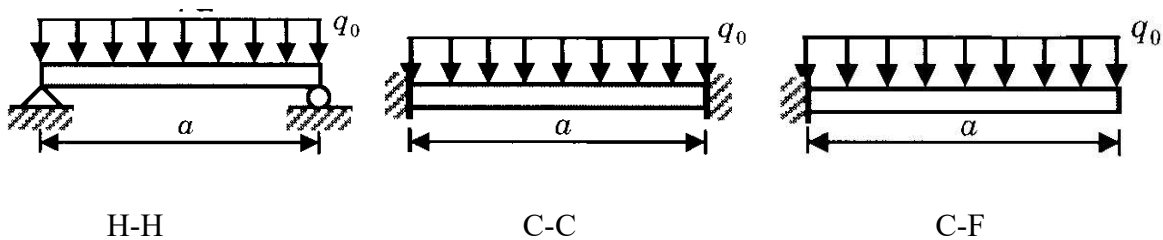


Figure 7.2 laminated composite beam subjected to UDL for different boundary conditions.

7.3.1 Validation of Semi analytical model

The model is validated with existing literature (table 7.2). Problems are taken from existing literature of KAW [52] and Reddy [3] as shown in table 7.2 and the semi analytical model of the thesis using the MATLAB tool is used to validate the results of existing literature.

Table 7.2 Validation of Semi analytical Model for Hinged-Hinged (H-H) beam

Stacking sequence	CLT deflection (m)		Stacking sequence	FSDT non dimensional deflection	
	KAW[52]	Present		Reddy[3]	Present
[0 90 -30 30] _s (Graphite-epoxy, UDL= 200 N/m, thickness= 0.125 mm, a=0.1 m, b=5 mm)	0.0052	0.0051	[45/-45] _s ($E_1/E_2 = 25$, $G_{12}=G_{13}=0.5E_2$, $G_{23}=0.2 E_2$, $\nu_{12}=0.25$, $a/h = 100$)	14.316	14.28

7.4 Finite element method (FEM)

The semi-analytical model is compared with the FEM using FEA software ANSYS15.0. The element selected for analysis is SHELL 181 (4 node element with 6 degrees of freedom at each node) because it is suitable for thin to moderately thick composite shell structures, and the inputs can easily be modified in the shell. The beam is being modeled by an creating area through key points. Then the beam is meshed with quadrilateral mapped meshing. The beam is constrained all d.o.f as zero at both ends for C-C condition and one end for the C-F condition. For H-H condition, it is constrained at x , y and z direction at one end whereas at other end, it is constrained only in x and z direction. A uniform pressure is applied along the surface area of the beam.

7.4.1 Convergence analysis

A convergence analysis is conducted to finalize the size of mesh. Convergence analysis is done by running the ANSYS code and deflection is determined for different mesh size until a size of mesh is obtained at which same result is repeated. In this problem (fig 7.3) 20 x100 mesh size is finalized since same result is obtained at 20 x 100, 25 x 120 and so on mesh size.

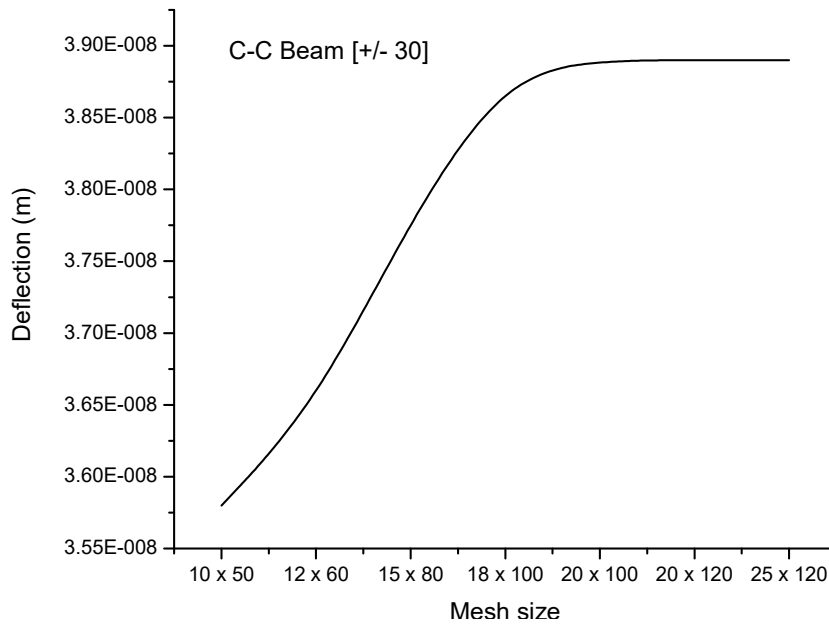


Figure 7.3 .Convergence analysis in ANSYS for Clamped-Clamped beam of stacking seq. [$\pm 30^\circ$]_s.

7.4.2 Validation of the FEM model

The FEM model built for the laminated composite plates under uniform pressure in chapter 6 is used to model the laminated composite beam under uniformly distributed load (UDL). The only difference between the models of plate and beam is the geometry. Fig 7.4 shows the geometry, boundary condition, and loading of both end hinged beams under UDL. In the case of beam width, is very small as compared to length. Since the plate model is validated in chapter 6 and the same model is used for the beam by changing the geometry, the beam model is not required to be validated.

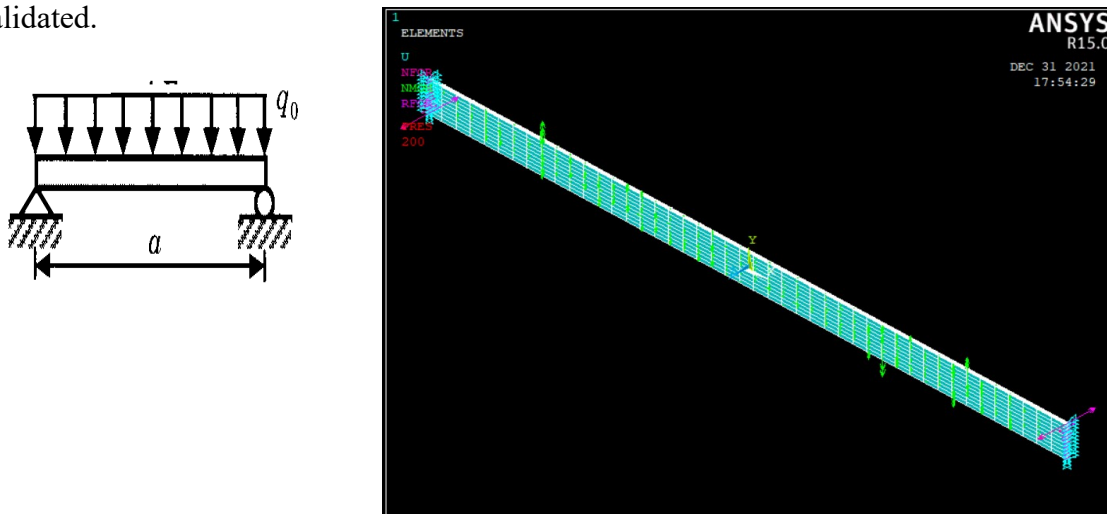


Figure 7.4 Geometry of hinged-hinged laminated composite beam under UDL

7.4.3 Numerical problem

A rectangular symmetrical angle ply laminated composite beam of length (a) 0.1m and width (b) 5mm, is considered. The beam is composed of four layers of graphite-epoxy composite material. The thickness of each layer is 0.125mm. The beam is hinged at both the ends and is subjected to uniformly distributed load (q_0b) of 200 N/m along the length (fig 7. 2). Transverse deflection is computed for different orientation angles ($0^\circ - 90^\circ$) by using semi-analytical method: Timoshenko beam theory (or FSDT). The results obtained from semi-analytical method solved in MATLAB software are compared with the results obtained from FEA software packages: ANSYS15.0.

The model of semi analytical method and FEM as discussed above is used to solve the numerical problem of a rectangular symmetric angle ply laminated composite beam of length (a) 0.2m and width (b) 5mm, composed of four layers of graphite-epoxy composite material subjected to uniformly distributed load (q_0b) of 200 N/m along the length. The thickness of each layer is 0.125mm. The beam is hinged at both ends. For symmetric angle ply laminate stacking sequence of $[\theta/-\theta]_s$ is represented by orientation angle “ θ ” in the y -axis. For example stacking sequence of $[90/-90]_s$ is represented by 90° (orientation angle). Transverse deflection is computed for different orientation angle ($0^\circ - 90^\circ$) by using analytical method: CLT and FSDT. The results obtained from semi-analytical method solved in MATLAB software are compared with the results obtained from FEA software packages: ANSYS.

7.4.3.1 Analysis of the results

Now the validated models as discussed above are extended for analysis of the present problem. The result obtained from the finite element software ANSYS is compared with the semi-analytical method for the problem defined in this thesis for Hinged-Hinged laminated composite beam and the percentage errors are noted. It is found that the error for orientation angles 15, 30 and 45 degree are above 5 percent and rests are below 5 percent. Below 5 percent error may be acceptable. This percentage error, therefore, depends on angle, thickness of laminate, and length to width ratio. The error may be varied (either reduced or increased) by varying these variables which is discussed in the next section. Also it is seen that the error percentage in deflection of beam is less as compared to plate. This may be due to: (a) beam equations are more simplified as compared to the plate, (b) Higher order terms are less, so the

solution is easier, (c) Beam is the 1D problem of the plate, so the equations are more simplified and the possibility of error in solving the equations get reduced.

In this chapter, deflection of beam is determined analytically by using two methods: Classical lamination theory (CLT) and First order shear deformation theory (FSDT). The results of both the theory are also compared. From the comparison, it is found that, the deflection obtained from FSDT is more than that of CLT because of the presence of shear deformation in Timoshenko beam theory (FSDT). The effect of shear deformation is to increase the total deflection of the beam. The contribution due to shear deformation to the deflection depends on the modulus ratio $\frac{E_{xx}^b}{G_{xz}^b}$ as well as the ratio of length to thickness ratio $(\frac{a}{h})$. The effect of shear deformation is negligible for thin and long beams. This term is not considered in CLT to simplify the analysis.

First order shear deformation theory is more accurate to solve the problem as compared to classical lamination theory due to the presence of shear deformation in the theory but it introduces shear correction factor for appropriate representation of strain energy of deformation which can be eliminated in the higher order shear deformation theory. So higher order theory may give more accurate result as compared to FSDT.

CLT results when compared with ANSYS results, it is found that the percentage error is less than the percentage error of FSDT with ANSYS. This may be due to the reason that FSDT deflection contains a higher order term in addition to CLT deflection. This higher order term introduces error. But the shear deformation term from the table 7.3, is very negligible because the beam is long and thin. Therefore the deflection obtained from CLT and FSDT are almost close. Therefore the percent error due to CLT and FSDT are almost same. The effect of shear deformation term is significant for short and thick beam.

Table 7.3 Comparison of the semi analytical model with FEM model for H-H beam, length=0.1m, width= 5mm, UDL= 200 N/m, thickness of each ply= 0.125mm

Stacking sequence [$\pm\theta$] _s (deg.)	Deflection (m) (Semi-Analytical Method)			Deflection(m) (FEM)	Percentage error of FEM with Semi analytical method	
	CLT	FSDT	Shear deformation (FSDT- CLT)		FSDT	CLT
0	0.0001381	0.0001382	6.9735e-08	1.38E-04	0.14	0.09
15	0.00023382	0.00023389	7.2477e-08	2.16E-04	8.28	8.25
30	0.00049905	0.00049913	8.1202e-08	4.50E-04	10.92	10.90
45	0.0011	0.0011	9.7182e-08	1.03E-03	6.80	6.80
60	0.0018	0.0018	1.2099e-07	1.79E-03	1.12	1.12
75	0.0023	0.0023	1.4744e-07	2.28E-03	1.32	1.32
90	0.0024	0.0024	1.6026e-07	2.42E-03	0.41	0.41

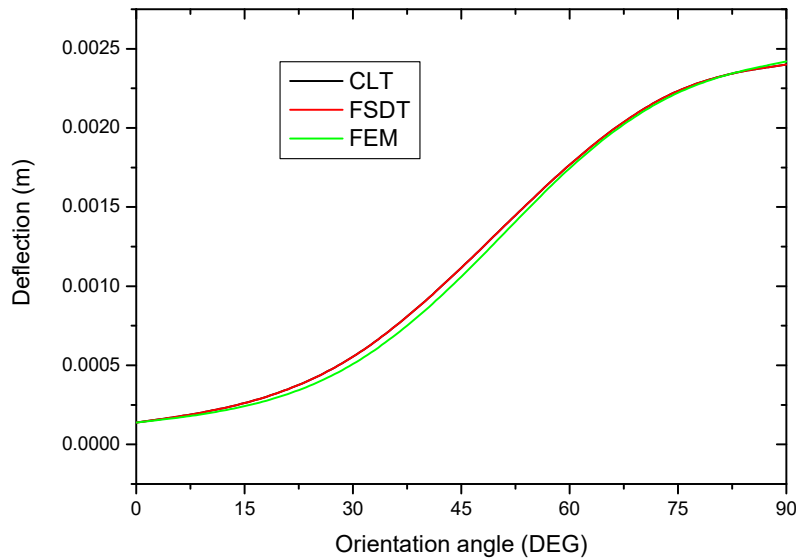


Figure 7.5(a). Comparison of the semi-analytical method (CLT & FSDT) with FEM

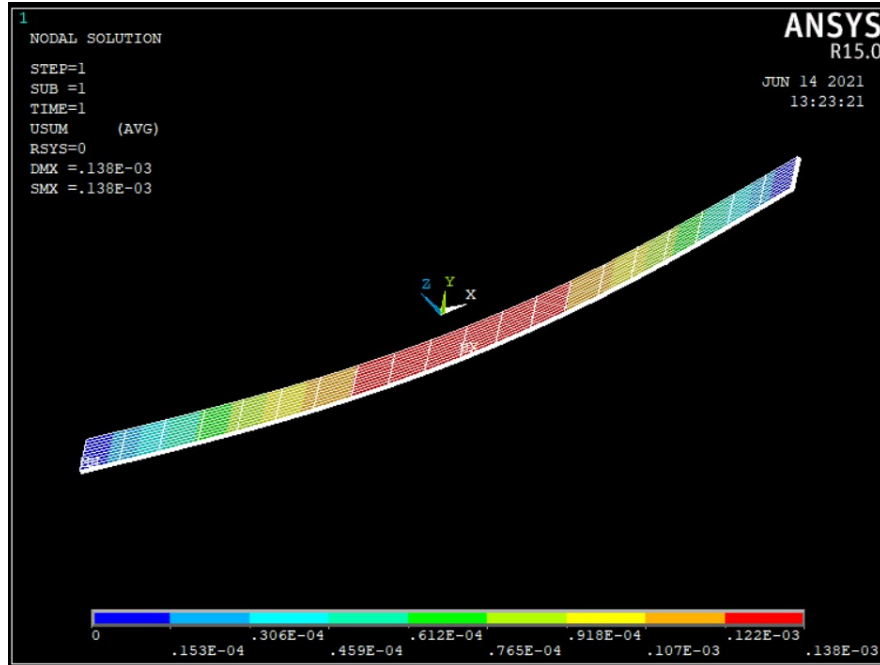


Figure 7.5 (b) Deflection of H-H beam for [0/-0]s

7.4.3.2 Effect of Orientation angle

The analysis is extended to evaluate the effect of orientation angle on non dimensional maximum deflection (\bar{w}) of Hinged- Hinged laminated composite beam under UDL. It is found that the non dimensional maximum transverse deflection (\bar{w}) increases as the fiber orientation angle increases from 0° to 90° (fig 7.5a) of symmetric four layer angle ply composite beam. Maximum deflection is obtained at a 90° angle and a minimum of 0° . Fig 7.5a also shows the comparison of three methods: semi analytical methods (CLT and FSDT) and FEM. The deflection found by FSDT is greater than that of CLT due to the presence of shear deformation, but this term is very small for thin and long beam and therefore deflection line of CLT and FSDT are almost coincide in fig 7.5(a) which is discussed in section 7.4.3.1. The difference in the deflection of the semi analytical method and FEM is not too much as compared to the plate. This may be due to the reason that the beam equations are more simplified and easy to solve as compared to plate equations because beam is the one dimensional representation of plate. Fig 7.5b shows the deflection of [0/0]s orientation at both end hinged laminated composite beam under UDL in FEM software ANSYS. The colour codes show the deflection at different regions of the beam whose values are given at the bottom of fig. 7.5 b.

7.4.3.3 Effect of boundary conditions

The above analysis is extended for different boundary conditions: Hinged-hinged (H-H), Clamped-Clamped (C-C) and Clamped-Free (C-F) beam under UDL. Fig 7.6 shows the effect of fiber orientation angle on the transverse deflection of a beam for different boundary conditions using first order shear deformation theory. From fig 7.6, the non dimensional deflection is minimum at 0 degree orientation angle and maximum at 90 degree angle and a sharp increase after 30 degree angle which may be conclude that the optimum orientation angle is 30 degree angle. Deflection of simply supported beam (H-H) with UDL is more as compared to fixed beam (C-C) with UDL, which can be inferred from their deflection formula (Table 7.1) and the cantilever beam (C-F) with UDL experiences the highest deflection.

7.4.3.4 Effect of the length to thickness ratio

The above analysis is further extended to different length to thickness ratios. The effect of the length to thickness ratio of the beam on the maximum transverse deflection is shown in fig 7.7. The effect of shear deformation is more significant for beams with (a/h) ratio of less than 10. As the a/h ratio increases, the maximum transverse deflection decreases and almost becomes constant. Length to thickness ratio has no effect on transverse deflection when the problem is solved by CLT due to the absence of shear deformation term in total deflection.

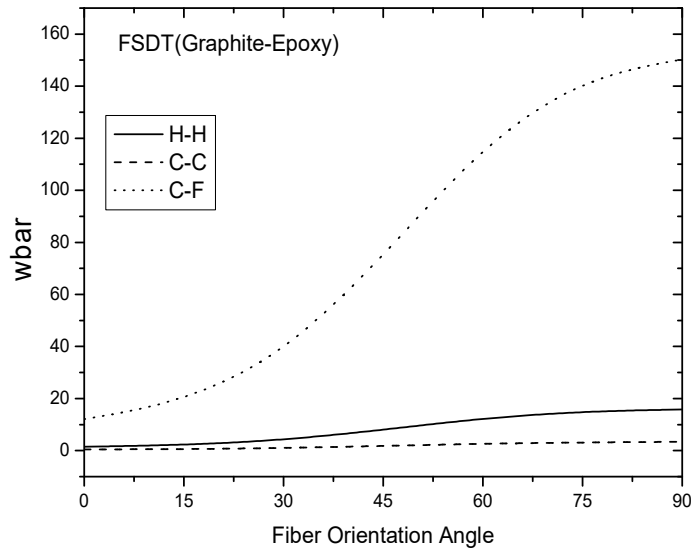


Figure 7.6 Effect of fiber orientation angle on non dimensional deflection for boundary conditions

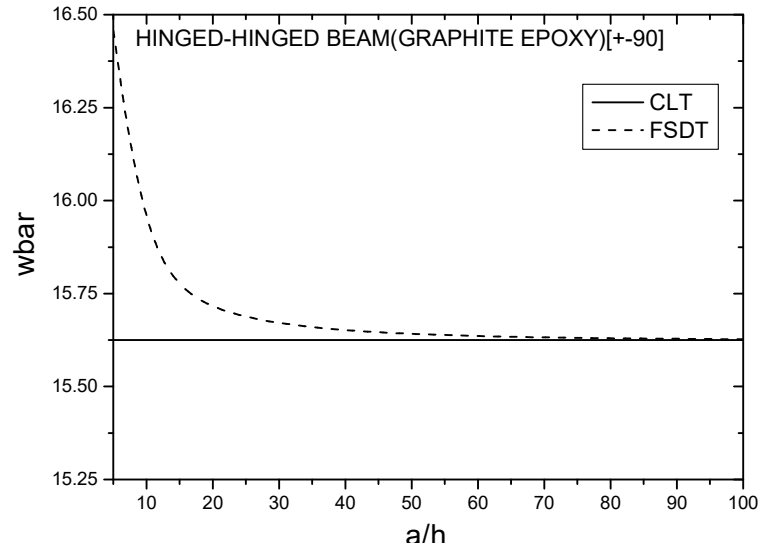


Figure 7.7 Effect of length to thickness ratio on non dimensional deflection for different methods.

7.4.3.5 Effect of no. of lamina

The analysis is extended to evaluate the effect of orientation angle on non dimensional maximum deflection (\bar{w}) of Hinged- Hinged laminated composite beam under UDL. As the number of lamina increases maximum transverse deflection decreases and almost becomes constant. The effect of non dimensional deflection is more significant for beams with number of lamina smaller than 8 (fig 7.8). Fig 7.9 shows the distribution of maximum normal stress along the thickness of the beam for different fiber orientation angle ranging from $\pm 0^\circ$ to $\pm 90^\circ$ and for different boundary conditions. There is a discontinuity in stress when the layers are changed i.e. stress distribution is not continuous along the thickness of beam.

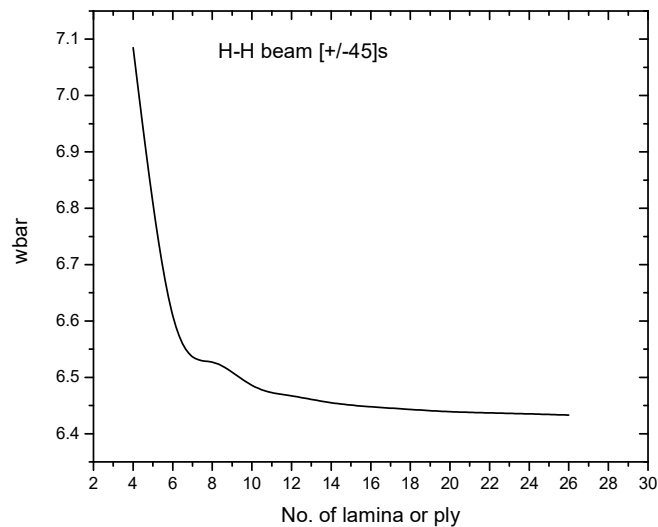
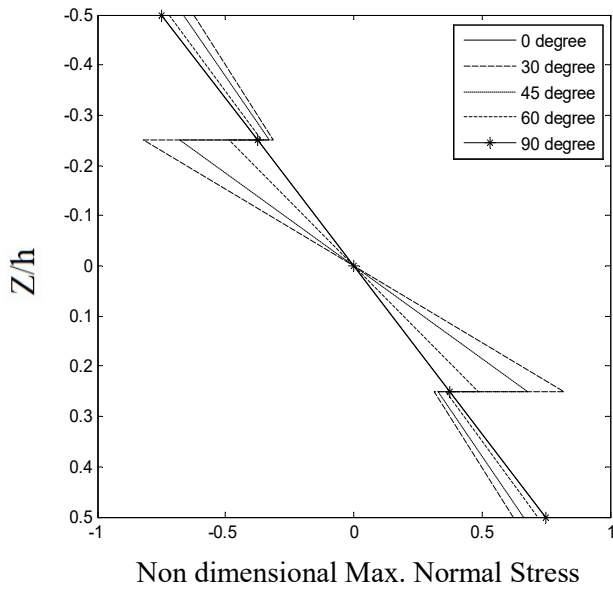
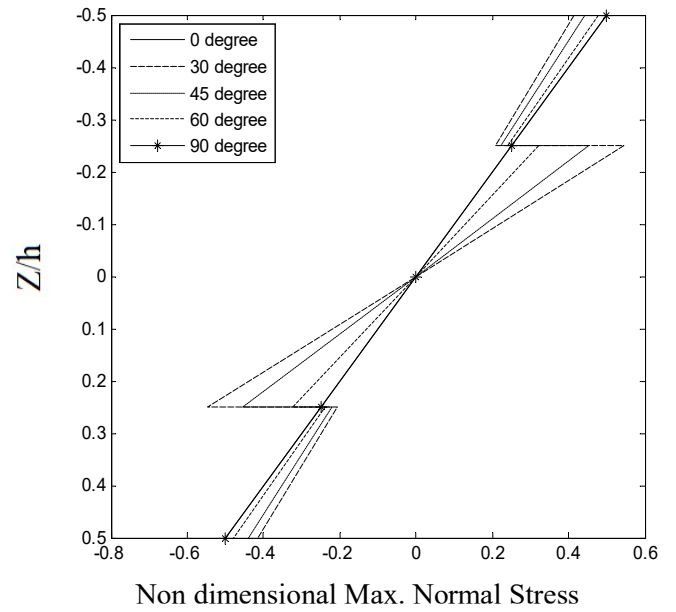


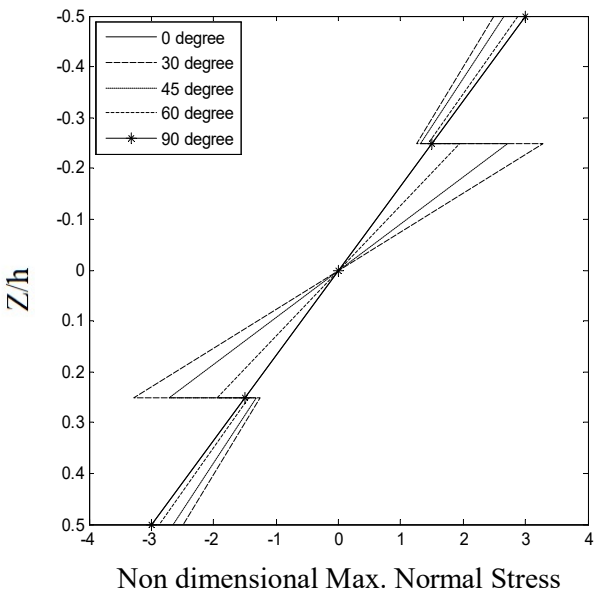
Figure 7.8 Effect of no. of lamina on non dimensional deflection solved by FSDT



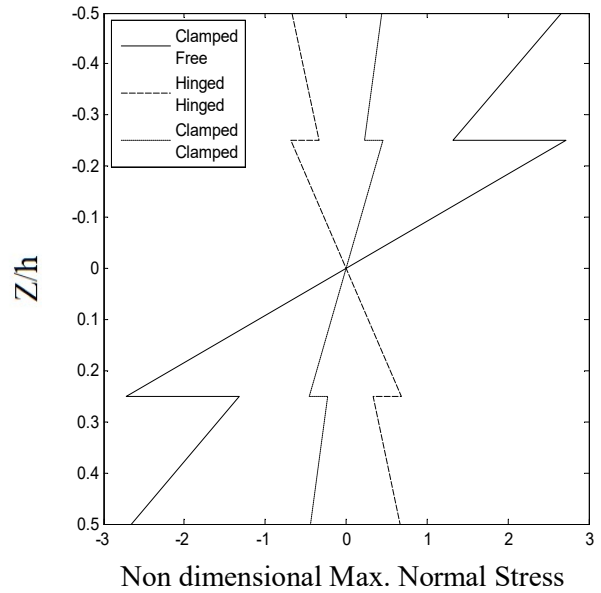
(a)



(b)



(c)



(d)

Figure 7.9 Distribution of maximum normal stress along the thickness of the beam for fiber orientation angle $[0/-0]_s$ to $[90/-90]_s$ for boundary conditions: (a) both end hinged (b) both end clamped (c) one end clamped and other end free. (d) Comparison of the variation of maximum normal stress along the beam thickness for different boundary conditions for $[45/-45]_s$ fiber orientation angle for Graphite/Epoxy

7.5 Analysis of Percentage error of laminated composite beam

As discussed in chapter 8, the results from the FEA software ANSYS are compared with the semi-analytical method (FSDT) solved in the MATLAB platform for different orientation angles, laminate thickness, mesh size, and length to width ratio for simply supported four layer laminated composite beam under a uniform distributed load of 200 N/m. Analysis of percentage error is performed for symmetric angle ply laminated beam of stacking sequence $[\theta/-\theta]_s$ which is represented by orientation angle “ θ ” as discussed above. Percentage error is the difference in results of FEA software with semi-analytical method with respect to semi-analytical results. From table 7.6, it is found that the percentage error depends on orientation angle, laminate thickness, and mesh size and length to width ratio.

7.5.1 Length to width ratio (L/W)

To find out the variation of the percentage error on the length to width ratio, other factors are kept constant. From figure 7.10 (a), it is seen that the variation of error is more significant for the L/W ratio below 10 as compared to after 10. After 10, the variation in error is almost constant. From the analysis, it can be concluded that, L/W ratio is below 10, beam equations are not applicable, i.e., a composite laminate below 10 cannot be considered as a beam, therefore it can be taken as plate. So, for problems with an L/W ratio below 10, if plate equation is applied, then error will be reduced. It is seen that after L/W ratio 10, the curve increases and decreases, i.e. no significant relationship can be established, but the variation in error is not too much.

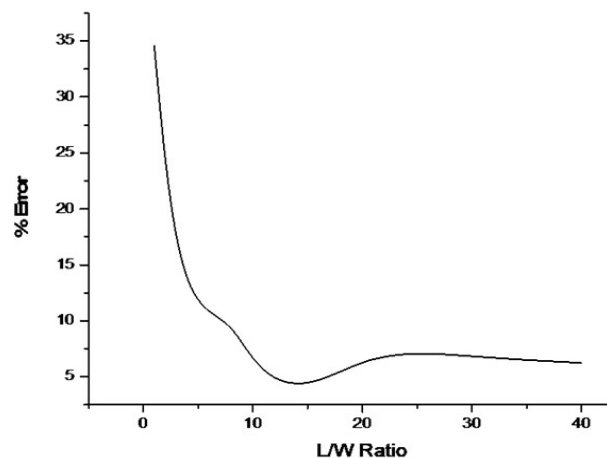


Figure 7.10 Variation of percentage error with L/W ratio from 1 and above for orientation angle of $[45/-45]_s$, mesh unit size of 0.25, thickness 0.5mm.

7.5.2 Mesh size unit

The variation of percentage error with mesh size is investigated, keeping the other factors constant, i.e. L/W ratio, angle, and thickness. Fig 7.11(a & b) show the variation for L/W ratio 10 and 20 respectively, thickness 0.5mm and angle 45 deg. It is found that the with the increase in mesh size or decrease in element size, the results gradually converge and, after a particular mesh size, the same results are obtained that is the solution becomes mesh size independent. This method is called convergence analysis. Therefore to obtain a better result, convergence analysis must be performed; otherwise the solution becomes mesh size dependent. So if convergence analysis is performed, this variable becomes insignificant. But it consumes more time for processing and computer memory.

7.5.3 Thickness of laminate

Another important variable in the analysis of laminated composites is the thickness of the laminate. From table 7.4 and fig 7.12, it is seen that as the thickness of the laminate increases, the percentage error decreases and approaches zero at a particular thickness, which is different for different L/W ratios, keeping the orientation angle constant. Therefore, thickness is a significant variable in the analysis of laminated composite beams. It is also found that though the L/W ratio is not as significant as discussed in the previous section, here in this section from table 7.4, it is seen that it has an effect on analysis. The percentage error approaches zero at different thicknesses for different L/W ratios, when the orientation angle is constant.

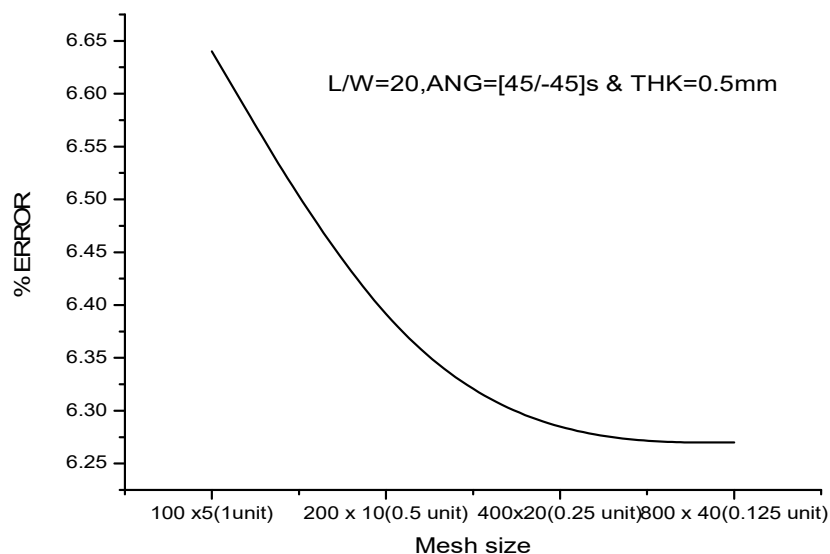


Figure 7.11(a) Variation of percentage error with mesh size (size of element) for L/W ratio of 20

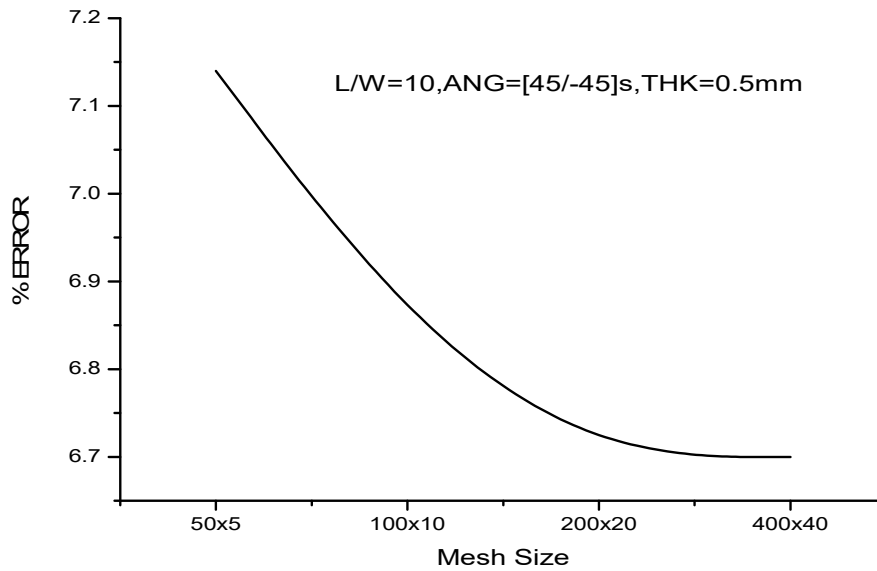


Figure 7.11(b) Variation of percentage error with mesh size (size of element) for L/W ratio of 10

Table 7.4: Percent error for different L/W and thickness of angle [45/-45]s

Thickness (mm)	L/W=10	L/W=20	L/W=30	L/W=40
0.5	6.7	6.27	6.84	6.25
1	4.77	4.81	4.96	4.95
1.5	3.36	3.66	3.6	3.88
2	1.93	3.03	2.89	3
2.5	1.11	1.97	2.06	2.09
3	0.47	1.4	1.67	1.7
3.5	0	0.69	1.08	1.1
4		0.55	1.01	1.05
4.5		0	0.62	0.65
5			0.42	0.45
5.5			0	0.38
6				0.3
6.5				0

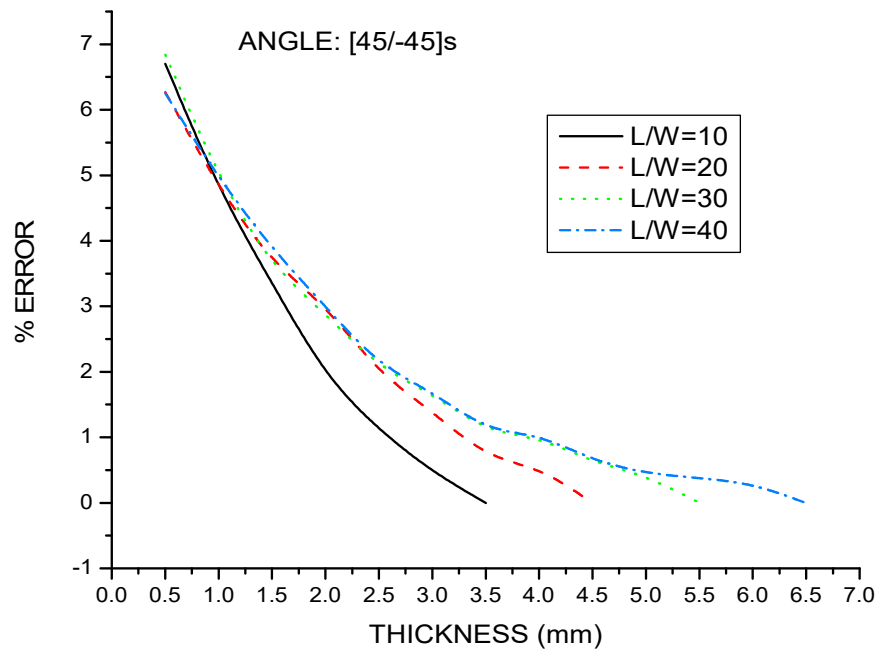


Figure 7.12 Percentage error for different L/W and thickness of angle [45/-45]s

7.5.4 Orientation angle

Another important variable is the orientation angle. In this section, a symmetrical arrangement of angle ply laminated composite beams is taken. As seen in the Chapter 7, the percentage error varies as the orientation angle changes from 0 deg to 90 deg. In the previous section 7.5.3, it is found that the percentage error approaches zero at a particular thickness of laminate when the L/W ratio and angle are kept constant. For example, the percentage error becomes zero at a laminate thickness of 3.5mm for an L/W ratio of 10 and an orientation angle of [45/-45]s. Now, keeping thickness and L/W ratio at 3.5mm and 10 mm, respectively constant, the orientation angle is changed, to study the effect of the orientation angle on percentage error. From table 7.5, it is seen that, %age error is zero at 45 degree angles but it is not zero at the other angles at the same L/W and thickness, which infers that orientation angle has a significant effect in the analysis of % age error (fig 7.13).

Table 7.5 Variation of %age error with orientation angle

Orientation Angle (deg)	semi analytical method (mm)	FEM (mm)	% Error
0	2.72E-08	2.78E-08	2.14
15	4.45E-08	4.22E-08	-5.08
30	9.23E-08	9.15E-08	-0.84
45	2.01E-07	2.01E-07	0.00
60	3.34E-07	3.34E-07	0.14
75	4.17E-07	4.18E-07	0.30
90	4.40E-07	4.42E-07	0.35

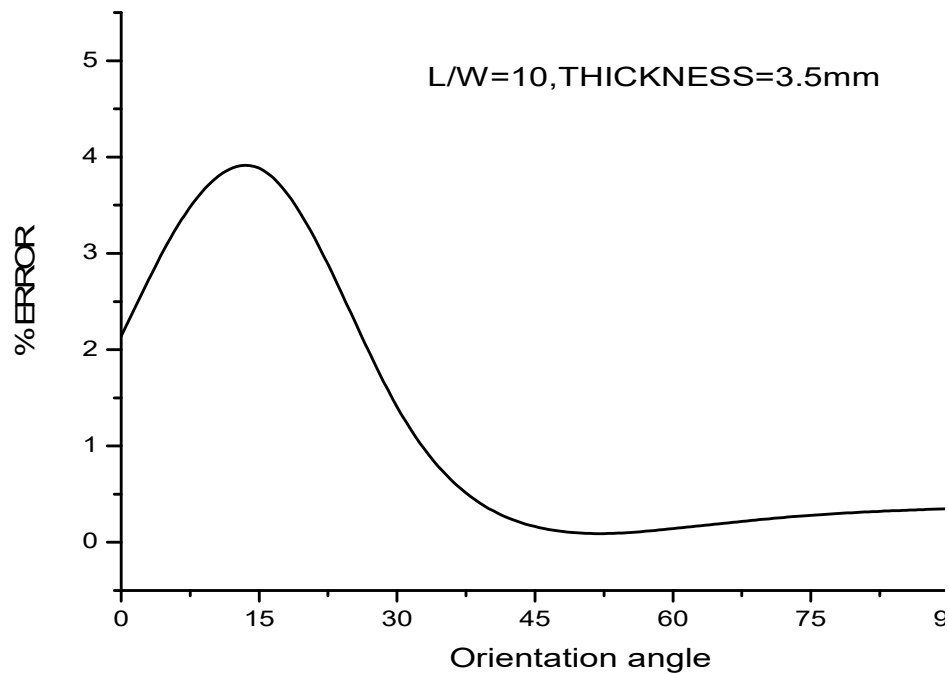


Figure 7.13 Effect of Orientation angle on Percentage (%) error

7.5.5 Statistical Analysis of Percentage Error in deflection

From the above discussion, it is seen that, the percentage error of deflection depends on several variables: L/W ratio, thickness of the laminate, mesh size, and orientation angle. The dependencies of %age error on these variables are discussed:

- The variation of % error with L/W ratio is not too much significant from L/W ratio 10 and above.
- The variation of %age error with mesh size is not too significant. It is found that with the increase in mesh size or decrease in element size, the results gradually converge and, after a particular mesh size, the same results are obtained i.e. the solution becomes mesh size independent. This method is time consuming.
- The variation of %age error with thickness and orientation angle has significant effect. It is seen that as the thickness increases, %age error decreases and gradually becomes zero at a particular thickness. The percentage error approaches zero at different thicknesses for different L/W ratios, when the orientation angle is constant. Therefore the L/W ratio, has an effect on the %age error. Whereas on the other hand, it is seen that % error changes with the change in orientation angle, keeping the other variables constant.
- It is also found out that the % error changes with different combinations of these variables.

Therefore, it is very difficult to establish a relationship between these variables with %age error. Also, it is very necessary to find out the contribution or significance of these variables in the analysis of the % error. So, statistical analysis of the percentage error is necessary to get a probable relationship between these variables and to find out the significance of these variables in the analysis.

7.5.5 (a) ANOVA

To understand the effect of these variables, length to width ratio (A), thickness of laminate (B), orientation angle (C) and Mesh size (D) on percentage error (E), data from table 7.6 is analysed using the analysis of variance (ANOVA) statistical tool. Three levels of these variables are chosen for creating the ANOVA table (table 7.7). The data are arranged for creating ANOVA table in table 7.8. In this analysis, length to width ratio (A), thickness of the laminate (B), orientation angle (C) and Mesh size (D) are independent variables, whereas percentage error (E) is a dependent variable or response factor. The significance level was based on the P-value,

i.e. Significant if $P < 0.05$ and insignificant for $P > 0.05$ (5% significant level or 95% confidence level). The MATLAB tool is used to solve the ANOVA table.

A one way ANOVA test is conducted on the response variable: percentage error and the output are presented in table 7.9. It is found that variables L/W ratio (A) and mesh size (D) are in significant ($P > 0.05$) whereas thickness (B) and orientation angle (C) are significant. L/W ratio is less insignificant with a probability of 0.279 as compared to a mesh size of 0.9668. To get the significance of the interaction of these variables, a two ways ANOVA with two-factor interaction test is conducted on response factor % error and the output is shown in table 7.10.

In table 7.10, the probability value of 0.289 indicates that the mean responses of % error for different levels of mesh size are not that significant. But thickness, orientation angle and L/W ratio have strong evidence of effect on %age error as corresponding probability values are zero. But one way ANOVA table shows that L/W ratio is insignificant with probability of 0.279, whereas mesh size is insignificant in both one way and two ways ANOVA. To understand the significance of the L/W ratio, an analysis of its interaction with other variables should be performed. Last four entries of probability column of table 7.10 are the probability value of null hypothesis for the two way interactions. The interaction between L/W ratio (A), thickness (B) and angle (C) i.e. AB, AC and BC are significant with probability value zero since A, B and C is significant. The interaction of D with A, B and C (AD, BD & CD) is not significant with probability value of 0.9859, 0.8592 and 0.5781 respectively. The interaction between the L/W ratio (A) and mesh size (D) is much higher than others with probability 0.9859, which shows that the L/W ratio is to some extent insignificant. The interaction between angle (C) and mesh size (D) is least significant as the probability value shows 0.5781 as compared to others. This shows that the significance of orientation angle (C) is greater than thickness (B).

To further study the significance between the variables A, B and C on E, variable D is eliminated because D is insignificant in both the test. An ANOVA table 7.11 is created using A, B and C and the results are noted in table 7.12. From table 7.12, it is seen that variable A (L/W ratio) is insignificant with a probability of 0.0747. Also, orientation angle is more significant with probability zero as compared to thickness, whose probability is 0.00036.

7.5.5 (b) Regression equation

In this thesis Design Expert 13.0 software has been applied to the data to obtain the mathematical equations for % error. In the present study responses, % error (E) are function of L/W ratio (A), thickness (B), Orientation angle (C) and mesh size (D). A second order polynomial equation used in RSM (Response surface methodology) is given below:

$$Y = b_0 + \sum_{i=1}^k (b_i x_i) + \sum_{i=1}^k (b_i x_i^2) + \sum \sum (b_{ij} x_i x_j) + \epsilon \quad (7.21)$$

Where Y= response variables i.e. dependent variables

x_i = predicted variables i.e. independent variables

b_0 = model constant

ϵ = random error

Parameters b_i , b_{ii} , b_{ij} are known as regression coefficient, where $i = 1, 2, 3, \dots, k$ and $j = 1, 2, 3, \dots, k$.

In the present study three parameters have been considered. Therefore for 4 factors, the selected polynomial equations are given as:

$$E = b_0 + b_1 A + b_2 B + b_3 C + b_4 D + b_{12} AB + b_{13} AC + b_{14} AD + b_{23} BC + b_{24} BD + b_{34} CD + b_{11} A^2 + b_{22} B^2 + b_{33} C^2 + b_{44} D^2 \quad (7.22)$$

Where E is the predicted response, b_0 model constant, b_1 , b_2 , b_3 and b_4 are linear coefficients,

b_{11} , b_{22} , b_{33} and b_{44} are quadratic coefficients and b_{12} , b_{13} , b_{14} , b_{23} , b_{24} , b_{34} are cross interaction coefficients.

The regression equations developed by RSM, used for predicting responses of % error (E) in terms of L/W ratio (A), thickness (B), Orientation angle (C) and mesh size (D) are given as:

$$E = 4.525 - 1.02333 * A - 2.89583 * B - 6.465 * C - 0.339167 * D + 0.32 * AB + 3.145 * AC + 0.55 * AD + 2.9325 * BC - 0.08 * BD + 0.5125 * CD - 1.87333 * A^2 + 0.270417 * B^2 + 3.18167 * C^2 + 0.357917 * D^2 \quad (7.23)$$

The equation in terms of coded factors can be used to make predictions about the response for given levels of each factor. By default, the high levels of the factors are coded as +1 and the

low levels are coded as -1. The coded equation is useful for identifying the relative impact of the factors by comparing the factor coefficients.

7.5.5 (C) Validation of a model

The adequacy of the developed model for %age error has been tested using the statistical analysis of variance (ANOVA) technique, which shows that the regression is significant with linear and quadratic terms for %age error at 95% confidence level as its p-value is less than 0.05. Adequate precision measures the signal to noise ratio. A ratio greater than 4 is desirable. This model shows a ratio of 13.249 which indicates an adequate signal. Therefore, this model can be used to navigate the design space. The validation of the developed model has also been checked by the normal probability plot of the residuals for %age error as shown in Fig. 7.14 and it is seen that the residuals fall on the straight line, which means the errors are distributed normally and the mathematical relationship has been correctly developed.

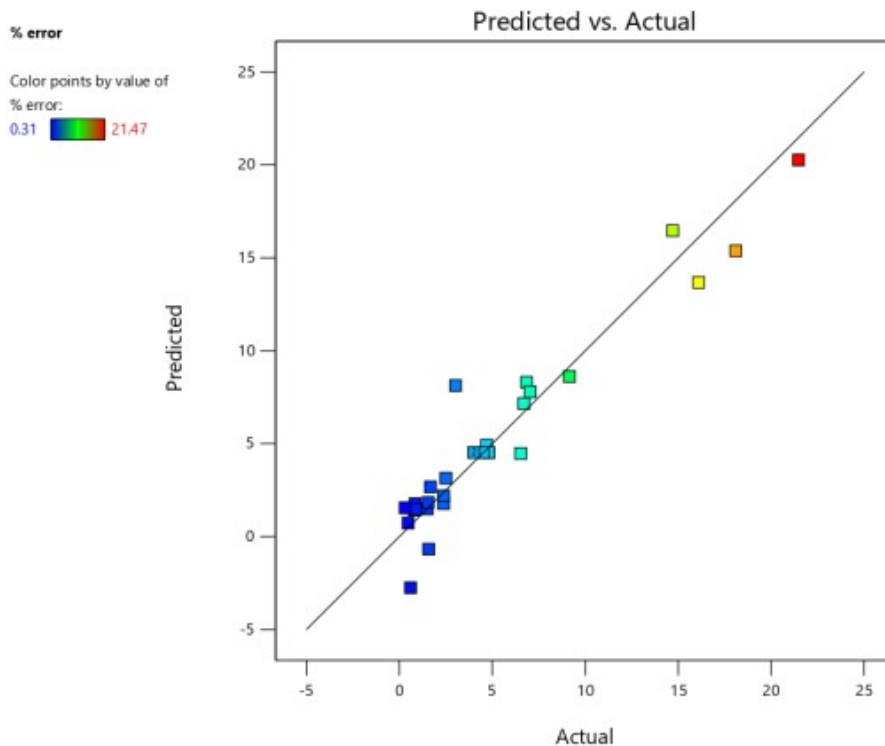


Figure 7.14 Residual plot of percentage (%) error

7.5.5 (d) Effect of Process Parameters

Fig 7.15 and 7.16 show the variation of factors with the response in surface plot and 2D plot respectively. From the plot, it is seen that the variation of %age error with mesh size is almost constant, because the graph is almost horizontal, which shows that the mesh size is insignificant. Also, the graph of the length to width ratio is slightly curved from horizontal, which shows that its significance is very small. The surface plot of mesh size and length to width ratio with % error is almost flat with a slight curvature (fig 7.15a). This curvature shows the little effect of length to width ratio on %age error. The slope of the curve of angle is greater than the thickness with a %age error, which shows that the effect of orientation angle is greater than thickness on %age error. The surface plot of combined thickness and angle with % age error is shown in fig 7.15 d which shows a gradual decrease with a slight bend. Therefore, as thickness increases, %age error decreases. Fig 7.15 b shows the combined effect of mesh size and thickness with %age error which is an almost flat decreasing curve. It shows that mesh size is insignificant, which is also reflected in ANOVA table 10.7. The same is the case for fig 7.15 c. The fig 7.16 (a) shows the 2d plot of percentage error with length to width ratio and thickness of laminate. The variation of percentage error with length to width ratio within the range of L/W ratio of 10 to 50 is almost the same as explained in section 7.5.1. The variation in %age error is less after 10, as seen in the previous fig 7.10. The black line is the mean of the two blue lines (upper and lower limit). The variation in %age error with the thickness of laminate is same as seen in the section 7.5.3. Fig 7.16 (b) shows the 2d plot of percentage error with orientation angle and mesh size. The variation in %age error with angle is same as seen in the section 7.5.4. The variation in %age error with mesh size is almost constant, which shows that mesh size is insignificant factor which can be eliminated by convergence.

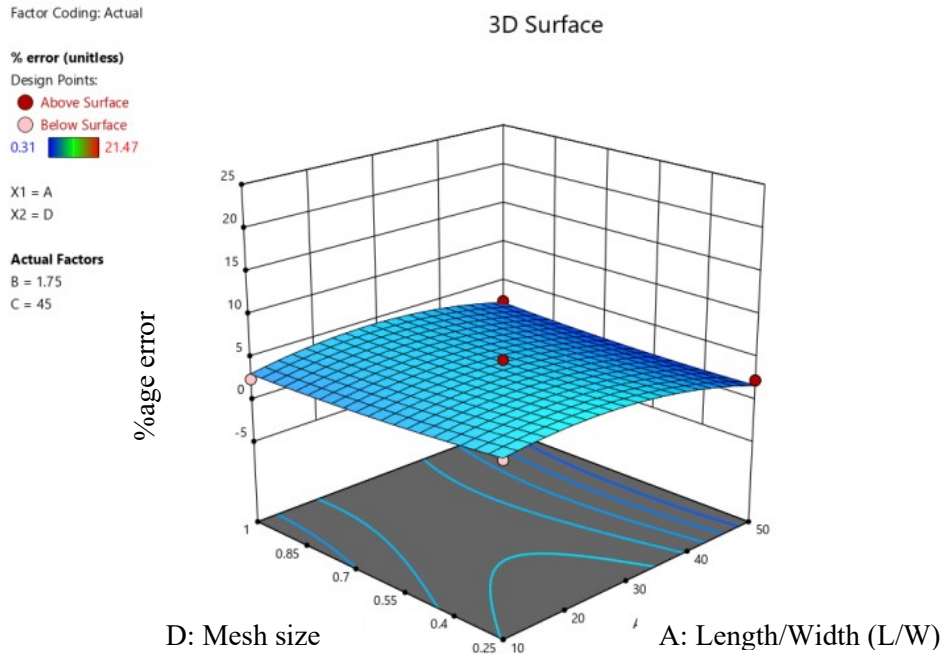


Figure 7.15(a) . Surface plot of factors with response (%age Error)

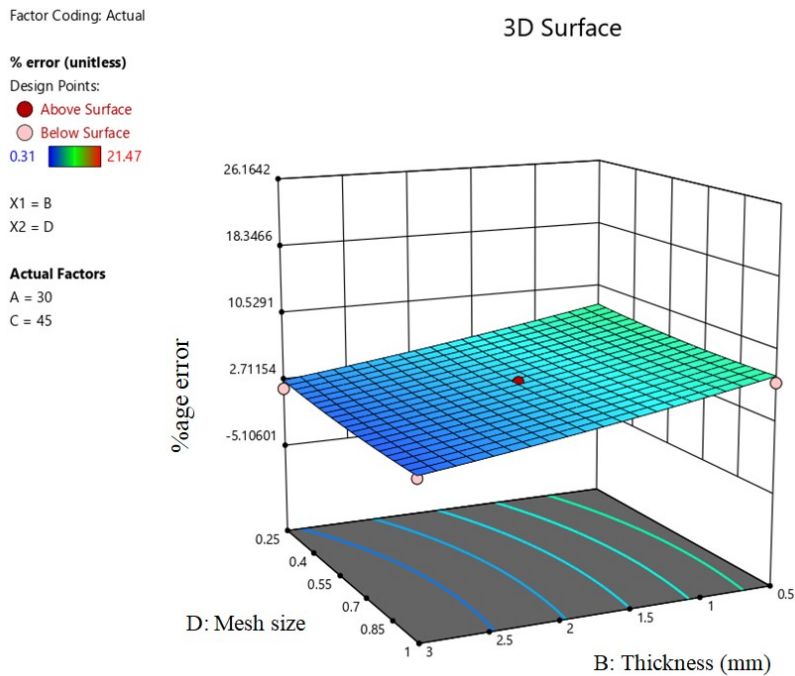


Figure 7.15(b) . Surface plot of factors with response (%age Error)

Factor Coding: Actual

% error (unitless)

Design Points:

● Above Surface

○ Below Surface

0.31  21.47

X1 = C

X2 = D

Actual Factors

A = 30

B = 1.75

D: Mesh size

3D Surface

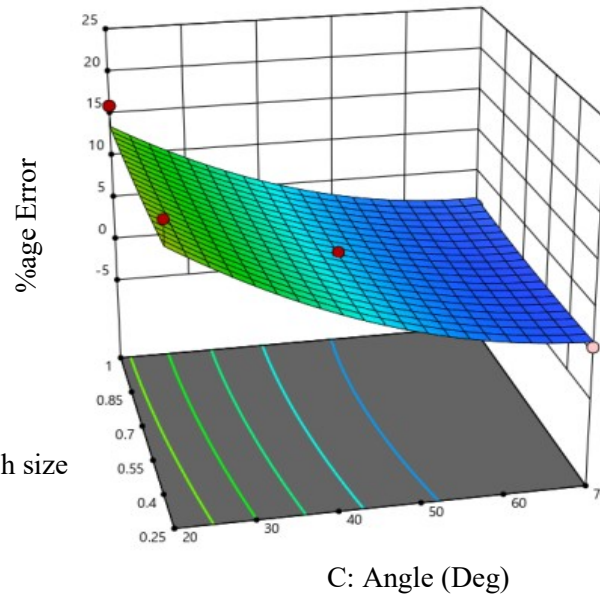


Figure 7.15(c) . Surface plot of factors with response (%age Error)

Factor Coding: Actual

% error (unitless)

Design Points:

● Above Surface

○ Below Surface

0.31  21.47

X1 = B

X2 = C

Actual Factors

A = 30

D = 0.625

B: Thickness (mm)

3D Surface

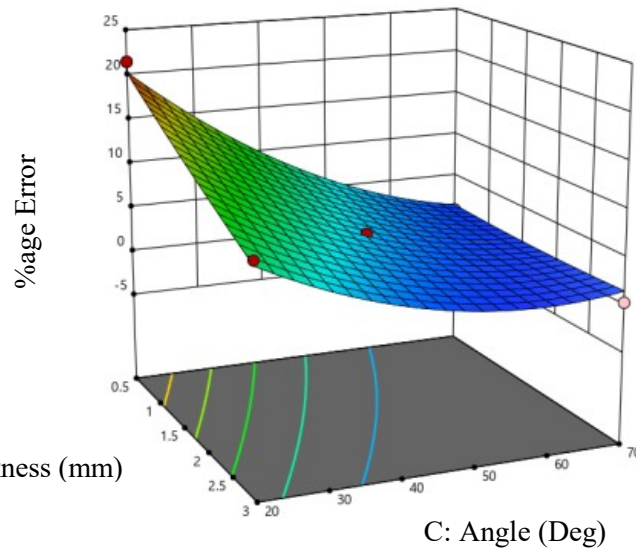


Figure 7.15(d) . Surface plot of factors with response (%age Error)

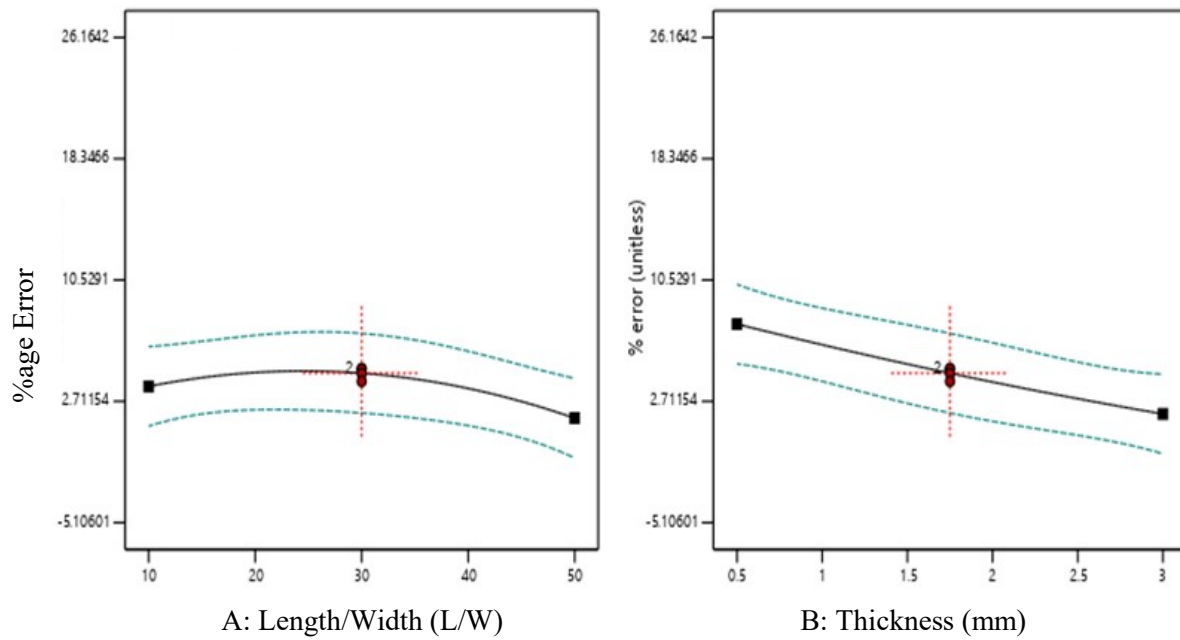


Figure 7.16 (a) 2 D plot of factors with response (%age Error)

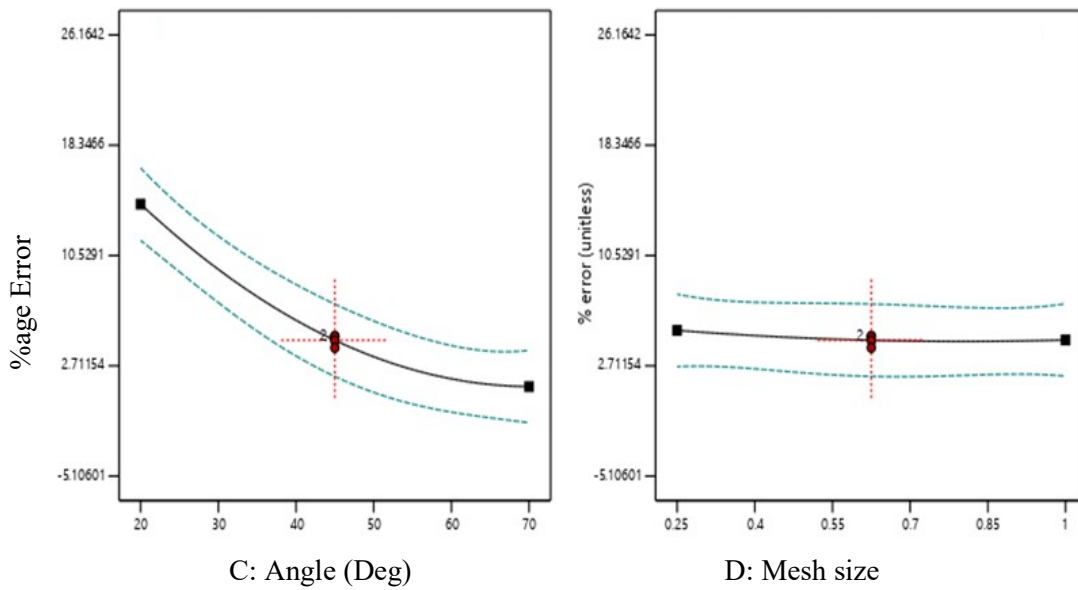


Figure 7.16 (b) 2 D plot of factors with response (%age Error)

Table 7.6. Percentage error in deflection (E) of semi analytical method with FEM (ANSYS) for simply supported beam under UDL of 200 N/m

ANGLE (Deg)		20			45			70		
		Thickness (mm)								
Length to width ratio (L/W)	Mesh Unit size	0.5	2	3	0.5	2	3	0.5	2	3
		10	1	22.14	12.05	6.37	7.14	1.93	0.47	1.16
0.5	21.60		11.71	6.15	6.85	1.93	0.47	1.16	0.11	0.01
0.25	21.06		11.71	6.15	6.70	1.93	0.47	1.16	0.11	0.01
30	1	21.93	13.77	9.29	7.04	2.89	1.67	1.24	0.52	0.31
	0.5	21.47	13.34	9.15	6.84	2.89	1.67	1.20	0.52	0.31
	0.25	21.47	13.34	9.15	6.84	2.89	1.67	1.20	0.52	0.31
50	1	21.43	13.60	9.60	6.53	2.96	1.58	0.84	2.08	0.32
	0.5	20.98	13.60	9.41	6.53	2.96	1.58	0.81	2.08	0.32
	0.25	20.81	13.60	9.41	6.53	2.96	1.58	0.81	2.08	0.32

Table 7.7 Variables for statistical analysis with levels.

Variables	Unit	Notation	Level		
			1	2	3
Length/Width	unit less	A	10	30	50
Thickness	mm	B	0.5	2	3
Angle	deg	C	20	45	70
Mesh Size	unit less	D	0.25	0.5	1

Table 7.8 Arrangement of data for ANOVA of simply supported beam

Sl.No.	A	B	C	D	E	Sl.No.	A	B	C	D	E
1	10	0.5	20	1	22.14	41	30	2	45	0.5	2.89
2	10	0.5	20	0.5	21.6	42	30	2	45	0.25	2.89
3	10	0.5	20	0.25	21.06	43	30	2	70	1	0.52
4	10	0.5	45	1	7.14	44	30	2	70	0.5	0.52
5	10	0.5	45	0.5	6.85	45	30	2	70	0.25	0.52

Sl.No.	A	B	C	D	E	Sl.No.	A	B	C	D	E
6	10	0.5	45	0.25	6.7	46	30	3	20	1	9.29
7	10	0.5	70	1	1.16	47	30	3	20	0.5	9.15
8	10	0.5	70	0.5	1.16	48	30	3	20	0.25	9.15
9	10	0.5	70	0.25	1.16	49	30	3	45	1	1.67
10	10	2	20	1	12.05	50	30	3	45	0.5	1.67
11	10	2	20	0.5	11.71	51	30	3	45	0.25	1.67
12	10	2	20	0.25	11.71	52	30	3	70	1	0.31
13	10	2	45	1	1.93	53	30	3	70	0.5	0.31
14	10	2	45	0.5	1.93	54	30	3	70	0.25	0.31
15	10	2	45	0.25	1.93	55	50	0.5	20	1	21.43
16	10	2	70	1	0.11	56	50	0.5	20	0.5	20.98
17	10	2	70	0.5	0.11	57	50	0.5	20	0.25	20.81
18	10	2	70	0.25	0.11	58	50	0.5	45	1	6.53
19	10	3	20	1	6.37	59	50	0.5	45	0.5	6.53
20	10	3	20	0.5	6.15	60	50	0.5	45	0.25	6.53
21	10	3	20	0.25	6.15	61	50	0.5	70	1	0.84
22	10	3	45	1	0.47	62	50	0.5	70	0.5	0.81
23	10	3	45	0.5	0.47	63	50	0.5	70	0.25	0.81
24	10	3	45	0.25	0.47	64	50	2	20	1	13.6
25	10	3	70	1	0.01	65	50	2	20	0.5	13.6
26	10	3	70	0.5	0.01	66	50	2	20	0.25	13.6
27	10	3	70	0.25	0.01	67	50	2	45	1	2.96
28	30	0.5	20	1	21.93	68	50	2	45	0.5	2.96
29	30	0.5	20	0.5	21.47	69	50	2	45	0.25	2.96
30	30	0.5	20	0.25	21.47	70	50	2	70	1	2.08
31	30	0.5	45	1	7.04	71	50	2	70	0.5	2.08
32	30	0.5	45	0.5	6.84	72	50	2	70	0.25	2.08
33	30	0.5	45	0.25	6.84	73	50	3	20	1	9.6
34	30	0.5	70	1	1.24	74	50	3	20	0.5	9.41
35	30	0.5	70	0.5	1.2	75	50	3	20	0.25	9.41
36	30	0.5	70	0.25	1.2	76	50	3	45	1	1.58
37	30	2	20	1	13.77	77	50	3	45	0.5	1.58
38	30	2	20	0.5	13.34	78	50	3	45	0.25	1.58
39	30	2	20	0.25	13.34	79	50	3	70	1	0.32
40	30	2	45	1	2.89	80	50	3	70	0.5	0.32
						81	50	3	70	0.25	0.32

Table 7.9 Results for one way ANOVA

Source	Sum of Square	Degree of freedom	Mean Square	F	Probability (P)	Remarks
L/W (A)	13.9395	2	6.9697	1.2995	0.2790	In significant
Thickness (B)	590.3119	2	295.1560	55.0305	0.0000	significant
Angle (C)	2742.3807	2	1371.1903	255.6524	0.0000	significant
Mesh size (D)	0.3628	2	0.1814	0.0338	0.9668	In significant
Error	386.1717	72	5.3635			
Total	3733.1666	80				

Table 7.10 Results for two ways ANOVA

Source	Sum of Square	Degree of freedom	Mean Square	F-value	P-value	Remark
A	13.9395	2	6.969749383	48.95346362	0	Significant
B	590.3119	2	295.1559716	2073.088475	0	Significant
C	2742.381	2	1371.190349	9630.836519	0	Significant
D	0.362773	2	0.18138642	1.274004704	0.289	In Significant
A*B	12.78637	4	3.196591975	22.45191905	0	Significant
A*C	4.627457	4	1.156864198	8.125472854	0	Significant
A*D	0.04996	4	0.012490123	0.087726943	0.9859	In Significant
B*C	361.2744	4	90.31859198	634.3711464	0	Significant
B*D	0.185649	4	0.046412346	0.325986625	0.8592	InSignificant
C*D	0.413872	4	0.103467901	0.726728016	0.5781	In Significant
Error	6.834	48	0.142375			
Total	3733.167	80				

Table 7.11. Arrangement of data for ANOVA eliminating the insignificant term

L/W	Thickness (mm)	Orientation Angle (Deg)	% Error (Deflection)
10	0.5	20	21.06
10	2	45	1.93
10	3	70	0.01
30	0.5	45	6.84
30	2	70	0.52
30	3	20	9.15
50	0.5	70	0.81
50	2	20	13.6
50	3	45	1.58
10	0.5	20	21.06
10	2	45	1.93
10	3	70	0.01
30	0.5	45	6.84
30	2	70	0.52
30	3	20	9.15
50	0.5	70	0.81
50	2	20	13.6
50	3	45	1.58
10	0.5	20	21.06

Table 7.12 Results of ANOVA eliminating the insignificant term

Source	Sum of Square	degree of freedom	Mean Square	F-value	P-value	Remarks
A	25.8990	2	12.9495	3.2457	0.0747	In significant
B	131.1331	2	65.5666	16.4336	0.00036	significant
C	744.0233	2	372.0117	93.2411	0	significant
Error	47.8774	12	3.9898			
Total	1057.9163	18				

7.6 Closure

From the discussion in this chapter, it may be concluded that the percentage error of problems solved by CLT with finite element method is less than that of FSDT because FSDT deflection contains a higher order term in addition to CLT deflection which introduces an error. The deflection obtained by CLT and FSDT in this chapter is almost close because the shear deformation term is negligible for long and thin beams. Therefore, the percentage error due to CLT and FSDT is almost the close. The effect of the shear deformation term is significant for short and thick beams. From this chapter, it is concluded that laminate thickness and orientation angle has more significant effect on percentage error as compared to other variables. Therefore, the percentage error for a laminated composite beam can be reduced by the optimum combination of laminate thickness and orientation angle.

CHAPTER 8

FAILURE ANALYSIS OF LAMINATED COMPOSITE

8.1 Introduction, 8.2 Methodology to find Strength ratio & First ply failure load, 8.2.1 Thermo mechanical stress 8.3. Failure theories, 8.3.1 Maximum stress criteria, 8.3.2 Maximum strain criteria, 8.3.3 Tsai–Wu Failure Theory, 8.3.4 Tsai–Hill failure theory, 8.3.5 Strength ratio, 8.4 Failure of laminated composite plate under in-plane tensile load, 8.4.1 Numerical Problem 8.4.1.1 Validation of semi analytical & FEM model, 8.4.1.2 Comparison of semi analytical and FEM model, 8.4.2 Effect of fiber orientation angle on failure analysis, 8.4.2.1 Symmetric Angle ply composite subjected to different mechanical loading condition, 8.4.3 Comparative study of different failure criteria based on first ply failure load, 8.4.4 Last ply failure analysis of laminate under tensile loading, 8.4.5. Mode of failure, 8.4.6 Effect of hygro-thermo mechanical loading on strength ratio 8.5 Failure analysis of Laminated Composite Beam, 8.5.1. Numerical Problem, 8.5.2. Results and discussion, 8.5.2.1 Comparative study of different failure theories for beam fixed at both ends under UDL, 8.5.2.2 Effect of fiber orientation angle on strength ratio for different boundary conditions of composite beam subjected to mechanical load (Uniformly distributed load), 8.5.2.3 Effect of thermal load on strength ratio of composite beam, 8.5.2.4 Effect of length to thickness ratio (a/h) on strength ratio based on FPF load, 8.5.2.5 Mode of failure, 8.6 Comparison of FEM results with Analytical method (FSDT), 8.7 Closure

8.1 Introduction

Failure analysis of a laminate is more complex than that of a single lamina, which requires accurate prediction of the strength of each lamina by assessing the stresses to its principal axis in each lamina and by applying suitable failure criteria. The strength of a laminate depends on lamina orientation angle, strength, stiffness, coefficient of thermal and moisture expansion, stacking sequence, and finally the fabrication process, which affect the residual stresses, which in turn affect the strength of laminate. A Composite structure failed due to an increase in load. The whole laminate does not fail at the same time. It happens that, due to an increase in load, a single ply fail within the laminate and the rest of the ply continues to take the load. Due to an increase in further load, the next ply fails and it continues till all the plies fail. The load at which the first ply and last ply of the laminate fail is called the first ply failure load and last ply failure load, respectively. When the first ply fails, the rest of the ply bears the strength and

stiffness of the laminate. When a ply fails, replace the failed ply with a hypothetical ply of near zero stiffness and strength to remove singularities in the matrix.

A laminate may fail by the failure of individual lamina (*intra laminar failure*) or by the separation of laminas or layers (*inter laminar failure*). First ply failure (FPF) can be determined by performing a stress analysis of the laminate under a given loading condition, determining the state of stress in each layer and assessing the strength of each layer by applying selected failure criteria. The FPF approach is conservative and it is used with low factor of safety or strength ratio. In ultimate laminate failure, a laminate fails when the maximum load level is reached. In a progressive failure scheme, after each ply failure, the influence and contribution of the damaged ply on the remaining ply must be evaluated until the final lamina fails. Ultimate laminate failure (ULF) can occur at a much higher load than FPF. After FPF, the failure process continues up to ULF. Laminate efficiency is the ratio of FPF and ULF. Failure of composite material can take place in different ways. First ply failure (FPF) occurs when the first lamina of the laminate fails either in the longitudinal or in the transverse direction of fibers. Then the last ply failure occurs when the laminate is not capable of taking any further additional load. A laminate can fail by (a) breaking of fibers (b) matrix cracking, (c) debonding of fiber and matrix, (d) de lamination of one lamina from another.

8.2 Methodology for determining Strength ratio & first ply failure load

- I. Enter the fundamental lamina properties ($E_1, E_2, G_{12}, \nu_{12}$).
- II. Calculate the ply stiffness $[Q]_{12}$ referred to their principle material axis.
- III. Input the orientation θ_k , number of layers n , through the thickness coordinate z .
- IV. Find out the transformed layer stiffness $[Q]_{xy}^k$ referred to the laminate coordinate system(x, y).
- V. Calculate the laminate stiffness matrix $[A], [B], [D]$ and their compliance matrix.
- VI. Enter the mechanical load, $[N]_{x,y}, [M]_{x,y}$.
- VII. Calculate midplane strain $[\varepsilon^0]_{xy}$ and curvature $[k]_{xy}$ using laminate analysis.
- VIII. Calculate the layer strain $[\varepsilon]_{1,2}^k$ and stress $[\sigma]_{1,2}^k$ with reference to the principal axis (1, 2) in each layer under the given load.

- IX. Enter the five lamina strength and using a suitable failure theory as discussed in the paper find out the strength ratio/ safety factor of each of the lamina. Then the minimum strength ratio is the desired strength ratio of the laminate.
- X. Multiply the minimum strength ratio to the applied load to give the load level of the failure of the first ply. This load is called the **First Ply Failure load (FPF)**.

8.2.1 Thermo mechanical stress

Composite materials are processed at high temperatures and then cooled down to room temperatures. Some composite structures operate at a high temperature, different from the operating temperature. Due to a mismatch of the coefficients of thermal expansion of the fiber and matrix, residual stresses develop in a lamina. Due to this, a thermal strain has developed in the lamina. Laminae oriented at different angles within the laminate have different thermal strains. Each lamina in a laminate gets stressed by the deformation differences between adjacent laminas. This difference produces mechanical strain and stress.

The mechanical strains developed by thermal loads are:

$$[\varepsilon^M] = [\varepsilon] - [\varepsilon^T] \quad \text{Where} \quad [\varepsilon] = [\varepsilon^0] + z[k] \quad (8.1)$$

Where M and T represent mechanical and free expansion thermal strain respectively.

The thermal stresses are given by:

$$[\sigma^T] = [\bar{Q}][\varepsilon^M] \quad (8.2)$$

Mid plane strain and curvature is calculated by:

$$\begin{bmatrix} N^T \\ M^T \end{bmatrix} = \begin{bmatrix} A & B \\ B & D \end{bmatrix} \begin{bmatrix} \varepsilon^0 \\ k \end{bmatrix} \quad (8.3)$$

Where $[N^T] = \Delta T \sum_{k=1}^n [\bar{Q}_{ij}]_k [\alpha]_k (h_k - h_{k-1})$

$$[M^T] = \frac{1}{2} \Delta T \sum_{k=1}^n [\bar{Q}_{ij}]_k [\alpha]_k (h_k^2 - h_{k-1}^2) \quad (8.4)$$

Thus, if both mechanical and thermal loads are applied, then superpose the mechanical loads to the fictitious thermal loads to find the ply-by-ply stresses and strains in the laminate or separately apply the mechanical and thermal loads and then add the resulting stresses and strains from the solution of the two problems.

8.2.2 Hygro thermal stress

Hygro thermal stresses are developed in composite laminate when they are cooled from processing temperature, operating temperature which is different from processing temperature and humid atmosphere.

The mechanical strain developed in the laminate by hygro thermal load alone

$$[\varepsilon^M] = [\varepsilon] - [\varepsilon^T] - [\varepsilon^c] \quad (8.5)$$

Where c represent free expansion moisture strains.

Mid plane strain and curvature can be calculated as

$$\begin{bmatrix} N^T \\ M^T \end{bmatrix} + \begin{bmatrix} N^c \\ M^c \end{bmatrix} = \begin{bmatrix} A & B \\ B & D \end{bmatrix} \begin{bmatrix} \varepsilon^0 \\ k \end{bmatrix} \quad (8.6)$$

The mechanical strain in the kth ply can be calculated from the eq. 8.5 and mechanical stress can therefore calculated as

$$[\sigma^M] = [\bar{Q}][\varepsilon^M] \quad (8.7)$$

Therefore, if both mechanical and hygro thermal loads are present (for example aero plane flying at high altitude), ply-by-ply stresses and strains in the laminate can be found out by adding the mechanical loads to the fictitious hygro thermal loads.

8.3 Failure theories

Single failure criteria are not sufficient to predict the failure of all types of laminate. Failure theories are classified into three groups:

1. Non- interactive theories (Maximum stress, Maximum strain theory).
2. Interactive theories (Tsai-Hill, Tsai- Wu failure theory).
3. Failure mode based theories (Hashin- Rotem, Puck theory).

Non- interactive theories such as Maximum stress, Maximum strain theory are simple to apply and can be used to determine the mode of failure, but Interactive theories like Tsai-Hill, Tsai-Wu failure theories cannot tell the mode of failure, but they can explain the interaction of stress in failure. Failure mode based theories like Hashin- Rotem, Puck theory is used to determine the mode of failure effectively. In the present study, interactive and non-interactive theories are used to determine the strength ratio or safety factor of a laminated composite plate under in plane loading. Maximum strain theory or maximum stress theory can be used to determine the mode of failure.

8.3.1 Maximum stress criteria

Failure is predicted in a lamina, if any of the normal or shear stresses in the local axes of a lamina is equal to or exceeds the corresponding ultimate strengths of the unidirectional lamina.

The lamina is considered to be failed if

$$\begin{aligned} -(\sigma_1^c)_{ult} < \sigma_1 < (\sigma_1^T)_{ult} \\ -(\sigma_2^c)_{ult} < \sigma_2 < (\sigma_2^T)_{ult} \\ -(\tau_{12})_{ult} < \tau_{12} < (\tau_{12})_{ult} \text{ is violated.} \end{aligned} \quad (8.8)$$

8.3.2 Maximum strain criteria

Failure is predicted in a lamina, if any of the normal or shearing strains in the local axes of a lamina equal or exceed the corresponding ultimate strains of the unidirectional lamina. A lamina is considered to be failed if

$$\begin{aligned} -(\varepsilon_1^c)_{ult} < \varepsilon_1 < (\varepsilon_1^T)_{ult} \\ -(\varepsilon_2^c)_{ult} < \varepsilon_2 < (\varepsilon_2^T)_{ult} \\ -(\gamma_{12})_{ult} < \gamma_{12} < (\gamma_{12})_{ult} \text{ is violated.} \end{aligned} \quad (8.9)$$

8.3.3 Tsai–Wu Failure Theory

This failure theory is based on the total strain energy failure theory. Tsai- Wu failure criteria is a quadratic failure criteria which take into account the interaction of stress components but it cannot be used to determine the mode of failure. A lamina is considered to be failed if:

$$H_1\sigma_1 + H_2\sigma_2 + H_6\tau_{12} + H_{11}\sigma_1^2 + H_{22}\sigma_2^2 + H_{11}\sigma_1^2 + H_{66}\tau_{12}^2 + 2H_{12}\sigma_1\sigma_2 < 1 \quad (8.10)$$

is violated. This failure theory is more general than the Tsai–Hill failure theory because it distinguishes between the compressive and tensile strengths of a lamina. The components H_1 , H_2 , H_6 , H_{11} , H_{22} , and H_{66} of the failure theory are found using the five strength parameters of a unidirectional lamina.

8.3.4 Tsai–Hill failure theory

This theory is based on the distortion energy failure theory of Von-Misses. Hill adopted the Von- Mises' distortional energy yield criterion to anisotropic materials. Then, Tsai adapted it to a unidirectional lamina. Based on the distortion energy theory, he proposed that a lamina has failed if

$$(G_2 + G_3)\sigma_1^2 + (G_1 + G_3)\sigma_2^2 + (G_1 + G_2)\sigma_3^2 - 2G_3\sigma_1\sigma_2 - 2G_2\sigma_1\sigma_3 - 2G_1\sigma_2\sigma_3 + 2G_4\tau_{23}^2 + 2G_5\tau_{13}^2 + 2G_6\tau_{12}^2 < 1 \quad (8.11)$$

is violated. The components G_1 , G_2 , G_3 , G_4 , G_5 , and G_6 of the strength criterion depend on the failure strengths.

8.3.5 Strength ratio

The failure theories only state that whether the lamina fails or not when the inequalities are violated but it cannot state how much the load can be increased or decreased if the lamina is safe or fails respectively. The definition of strength ratio (SR) is helpful here. The strength ratio is defined as

$$SR = \frac{\text{Maximum load applied}}{\text{Load applied}} = \frac{\text{ultimate strength}}{\text{applied stress}} \quad (8.12)$$

8.4 Failure of laminated composite plate under in-plane tensile load

The semi analytical method to find the strength ratio using different failure theories as discussed above is applied to determine the failure of a laminated composite plate under in plane tensile load. The semi analytical model of failure is solved by using the MATLAB tool. A programme to find the strength ratio and first ply failure load is developed by using the methodology discussed in section 8.2 of this chapter.

8.4.1 Numerical Problem

A fiber reinforced composite square plate is subjected to uniform tensile in plane load on top and bottom surfaces (y direction) or on the side surfaces (x direction) or combination of both. The fibers are oriented at different angles ranging from 0° to 90° with stacking sequence of $[\theta/-\theta]_s$ for symmetric angle ply laminate which is represented by orientation angle “ θ ”. The material used is graphite- epoxy composite material. Strength ratios and first ply failure loads are calculated for different orientation angles and loads by both semi analytical method and FEM. The models built up by both methods are validated with literature and then compared. The mode of failure is also determined. Strength ratios are calculated using different failure theories and compared.

8.4.1.1 Validation of semi analytical and FEM models

Stresses are determined by using the equation 3.8 as discussed in chapter 3. The equations are solved using MATLAB platform for different orientation angles ranging from 0° to 90° . First ply failure load is determined by following the steps as discussed in section 8.2 of this chapter. The results are compared with the results of FEM using finite element software (ANSYS 15.0). The semi analytical model is validated with KAW [52] and the FEM model is validated with Barberio et al. [2]. FEM results are compared with semi analytical results for the problem mentioned in reference 52 in table 8.2. It is seen that both results found good agreement with each other. This is due to the reason that the equations of laminate under in plane load are free from higher order terms and are solved by simple matrix operations.

The FEA package presents the failure criteria by using the failure index, I_F which is the reciprocal of the strength ratio SR. The finite element model of the laminated composite plate is built up in ANSYS 15.0 software using SHELL elements and a failure index is computed for the problem in the reference [2]. The results are compared with the results of the reference to validate the FEA model presented in table 8.1. In the same way, the semi analytical model, built up using Classical lamination theory (CLT) is solved in MATLAB platform. This semi analytical model is validated with the results of the problem mentioned in the literature [52], presented in table 8.2.

Table 8.1 Comparison of FEM results with published literature [2]

Layers		Maximum Stress I_F		Tsai-Wu I_F	
No.	Angle (deg)	Present	Literature	Present	Literature
1	0	0.0144	0.0144	0.0144	0.0144
2	90	0.0243	0.0243	0.0294	0.0294
3	45	0.0157	0.0157	0.0199	0.0199
4	-45	0.0157	0.0157	0.0199	0.0199

Table 8.2 Comparison of CLT with published literature [52]

Layers		Maximum Strain SR		Tsai-Wu SR	
No.	Angle (deg)	Present	KAW (2006)	Present	KAW (2006)
1	0	1.548×10^7	1.548×10^7	1.339×10^7	1.339×10^7
2	90	7.254×10^6	7.254×10^6	7.277×10^6	7.277×10^6
3	0	1.548×10^7	1.548×10^7	1.339×10^7	1.339×10^7

Table 8.3 Comparison of CLT with FEM [52]

Layers		Tsai-Wu SR	
No.	Angle (deg)	CLT	FEM
1	0	1.339×10^7	1.339×10^7
2	90	7.277×10^6	7.277×10^6
3	0	1.339×10^7	1.339×10^7

8.4.1.2 Comparison of semi analytical and FEM model

Finite element results is compared with the semi analytical results (CLT) and good agreement found. Failure analysis depends on the stress at each lamina. In chapter 5, it is shown that semi analytical results (CLT) and Finite element results show good agreement with each other with zero percent error. Therefore, strength ratios obtained from both models are the same. Analysis of a laminated plate under in-plane load is the simplest case of analysis of laminated composite since its equations are free from expansion terms. An exact solution is obtained by solving a definite number of equations by CLT. In the case of complex loading and boundary conditions, the accuracy of the solution is determined by the number of equations used, and the solution is approximate, as discussed in Chapter 6. Table 8.4 shows the comparison of FEM results with CLT for graphite/epoxy symmetric 4 layer angle ply laminated composite plate subjected to in-plane loading, $N_x = 1$, length to thickness ratio of 10. From the table it is seen that results obtained from both the methods are same due to the reason as described above.

Table 8.4 Comparison of CLT with FEM for 4 layer symmetric angle ply laminated composite plate under in plane load (N_x) of 1 N/m, $a/h= 10$.

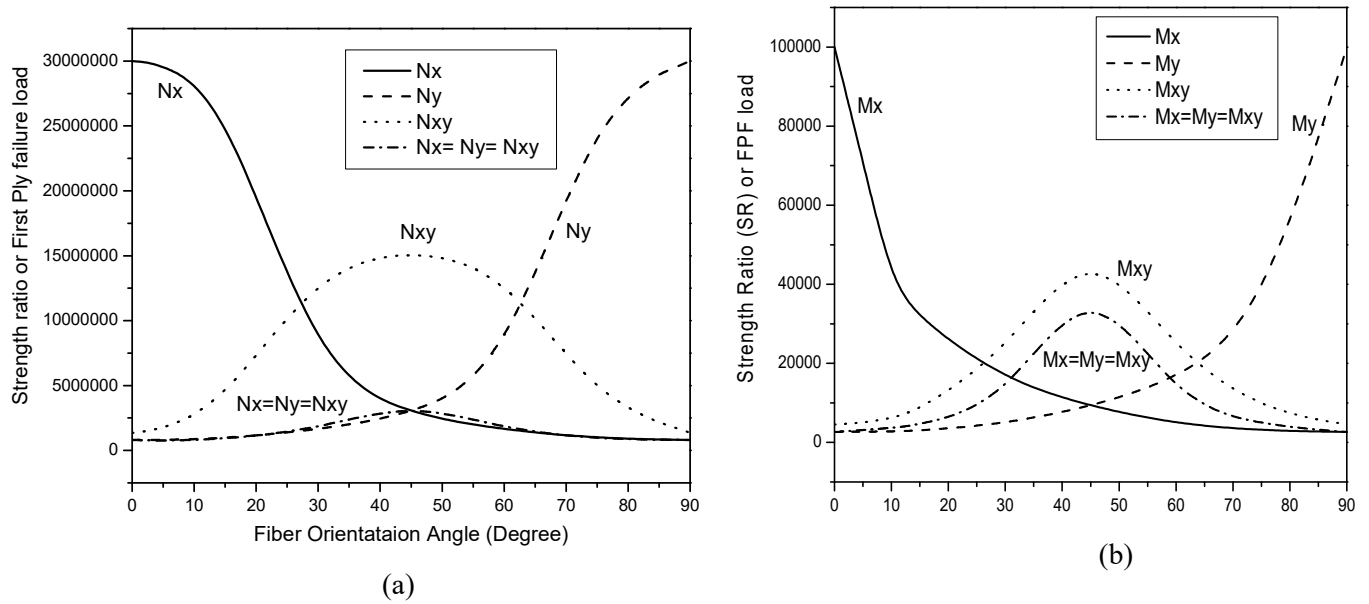
Orientation angle [$\theta/-\theta$]s in deg.	SR (MAX. STRESS CRITERIA)		SR (TSAI-WU CRITERIA)	
	CLT	FEM	CLT	FEM
0	7500000	7500000	7.50e6	7.50e6
15	7.56e5	7.56e5	5.57e5	5.57e5
30	3.30e5	3.30e5	2.61e5	2.61e5
45	2.14e5	2.14e5	1.99e5	1.99e5
60	2.01e5	2.01e5	1.96e5	1.96e5
75	2.02e5	2.02e5	2.00e5	2.00e5
90	2.00e5	2.00e5	2.00e5	2.00e5

8.4.2 Effect of fiber orientation angle on failure analysis

The semi analytical method as discussed above is extended to study the effect of fiber orientation angle on strength ratio and first ply failure load. The first ply failure load is calculated by multiplying the strength ratio by the applied load. If load is unity, then the strength ratio and first ply failure load are the same.

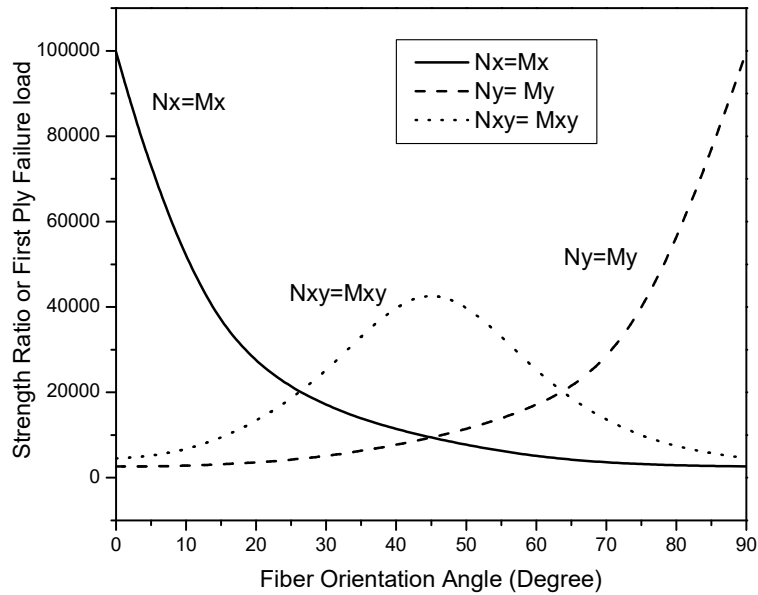
8.4.2.1 Symmetric Angle ply composite subjected to different mechanical loading condition

Consider four layers of symmetric angle ply laminated composite plate subjected to in plane normal (N_x, N_y) and shear loading (N_{xy}), bending (M_x, M_y) and twisting moments (M_{xy}). The plate is made up of graphite epoxy composite. The effect of fiber orientation angle on the strength ratio based on first ply failure is discussed in this thesis.



(a)

(b)



(c)

Figure 8.1: Strength ratio calculated using Maximum stress criteria base on FPF for angle ply laminate for a range of fiber orientation angle subjected to (a) in plane normal and shear loading (only $N_x = 1$, $N_y = 1$, $N_{xy} = 1$, $N_x = N_y = N_{xy} = 1$) (b) bending and twisting moment (only $M_x = 1$, $M_y = 1$, $M_{xy} = 1$, $M_x = M_y = M_{xy} = 1$) and (c) combination of all loading ($N_x = M_x = 1$, $N_y = M_y = 1$, $N_{xy} = M_{xy} = 1$)

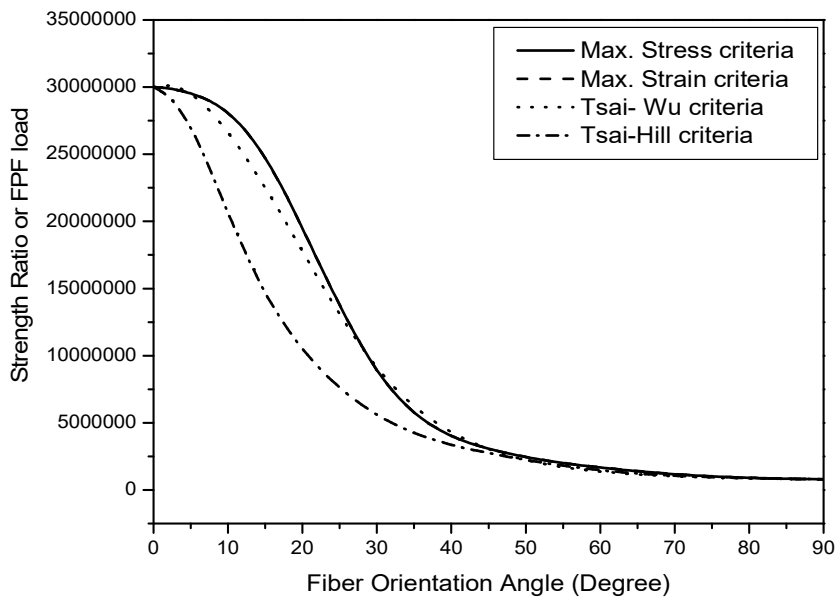
Figure 8.1 shows the Strength ratio calculated using maximum stress criteria based on first ply failure load for symmetric angle ply laminate for a range of fiber orientation angles subjected to in plane normal, shear loading, bending and twisting moments and their combinations. Strength

ratio multiplied to the applied load gives the first ply failure load. Since the load taken is taken unity, therefore strength ratio and first ply failure load is same. For loading *only* N_x (fig 8.1a), *only* M_x (fig 8.1b), *and* $N_x = M_x$ (fig 8.1 c) the failure criteria show that the laminate is strongest at 0° fiber orientation angle (θ) and that the strength ratio or first ply failure load decreases with the increase in θ . Whereas opposite case happens for loading *only* N_y (fig 8.1a), *only* M_y (fig 8.1b), *and* $N_y = M_y$ (fig 8.1 c), the laminate is strongest at 90° fiber orientation angle (θ) and strength ratio or first ply failure load increases with the increase in θ . For only shear loading N_{xy} (fig 8.1a) or twisting moment, M_{xy} (fig 8.1b), the laminate is strongest at optimum angle of 45° and the strength ratio first increases from 0° attaining the maximum value at 45° and then decreases to the initial value at 90° . The same nature is followed by the laminate subjected to loading $N_x = N_y = N_{xy}$ (fig 8.1a), $M_x = M_y = M_{xy}$ (fig 8.1b), $N_{xy} = M_{xy}$ (fig 8.1c) and the maximum strength ratio of the laminate under these loadings ($N_x = N_y = N_{xy}$, $M_x = M_y = M_{xy}$, $N_{xy} = M_{xy}$) occurs at $[+45/-45]_s$.

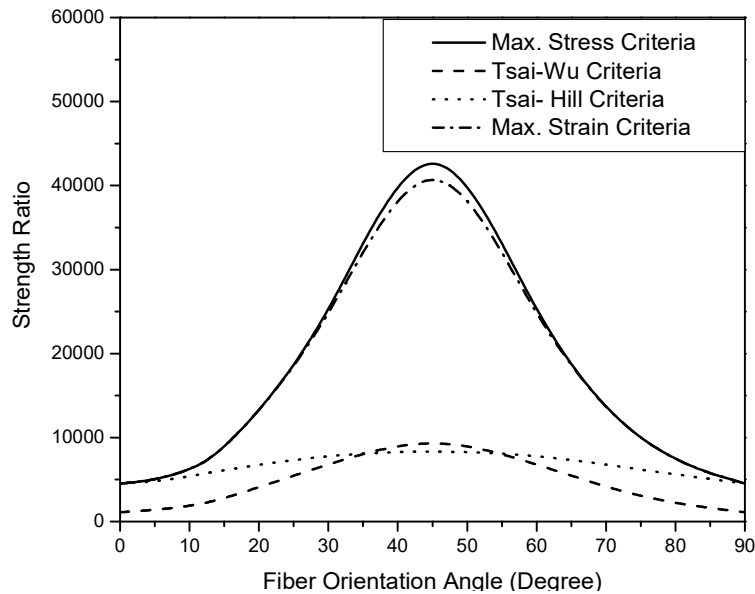
8.4.3 Comparative study of different failure criteria based on first ply failure load

Interactive and non interactive failure criteria are compared for graphite epoxy laminates subjected to in plane normal and shear loading, bending and twisting moments based on first ply failure load. Strength ratios are calculated using four different failures for the symmetric angle ply laminate for different range of orientation angles. For in plane loading $N_x \neq 0$ considering the four failure criteria, maximum strength ratio is obtained at $\theta = 0^\circ$ for all the criteria except the Tsai Wu criteria (fig 8.2 a) and minimum strength ratio is obtained at 90° for all criteria. Considering Tsai-Wu criteria the maximum strength ratio is obtained at $\theta = 5^\circ$. So both Interactive and non interactive failure criteria yield maximum strength ratio of laminate at different orientation angles. To find the same orientation angle by satisfying both the maximum stress and Tsai- Wu criteria, 80 % and 10% of the strength ratio calculated by using maximum stress and Tsai Wu criteria, respectively, are added (fig 8.3). Fig 8.3 shows that maximum strength ratio is obtained at $\theta = 0^\circ$ by using combined failure criteria which satisfy the other criteria for in plane normal tensile load ($N_x \neq 0$). Mustafa Akbulut et al. [62] in their paper added 90% and 10% of the safety factors calculated according to the maximum stress and the Tsai–Wu criteria, respectively, to find the combined safety factor which better conforms to the trend of the in-plane laminate strength. For loading $N_y \neq 0$ in fig 8.2b the maximum strength

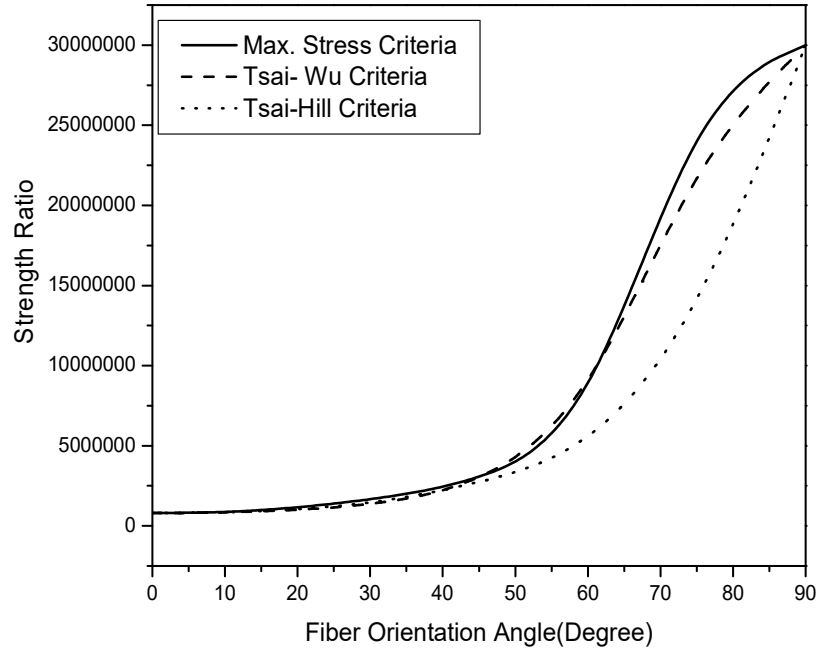
ratio of the laminate is obtained at $\theta = 90^\circ$ and the minimum at $\theta = 0^\circ$ for all criteria. Whereas for twisting moment $M_{xy} \neq 0$, maximum strength ratio is obtained at $\theta = 45^\circ$ for all the failure criteria (fig 8.2c). Strength ratio or first ply failure load calculated for the interactive failure criteria is larger than that of the non interactive failure criteria for all the cases of loading for angle ply composite. For cross ply composites, maximum strength ratio calculated by maximum stress criteria is greater than that of other criteria. Fig 8.4 shows the comparison of the maximum strength ratio calculated by all the criteria for cross ply composite.



(a)



(b)



(c)

Figure 8.2 Strength ratio calculated using interactive and non interactive failure criteria for angle ply laminate subjected to (a) inplane normal tensile loading ($N_x \neq 0$) (b) twisting moment $M_{xy} \neq 0$ and (c) in plane loading ($N_y \neq 0$) for range of fiber orientation angle.

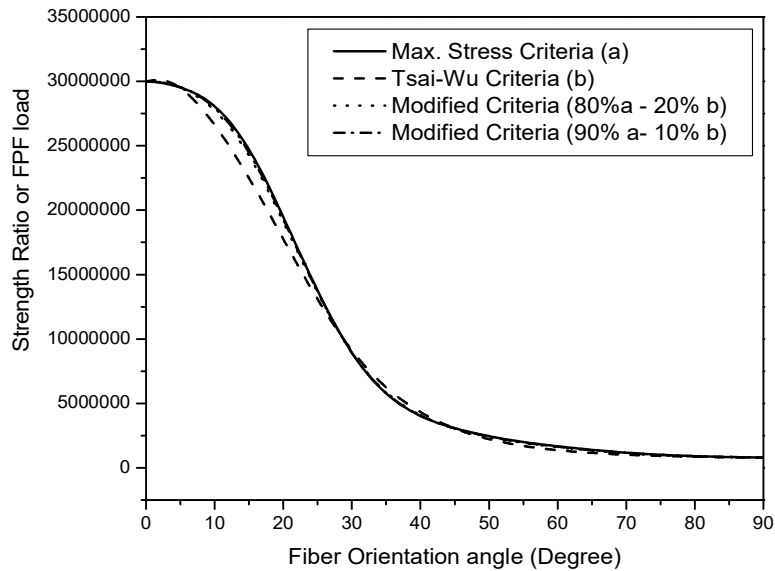


Figure 8.3 Comparison of Strength ratio calculated using Max. Stress, Tsai –Wu and modified failure criteria for angle ply laminate subjected to inplane normal tensile loading ($N_x \neq 0$) for range of fiber orientation angle

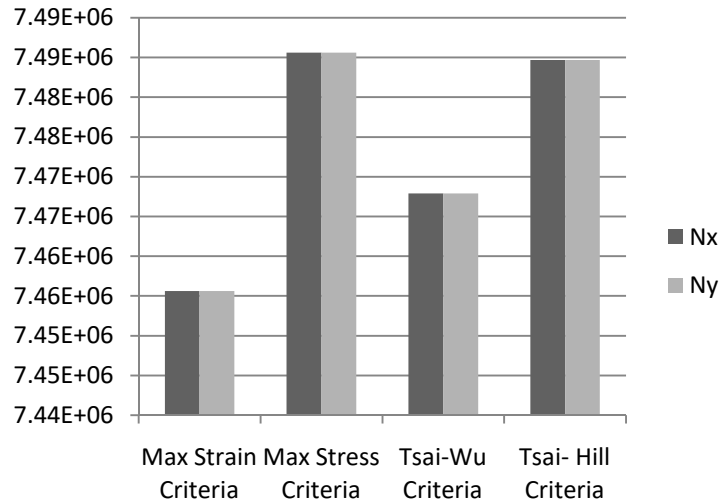


Figure 8.4 Strength ratio calculated using interactive and non interactive failure criteria for cross ply laminate subjected to in plane normal tensile loading ($N_x \neq 0, N_y \neq 0$)

8.4.4 Last ply failure analysis of laminate under tensile loading

After the failure of the first ply in a laminate, the next weaker ply fails and so it continues up to the last ply when the whole laminate fails. The load, at which the last ply fails, is called the last ply failure load (LPF). The last ply failure load is determined by the fully discounted method [author K W KAW] which states that when a ply fails, fully discount the ply and replace it with a ply of near zero stiffness and strength. This process continues till the last ply fails. First ply failure and fully discounted method is discussed in the section. The mode of failure is determined by using maximum stress theory (table 8.5). The table shows the first ply failure and last ply failure loads for different stacking sequences of the laminate. FPF and LPF loads are the same for symmetric angle ply composite.

Table 8.5. First ply failure load (FPF) and last ply failure load (LPF) for different laminate under tensile load (1MN), thickness/ply: 5 mm, Graphite epoxy composite laminate.

Stacking sequence	FPF (MN)	LPF (MN)	Laminate efficiency
0/90/0 (K A KAW)	7.28	15	48.5
0/90/90/0	7.47	15	49.7
45/-45/-45/45	2.46	2.46	100
45/45/45/45	1.29	1.29	100

8.4.5 Mode of failure

Mode of failure is determined by using maximum stress failure theory which states that [5]:

$\sigma_1 > 0$,Fiber failure in tension (1T)

$\sigma_1 < 0$,Fiber failure in compression(1C)

$\sigma_2 > 0$,Matrix Failure in tension (2T)

$\sigma_2 < 0$,Matrix failure in compression (2C)

$S = \text{shear failure } (\gamma_{12} > 0, \gamma_{12} < 0) (S)$ (8.13)

If $SR > 1$, then the lamina is safe and the applied stress can be increased by a factor of SR . If $SR < 1$, the lamina is unsafe and the applied stress needs to be reduced by a factor of SR . A value of $SR = 1$ implies the failure load. Table 8.6 and 8.7 show the modes of failure for symmetric angle ply and cross ply composite laminates under in plane tensile loading $N_x \neq 0$ respectively. The mode of failure for each lamina within the laminate is found by using maximum stress failure theory. Determine the stress of each lamina, then apply the conditions of eq. 8.13, the modes of failure of each lamina are determined.

Table 8.6 Mode of failure of symmetric angle ply composite laminate under in plane tensile load

Stacking sequence	Angle	Position	SR	MODE	Stacking sequence	Ply No.	Position	SR	MODE	
[0/-0] _s	0°	TOP	30	1T	[60/-60] _s	-45°	TOP	2.72	ST	
		BOTTOM	30	1T			BOTTOM	2.72	ST	
	-0°	TOP	30	1T		45°	TOP	2.72	SC	
		BOTTOM	30	1T			BOTTOM	2.72	SC	
	-0°	TOP	30	1T		60°	TOP	1.6104	SC	
		BOTTOM	30	1T			BOTTOM	1.6104	SC	
	0°	TOP	30	1T	-60°	TOP	1.6104	ST		
		BOTTOM	30	1T		BOTTOM	1.6104	ST		
	[30/-30] _s	30°	TOP	5.9827	SC	[90/-90] _s	-60°	TOP	1.6104	ST
			BOTTOM	5.9827	SC			BOTTOM	1.6104	ST
		-30°	TOP	5.9827	ST		60°	TOP	1.6104	SC
			BOTTOM	5.9827	ST			BOTTOM	1.6104	SC
-30°		TOP	5.9827	ST	90°	TOP	0.8	2T		
		BOTTOM	5.9827	ST		BOTTOM	0.8	2T		
30°		TOP	5.9827	SC	-90°	TOP	0.8	2T		
		BOTTOM	5.9827	SC		BOTTOM	0.8	2T		
[45/-45] _s	45°	TOP	2.72	SC	-90°	TOP	0.8	2T		
		BOTTOM	2.72	SC		BOTTOM	0.8	2T		
	-45°	TOP	2.72	ST	90°	TOP	0.8	2T		
		BOTTOM	2.72	ST		BOTTOM	0.8	2T		

Table 8.7 Mode of failure of symmetric cross ply composite laminate under in plane tensile load

Stacking sequence	Angle	Position	SR	MODE
[0/90] _s	0°	TOP	15.9102	1T
		BOTTOM	15.9102	1T
	90°	TOP	7.4556	2T
		BOTTOM	7.4556	2T
	90°	TOP	7.4556	2T
		BOTTOM	7.4556	2T
	0°	TOP	15.9102	1T
		BOTTOM	15.9102	1T

Notation of mode of failure [52]

1T- Longitudinal Tensile failure

2T- Transverse Tensile failure

1C – Longitudinal compressive failure

2C – Transverse compressive failure

ST- Tensile Shear failure

SC- Compressive shear failure

8.4.6 Effect of hygro-thermo mechanical loading on strength ratio

During fabrication, composite laminates are subjected to a variety of thermal and moisture environments which introduce residual stresses into them. These stresses are called “hygro thermal stresses” which affect the performance of composite laminates. If the laminate is exposed only a thermal environment, i.e. it is cooled from curing temperature to room temperature or heated from room temperature to processing temperature, then the stress generated in them is called residual thermal stress. When the same laminate is subjected to mechanical load, then the stress developed in it is called thermo mechanical stress and if it is exposed to moisture along with thermal and mechanical load, then hygro thermo mechanical stress is developed. A comparison of the strength ratio calculated by the Tsai- Wu failure criteria for graphite epoxy laminated composite plates subjected to mechanical, thermo mechanical; and hygro thermo mechanical loading is presented using the semi analytical method as discussed above. The strength ratio is calculated for the angle from 0° to 90° at an increment of 15°. It is assumed that any change in value within 15° is neglected. Fig 6 and 7 show that, the strength ratio for a range of orientation angles of angle ply laminates subjected to two types of mechanical loading and their combination with thermal (positive temperature

difference) and hygro thermal loading. Fig 8.5 a, in plane tensile mechanical loading is applied and fig 8.5b, a combination of tensile load and bending moment is applied. In both the cases maximum and minimum strength ratios are obtained at 0° and 90° , respectively, and they are the same for all types of loading. The strength ratio of hygro thermo mechanical loading is greater than that of thermo mechanical loading, which is again greater than mechanical loading for the rest of the orientation angle. Also, the strength ratio of mechanical loading is greater than that of combined mechanical loading. In fig 8.6, due to the presence of negative residual thermal stress (negative temperature difference), the strength ratio of the thermo mechanical load is less than that of the mechanical load but in the previous case (fig 8.5), positive thermal stress increases the thermo mechanical load. In the entire cases, hygro thermo mechanical load is greater than the other loading. This implies that the presence of moisture causes the stresses to be greater than with other loadings. The comparison of the strength ratio using Tsai–Wu failure criteria for thermo mechanical loading for a range of temperature changes is shown in Fig 8.7. Strength ratio increases with the increase in temperature difference whereas it is the same for orientation angles of 0° and 90° which shows that the temperature change has no effect on the strength ratio for the above stated orientation angle. Fig 8.8 shows the comparison of the strength ratio calculated by Tsai Wu failure criteria, based on FPF load for cross ply composite subjected to in plane tensile load. The strength ratio of the hygro thermo mechanical load is greater than that of other loading and it draws the same conclusion.

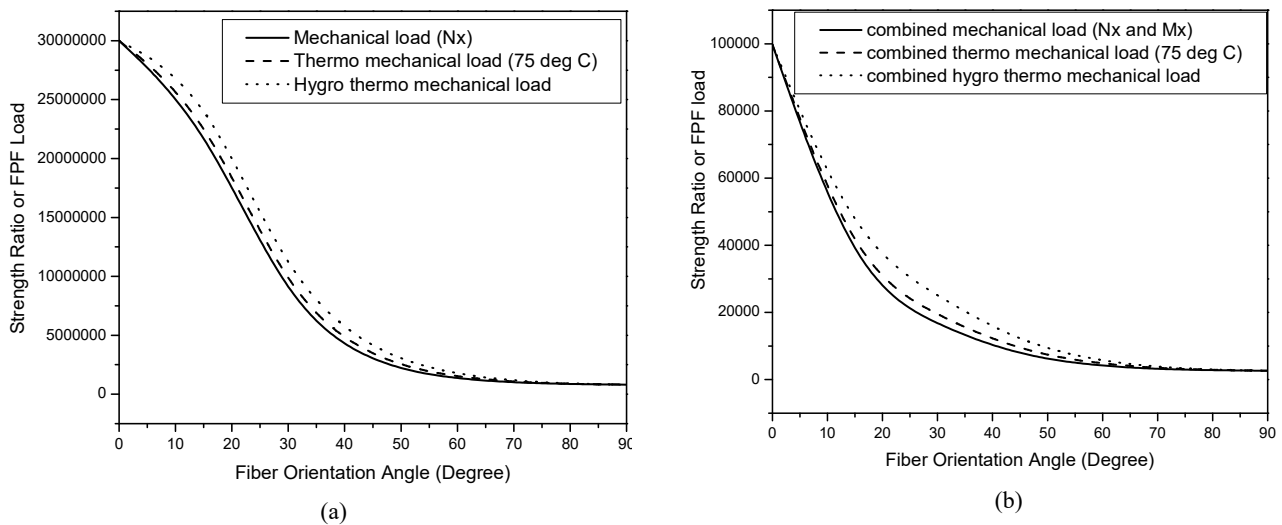


Figure 8.5 Comparison of the Strength ratio calculated using Tsai-Wu criteria based on FPF for angle ply laminate for a range of fiber orientation angle subjected to (a) Hygro thermo mechanical loading (b) Combined Hygro thermo mechanical loading for positive temperature difference

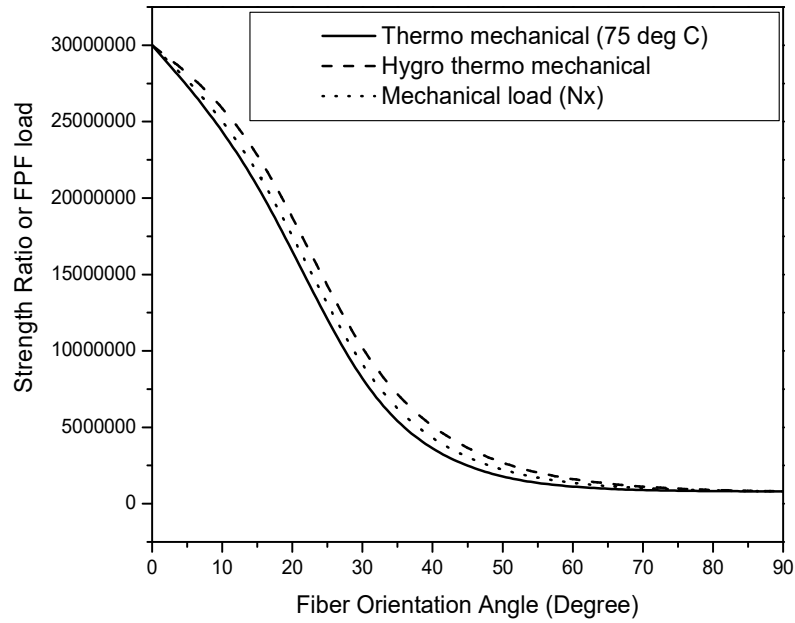


Figure 8.6 Comparison of the Strength ratio calculated using Tsai-Wu criteria subjected to Hygro thermo mechanical loading for negative temperature difference .

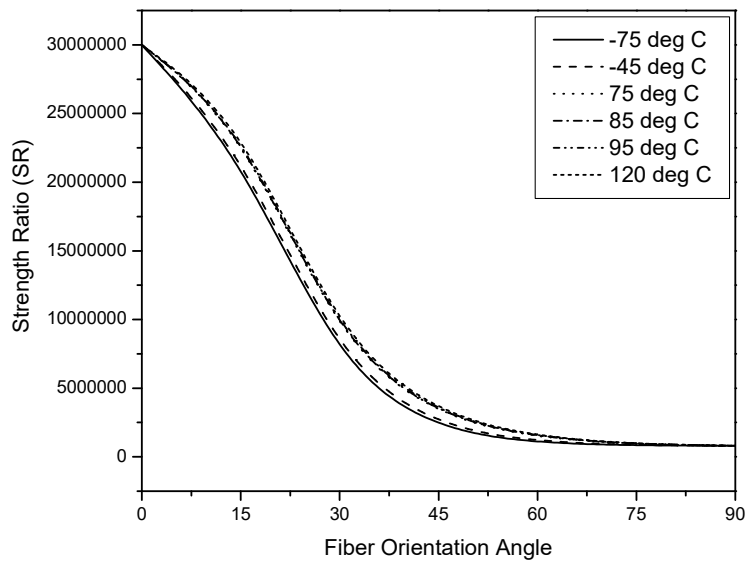


Figure 8.7 Comparison of the Strength ratio calculated using Tsai-Wu criteria subjected to thermo mechanical loading for a range of temperature difference

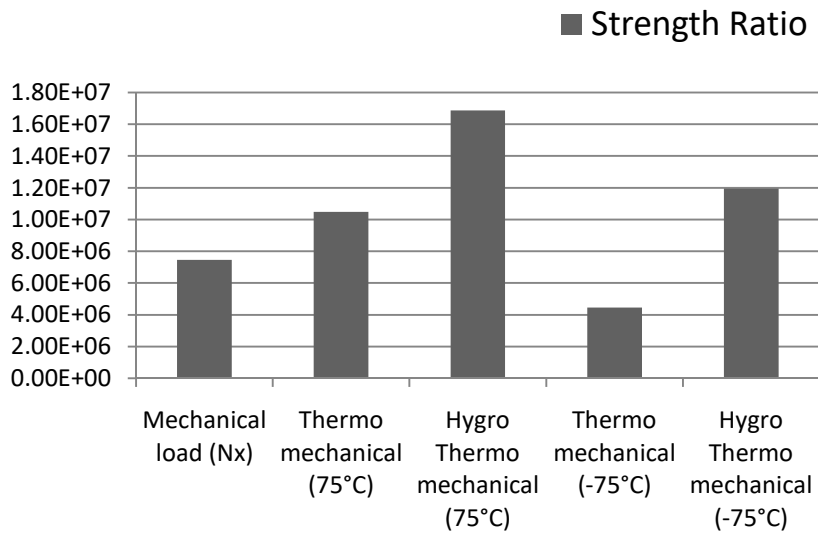


Figure 8.8 Comparison of the Strength ratio calculated using Tsai-Wu criteria subjected to Hygro thermo mechanical loading for cross ply composite.

8.5 Failure analysis of Laminated Composite Beam

The semi analytical method to find the strength ratio using different failure theories as discussed above is applied to determine the failure of a laminated composite beam under transverse load. The semi analytical model of failure is solved by using the MATLAB tool. A programme to find the strength ratio and first ply failure load has been developed by using the methodology discussed in section 8.2 of this chapter.

8.5.1 Numerical Problem

Consider a laminated composite beam of length 1 m and width 0.2 m, composed of four plies, symmetrically arranged about the mid plane. Symmetric angle ply and cross ply arrangement are considered for the study. The thickness of each lamina is 0.005 m. Strength ratio is calculated for the beam using the algorithm developed based on the first ply failure load for two different loading conditions: Mechanical load (UDL of 1000 N/m) and thermo mechanical (UDL and $\Delta T = -75^\circ\text{C}$) and for three different boundary conditions (Table 7.1).

First ply failure load is chosen for analysis because it is the starting point of failure of lamina within a laminate and the process continues until all the lamina fails. So, after the first ply fails,

there are options to stop or delay the failure process by modifying the parameters that contribute to failure, but after the last ply or ultimate failure, all plies fail and there is no way to rectify. So first ply failure load is a very important parameter for failure analysis of composite structures.

8.5.2 Results and discussion

Two failure theories, interactive and non interactive, are compared in this thesis. Maximum stress falls in the category of non-interactive failure theory whereas Tsai-Wu and Tsai-Hill fall under the category of interactive failure theory which shows the interaction between the different stress components. But it cannot determine the mode of failure. The mode of failure is determined by maximum stress or strain failure theory. The strength ratio is calculated for different orientation angles and boundary conditions using interactive and non interactive failure theories and compared by using semi analytical method. The semi analytical model is solved by using the MATLAB tool.

8.5.2.1 Comparative study of different failure theories for beam fixed at both ends under UDL

The strength ratio is computed and compared for different failure theories based on first ply failure load for a composite beam clamped at both ends and subjected to uniformly distributed load in table 8.8. The beam is composed of four plies of graphite/epoxy composite material. Maximum deflection is obtained at the centre of the clamped beam, and the strength ratio is minimum at both the ends of the beam. From fig. 8.9 and fig 8.10, it is found that the strength ratio of non interactive failure criteria (maximum stress, maximum strain) is greater than that of interactive failure criteria (Tsai-Wu and Tsai-Hill) for both angle ply symmetric and cross ply symmetric arrangement of laminated composite beams. Whereas the strength ratio is the same for 0° and 90° orientation angle for all the failure criteria, which concludes that the strength ratio does not depend upon failure criteria for 0° and 90° orientation angles only. Also, it is found out that strength ratio obtained from Tsai-Hill failure criteria is greater than that of Tsai-Wu failure criteria. So a minimum value of strength ratio is obtained at Tsai-Wu failure criteria as compared to other failure criteria which are desirable to find the first ply failure load. So, in this case, the Tsai-Wu failure criteria is used to find the strength ratio for all the cases, but it is

not able to state the mode of failure, which is computed by using the maximum stress failure theory.

Table 8.8 Comparison of strength ratio from different failure criteria for different fiber orientation angle

Fiber orientation angle	Strength Ratio at $x=0, a$			Max deflection at $x=a/2$	
Angle Ply Sym.	Maximum Stress	Tsai Wu	Tsai-Hill	$w (m)$	$wbar$
0	240	240	240	1.08E-04	0.1778
15	74.4047	71.7765	71.9947	1.83E-04	0.301
30	37.6785	36.3866	37.3498	3.90E-04	0.6425
45	21.76	16.8792	18.8729	8.60E-04	1.417
60	11.2204	9.2311	9.8363	0.0014	2.3663
75	7.1203	6.8941	6.9839	0.0018	2.9577
90	6.4	6.4	6.4	0.0019	3.125
Cross ply Sym.					
0/90/90/0	203.2773	190.0751	197.1989	1.22E-04	0.201

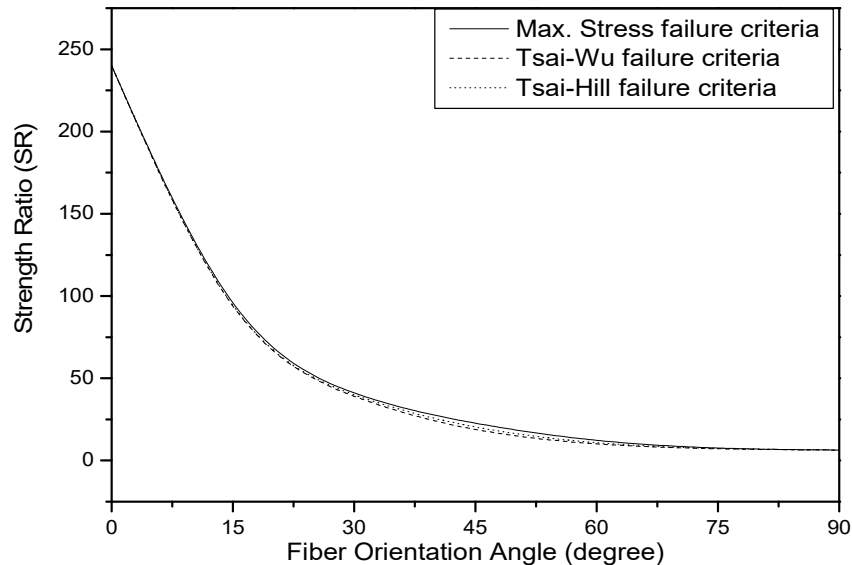


Figure 8.9 Comparative study of different failure criteria for clamped – clamped symmetric angle ply composite beam.

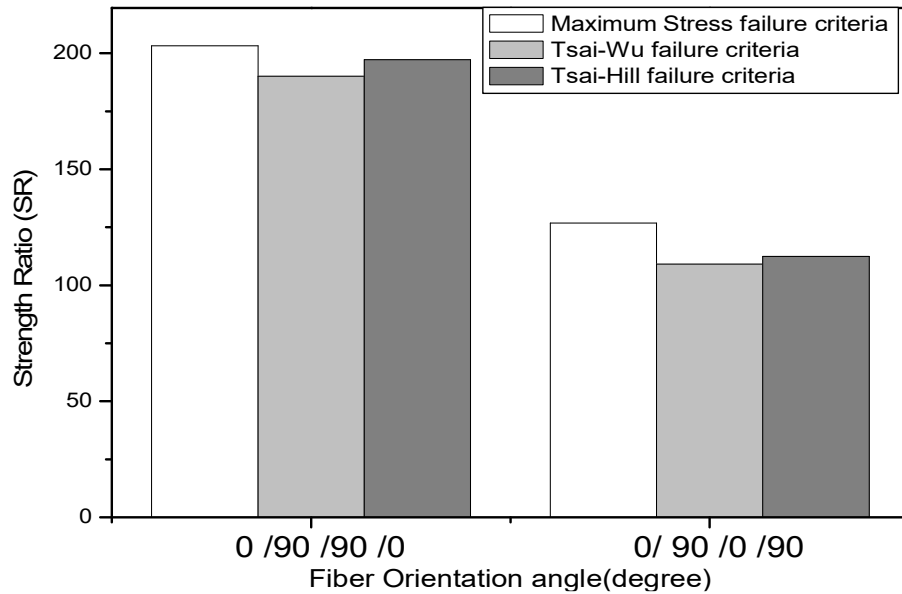


Figure 8.10 Comparative study of different failure criteria for fixed – fixed symmetric Cross ply composite beam.

8.5.2.2 Effect of fiber orientation angle on strength ratio for different boundary conditions of a composite beam subjected to mechanical load (uniformly distributed load)

The effect of fiber orientation angle on symmetric angle ply and cross ply composite beams is studied for different boundary conditions and subjected to uniformly distributed load. The strength ratio is determined by using Tsai-Wu failure criteria, based on first ply failure load. The beam is composed of four plies of graphite/epoxy composite material. It is observed from table 8.9 (fig 8.11) that the strength ratio is maximum at 0° and it gradually decreases and becomes minimum at 90° fiber orientation angle. It is also found that the strength ratio is minimum at maximum transverse deflection and vice versa. At 90° orientation angle, transverse deflection is maximum but strength ratio is minimum and at 0° orientation angle, transverse deflection is minimum and strength ratio is maximum. The strength ratio of both end clamped beam is greater than the other boundary conditions, whereas the strength ratio of the hinged-hinged beam is greater than the clamped – free (cantilever) beam.

Table 8.9 Strength ratio and transverse deflection of composite beam for different boundary conditions under UDL. (Graphite/Epoxy composite material)

Fiber Orientation angle	Hinged-hinged		Clamped-Clamped		Clamped-Free	
	Strength Ratio	$wbar$	Strength Ratio	$wbar$	Strength Ratio	$wbar$
[0/-0/-0/0]	160	0.88	240	0.1778	40	8.5359
[15/-15/-15/15]	47.85	1.5	71.7765	0.301	11.96	14.45
[30/-30/-30/30]	24.2577	3.21	36.3866	0.6425	6.06	30.84
[45/-45/-45/45]	11.2528	7.08	16.8792	1.417	2.81	68.017
[60/-60/-60/60]	6.15	11.83	9.2311	2.3663	1.54	113.58
[75/-75/-75/75]	4.59	14.78	6.8941	2.9577	1.149	141.96
[90/-90/-90/90]	4.26	15.62	6.4	3.125	1.06	150
[0/ 90/ 90/ 0]	126.7	1.0051	190.0751	0.201	31.67	9.6494

N.B: $wbar$ is non dimensional quantity.

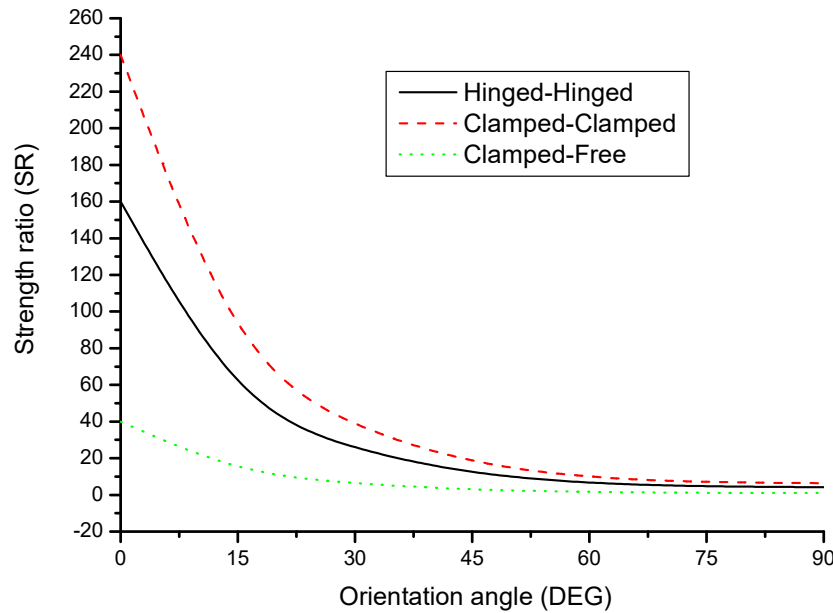


Figure 8.11 Effect of fiber orientation angle on strength ratio for different boundary conditions

8.5.2.3 Effect of thermal load on strength ratio of laminated composite beam

During fabrication, composite laminates are subjected to a variety of thermal environments which introduce residual stresses into them. These stresses are called thermal stresses, which

affect the performance of composite laminates. If the laminate is exposed only thermal environment, i.e. if it is cooled from curing temperature to room temperature or heated from room temperature to processing temperature, then the stress generated in them is called residual thermal stress. When the same laminate is subjected to mechanical load, the stress developed in it is called thermo mechanical stress. A comparison of the strength ratio calculated by Tsai-Wu failure criteria for graphite epoxy laminated composite beams subjected to mechanical and thermo mechanical loading for different boundary conditions is presented in table 8.10. Strength ratio is calculated for the angle from 0° to 90° at an increment of 15° . It is assumed that any change in value within 15° is neglected. Fig 8.12 shows the strength ratio for a range of orientation angles of an angle ply laminate subjected to mechanical and thermo mechanical loading. It is found that due to negative thermal stress, the thermo mechanical stress increases and the strength ratio of the beam under thermo mechanical load is less than that of mechanical load (Table. 8.10)

Table 8.10. Comparison of strength ratio of composite beam subjected to mechanical (UDL=1000 N/m) and thermo mechanical load ($\Delta T = -75^\circ\text{C}$, $UDL = 1000 \text{ N/m}$)

Fiber Orientation angle	Strength ratio based on first ply failure load					
	Simply Supported		Fixed-Fixed		Fixed-Free	
	Mechanical	Thermo mechanical	Mechanical	Thermo mechanical	Mechanical	Thermo mechanical
[0/-0/-0/0]	160	160	240	240	40	40
[15/-15/-15/15]	47.85	42.5718	71.7765	63.857	11.96	10.64
[30/-30/-30/30]	24.2577	20.147	36.3866	30.22	6.06	5.036
[45/-45/-45/45]	11.2528	8.16	16.8792	12.247	2.81	2.04
[60/-60/-60/60]	6.15	4.94	9.2311	7.411	1.54	1.235
[75/-75/-75/75]	4.59	4.32	6.8941	6.4837	1.149	1.08
[90/-90/-90/90]	4.26	4.2667	6.4	6.4	1.06	1.06
[0/ 90/ 90/ 0]	126.7	79.8749	190.0751	119.8124	31.67	19.96

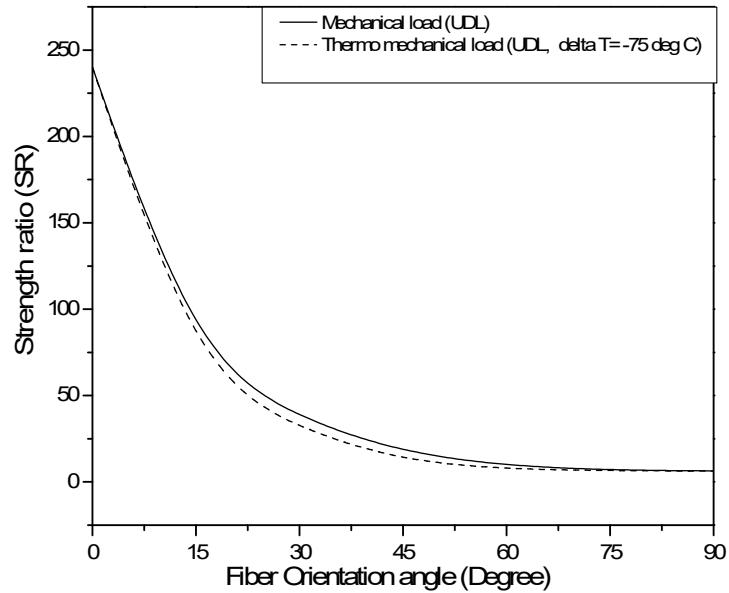


Figure 8.12 Comparison of strength ratio obtained for mechanical and thermo mechanical load for different fiber orientation angle for laminated composite beam (Clamped-clamped)

8.5.2.4 Effect of length to thickness ratio (a/h) on strength ratio based on FPF load

As the length to thickness ratio (a/h) increases, the thickness of the beam decreases, keeping the length of the beam constant. The strength ratio also decreases and becomes constant (fig 8.13). Strength ratio is more significant for the beam whose a/h ratio is less than 10, because from a/h ratio 5 to 10, the strength ratio decreases sharply, and after 10, it decreases gradually and becomes almost constant after 40. So, the strength ratio does not depend upon the length to thickness ratio when the composite laminated beam has an a/h ratio of 40 and above.

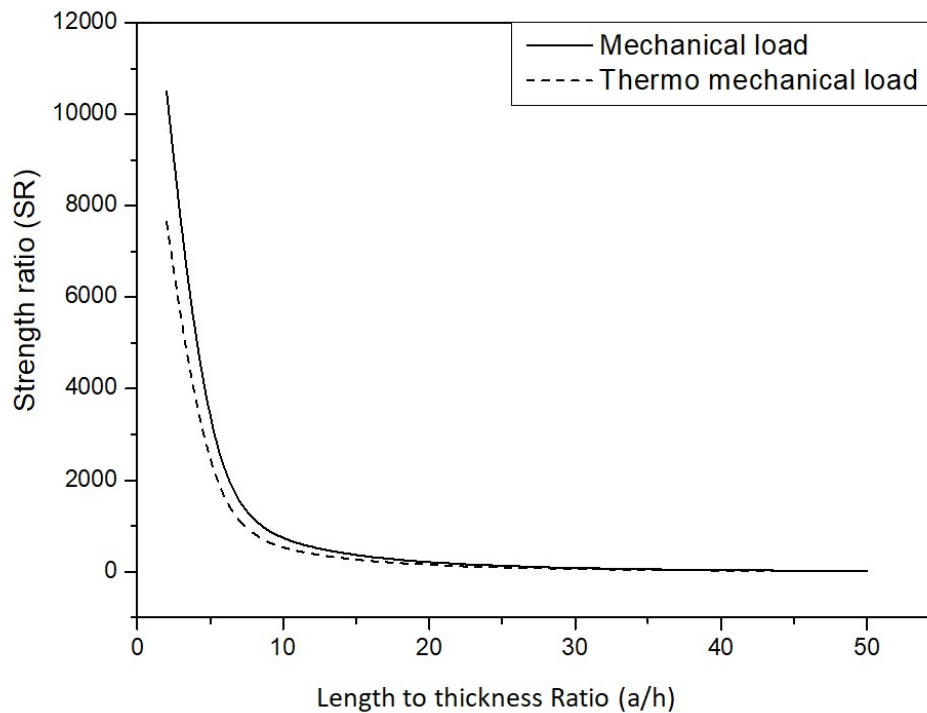


Figure 8.13 Effect of length to thickness ratio on strength ratio for composite beam (Clamped-clamped) subjected to Mechanical and thermo mechanical load

8.5.2.5 Mode of Failure

The mode of failure is determined by using a non interactive failure theory (Maximum stress theory). A laminated composite laminate may fail due to breakage of fiber, matrix cracking, or shear failure. The mode of failure of a laminate is very important to find out the ultimate failure load and to predict the nature of failure of the lamina within the laminate so that proper preventive measures may be taken to avoid failure. Table 8.11 shows the mode of failure of a composite beam under mechanical and thermo mechanical load.

Table 8.11. Mode of failure of composite beam for different boundary conditions subjected to mechanical and thermo mechanical load

B.C	Mechanical Load			Thermo mechanical load		
	Fiber Orientation angle (deg)	Failure location	First failed ply	Mode of failure	First failed ply	Mode of failure
Hinged-Hinged with UDL	[0/-0/-0/0]	(0.5,0.5)	1,4	4- Fiber failure in tension, 1-Fiber failure in Compression	1,4	1- Fiber failure in compression, 4-Fiber failure in tension
	[15/-15/-15/15]	(0.5,0.5)	4	Fiber failure in tension	4	Shear failure in comp
	[30/-30/-30/30]	(0.5,0.5)	1	Fiber failure in compression	4	Matrix failure in tension
	[45/-45/-45/45]	(0.5,0.5)	4	Fiber failure in tension	4	Matrix failure in tension
	[60/-60/-60/60]	(0.5,0.5)	4	Matrix failure in tension	4	Matrix failure in tension
	[75/-75/-75/75]	(0.5,0.5)	4	Matrix failure in tension	4	Matrix failure in tension
	[90/-90/-90/90]	(0.5,0.5)	4	Matrix failure in tension	4	Matrix failure in tension
	[0/ 90/ 90/ 0]	(0.5,0.5)	4	Fiber failure in tension	3	Fiber failure in compression
	Clamped-Free with UDL	[0/-0/-0/0]	(0,0)	1,4	4- Fiber failure in compression, 1-Fiber failure in tension	1,4
[15/-15/-15/15]		(0,0)	1	Fiber failure in tension	1	Fiber failure in tension
[30/-30/-30/30]		(0,0)	4	Fiber failure in compression	1	Fiber failure in tension
[45/-45/-45/45]		(0,0)	1	Fiber failure in tension	1	Matrix failure in tension
[60/-60/-60/60]		(0,0)	1	Matrix failure in tension	1	Matrix failure in tension
[75/-75/-75/75]		(0,0)	1	Matrix failure in tension	1	Matrix failure in tension
[90/-90/-90/90]		(0,0)	1	Matrix failure in tension	1	Matrix failure in tension
[0/ 90/ 90/ 0]		(0,0)	1	Fiber failure in tension	2	Fiber failure in compression
Clamped-Clamped (UDL)	[0/-0/-0/0]	(0,0)	1,4	4- Fiber failure in compression, 1-Fiber failure in tension	1,4	4- Fiber failure in compression, 1-Fiber failure in tension
	[15/-15/-15/15]	(0,0)	1	Fiber failure in tension	1	Shear failure
	[30/-30/-30/30]	(0,0)	4	Fiber failure in compression	1	Matrix failure in tension
	[45/-45/-45/45]	(0,0)	1	Shear failure	1	Matrix failure in tension
	[60/-60/-60/60]	(0,0)	1	Matrix failure in tension	1	Matrix failure in tension
	[75/-75/-75/75]	(0,0)	1	Matrix failure in tension	1	Matrix failure in tension
	[90/-90/-90/90]	(0,0)	1	Matrix failure in tension	1	Matrix failure in tension
	[0/ 90/ 90/ 0]	(0,0)	1	Fiber failure in tension	2	Matrix failure in tension

8.6 Comparison of FEM results with the Semi-Analytical method (FSDT)

Now the validated models as discussed above are extended for analysis of the present problem. The result obtained from the finite element software ANSYS is compared with the semi-analytical method for the problem defined in this thesis for hinged-hinged laminated composite beams and the percentage errors are noted in table 8.12. It is found that the errors for orientation angles of 15, 30 and 45 degrees are above 5 percent and the rest are below 5 percent. Below 5 percent, error may be acceptable. This percentage error therefore depends on the angle, thickness of the laminate and aspect ratio (length to width ratio). The error may be varied (either reduced or increased) by varying these variables. The percentage error in results of semi-analytical method (FSDT) solved in MATLAB platform with FEM is due to the reason that:

1. Beam equations are derived from general composite material equations by using the assumptions of section 7.1.1. The beam problem is a 1 dimensional problem, Higher order terms are eliminated, which introduces the error.
2. Though FEA software is presently widely used to solve simple to complex problems, but its solution depends on various factors like mesh size and type, interpolation function, etc., which give an approximate solution. It is also noted from the discussion of the semi-analytical method (FSDT) of composite beam, that its result also contains error due to approximation to solve the equations. The error in table 8.11 may be reduced by changing the different variables; the effect of these variables on the error is discussed in detail in the previous chapter.

Table 8.12 Percentage error of FEA results with FSDT results for Tsai-Wu Criteria

Orientation angle	Strength ratio (Tsai-Wu criteria)		Percentage error
	FSDT	ANSYS	
0°	160	159.81	0.12
15°	47.85	44.02	8.01
30°	24.26	21.57	11.1
45°	11.25	10.41	7.5
60°	6.15	6.04	1.8
75°	4.59	4.48	2.41
90°	4.26	4.23	0.6

8.7 Closure

Results obtained by semi analytical (CLT) and finite element show good agreement with each other with zero percent error for laminated composite plates under in-plane loads because; it is the simplest case of analysis of a laminated composite which is free from expansion terms. It can be concluded that the percentage error of composite beam depends on angle, thickness of laminate and aspect ratio (length to width ratio) which may be reduced by an optimum combination of these variables. Since the beam problem is the one dimensional problem of a laminated composite plate, all the higher order terms are neglected for simplification. Beam problems are solved by CLT and FSDT. In both theories, stress is the same. Failure analysis is based on stresses in each lamina, so both the theories yield the same results. Therefore, the results obtained from these theories may contain some errors due to the simplifications.

CHAPTER 9

ANALYSIS OF HYBRID LAMINATED COMPOSITE

9.1 Introduction, 9.2 Analysis of Hybrid composite Laminate, 9.2.1 Numerical Problem, 9.2.2 Semi analytical model, 9.2.3 FEM model, 9.3 Discussion, 9.3.1 Stress and displacement, 9.3.2 Failure analysis, 9.4 Analysis of hybrid composite beam and plate 9.5 Closure

9.1 Introduction

The laminated composite design includes optimization in cost, mass, strength ratio, stiffness, etc. A hybrid composite is the optimum combination of different composite materials in such a way that it minimises cost and mass without compromising strength. In this thesis two composite materials are considered, graphite/epoxy (G) and glass/epoxy (C) composite. Different combinations of above two materials are studied, to get the optimum combination whose properties are superior as compared to its constituents. The probable combinations of hybrid composites are G-C-G-C, G-C-C-G and C-G-G-C.

To produce a light weight flexible superior structure, hybridization of composite materials is being explored recently. The main purpose of designing hybrid composites is to produce a superior material with balanced strength and stiffness, balanced bending and membrane mechanical properties, balanced thermal distortion stability, reduced weight and cost, improved fracture toughness and crack arresting properties, and other desirable properties. A hybrid composite is the best combination of mechanical properties and cost. It improves the mechanical properties as well as reduces the cost.

Hybrid laminate can be manufactured in two different ways, either by combining different fibers for example, carbon and glass fibers are embedded in a common epoxy matrix, or by combining different composite materials in alternative layer for example, carbon/epoxy composite material and glass/epoxy composite materials are laminated in alternative layers. In this thesis, a second type of hybrid composite is explored.

There are numerous research works in this field. Jin Zhang et al.[58] find the effect of stacking sequence on the strength of hybrid composites which are composed of materials of different strengths and stiffness. The author investigates the strength of hybrid composites, which are manufactured by using varying ratios of glass woven fabric and carbon woven fabric in an epoxy matrix by static tests like tension, compression, and three point bending. The results of the paper show that hybrid composite laminates with 50% carbon fiber reinforcement give the best flexural properties when the carbon layers are at the exterior, and the alternating carbon/glass lay-up shows the highest compressive strength. Guru Raja M N et al. [59] studied the tensile strength, tensile modulus, and peak load of the carbon /glass epoxy hybrid for orientation angles of 0/90, 45/45, 30/60. A vacuum bagging technique was used for the fabrication of hybrid specimens. It was found that angle ply orientation at 0 / 90 showed a significant increase in tensile properties as compared to other orientations. M.M.W. Irina et al. [60] investigated the mechanical properties of three different arrangements of glass fiber hybrid composites (plain-woven and stitched bi-axial 45) and plain-woven carbon fiber. The hybrid composite panels were manufactured by Vacuum assisted resin transfer molding method. Experimental results show that the [CWW]₆ arrangement, where C and W are weaved carbon fiber and glass fiber respectively, were superior in terms of mechanical properties such as tensile strength, flexural strength, and volume fraction.

In this thesis the results obtained from finite element software ANSYS is compared with that of semi-analytical methods in solving the problem of hybrid laminated composite plate or beam under various loading conditions. Also, it studies the stress, deflection, and failure loads of various combinations of hybrid composites to get the optimum combination whose properties are superior as compared to their constituents. As discussed above, two composite materials are considered, graphite/epoxy (G) and glass/epoxy (C) composite, to obtain a hybrid composite.

9.2 Analysis of Hybrid composite Laminate

Hybrid composite laminate under in plane tensile load was analyzed analytically by classical lamination theory (CLT). The programme is solved on the MATLAB platform. The equations to solve the problem of hybrid composite using CLT are the same as discussed in chapter 3. The results obtained analytically were verified with existing literature to validate the semi analytical model.

A FEM model of the hybrid composite laminate was built up using finite element software ANSYS and using the same method as discussed in Chapter 4. The results obtained from finite element software were compared with semi-analytical methods. The FEA model was validated with published literature to validate the model.

9.2.1 Numerical Problem

A $[\theta/-\theta]$ s symmetric angle ply hybrid composite laminate made of plies of graphite /epoxy (G) and glass/epoxy (C) subjected to a uni axial or biaxial tensile load of $N_x=N_y=500$ N/m is considered for the study. Each lamina is 5mm thick, and the cross section of laminate is 2000mm \times 2000mm. Stresses are found for different combinations of G and C and compared with either G or C to get the optimum combination. Stresses are found by both the methods CLT and FEA.

9.2.2 Semi analytical Method

Semi analytical model is built up by using the laminate equations as discussed in Chapter 3. The equations are solved in MATLAB tools discussed in Chapter 3. The only difference between the composite laminate of a single material and a hybrid is that, in the case of a hybrid, the material properties of both the materials are input in matrix form and, accordingly, the programme is changed. The Semi analytical model is validated with published literature [61] and good agreement is found which validates the programme (table 9.2).

9.2.3 Finite element method

The FEM model is built up using Shell 4 node 181 elements. Figure 9.1(a) depicts the stacking sequence, or shell lay up of laminate in ANSYS. Meshing is done by quadrilateral mapped meshing (fig 9.1b). A convergence analysis is performed to find the optimum level of meshing. Loading and boundary conditions are applied to the laminate. Two types of loading are investigated: uni-axial tensile load N_x and biaxial tensile load $N_x=N_y$. The same method can be applied to compressive loading, which is not discussed in this thesis. The FEM model is validated with published literature [60] and good agreement is found which validates the programme (table 9.1).

Table 9.1 Validation of FEM model with existing literature [60]

Lamina	Stress		Present (FEM) (Pa)	Reference [60] (Pa)
0° (Carbon/epoxy)	(σ_x)	Min	-73104.9	-73105.3
		Max	349235.8	349236
	(σ_y)	Min	91722.8	91722.9
		Max	113301.5	113302
	(τ_{xy})	Min	55405.3	55405.3
		Max	86861.1	86861.2
45° (Glass/epoxy)	(σ_x)	Min	93768.45	93768.7
		Max	141148.7	141149
	(σ_y)	Min	141148.7	141149
		Max	142775.8	142776
	(τ_{xy})	Min	55405.3	55405.3
		Max	86861.12	86861.2
-45° (Glass/epoxy)	(σ_x)	Min	141148.7	141149
		Max	142776	142776
	(σ_y)	Min	93768.6	93768.7
		Max	141148.7	141149
	(τ_{xy})	Min	-86861.1	-86861.2
		Max	-55405.15	-55405.3
90° (Carbon/epoxy)	(σ_x)	Min	91722.8	91722.9
		Max	113301.6	113302
	(σ_y)	Min	-73105.3	-73105.3
		Max	349235.6	349236
	(τ_{xy})	Min	14119.38	14119.4
		Max	28238.78	28238.8

Table 9.2 Validation of Semi analytical model with existing literature [60]

Lamina	Stress		Present (Pa)	Reference [60] (Pa)
0° (Carbon/epoxy)	(σ_x)	Min	-73110	-73198
		Max	349240	349310
	(σ_y)	Min	91720	91700
		Max	113300	113300
	(τ_{xy})	Min	-28240	-28246
		Max	-14120	-14123
45° (Glass/epoxy)	(σ_x)	Min	93770	93768
		Max	141150	141160
	(σ_y)	Min	141150	141160
		Max	142780	142790
	(τ_{xy})	Min	55410	55419
		Max	86860	86884

Lamina	Stress		Present (Pa)	Reference [60] (Pa)
-45° (Glass/epoxy)	(σ_x)	Min	141150	141160
		Max	142780	142790
	(σ_y)	Min	93770	93768
		Max	141150	141160
	(τ_{xy})	Min	-86860	-86884
		Max	-55410	-55419
90° (Carbon/epoxy)	(σ_x)	Min	91720	91700
		Max	113300	113300
	(σ_y)	Min	-73110	-73198
		Max	349240	349310
	(τ_{xy})	Min	14120	14123
		Max	28240	28246

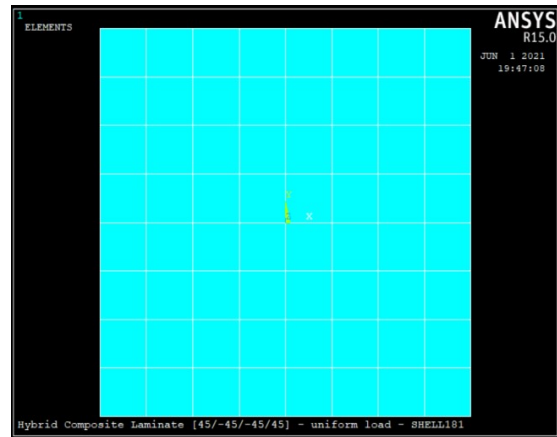
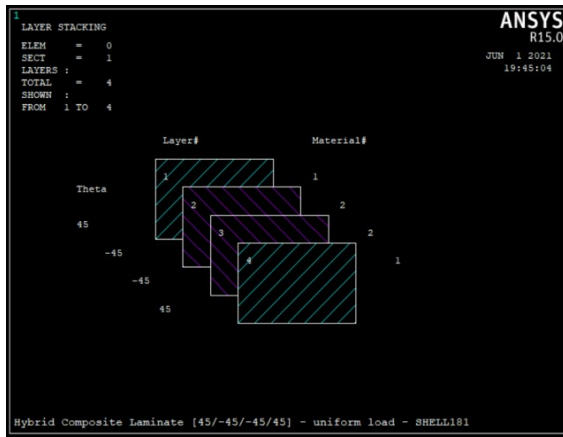


Fig 9.1 (a) Stacking sequence of laminate

(b) Quadrilateral Mapped meshing of laminate

9.3 Discussion

9.3.1 Stress and displacement

The stresses and deflections of various combinations of hybrid composite laminates obtained by FEM are compared to semi-analytical methods solved in the MATLAB platform, and less than 1% error is calculated. $[45/-45]_s$ Hybrid composite laminate composed of layers of Graphite/epoxy (G) and Glass/epoxy (C) composite under 1000 N tensile load in x direction are analyzed. Table 9.3a and 9.3b show the comparison of the local stress and global stress of G-C-C-G hybrid composite of FEM with semi analytical method. Displacement vector sum (USUM) is found out for different combinations of composite materials (table 9.4). The composite materials chosen to make hybrid composites are: Graphite/epoxy (G) and Glass/epoxy (C).

Different combinations of these composite materials are analyzed and compared to find out the optimum combination.

Table 9.3(a) Comparison of the Local stress of G-C-C-G hybrid composite of FEM with Semi analytical method

Lamina	Local Stress			
			FEM (Pa)	Semi analytical method (Pa)
45° (Graphite /epoxy)	(σ_x)	Top/Bottom	45865	45865
	(σ_y)	Top/Bottom	10882	10882
	(τ_{xy})	Top/Bottom	-31698	-31698
-45° (Glass/epoxy)	(σ_x)	Top/Bottom	39118	39118
	(σ_y)	Top/Bottom	4135.4	4135
	(τ_{xy})	Top/Bottom	18302	18302
-45° (Glass/epoxy)	(σ_x)	Top/Bottom	39118	39118
	(σ_y)	Top/Bottom	4135.4	4135
	(τ_{xy})	Top/Bottom	18302	18302
45° (Graphite/epoxy)	(σ_x)	Top/Bottom	45865	45865
	(σ_y)	Top/Bottom	10882	10882
	(τ_{xy})	Top/Bottom	-31698	-31698

Table 9.3(b) Comparison of the Global stress of G-C-C-G hybrid composite of FEM with Semi analytical method

Lamina	Global Stress		FEM(Pa)	Semi analytical method (Pa)	% age error
45° (Graphite /epoxy)	(σ_x)	Top/Bottom	60071	60071	0
	(σ_y)	Top/Bottom	-3324.3	-3324	0.001
	(τ_{xy})	Top/Bottom	17491	17491	0

-45° (Glass/epoxy)	(σ_x)	Top/Bottom	39929	39929	0
	(σ_y)	Top/Bottom	3324	3324	0
	(τ_{xy})	Top/Bottom	-17491	-17491	0
-45° (Glass/epoxy)	(σ_x)	Top/Bottom	39929	39929	0
	(σ_y)	Top/Bottom	3324	3324	0
	(τ_{xy})	Top/Bottom	-17491	-17491	0
45° (Graphite/epoxy)	(σ_x)	Top/Bottom	60071	60071	0
	(σ_y)	Top/Bottom	-3324.3	-3324	0.001
	(τ_{xy})	Top/Bottom	17491	17491	0

Table 9.4 Comparison of different hybrid laminated composite.

Hybrid Composite	USUM (mtr)
G-G-G-G	0.002491
G-C-C-G	0.003912
C-C-C-C	0.004482
C-G-C-G	8.6441

From table 9.4, the displacement vector sum (USUM) of graphite/epoxy laminate is less as compared to Glass/epoxy since the elastic and shear modulus of graphite/epoxy material are greater as compared to others. When hybrid laminate is built up using graphite/epoxy and glass/epoxy, it is found that G-C-C-G combination shows the displacement which is more than Graphite/epoxy but less than Glass/epoxy. G-C-C-G combination of hybrid composites shows the least displacement vector sum (USUM) as compared to other hybrid combinations. Fig 9.2 shows the deflection of G-C-C-G

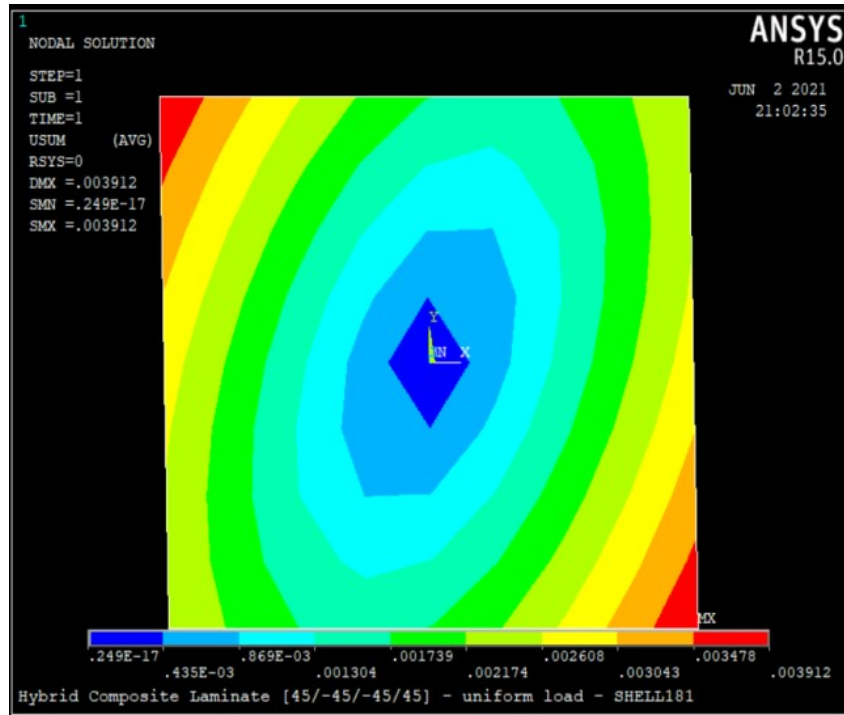


Figure 9.2 USUM of G-C-C-G

9.3.2 Failure analysis

Failure analysis of laminate was discussed in detail in the previous chapter-8. In this chapter, strength ratios are calculated for different combinations of hybrid composites. Tsai-Wu and maximum stress criteria are used to calculate the strength ratio. The ply having minimum strength ratio fails first. The minimum strength ratio when multiplied with load gives the first ply failure load. Here the load is taken as a unit tensile load. Therefore, strength ratio and first ply failure load are the same. Strength ratio using Tsai-Wu criteria is calculated for a cross ply hybrid composite and is compared with glass and graphite epoxy composite. Graphite epoxy composite forms the outer layer and glass epoxy composite forms the inner layer because the longitudinal tensile and compressive strengths are larger in the graphite/epoxy lamina than in a glass/epoxy lamina. Table 9.5 shows the comparison of the strength ratio, cost and mass of four layer cross ply hybrid composites with other composites. The thickness of each layer is assumed to be constant. Based on first ply failure analysis, the strength ratio (SR) of hybrid composite is superior to that of glass/epoxy composite and less than the SR of graphite/epoxy. Also, the cost of the hybrid composite is less than that of the graphite epoxy composite and the mass is less than glass/epoxy and slightly greater than graphite epoxy composite . Table 9.6

shows the strength ratio of the G-C-C-G hybrid composite lamina by lamina for $[45/-45]_s$ using Tsai-Wu and Max. Stress criteria. The results are compared with FEA software ANSYS and good agreement is found. It is found that graphite/epoxy lamina shows the least strength ratio, which infers that this lamina fails first. Since the applied load is unit, the strength ratio and first ply load are the same. Table 9.7 shows the comparison of $[45/-45]_s$ angle ply Graphite/epoxy and Glass/epoxy composite with hybrid combinations i.e. G-C-C-G combination as discussed above and found that G-C-C-G hybrid composite, shows the least strength ratio or first ply failure load as compared to the others.

Table 9.5. Comparison of four layers Cross ply $[0/90/90/0]$ Glass/Epoxy and Graphite/ Epoxy composite with Hybrid composite, thickness/layer: 5 mm, length: 1m and width: 0.2 m under in plane tensile load (1N) based on Tsai-Wu Criteria.

Type of composite	Strength Ratio	Cost/ply	Total cost	Mass
Graphite/Epoxy	7.47E6	2.5 unit	10 unit	6.36 kg
Glass/Epoxy	1.77E6	1 unit	4 unit	8 kg
Gr-E/Gl-E/Gl-E/Gr-E (Hybrid composite)	7.14E6		7 unit	7.12 kg

Table 9.6 Strength ratio of G-C-C-G sym. Angle ply hybrid composite $[45/-45]_s$

Lamina/ply	Orientation Angle	Strength Ratio			
		TSAI-WU		MAX. STRESS	
		Semi analytical method	FEM	Semi analytical method	FEM
G	45°	1.6565E6	1.6565E6	2.1453E6	2.1453E6
C	-45°	3.3407E6	3.3407E6	3.9339E6	3.9339E6
C	-45°	3.3407E6	3.3407E6	3.9339E6	3.9339E6
G	45°	1.6565E6	1.6565E6	2.1453E6	2.1453E6

Table 9.7 Comparison of four layers Angle ply [45/-45/-45/45] Glass/Epoxy and Graphite/Epoxy composite with Hybrid composite, thickness/layer: 5 mm, length: 1m and width: 0.2 m under in plane tensile load (1N) based on Tsai-Wu Criteria and Max. Stress Criteria.

Hybrid composite	Tsai-Wu criteria	Max. Stress criteria	Mode of failure
C-C-C-C	1.9989E6	2.88E6	1T
G-C-C-G	1.6565E6	2.15E6	1T (G ply)
G-G-G-G	2.4646E6	2.72E6	1T

9.4 Analysis of hybrid composite beam and plate

A comparative study of the deflection, strength ratio, cost, and mass of graphite epoxy and glass epoxy composite beams for different boundary conditions is presented in the table 9.8, which shows that deflection of glass epoxy composite is more than that of graphite epoxy. Also the cost per ply of graphite epoxy is 2.5 times greater than that of glass epoxy and the density of glass epoxy is less than that of graphite epoxy. Laminated composite design includes optimization in cost, mass, strength ratio, stiffness etc. A hybrid composite is the optimum combination of different composite materials in such a way that it minimises cost and mass without compromising its strength. Plies of graphite and glass epoxy are combined in such a way that it minimizes cost and mass.

It is found that the G-C-C-G (G: graphite epoxy and C: glass epoxy material) combination of composite materials (hybrid composite) shows the minimum transverse deflection as compared to glass/Epoxy composite and very close to graphite/Epoxy composite (Table 9.8). A graphite/epoxy composite forms the facing material and the glass epoxy composite forms the inner core layer. Because the longitudinal tensile and compressive strengths are larger in the graphite/epoxy lamina than in a glass/epoxy lamina. Also, hybrid composite shows minimum mass as compared to glass/epoxy and the mass is slightly greater than graphite/epoxy and also its cost is less than graphite/epoxy but greater than glass/epoxy composite. Based on first ply failure analysis, strength ratio (SR) of the G-C-C-G hybrid composite is superior than glass/epoxy composite and close to the strength ratio of graphite/epoxy. Therefore, the G-C-C-G, hybrid composite is relatively superior to that of constituent composite material. Table 9.9 shows the comparison of the results of FSDT method with Finite element software ANSYS for four layers angle ply [60/-60]_s glass/epoxy and graphite/epoxy composites with hybrid composite beam, thickness/layer: 0.125 mm, length: 0.1m and width: 5mm under UDL

(200N/m) and percentage error is noted. Table 9.10 shows the comparison of the Semi analytical method results with FEM for simply supported 20 m x 20 m laminated composite plate for G-C-C-G combination under uniform transverse load (100 N/m) of thickness per lamina of 5mm for orientation angle ranging from 0 deg to 90 deg. Fig 9.3 shows the finite element model of the G-C-C-G hybrid composite beam.

Table 9.8. Comparison of four layers Angle ply $[60/-60]_s$ Glass/Epoxy and Graphite/ Epoxy composite with Hybrid composite beam, thickness/layer: 0.125 mm, length: 0.1m and width: 5mm under UDL (200N/m) based on Tsai-Wu Criteria.

Hybrid composite	Deflection (m)	Strength Ratio (Tsai-Wu criteria)	First failed ply	Mode of failure	Cost	Mass (gm)
G-G-G-G	0.0018	0.0481	4	SC	10 unit	0.3975
G-C-C-G	0.002	0.0422	4	2T	7 unit	0.445
G-C-G-C	0.0022	0.0442	4	2T	7 unit	0.445
C-C-C-C	0.0028	0.0429	4	2T	4 unit	0.4925

Table 9.9 Comparison of the analytical results (FSDT) with FEM results.

Hybrid composite	Deflection (m)			Strength Ratio (Tsai-Wu criteria)		
	Analytical	FEM	% error	Analytical	FEM	% error
G-G-G-G	0.0018	0.001794	0.33	0.0481	0.0475	1.25
G-C-C-G	0.002	0.001897	5.15	0.0422	0.04	5.21
G-C-G-C	0.0022	0.0022	0.00	0.0442	0.0441	0.23
C-C-C-C	0.0028	0.002732	2.43	0.0429	0.0417	2.80

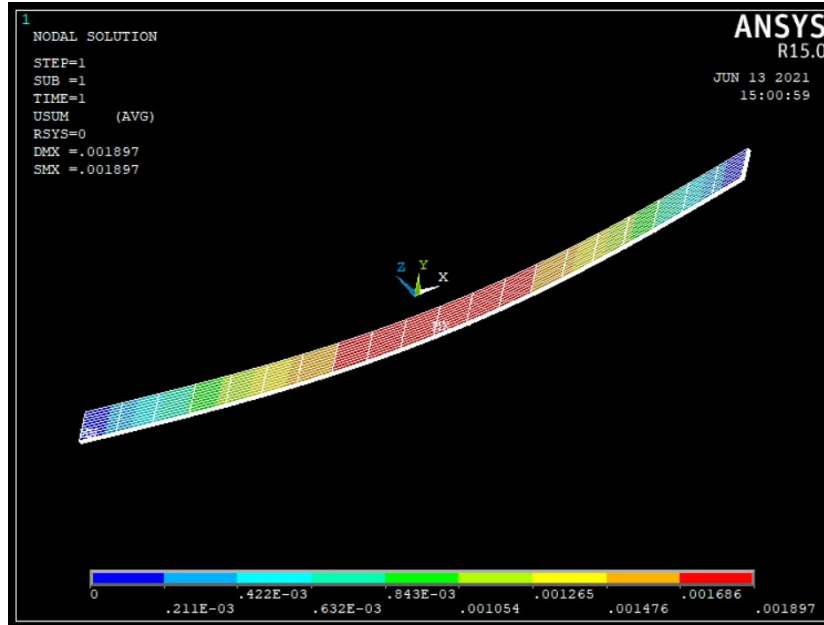


Figure 9.3 Deflection of G-C-C-G hybrid composite beam

Table 9.10 Comparison of the analytical results (Navier Method) with FEM results.

Angle Orientation [+0]s	Navier method m	FEM m	% Error
0	1.8281	1.8427	0.8
15	1.5758	2.3338	48.1
30	1.2319	1.9464	58
45	1.1104	1.8821	69.5
60	1.2319	1.7628	43.1
75	1.5758	2.0879	32.5
90	1.8281	1.8427	0.8

9.5 Closure

The problem of the hybrid laminated composites under different boundary conditions and loading conditions is studied. Different combinations of graphite epoxy and glass epoxy composites are studied by semi analytical and finite element methods and compared to get the best combination. The G-C-C-G combinations is found suitable with respect to cost and mass as compared to graphite epoxy (G) and glass epoxy composite (C). Percentage errors of analytical results with ANSYS results are noted for plate and beam.

CHAPTER 10

CONCLUSION

The results from FEA software like ANSYS are compared with analytical methods in solving problems like deflection, stress, and failure loads of laminated composite structures (plates or beams) under different boundary conditions and loads. Simple laminate equations are used to solve the problems of laminated composite plates under in-plane load. Beam problems are solved by classical lamination theory and first-order shear deformation theory. The problem of simply supporting a plate under transverse load is solved by the Navier method and the Rayleigh-Ritz method. The results from the FEA software exactly match the semi-analytical method for composite plates under in-plane load because the equations used in this problem are simple and free from higher order terms. But for complex problems like beams and simply supported plates, FEA results do not match with the analytical method, so a percentage error is obtained. This percentage error varies with the variation of the orientation angle, the thickness of the laminate, number of laminae, aspect ratio, and length to thickness ratio. Due to assumptions in solving the equations, both semi-analytical and FEA software give approximate solutions to the problems. As the complexity of the problem increases, the higher order terms also increase. Therefore, to solve the equations, certain assumptions are made, which introduces the error. The significance of the various factors for the analysis of the error is studied by the statistical method ANOVA, and the relationship between them is established by regression analysis. The percentage error for a laminated composite plate and beam under transverse load depends on the laminate thickness and orientation angle (or stacking sequence). Mesh size is an insignificant variable because mesh size can be converged by convergence analysis. The analysis is also extended to hybrid beams and the buckling problem of simply supported plates. The analysis is further extended to study the effects of these factors on deflection and strength ratio based on first-ply failure load. A comparative study of different failure criteria was conducted based on first-ply failure load. The deflection and stress obtained from FEA software are compared with semi-analytical methods for different problems of laminated composite structures, from simpler to complex problems, using 2-dimensional models, and an error is noted. It is found that for simpler problems, the error rate is very low, but as the complexity increases, the error rate also increases. Also, it is noted that error reduces as the thickness of the laminate increases, and this error varies for different variables, i.e.,

orientation angle, length to width ratio, etc. Therefore, it may be possible to reduce the error by optimizing these variables. Different researchers have proposed different methods of optimization, but in this thesis, a statistical method is used to study the error. The semi-analytical method is used to study the effects of orientation angle, the number of the lamina, and length to thickness ratio on deflection, stress, and first ply failure load of laminated composite plates under different boundary conditions and loads. The semi-analytical method is also used to study the effect of thermal and hygro-thermal loads on the failure analysis of laminated composite plates under in-plane load and beams under transverse load. The comparison is also extended to hybrid composite plates and beams. A comparative study of different hybrid composites made of different combinations of graphite epoxy and glass epoxy materials was also done to obtain a better or optimum hybrid composite material suitable for the application.

The comparative study and analysis of the errors of the semi-analytical and finite element methods in solving the problem of laminated composite plates or beams is essential to study the degree of approximation in the results. And after getting the error, it is very essential to study the method of reducing the error and select the factors to be optimized for error reduction. In this thesis, a comparative study of semi-analytical and finite element methods is done to get the error and the error analysis is done by statistical method.

CHAPTER 11

FUTURE SCOPE

In this thesis, the results from FEM using finite element software are compared with those from a semi-analytical method. The problems of laminating composite plates under in-plane load are solved by using laminate equations, whereas, for simply supported plates under transverse loading, they are solved by the Navier-Stokes method and the Rayleigh-Ritz method. The problems of laminated composite beams under different boundary conditions and subjected to different loading conditions are solved by CLT and FSDT. The algorithms based on these theories are solved on the MATLAB platform. The FEA software ANSYS is used to solve the problem by the finite element method. The results from the FEA software are compared with semi-analytical methods, and percentage errors are noted. A significant percentage error is found for simply supported plate and beam under transverse load. The reason behind the error is discussed in this thesis. It is found from the investigation that the semi-analytical method for simply supported plate and beam under transverse load gives an approximate result because the method solves the problem by assuming certain assumptions, whereas FEM solves the problem by a numerical method which gives an approximate solution. Even better ideas can be obtained if the results are compared with a third method, i.e., an experimental method. Although experimental methods contain certain experimental errors, the results from the experiment may be used to compare the results of FEA software and semi-analytical methods. Experimental methods are beyond the scope of this thesis. The accuracy of these methods may be checked with higher order theories, which are beyond the scope of this thesis. The percentage error depends on different factors as discussed in this thesis. The significance of these factors in solving the problem is discussed by means of a statistical method in this thesis. The percentage error may be reduced by an optimum combination of these factors, which is beyond the scope of this thesis. Different optimization methods are available to optimize the percentage error, which is beyond the scope of this report. Therefore, future research work may be directed along the following lines, which are not discussed in this thesis:

- In this thesis, the problem is solved using FEA software and a semi-analytical method. Newer research may be targeted towards experimental methods to compare the results of the FEA software and analytical methods.

- Future research may also be concentrated on higher-order theories to get better results.
- Future research may be done to optimize the percentage error to get a more accurate result.
- A two-dimensional model of the laminated composite plate or beam is built up using the SHELL element in FEA software to solve the problem. Future research may be concentrated on a three-dimensional model of the plate or beam to get a more accurate result.

REFERENCES

- [1] Isaac M. Danial, Ori Ishai (2007): Engineering Mechanics of Composite materials, Oxford University Press, Inc., New York. ISBN 978-0195150971.
- [2] Ever J. Barbero (2014): Finite Element Analysis of Composite Material Using ANSYS, CRC Press, Taylor & Francis Group, 6000 Broken Sound Parkway NW, Suite. ISBN 978-1-4665-1690-8.
- [3] J.N. Reddy (1997): Mechanics of Laminated composite plates and shells- Theory and analysis, CRC Press, London, New York. ISBN 0-8493-1592-1.
- [4] Ever J. Barbero (2018): Introduction to Composite Material Design, CRC Press, Taylor & Francis Group, 6000 Broken Sound Parkway NW, Suite. ISBN 978-1-1381-9680-3.
- [5] B. N. Pandya, T. Kant (1988): Finite element analysis of laminated composite plates using a higher-order displacement model, Composite Science and Technology, 32(2), pp. 137-155.
- [6] T.Y. Kam, S.C. Lin, K.M. Hsiao (1993): Reliability analysis of nonlinear laminated composite plate structures, Composite Structure, 25(1-4), pp. 503-10.
- [7] Han Wanmin, Petyt Maurice, Hsiao Kuo-Mo (1994): Investigation into geometrically nonlinear analysis of rectangular laminated plates using the hierarchical finite element method. Finite Element Analysis Des, 18(1-3), pp.273-88.
- [8] C. Sridhar and K.P. Rao (1995): Large deformation finite element analysis of laminated circular composite plates, Computers and structures, 54(1), pp. 59-64.
- [9] M. Ganapathi, O. Polit, M. Touratier (1996): C^0 eight-node membrane shear-bending element for geometrically non-linear (static and dynamic) analysis of laminates. Int. Journal for Numerical Methods in Engineering, 39(20), pp. 3453-74.

- [10] G. Bao, W. Jiang , J.C. Roberts (1997): Analytic and finite element solutions for bending and buckling of orthotropic rectangular plates, *Int. of Journal of solids and structures*, 34 (14), pp. 1797-1822.
- [11] K.Y. Sze, L.W. He, Y.K. Cheung (2000): Predictor corrector procedures for analysis of laminated plates using standard Mindlin finite element models, *Int. Journal for Composite Structures*, 50(2), pp.171-182.
- [12] Y.X. Zhang, K.S. Kim. (2004): Two simple and efficient displacement-based quadrilateral elements for the analysis of composite laminated plates. *Int. Journal Numerical Meth Eng*, 61, pp. 1771–96.
- [13] Y.X. Zhang, K.S. Kim (2005): A simple displacement-based 3-node triangular element for linear and geometrically nonlinear analysis of laminated composite plates. *Comput Meth Appl Mech Eng*, 194, pp. 4607–32.
- [14] Y.X. Zhang , C.H. Yang (2009): Recent developments in finite element analysis for laminated composite plates, *Composite structure*, 88(1), pp. 147-157.
- [15] Mauricio F. Caliri Jr., Antonio J.M. Ferreira, Volnei Tita (2016): A review on plate and shell theories for laminated and sandwich structures highlighting the Finite Element Method, *Int. Journal of Composite structures*, 156, pg-63-67.
- [16] Chalida Anakpotchanakul and Pongtorn Prombut (2019): Influence of aspect ratios on vibration and bending of composite laminates, *Materials today proceedings*, 17(4), pp. 1588-1594.
- [17] K.H. Lo, R.M. Christensen, E.M. Wu (1977): A higher order theory for plate deformations, part 2: laminated plates, *ASME J. Appl. Mech.* 44, pp. 669–676.
- [18] Deepak ku. Maity, P.K Sinha (1994): Bending and free vibration analysis of shear deformable laminated composite beams by finite element method, *Composite Structure*, 29(4), pp. 421-431.
- [19] Hemendra Arya, Rameshchandra Shimpi, Niranjan K. Naik (2002): zigzag model for laminated composite beams, *Composite Structures*, 56 (1), pp. 21-24.
- [20] Masoud Tahani (2007): Analysis of laminated composite beams using layerwise displacement theories, *Composite Structures* 79, pp. 535–547.

- [21] R. R. Borkar, A. S. Sayyad, S. M. Ghumare (2013): Assessment of Refined Beam Theories For The Bending Analysis of Composite Beam. *Int. Journal of Advanced Technology in Civil Engineering*, 2(1), pp. 73-78.
- [22] Mohammed Fahmy Aly , Galal. A. Hassan , Ibrahim Goda (2013), The effect of fiber orientation and laminate stacking sequences on the torsional natural frequencies of laminated composite beams, *IJRET: International Journal of Research in Engineering and Technology* 2(12), pp. 203-2018.
- [23] Trung Kien Nguyen, Ngoc Duong Nguyen, Thuc P. Vo, Huu Tai Thai (2017): Trigonometric-series solution for analysis of laminated composite beams, *Composite Structures* 160, pp. 142–151.
- [24] Atteshamuddin S. Sayyad, Yuwaraj M. Ghugal (2017): Bending, buckling and free vibration of laminated composite and sandwich beams: A critical review of literature, *Composite Structures* 171, pp. 486–504.
- [25] Atilla and Emrah (2017): Static analysis of laminated composite beams based on higher-order shear deformation theory by using mixed-type finite element method, *Int. journal of Mechanical Sciences*, 130, pp. 234-243.
- [26] Krishna Chaitany, Gantasal, Nitin Kotkunde (2017): Theoretical and finite element investigation of inter-laminar stresses for laminated composite beam, *Materials today proceedings*, 4(8), pp. 7731-7740.
- [27] Nivedan Pandey, Appaso M. Gadade (2019): Static Response of Laminated Composite Beam Subjected to Transverse Loading, *Materials today proceedings*, 16(2), pp. 956-963.
- [28] Joshi, M.G. and Biggers Jr., S.B. (1996): Thickness optimization for maximum buckling loads in composite laminated plates, *Composites: Part B*, 27 B, pp. 105–114.
- [29] I. Shufrin, O. Rabinovitch. and M. Eisenberger (2008): Buckling of laminated plates with general boundary conditions under combined compression, tension, and shear- a semi-analytical solution, *Thin-Walled Structures*, 46(7-9), pp. 925-938.
- [30] A. Lakshmi Narayana, K.M. Rao. and R. Vijaya Kumar (2014): Buckling analysis of rectangular composite plates with rectangular cut out subjected to linearly varying in-plane loading using FEM, *Sadhana*, 39(3), pp. 583–596.

- [31] Volkan Kahya (2016): Buckling analysis of laminated composite and sandwich beams by the finite element method, *Composites Part B Engineering*, 91, pp. 126-134.
- [32] A. Madeo , R.M. J. Groh, G. Zucco, P.M. Weaver, G. Zagari, R. Zinno (2017): Post-buckling analysis of variable-angle tow composite plates using Koiter's approach and the finite element method, *Thin walled structure*, 110, pp. 1-13.
- [33] M. Kazemi. and Verchery (2016): Design of composite laminated plates for maximum buckling load with stiffness and elastic modulus constraints, *Composite Structures*, 148, pp. 27-38.
- [34] G.J. Turvey (1980): An initial flexural failure analysis of symmetrically laminated cross-ply rectangular plates. *Int. J of Solids & Struct.*, 16, pp. 451-63.
- [35] G.J. Turvey (1980): Flexural failure analysis of angle-ply laminates of GFRP and CFRP, *Int. Journal Strain Analysis*, 15, pp. 43-49.
- [36] G.J. Turvey. (1980): A study of the onset of flexural failure in cross-ply laminated strips. *Fibre Sci. Tech.*, 13, pp. 325-326.
- [37] G. J. Turvey (1981): Initial flexural failure of square, simply supported, angle-ply plates. *Fibre Sci. Tech.*, 15 , pp. 47-63.
- [38] J. N. Reddy & A. K. Pandey (1987): A first-ply failure analysis of composite laminates. *Computers & Struct.*, 25, pp. 371-393.
- [39] Y. S. N. Reddy & J. N. Reddy (1992): Linear and nonlinear failure analysis of composite laminates with transverse shear. *Comp. Sci. Tech.*, 44, pp. 227-255.
- [40] S. Tolson and N. Zabararas (1991): finite element analysis of progressive failure in laminated composite plate, *Composite & Structures*, 38(3), pp. 361-376.
- [41] T. Y. Kam & S. C. Lin (1995): First ply failure analysis of laminated composite plate based on the layer wise linear displacement theory, *Int. Journal composite Structure*, 32, pp. 583-91.
- [42] P. Subramanian (2001), Flexural analysis of symmetric laminated composite beams using C¹ finite element, *Composite structure*, 54(1), pp. 121-126.

- [43] A.K. Onkar, C.S. Upadhyay, D. Yadav (2007): Probabilistic failure of laminated composite plates using the stochastic finite element method, *Composite structure*, 77(1), pp. 79-91.
- [44] Y.X. Zhang, H.S. Zhang (2010): Multiscale finite element modeling of failure process of composite laminates, *Composite structure*, 92(9), pp. 2159-65.
- [45] M. Meng, H.R. Le, M.J. Rizvi, S.M. Grove (2015): 3D FEA modelling of laminated composites in bending and their failure mechanisms, *Composite Structures* 119, pp. 693–708.
- [46] Ever J. Barbero , Mehdi Shahbazi (2017): Determination of material properties for ANSYS progressive damage analysis of laminated composites, *Composite Structures* 176, pp. 768–779.
- [47] Meenu Teotia and R.K. Soni (2018): Applications of finite element modelling in failure analysis of laminated glass composites: A review, *Engineering failure analysis*, 94, pp. 412-437.
- [48] Dhiraj Biswas, Chaitali Ray (2019): Effect of hybridisation in laminated composites on the first ply failure behaviour: Experimental and numerical studies, *Int. J. of Mechanical Sciences*, 161-162, pp. 1050-57.
- [49] M. Patni , S. Minera ,C. Bisagni , P.M. Weaver , A. Pirrera (2019): Geometrically nonlinear finite element model for predicting failure in composite structures, *composite structures*, 225, pp. 1110-68.
- [50] Ravi Joshi, P. Pal, S.K. Duggal (2020): Ply-by-ply failure analysis of laminates using finite element method, *Europien Journal of Mechanics*, 81, pp. 1039-1064.
- [51] Jianyu Zhang , Dexuan Qi , Longwei Zhou , Libin Zhao , Ning Hua (2015): A progressive failure analysis model for composite structures in hygro thermal environments, *Composite Structures* 133, pp. 331–342.
- [52] Autar K. Kaw (2006): *Mechanics of Composite material*, second edition, Taylor & Francis, ISBN 978-0-8493-1343-1.
- [53] Guven, E. Madanci (2006): *Finite element method and application in engineering using ANSYS*, University of Arizona, Springer, ISBN 978-0387-28289-3,

- [54] Ever J. Barbero (2013): Finite Element Analysis of Composite Material Using ABAQUS, CRC Press, Taylor & Francis Group, 6000 Broken Sound Parkway NW, Suite, ISBN 978-1-4665-1663-2
- [55] Mer Arnel Manahan (2011): A Finite Element Study of the Deflection of Simply Supported Composite Plates Subject to Uniform Load, M.E Thesis, Rensselaer Polytechnic Institute Hartford, Connecticut.
- [56] Kenneth Carroll (2013): Maximum Deflection Analysis of Simply Supported Aluminum and Composite Plates Under Uniform Pressure Using Rayleigh-Ritz Method and Finite Element Method, M.E Thesis, Rensselaer Polytechnic Institute Hartford, Connecticut.
- [57] Qiao Jie Yang (2009): Simplified Approaches to Buckling of Composite Plates, Thesis for Master of Science, University of Oslo.
- [58] J. Zhang, K. Chaisombat, S. He, C. H. Wang (2012): Hybrid Composite Laminates Reinforced With Glass / Carbon Woven Fabrics For Light Weight Load Bearing Structures, Materials and Design, 36, pp. 75–80.
- [59] Irina M.M.W., A.I. Azmi1, Tan C.L., Lee C.C. and A.N.M Khalil (2015): Evaluation of Mechanical Properties of Hybrid Fiber Reinforced Polymer Composites and Their Architecture, Procedia Manufacturing, 2, pp. 236–240.
- [60] Abhishek S. Patil, U. B. Khadabadi (2016): ANSYS as a Tool to Perform FEA and Failure Analysis of Hybrid Laminated Composites, International Research Journal of Engineering and Technology, 3(5), pp. 1235-1241.
- [61] Mustafa Akbulut, O. Fazil. Sonmez (2011): Design optimization of laminated composites using a new variant of simulated annealing- Computers and Structures, 89, pp- 1712–1724.
- [62] Krishna Chaitany, Gantasal, Nitin Kotkunde (2017): Theoretical and finite element investigation of inter-laminar stresses for laminated composite beam, Materials today proceedings, 4(8), pp. 7731-7740.

APPENDIX

- MATLAB code for simply supported beam under UDL (CLT)

```
clc
E1 = 181e9 ; % Pa
nu12 = 0.28 ;
E2 = 10.3e9 ; % Pa
G12 = 7.17e9 ; % Pa
nu21 = nu12 * E2 / E1 ;
orient=[0 90 -30 30 30 -30 90 0];
N=length(orient);
thick =0.000125; % m each layer thickness
h = N * thick; % total laminate thickness
z = -h/2 : thick : h/2;
b = 0.005; % m width of beam
L = 0.1; % m (a) length of beam
q = 200; % N/m distributed load
Aij = zeros(3,3);
Bij = zeros(3,3);
Dij = zeros(3,3);
Aij_vect = zeros(1,N);
Bij_vect = zeros(1,N);
Dij_vect = zeros(1,N);
NT = zeros(3,1);
MT = zeros(3,1);
% Q matrix (material coordinates)
denom = 1 - nu12 * nu21 ;
Q11 = E1 / denom ;
Q12 = nu12 * E2 / denom ;
Q22 = E2 / denom ;
Q66 = G12 ;
Q = [ Q11 Q12 0; Q12 Q22 0; 0 0 Q66];
for i = 1:3
for j = 1:3
for k=1:N
theta = orient(k) * pi / 180; % ply i angle in radians, from bottom
m = cos(theta) ;
n = sin(theta) ;
```

```

T = [ m^2 n^2 2*m*n; n^2 m^2 -2*m*n; -m*n m*n (m^2 - n^2)];
%abar = T' * a;
Qbar = inv(T) * Q * (inv(T))';

Aij_vect(k) = Qbar(i,j).*(z(k+1)-z(k));
Bij_vect(k) = Qbar(i,j).*((z(k+1)).^2-(z(k)).^2);
Dij_vect(k) = Qbar(i,j).*((z(k+1)).^3-(z(k)).^3);
end
Aij(i,j) = sum(Aij_vect);
Bij(i,j) = sum(Bij_vect)/2;
Dij(i,j) = sum(Dij_vect)/3;
end
end
Aij;
Bij;
Dij;
Dstar = inv(Dij); % Pa- m3
Dstar11 = Dstar(1); % 1/Pa-m3
Dstar12 = Dstar(2); % 1/Pa-m3
Dstar16 = Dstar(3); % 1/Pa-m3
Ex = 12/(Dstar11*h^3); % Pa
I = (b*h^3)/12 % m4 moment of inertia of the section of beam
wmax = (5*q*L^4)/(384*Ex*I)% m deflection of simply supported beam of uniformly
distributed load
wbar = wmax*(E2*h^3*b)/(q*L^4)*100
Mmax = (q*L^2)/8
Dm = [Dstar11;Dstar12;Dstar16];
Kappa = Dm*(Mmax/b)% unit: 1/m
stress = [];
LayerZ = zeros(1,N*2);
for i = 0:N-1
LayerZ(2*i+2) = z(i+2);
LayerZ(2*i+1) = z(i+1);
theta = orient(i+1) * pi / 180; % ply i angle in radians, from bottom
m = cos(theta) ;
n = sin(theta) ;
T = [ m^2 n^2 2*m*n; n^2 m^2 -2*m*n; -m*n m*n (m^2 - n^2)];
Qbar = inv(T) * Q * (inv(T))';
tempX = T*Qbar*(z(i+1)*(Kappa));

```

```

    tempy = T*Qbar*(z(i+2)*(Kappa));
    stress = [stress,tempx,tempy];    %local stress
    strain = inv(Q)* stress;        %local strain
end
LayerZ;
stress
strain
%.....
globalstress = [];
globalstrain = [];
LayerZ = zeros(1,N*2);
for i = 0:N-1
    LayerZ(2*i+2) = z(i+2);
    LayerZ(2*i+1) = z(i+1);
    theta = orient(i+1) * pi / 180; % ply i angle in radians, from bottom
    m = cos(theta) ;
    n = sin(theta) ;
    T = [ m^2 n^2 2*m*n; n^2 m^2 -2*m*n; -m*n m*n (m^2 - n^2)];
    Qbar = inv(T) * Q * (inv(T))';
    tempx = Qbar*(z(i+1)*(Kappa));
    tempy = Qbar*(z(i+2)*(Kappa));
    globalstress = [globalstress,tempx,tempy];
    tempx1 = (z(i+1)*(Kappa));
    tempy1 = (z(i+2)*(Kappa));
    globalstrain = [globalstrain,tempx1,tempy1];
end
LayerZ;
globalstress
globalstrain

```

- Failure analysis of simply supported beam based on TSAI-WU criteria

```

clc
E1 = 181e9 ; % Psi
nu12 = 0.28 ;
nu13 = 0.28 ;
nu23 = 0.6 ;
E2 = 10.3e9 ; % Psi
E3 = 10.3e9 ; % Psi
G12 = 7.17e9 ; % Psi
G13 = 7.17e9 ; % Psi

```

```

G23 = 3.12e9;
nu21 = nu12 * E2 / E1 ;
nu31 = nu13 * E3 / E1 ;
nu32 = nu23 * E3 / E2 ;
%[moduli]=[E1 E2 nu12 G12];
s1tu= 1500e6; %ultimite longitudinal tensile strength
s1cu= 1500e6 ; %ultimite longitudinal compressive strength
s2tu=40e6 ; %ultimite transverse tensile strength
s2cu=246e6 ; %ultimite transverse compressive strength
s12u=68e6 ; %ultimite in-plane shear strength
[strength]=[s1tu s1cu s2tu s2cu s12u];
%.....
orient=[0 90 -30 30 30 -30 90 0]; % ANTY SYMMETRIC ANGLE PLY LAMINATE
N=length(orient);
thick =0.000125; % m each layer thickness
h = N * thick; % total laminate thickness
z = -h/2 : thick : h/2;
b = .005; % m wiidth of beam
L = 0.1; % m (a) length of beam
q = 200; % N/m distributed load
Aij = zeros(5,5);
Bij = zeros(5,5);
Dij = zeros(5,5);
Aij_vect = zeros(1,N);
Bij_vect = zeros(1,N);
Dij_vect = zeros(1,N);
%.....
denom = 1 - nu12 * nu21 ;
Q11 = E1 / denom ;
Q12 = nu12 * E2 / denom ;
Q22 = E2 / denom ;
Q66 = G12 ;
Q44 = G23 ;
Q55 = G13;
Q = [ Q11 Q12 0 0 0; Q12 Q22 0 0 0; 0 0 Q44 0 0; 0 0 0 Q55 0; 0 0 0 0 Q66]
%.....
for i = 1:5
for j = 1:5
for k=1:N
theta = orient(k) * pi / 180; % ply i angle in radians, from bottom

```

```

m = cos(theta) ;
n = sin(theta) ;
T = [ m^2 n^2 0 0 2*m*n; n^2 m^2 0 0 -2*m*n; 0 0 m -n 0; 0 0 n m 0; -m*n m*n 0 0
(m^2 - n^2)];
Qbar = inv(T) * Q * (inv(T))';
Aij_vect(k) = Qbar(i,j).*(z(k+1)-z(k));
Bij_vect(k) = Qbar(i,j).*((z(k+1)).^2-(z(k)).^2);
Dij_vect(k) = Qbar(i,j).*((z(k+1)).^3-(z(k)).^3);
end
Aij(i,j) = sum(Aij_vect);
Bij(i,j) = sum(Bij_vect)/2;
Dij(i,j) = sum(Dij_vect)/3;
end
end
Aij;
Bij;
Dij;
ASTAR = inv(Aij);
ASTAR55 = ASTAR(19);
Dstar = inv(Dij); % Pa- m3
Dstar11 = Dstar(1); % 1/Pa-m3
Dstar12 = Dstar(2); % 1/Pa-m3
Dstar16 = Dstar(5); % 1/Pa-m3
Ex = 12/(Dstar11*h^3) % Pa
I = (b*h^3)/12% m4 moment of inertia of the section of beam
G = 1/(ASTAR55*h);
wmax1 = (5*q*L^4)/(384*Ex*I)
wmax = (5*q*b*L^4)/(384*Ex*I)+((q*b*L^2)/(8*G*b*h))
Mmax = (q*L^2)/8
Dm = [Dstar11;Dstar12;Dstar16];
Kappa = Dm*(Mmax/b)% unit: 1/m
stress = [];
LayerZ = zeros(1,N*2);
for i = 0:N-1
LayerZ(2*i+2) = z(i+2);
LayerZ(2*i+1) = z(i+1);
theta = orient(i+1) * pi / 180; % ply i angle in radians, from bottom
m = cos(theta) ;
n = sin(theta) ;
T = [ m^2 n^2 2*m*n; n^2 m^2 -2*m*n; -m*n m*n (m^2 - n^2)];

```

```

Qbar = inv(T) * Q * (inv(T))';
tempx = T*Qbar*(z(i+1)*(Kappa));
tempy = T*Qbar*(z(i+2)*(Kappa));
stress = [stress,tempx,tempy];    %local stress
strain = inv(Q)* stress;        %local strain
end
LayerZ;
stress
strain;
H1=(1/((strength(1))) - (1/(strength(2))));
H2=(1/((strength(3))) - (1/(strength(4))));
H11=(1/((strength(1)*strength(2))));
H22=(1/((strength(3)*strength(4))));
H66=(1/((strength(5))^2));
H6=0;
% Finding H12 using Mises-Hencky criterion
H12=(-1/2)*sqrt(1/((strength(1))*(strength(2))*(strength(3))*(strength(4))));
%SR=[3,2];
for i=1:3:24
b=(H1*stress(i)+(H2*stress(i+1)+(H6*stress(i+2)));
a=(H11*(stress(i)^2)+(H22*(stress(i+1)^2)+(H66*(stress(i+2)^2)+(2*H12*stress(i)*stress(i+1))));
c=-1;
% Quadratic formula
R(1)=((-b)+sqrt((b^2)-(4*a*c)))/(2*a);
R(2)=((-b)-sqrt((b^2)-(4*a*c)))/(2*a);
% Strength ratio per Tsai-Wu criterion
if(R(1)<0)
    SR=R(2);
else
    SR=R(1);

end
SR
end

```

- MATLAB code of ANOVA

```
E = data(:,5);
```

```
A = data(:,1);
```

```

B = data(:,2);
C = data(:,3);
D = data(:,4);

%p = anovan(deflectionerror, {aspectratio, thickness, orientationangle})

[p1, tb1, stat1] = anovan(E, {A, B, C, D}, 'model', 1, 'varnames', {'A', 'B', 'C', 'D'}, 'alpha', 0.05)

[p2, tb2, stat2] = anovan(E, {A, B, C, D}, 'model', 2, 'varnames', {'A', 'B', 'C', 'D'}, 'alpha', 0.05)

results = multcompare(stat1, 'Dimension', [1 2 3 4]);

```

- MATLAB code for laminate under in plane load (stress)

```

clc
E1 = 181e9 ; % Pa
nu12 = 0.28 ;
E2 = 10.3e9 ; % Pa
G12 = 7.17e9 ; % Pa
nu21 = nu12 * E2 / E1 ;
orient=[0 90 0];
N=length(orient);
thick =0.005; % m each layer thickness
t = N * thick; % total laminate thickness
z = -t/2 : thick : t/2;
Aij = zeros(3,3);
Bij = zeros(3,3);
Dij = zeros(3,3);
Aij_vect = zeros(1,N);
Bij_vect = zeros(1,N);
Dij_vect = zeros(1,N);
% Q matrix (material coordinates)
denom = 1 - nu12 * nu21 ;
Q11 = E1 / denom ;
Q12 = nu12 * E2 / denom ;
Q22 = E2 / denom ;
Q66 = G12 ;
Q = [ Q11 Q12 0; Q12 Q22 0; 0 0 Q66];
for i = 1:3
for j = 1:3
for k=1:N
theta = orient(k) * pi / 180; % ply i angle in radians, from bottom

```



```

m = cos(theta) ;
n = sin(theta) ;
T = [ m^2 n^2 2*m*n; n^2 m^2 -2*m*n; -m*n m*n (m^2 - n^2)];
Qbar = inv(T) * Q * (inv(T))' ;
%Qb=Qbar(Orient(k))
Aij_vect(k) = Qbar(i,j).*(z(k+1)-z(k));
Bij_vect(k) = Qbar(i,j).*((z(k+1)).^2-(z(k)).^2);
Dij_vect(k) = Qbar(i,j).*((z(k+1)).^3-(z(k)).^3);
end
Aij(i,j) = sum(Aij_vect);
Bij(i,j) = sum(Bij_vect)/2;
Dij(i,j) = sum(Dij_vect)/3;
end
end
Aij
Bij
Dij
MM = [0; 0; 0];
NN = [1; 0; 0];
ABD= [Aij Bij;Bij Dij]
Astar = inv(Aij);
Bstar = -inv(Aij)*Bij;
Dstar = Dij-(Bij/Aij*Bij);
Hstar = Bij/Aij;
Aprime = Astar-(Bstar/Dstar*Hstar);
Bprime = Bstar/Dstar;
Dprime = inv(Dstar);
Hprime = -Dstar\Hstar;
Kappa = Dstar\MM-Dstar\Hstar*NN
Eps_o = Bstar/Dstar*MM+(Astar-Bstar/Dstar*Hstar)*NN
stress = [];
LayerZ = zeros(1,N*2);
for i = 0:N-1
LayerZ(2*i+2) = z(i+2)
LayerZ(2*i+1) = z(i+1)
theta = orient(i+1) * pi / 180; % ply i angle in radians, from bottom
m = cos(theta) ;
n = sin(theta) ;
T = [ m^2 n^2 2*m*n; n^2 m^2 -2*m*n; -m*n m*n (m^2 - n^2)];
Qbar = inv(T) * Q * (inv(T))';

```

```

tempX = Qbar*(Eps_o+z(i+1)*(Kappa));
tempY = Qbar*(Eps_o+z(i+2)*(Kappa));
stress = [stress,tempX,tempY];
end
LayerZ;
stress
sigmaX = stress(1,:);
sigmaY = stress(2,:);
TaoXY = stress(3,:);
hold on
plot(sigmaX, LayerZ./t,'k:')
axis ij
xlabel('pa');
ylabel('z/h');
title('Stresses(Mechanical load) on Laminate (a/h=5 & [+0]s)');
hold on
plot(sigmaY,LayerZ./t,'k')
axis ij
xlabel('pa');
ylabel('z/h');
plot(TaoXY,LayerZ./t,'k--');
axis ij
xlabel('pa');
ylabel('z/h');
legend ('SigmaX','Sigma Y','TaoXY XY');
pause(2);

```

- MATLAB Code of thermo mechanical stress of laminate

```

clc
E1 = 181e9 ; % Pa
nu12 = 0.28 ;
E2 = 10.3e9 ; % Pa
G12 = 7.17e9 ; % Pa
nu21 = nu12 * E2 / E1 ;
a1 = 0.2e-7 ; % coefficients of thermal expansion
a2 = 0.225e-4 ;
deltaT = -75 ;
% [-0 +0 -0 +0]

```

```

orient=[0 90];
N=length(orient);
thick =0.005; % m each layer thickness
t = N * thick; % total laminate thickness
z = -t/2 : thick : t/2;
a = [a1 a2 0]';
Aij = zeros(3,3);
Bij = zeros(3,3);
Dij = zeros(3,3);
Aij_vect = zeros(1,N);
Bij_vect = zeros(1,N);
Dij_vect = zeros(1,N);
NT = zeros(3,1);
MT = zeros(3,1);
% Q matrix (material coordinates)
denom = 1 - nu12 * nu21 ;
Q11 = E1 / denom ;
Q12 = nu12 * E2 / denom ;
Q22 = E2 / denom ;
Q66 = G12 ;
Q = [ Q11 Q12 0; Q12 Q22 0; 0 0 Q66];
for i = 1:3
for j = 1:3
for k=1:N
theta = orient(k) * pi / 180; % ply i angle in radians, from bottom
m = cos(theta) ;
n = sin(theta) ;
T = [ m^2 n^2 2*m*n; n^2 m^2 -2*m*n; -m*n m*n (m^2 - n^2)];
abar = T' * a;
Qbar = inv(T) * Q * (inv(T))';

```

```

%Qb=Qbar(Orient(k))
Aij_vect(k) = Qbar(i,j).*(z(k+1)-z(k));
Bij_vect(k) = Qbar(i,j).*((z(k+1)).^2-(z(k)).^2);
Dij_vect(k) = Qbar(i,j).*((z(k+1)).^3-(z(k)).^3);
end
Aij(i,j) = sum(Aij_vect);
Bij(i,j) = sum(Bij_vect)/2;
Dij(i,j) = sum(Dij_vect)/3;
end
end
Aij
Bij
Dij
for k=1:N
    theta = orient(k) * pi / 180; % ply i angle in radians, from bottom
    m = cos(theta) ;
    n = sin(theta) ;
    T = [ m^2 n^2 2*m*n; n^2 m^2 -2*m*n; -m*n m*n (m^2 - n^2)];
    abar = T' * a;
    Qbar = inv(T) * Q * (inv(T))' ;
    zbar(k) = - (t + thick)/2 + k*thick
    NT = NT + Qbar * abar * thick * deltaT;
    MT = MT + Qbar * abar * thick * zbar(k) * deltaT;
end;
NT
MT
%MM = [0; 0; 0]; % N-m
%NN = [1000; 1000 ; 0]; % N/m
ABD= [Aij Bij;Bij Dij]
Astar = inv(Aij);
Bstar = -inv(Aij)*Bij;

```

```

Dstar = Dij-(Bij/Aij*Bij);
Hstar = Bij/Aij;
Aprime = Astar-(Bstar/Dstar*Hstar);
Bprime = Bstar/Dstar;
Dprime = inv(Dstar);
Hprime = -Dstar\Hstar;
Kappa = Dstar\MT-Dstar\Hstar*NT
Eps_o = Bstar/Dstar*MT+(Astar-Bstar/Dstar*Hstar)*NT
stress = [];
strain = [];
LayerZ = zeros(1,N*2);
for i = 0:N-1
LayerZ(2*i+2) = z(i+2)
LayerZ(2*i+1) = z(i+1)
theta = orient(i+1) * pi / 180; % ply i angle in radians, from bottom
m = cos(theta) ;
n = sin(theta) ;
T = [ m^2 n^2 2*m*n; n^2 m^2 -2*m*n; -m*n m*n (m^2 - n^2)]
Qbar = inv(T) * Q * (inv(T))';
abar = T' * a;
epsilonX = (Eps_o+z(i+1))*(Kappa)- abar* deltaT;
epsilonY = (Eps_o+z(i+2))*(Kappa)- abar* deltaT;
strain = [strain,epsilonX,epsilonY];
tempX = Qbar*(Eps_o+z(i+1))*(Kappa));
tempY = Qbar*(Eps_o+z(i+2))*(Kappa));
stress = [stress,tempX,tempY];
end
LayerZ;
stress
strain
strainX = strain(1,:)

```

```

strainY = strain(2,:);
gammaXY = strain(3,:);
sigmaX = stress(1,:)/1000
sigmaY = stress(2,:)/1000 %KPa
TaoXY = stress(3,:)/1000
maxstressX = max(sigmaX)
maxstressY = max (sigmaY)
maxTaoXY = max(TaoXY)
minstressX = min(sigmaX);
%minstressY = min(sigmaY)
%minTaoXY = min(TaoXY)
STRESS_RATIO= abs(max(sigmaX)/min(sigmaX))
hold on
plot(sigmaX, LayerZ./t,'k:')
axis ij
xlabel('pa');
ylabel('z/h');
title('Stresses(Mechanical load, Nx & Mx) on Laminate (a/h=5 & [+0]as)');
hold on
plot(sigmaY,LayerZ./t,'k')
axis ij
xlabel('pa');
ylabel('z/h');
plot(TaoXY,LayerZ./t,'k--');
axis ij
xlabel('pa');
ylabel('z/h');
legend ('SigmaX','Sigma Y','TaoXY XY');
pause(2);

```